

# **Effects of Stretch on the Bladder Umbrella Cell Apical Junctional Ring**

by

**Amity Fenn Eaton**

B.A., Emory University, 2009

Submitted to the Graduate Faculty of  
School of Medicine in partial fulfillment  
of the requirements for the degree of  
Doctor of Philosophy

University of Pittsburgh

2019

UNIVERSITY OF PITTSBURGH  
SCHOOL OF MEDICINE

This dissertation was presented

by

**Amity Fenn Eaton**

It was defended on

October 14, 2019

and approved by

Thomas Kleyman, Professor, Renal-Electrolyte Division

Alexander Sorkin, Professor, Department of Cell Biology

Marcelo Carattino, Associate Professor, Renal-Electrolyte Division

Bruce McClane, Professor, Department of Microbiology and Molecular Genetics

Dissertation Director: Gerard Apodaca, Professor, Renal-Electrolyte Division

Copyright © by Amity Fenn Eaton

2019

# Effects of Stretch on the Bladder Umbrella Cell Apical Junctional Ring

Amity Fenn Eaton, PhD

University of Pittsburgh, 2019

A critical component of the epithelial barrier is the apical junctional complex (AJC), a ring-like structure circumscribing polarized epithelial cells, which is composed of the apical-most tight junction, the sub-adjacent adherens junction, and the punctate desmosomes. The AJC is physically associated with both actin and keratin filaments, which also form a belt encircling epithelial cells at the height of the AJC. Together the AJC and its associated cytoskeleton form the apical junctional ring (AJR). Critically, the AJR must maintain its continuity in the face of external mechanical forces that accompany normal physiological functions, such as during breathing, when blood flows through vessels, or when urine accumulates in the bladder; however, it is not well understood how this is accomplished.

To accommodate dramatic changes in urine volume, the AJR of umbrella cells, which line the luminal surface of the bladder, expands during bladder filling and contracts upon voiding; however, the mechanisms that drive these events are unknown. We hypothesize that the active expansion and contraction of the umbrella cell AJR during filling and voiding requires the membrane trafficking of junctional proteins. Using native umbrella cells as a model, we observed that the umbrella cells' AJR assumed a non-sarcomeric organization in which filamentous actin and  $\alpha$ -actinin-4 formed a continuous belt, while non-muscle myosin II A (NMMIIA) formed discontinuous linear tracts along either side of the actin ring. Expansion of the umbrella cell AJR required formin-dependent actin assembly but was independent of NMMII ATPase function. AJR expansion also required membrane traffic, Rab13-dependent exocytosis specifically, but not trafficking events regulated by Rab8a or Rab11a. In contrast, the voiding-induced contraction of the AJR depended on actomyosin dynamics, as well as on RhoA, and dynamin-dependent

endocytosis. Taken together, our studies indicate that an important mechanism by which the urothelium retains continuity in the face of cyclical changes in urine volume is the expansion and contraction of the AJR. Whereas AJR expansion depends on actin polymerization, it also requires exocytosis, presumably of vesicles containing AJR-associated proteins. In contrast, contraction of the AJR is likely driven by actomyosin contraction of the AJR and endocytosis of excess AJR proteins.

## Table of Contents

Preface .....	xiii
List of Abbreviations.....	xiv
1.0 Introduction.....	1
1.1 The Epithelial Permeability Barrier.....	2
1.2 The Epithelial Apical Junctional Ring .....	4
1.2.1 The tight junction.....	5
1.2.2 Role of claudins in defining tight junction permeability.....	9
1.2.3 The adherens junction.....	12
1.2.4 Desmosomes.....	17
1.2.5 The peri-junctional cytoskeletal ring.....	20
1.3 Formation, Maintenance, and Remodeling of the Apical Junctional Ring.....	24
1.3.1 Role of the actomyosin cytoskeleton in the formation and remodeling of the AJC .....	26
1.3.2 Role of membrane trafficking during the formation and remodeling of the AJC.. ..	28
1.3.3 Role of Rab GTPases during the formation and remodeling of the AJC .....	31
1.3.4 Role of Rho GTPases in the formation and remodeling of the AJR .....	34
1.4 Effects of Force on Epithelial Tissues .....	36
1.4.1 Intrinsic mechanical forces .....	37
1.4.2 Extrinsic mechanical forces.....	38
1.4.3 Effects of force on membrane trafficking in epithelia.....	38
1.5 Effects of Force on the Apical Junctional Ring .....	40
1.5.1 Effects of force on the tight junction.....	40

1.5.2 Effects of force on the adherens junction.....	42
1.5.3 Effects of force on desmosomes .....	44
1.5.4 Effects of force on the perijunctional cytoskeletal ring.....	45
1.5.5 Apical junctional ring contraction .....	46
1.5.6 Apical junctional ring expansion. ....	47
1.6 Goals of this Dissertation .....	48
2.0 Effects of Filling and Voiding on the Umbrella Cell Apical Junctional Ring .....	51
2.1 Introduction .....	51
2.1.1 Hypothesis .....	53
2.1.2 Structure and function of the urothelium .....	53
2.1.3 Effects of filling and voiding on the structure and function of the umbrella cell layer .....	55
2.1.4 Structure and function of the umbrella cell apical junctional ring.....	61
2.1.5 Claudin expression within the rat urothelium .....	63
2.1.6 Effects of filling and voiding on the structure and function of the umbrella cell apical junctional ring. ....	65
2.2 Results.....	69
2.2.1 The actomyosin cytoskeleton associated with the AJR of umbrella cells forms a non-sarcomeric network.....	69
2.2.2 AJR expansion depends on the actin cytoskeleton.....	74
2.2.3 Apical junctional ring expansion depends on Rab13-dependent exocytosis .....	78
2.2.4 Apical junctional ring contraction depends on the actomyosin cytoskeleton.....	82
2.2.5 Apical junctional ring contraction depends on the dynamin-2-dependent endocytosis.....	84
2.3 Discussion .....	87

2.3.1 Organization and dynamics of the AJR-associated actomyosin cytoskeleton in umbrella cells.....	87
2.3.2 Expansion of the umbrella cell apical junctional ring.....	90
2.3.3 Contraction of the umbrella cell apical junctional ring. ....	92
2.3.4 Summary .....	93
3.0 Perspectives and Future Directions.....	95
3.1 Umbrella cell mechanotransduction.....	95
3.1.1 Role of ENaC and a Nonselective Cation Channel .....	96
3.1.2 Junctional proteins as mechanosensors.....	97
3.1.3 The actomyosin cytoskeleton is mechanosensitive.....	100
3.2 Coordination of umbrella cell mechanotransduction. ....	101
3.2.1 Role of the umbrella cell cytoskeleton. ....	102
3.2.2 Role of $\alpha$ -actinin-4.....	104
3.2.3 Role of Rab GTPases .....	107
3.2.4 Role of Rab13/JRAB-MICAL-L2/ $\alpha$ -actinin-4 signaling cascade.....	108
3.3 Umbrella cell paracellular permeability .....	112
3.3.1 Tight junction strands .....	113
3.3.2 Lateral intercellular space. ....	113
3.3.3 Membrane trafficking of junctional proteins .....	115
3.4 Perspectives .....	118
3.4.1 The AJR: A mechanotransduction signaling complex .....	118
3.4.2 Paracellular permeability in health and disease.....	120
4.0 Materials and Methods .....	122
4.1 Animals.....	122
4.2 Antibodies and reagents.....	122
4.3 Preparation of filled, voided, and quiescent bladders .....	123

4.4 Indirect immunofluorescence and image capture. ....	126
4.4.1 Indirect immunofluorescent tissue labeling. ....	126
4.4.2 Image capture. ....	127
4.5 Production of adenoviruses and summary of viral constructs.....	127
4.5.1 Preparation of chemically competent AdEasier-1 cells.....	127
4.5.2 Production of DN-Rab13-GFP adenovirus.....	128
4.5.3 DN-Rab8a and DN-Rab11a adenoviruses.....	129
4.5.4 <i>In situ</i> adenoviral transduction.....	129
4.5.5 Lysate preparation and western blotting.....	130
4.6 Data and statistical analysis.....	131
4.6.1 Quantitation of AJR perimeter.....	131
4.6.2 Non-linear regression analysis of filling data.....	132
4.6.3 Data analysis.....	132
Appendix: Supplemental Material for Chapter 2.0.....	133
Bibliography.....	142

## List of Tables

Table 1. Tight junction-associated proteins .....	8
Table 2. Adherens junction-associated proteins .....	16
Table 3. Desmosome-associated proteins.....	19
Table 4. Effects of pharmacological inhibitors on AJR expansion. ....	77

## List of Figures

Figure 1. Structure of the tight junction.....	6
Figure 2. Model of the claudin paracellular pore .....	11
Figure 3. Structure of the adherens junction.....	14
Figure 4. Structure of the desmosome .....	17
Figure 5. Structure of the peri-junctional cytoskeletal ring.....	21
Figure 6. RhoA-ROCK-NMMII signaling pathway .....	22
Figure 7. Effects of filling and voiding on intact rat bladder .....	52
Figure 8. Structure of the urothelium .....	54
Figure 9. Filling and voiding alter umbrella cell structure .....	55
Figure 10. Characterization of the response to urothelial stretch. ....	57
Figure 11. ZO-1 is internalized upon voiding. ....	60
Figure 12. Structure and composition of the umbrella cell AJR.....	62
Figure 13. Claudin expression in the urothelium.....	64
Figure 14. Stretch augments urothelial ion transport .....	66
Figure 15. Stretch increases the junctional permeability of the urothelium.....	67
Figure 16. Claudin-8 expression in full, voided, and quiescent rat bladders.....	68
Figure 17. The AJR expands and contracts as a unit during bladder filling and voiding. ....	70
Figure 18. The junctional actomyosin cytoskeleton expands and contracts with the apical junctional complex during bladder filling and voiding.....	73
Figure 19. Effect of filling on average perimeterAJR per umbrella cell .....	74
Figure 20. F-actin disruption impairs AJR expansion during bladder filling.....	76
Figure 21. Inhibition of exocytosis impairs AJR expansion during bladder filling. ....	79
Figure 22. Expression of DN-RAB13-GFP impairs AJR expansion during bladder filling. ....	81

Figure 23. Disruption of the actin cytoskeleton or inhibition of NMMIIA contractility impairs AJR contraction during bladder voiding. ....	83
Figure 24. Expression of DN-RhoA or DN-dynamin-1 impairs AJR contraction during bladder voiding.....	85
Figure 25. Inhibition of endocytosis impairs AJR contraction during bladder voiding.....	86
Figure 26. Model for AJR dynamics during bladder filling and voiding. ....	94
Figure 27. $\alpha$ -actinin-4 colocalizes with the cytokeratin network.....	105
Figure 28. Proposed model of Rab13-JRAB/MICAL-L2- $\alpha$ -actinin-4 signaling cascade.....	111
Figure 29. Stretch increases umbrella lateral intercellular space. ....	114
Figure 30. Claudin-4 knockdown decreases paracellular permeability to anions.....	116
Figure 31. Claudin-4 localization is altered by filling and voiding.....	117
Figure S1. Modified Ussing chambers used to stretch bladder tissue.....	133
Figure S2. Claudin Antibody Specificity Assay .....	134
Figure S3. NMMII distribution within the bladder mucosa .....	135
Figure S4. NMMIIC distribution in the umbrella cell layer.....	136
Figure S5. The umbrella cell AJR can expand after DDM treatment.....	137
Figure S6. RAB13 expression in umbrella cells .....	138
Figure S7. Expression levels of endogenous Rab proteins relative to exogenously expressed DN-Rab mutants.....	139
Figure S8. Comparison of ear hair cell AJR organization versus that of umbrella cells .....	140
Figure S9. Drug filling/voiding assay schematic.....	141

## Preface

I want to take this opportunity to acknowledge everybody who helped me complete this work. I am especially grateful to my mentor, Gerry Apodaca, for his guidance and support. I want to thank the current and past members of the Apodaca lab including Dennis Clayton, Giovanni Ruiz, Luciana Gallo, Marianela Dalghi, Shawn Griffiths, and Steven Truschel. A special thanks goes to the members of my committee, Tom Kleyman, Sascha Sorkin, Marcelo Carattino, and Bruce McClane for sacrificing a lot of their time and energy to help me. I would, also, like to acknowledge the significant moral support of my mom, dad, brother, Andrea, and Kelsey, and my friends, without which I would not have been successful in completing my PhD. Finally, I want to thank both Sarah Biancardi and Carmella Londino for all of their indispensable help navigating the bureaucracy within the School of Medicine during my time as a graduate student.

This work was supported by a fellowship from the National Institute of Diabetes and Digestive and Kidney Diseases of the National Institutes of Health: F31-DK117547-02 (to A.F.E.).

## List of Abbreviations

AJC = apical junctional complex  
AJR = apical junctional ring  
BAECs = bovine aortic endothelial cells  
BfA = brefeldin A  
Bleb = blebbistatin  
CHX = cyclohexamide  
CK = cytokeratin  
CoIP = coimmunoprecipitation  
Cyto D = cytochalasin D  
DA = dominant active  
DDM = N-dodecyl- $\beta$ -D-maltoside  
DFV = discoidal and/or fusiform vesicles  
DN = dominant negative  
E-cadherin = epithelial-cadherin  
ECL = extracellular loop  
EEA1 = early endosome antigen 1  
ENaC = Epithelial sodium channel  
EpCAM = Epithelial cell adhesion molecule  
F-Actin = Filamentous actin  
FRAP = Fluorescence recovery after photobleaching  
GAP = GTPase-activating protein  
GEF = guanine nucleotide exchange factor  
GLUT4 = glucose transporter type 4  
HEK = human embryonic kidney cells  
JAM = junctional adhesion molecule

JRAB/MICAL-L2 = Junctional Rab13-Binding protein/Molecule Interacting with CAsL-Like2

LIS = Lateral intercellular space

MARVEL = MAL-Related proteins for VEsicle trafficking and membrane Link

MDCK = Madin-Darby canine kidney cells

MLCK = myosin light-chain kinase

MLCP = myosin light-chain phosphatase

Myo5B = myosin VB

NMMII = non-muscle myosin II

NSCC = Nonselective cation channel

PDZ = PSD-95/Discs large/ZO-1

PI3K = phosphoinositide 3-kinase

PJAEs = peripheral junction-associated endosomes

PJAR = peri-junctional actomyosin ring

$R_J$  = junctional resistance

ROCK = Rho-associated coiled-coil kinase

SEM = scanning electron microscopy

TEM = transmission electron microscopy

TER = transepithelial resistance

TGN = *Trans*-Golgi network

TRP = Transient receptor potential

WGA = wheat germ agglutinin

ZO = zonula occludens

## 1.0 Introduction

Epithelial tissues are continuous sheets of cells that cover the exterior of the body or line the internal surface of body cavities and hollow organs. The primary function of epithelial tissues is to form a selectively permeable barrier between the outside environment and the underlying tissues of the body. This barrier must be maintained in the face of a variety of stresses in order for multicellular organisms to maintain internal homeostasis in the face of changing external conditions. To create an effective barrier epithelial cells must first establish structurally and functionally distinct apical and basolateral plasma membrane domains. The apical domain forms the outer surface of the body and faces the lumen of internal body cavities, while the basolateral domain is oriented away from the lumen and contacts the underlying epithelium or connective tissue. The basolateral membrane includes both the lateral membrane where cell-cell junctional complexes adhere adjacent epithelial cells together, and the basal membrane domain where epithelial cells sit atop a basement membrane that contacts the underlying epithelial or lamina propria layer.

Within cohesive tissues epithelial cells are held together by the apical junctional complex (AJC), which includes the tight junction, the adherens junction, and the desmosomes. Together they form a ring-like structure that completely encircles polarized epithelial cells at their apico-lateral border. An intact AJC is necessary to establish the selectively permeable epithelial barrier. In the absence of a fully intact AJC, the barrier is lost, and the proper structure and function of the epithelial tissue is compromised. Once an epithelial barrier is formed, it must be maintained in the face of stresses that are experienced under normal conditions, including exposure to physiological forces. For example, epithelia experience forces when air fills the lungs, the stomach expands after eating or drinking, or when urine accumulates in the bladder. How the epithelial AJC is able

to remain dynamic enough to accommodate these physiological forces while being stable enough to maintain the permeability barrier is the question that I am addressing in my thesis work.

While there has been a fair amount of investigation into how the AJR responds to mechanical stimuli in invertebrates (Kong *et al.*, 2017), zebrafish (Han *et al.*, 2016), or cultured cell lines (Liu *et al.*, 2010), there has been very little research examining how vertebrate or mammalian epithelial tissues are able to adapt to these ubiquitous physiological forces without compromising their structure or function. To address this question, I use native rat urinary bladder epithelium (urothelium), which forms one of the least permeable epithelial barriers in the entire body. Of relevance to the question at hand, the urothelium must maintain its impermeable barrier in the face of dramatic changes in urine volume during repeated cycles of filling and voiding.

## **1.1 The Epithelial Permeability Barrier**

Epithelial tissues serve a variety of functions including protection from abrasion, selective secretion and absorption, and sensory perception. The proper function of an epithelial tissue, by definition, requires the maintenance of a selectively permeable barrier separating underlying tissues from the external or luminal environment. The integrity of this barrier is dependent upon an intact apical plasma membrane and AJC. Both the apical membrane and the apical-most tight junction within the AJC are selectively permeable to ions and water, which move across the epithelial sheet by two main routes: the *transcellular pathway* and the *paracellular pathway*. The *transcellular pathway*, defined as the transport or diffusion of substances through the cell across both the apical and basolateral membranes, is often an active process. This transport is classified as absorption when solutes are transported or diffuse through transmembrane channels in the apical membrane, and then are extruded out of the cell across the basolateral membrane. In contrast, secretion occurs when materials are transported from the basolateral surface into the

lumen. The second route, the *paracellular pathway* is the passive movement of ions and water down their concentration gradient across the AJC and through the intercellular space between adjacent epithelial cells. Using ion conductance scanning, Frömter and Diamond were the first to show that in epithelia the main route of passive ion permeation occurs through the intercellular space (Fromter and Diamond, 1972). The rate of paracellular diffusion and the ionic selectivity of the intercellular pathway is regulated by the molecular composition of the apical-most tight junction, which will be discussed further below.

There is increasing evidence that tight junction protein expression, strand organization, and barrier function are altered in numerous disease processes including during cancer metastasis (Martin and Jiang, 2009), in inflammatory diseases like Crohn's disease (Bruewer *et al.*, 2006) and Acute Respiratory Distress Syndrome (Jang, 2014), and in nervous system diseases including multiple sclerosis (Forster, 2008). Specifically, mutations in claudins -1, -14, -16, and -19 cause the genetic disorders neonatal sclerosing cholangitis, autosomal recessive deafness, and familial hypomagnesemic hypercalciuria with nephrocalcinosis, respectively, which are characterized by a compromised epithelial barrier (Gunzel and Yu, 2013). Although the tight junction is the main regulator of paracellular permeability, dysregulation of the adherens junction is also linked to a variety of pathologies associated with increased epithelial permeability, such as inflammatory bowel disease (Mehta *et al.*, 2015). Therefore, understanding how the paracellular barrier is maintained under normal conditions is critical to interpreting structural and functional abnormalities in pathologies characterized by a loss of the epithelial barrier. Specifically, in the bladder, the highly-impermeable urothelium acts as a protective barrier, and the highly impermeable umbrella cell AJC is critical to maintaining this barrier. Accordingly, the umbrella cell barrier is compromised in a variety of bladder pathologies including bacterial infections (Wood *et al.*, 2012), the bladder dysfunction associated with spinal cord injury (Apodaca *et al.*, 2003), and interstitial cystitis (Parsons, 2007).

Although the AJC plays an important role in the physiological maintenance of the epithelial barrier in healthy tissues, and is altered in certain disease states, there are few insights into the mechanisms controlling AJC composition and the preservation of the permeability barrier, even under normal conditions. In the case of interstitial cystitis, it was not previously understood whether increased epithelial permeability led to inflammation, or whether increased permeability occurred secondary to inflammation. However, we showed recently that increasing paracellular permeability across the umbrella cell tight junction, alone, by expressing the cationic, pore-forming, tight junction protein claudin-2, was sufficient to cause the downstream inflammation associated with interstitial cystitis (Montalbetti *et al.*, 2015). Therefore, understanding the mechanisms regulating the formation, maintenance, and remodeling of the AJC under normal conditions is likely critical to the understanding pathological conditions characterized by epithelial barrier dysfunction in the urothelium, and other epithelial tissues.

## 1.2 The Epithelial Apical Junctional Ring

The structural continuity and proper function of epithelial tissues requires an intact AJC, a tripartite structure which circumscribes polarized epithelial cells at their apico-lateral border. As noted above, its constituents include a continuous belt composed of the apical-most tight junction and the sub-adjacent adherens junction, as well as a discontinuous ring of punctate desmosomes (**Figure 1A**). The tight and adherens junctions are physically associated with the actomyosin cytoskeleton, which also forms a continuous ring around polarized epithelial cells at the height of the junctional complex; whereas the desmosomes associate with the keratin filament cytoskeleton. Together, the AJC and associated junctional actomyosin and keratin cytoskeletal belts form the apical junctional ring (AJR).

### 1.2.1 The tight junction.

When examined by transmission electron microscopy (TEM), the tight junction is the most apical portion of the AJC (**Figure 1A**, circled). The tight junction is a multi-protein complex, which contains a variety of transmembrane and cytoplasmic plaque proteins (a subset shown in **Figure 1B** and more in **Table 1**). The tight junction has at least two functions: it acts as a fence, preventing the diffusion of lipids and transmembrane proteins between the apical and basolateral membrane domains, maintaining epithelial identity. The tight junction, also, acts as a gate, regulating the movement of ions and water through the paracellular space between adjacent epithelial cells (Gunzel and Yu, 2013).

Ultrastructurally, the tight junction is composed of what are termed “kissing points”. These “kissing points” are formed by the lateral association of transmembrane tight junction proteins embedded in the plasma membranes of adjacent epithelial cells forming paired strands, which obliterate the space between the cells (**Figures 1, C-D**). These “kissing points” can be seen when the tight junction complex is examined in cross-section using TEM (**Figures 1, A**, circled, and **C**, arrowheads) (Furuse and Tsukita, 2006). The paired association of transmembrane proteins within the tight junction strands forming these “kissing points” establishes the selectively permeable barrier across the intercellular space. When viewed using freeze fracture electron microscopy these kissing points appear as a continuous belt of anastomosing strands made up of transmembrane proteins, mainly claudins and occludin, and lipids (**Figure 1E**) (Claude and Goodenough, 1973). The transmembrane tight junction proteins making up the strands are associated with an intracellular plaque, which in turn links the tight junction strands to the actomyosin cytoskeletal network (**Figure 1B**).

At the molecular level, the tight junction plaque is composed of cytoskeletal and membrane components. The best understood cytoplasmic adaptor proteins are the zonula

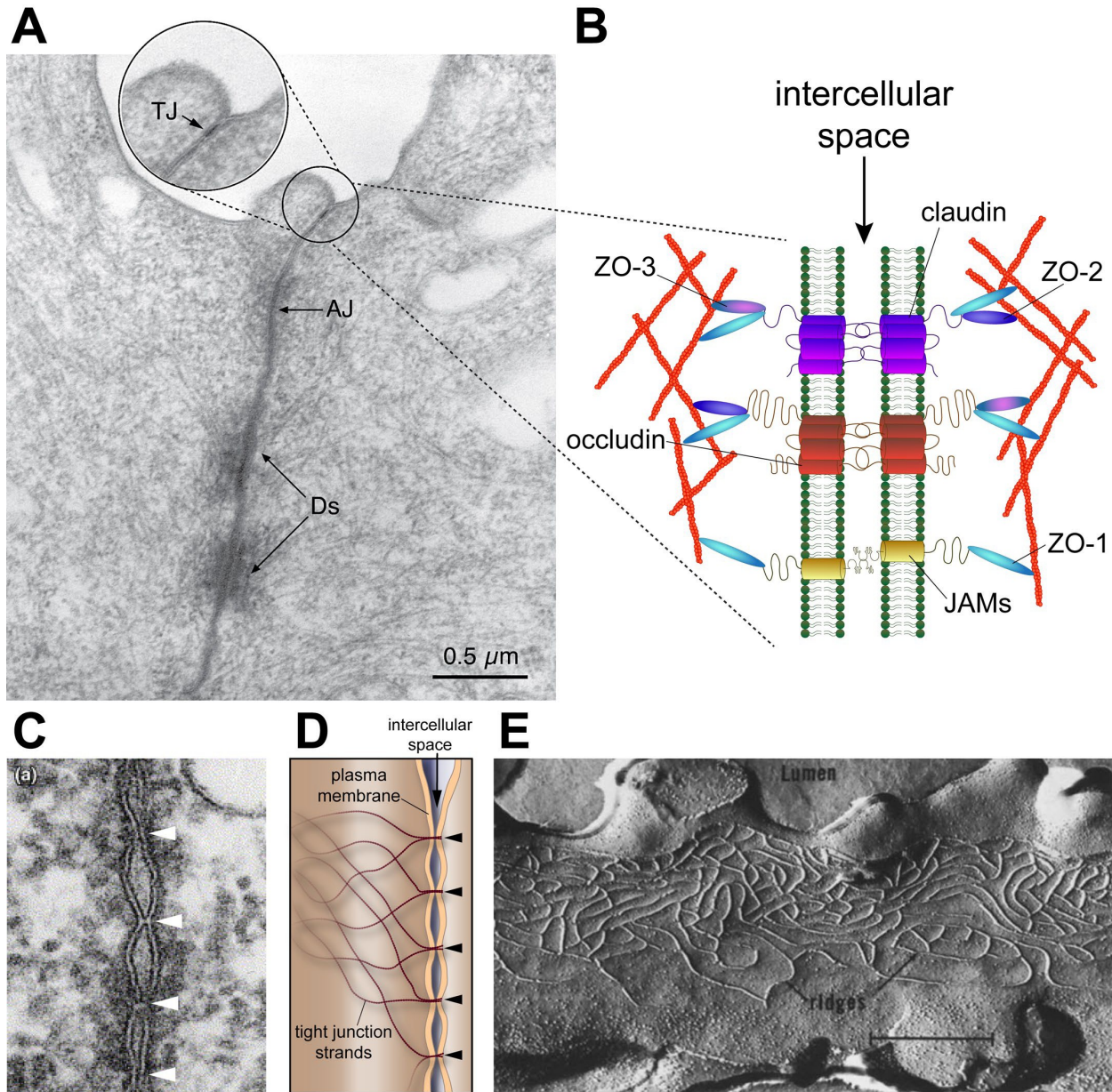


**Figure 1. Structure of the tight junction.**

(A) Cross-sectional TEM of rat bladder umbrella cell AJC with the apical-most tight junction (circled), the subadjacent adherens junction, and the most basal desmosomes. (B) The tight junction is a multi-protein complex consisting of transmembrane proteins linked to the actin cytoskeleton via cytoplasmic adaptor proteins. (C) Freeze fracture EM image of frog urinary bladder showing the tight junction strands. EM image reprinted from Claude and Goodenough, 1973 with permission from Rockefeller University Press © 2019. (D) Schematic representation of cross-sectional view of tight junction "kissing points" formed at the plasma membrane of adjacent epithelial cells by paired tight junction strands. (E) High-magnification view of the tight junction in cross-sectional TEM showing the "kissing points", indicated with arrowheads. EM image reprinted from Furuse and Tsukita, 2006 with permission from Elsevier © 2019.

occludens (ZO-1/2/3) proteins which bind f-actin and contain three PSD-95/discs large/ZO-1 (PDZ) domains which mediate dimerization between the ZO proteins, or the association of ZO proteins with the transmembrane tight junction proteins, linking them to the actomyosin cytoskeleton (**Figure 1B**) (Meyer *et al.*, 2002). Highlighting the importance of the ZO proteins, mice lacking either ZO-1 or ZO-2 are embryonic lethal (Katsuno *et al.*, 2008; Xu *et al.*, 2008); however ZO-3 knockout mice are not embryonic lethal (Xu *et al.*, 2008), suggesting some degree of functional redundancy. On the other hand, depletion of either ZO-1 or ZO-2 in cultured cell lines only causes minor structural or functional changes to the junction (Umeda *et al.*, 2004; McNeil *et al.*, 2006; Hernandez *et al.*, 2007). However, if both ZO-1 and ZO-2 are knocked down in Eph4 epithelial cells, transmembrane tight junction proteins fail to localize to the AJC and the tight junction barrier is completely lost indicating that the ZO proteins are essential for the formation of the tight junction (Umeda *et al.*, 2006). Intriguingly, when ZO-1 and ZO-2 are both depleted in Madin-Darby canine kidney cells (MDCK), loss of tight junction barrier function is accompanied by a delay in the formation of the adherens junction and the actomyosin junctional ring, but once formed the junctional cytoskeletal belt is wider and more linear than in control cells (Fanning *et al.*, 2012), indicating that the ZO proteins regulate the structure and function of the entire AJR. Other cytoplasmic proteins associated with the tight junction include other PDZ-containing scaffolding proteins such as MUPP1 (Adachi *et al.*, 2009) and MAGI-1/2/3 (Balbas *et al.*, 2014), and actin-binding proteins like cingulin (Guillemot *et al.*, 2012) and paracingulin (Guillemot *et al.*, 2008), and the proteins comprising the Pals-1/PATJ/CRB3 and PAR3/PAR6/aPKC polarity complexes (Bilder *et al.*, 2003; Tanentzapf and Tepass, 2003) (**Table 1**).

The transmembrane tight junction proteins include the four-pass transmembrane proteins occludin, tricellulin, angulin, marvelD3 (Raleigh *et al.*, 2010), and claudins, and the single-pass junctional adhesion molecules (JAMs) (Ebnet *et al.*, 2004) (**Table 1**). Occludin, tricellulin, and marvelD3, but not the claudins, contain tetra-spanning MAL-Related proteins for VEsicle trafficking and membrane Link (MARVEL) domains. The MARVEL domain is found in proteins

Table 1. Tight junction-associated proteins

Tight junction protein		Interactors	Function
<b>Four-pass transmembrane proteins</b>	Claudins	ZO-1/2/3, occludin, cingulin, PAR3, MUPP1, MAG11	Determine ionic selectivity of paracellular pathway; necessary for TJ establishment (Gunzel and Yu, 2013)
	Occludin	JAM-A, ZO-1/2/3, cingulin	Dispensable for TJ barrier establishment, may regulate barrier and fence function (Feldman <i>et al.</i> , 2005)
	Tricellulin	ZO-1	Tricellular TJs; required for establishment and maintenance of TJ barrier (Ikenouchi <i>et al.</i> , 2005)
	MarvelD3	Claudins, occludin, ZO-1/2/3, cingulin	Maintenance of TJ barrier (Raleigh <i>et al.</i> , 2010)
	Angulin-1/2/3	Tricellulin	Formation of high resistance tricellular tight junctions in endothelial cells (Sohet <i>et al.</i> , 2015), recruits tricellulin to TJ
<b>Single-pass transmembrane proteins</b>	JAM-A/B/C/D	Occludin, ZO-1, cingulin, PAR3, MUPP1, MAG11	Development of cell polarity (Ebnet <i>et al.</i> , 2004)
	Crumbs homologue-3 (CRB3)	Pals1, PATJ, PAR6	Development of cell polarity and TJ morphogenesis (Lemmers <i>et al.</i> , 2004); prevents lateral diffusion of PAR3/PAR6/aPKC complex (Tanentzapf and Tepass, 2003)
<b>Cytoplasmic adaptor proteins</b>	ZO-1	Occludin, claudins, JAMs, Bves, ZO-1/2/3, cingulin, $\alpha$ -actinin-4, $\alpha$ -catenin, F-actin	Connects transmembrane TJ proteins to the actin cytoskeleton; scaffolding protein (Meyer <i>et al.</i> , 2002)
	ZO-2	Occludin, claudins, ZO-1, cingulin, F-actin, $\alpha$ -catenin	
	ZO-3	Occludin, claudins, ZO-1, cingulin, PATJ, p120-catenin, F-actin	
	Multi-PDZ domain protein-1 (MUPP1)	JAMs, claudins, CAR	Scaffolding protein; dispensable for TJ establishment (Adachi <i>et al.</i> , 2009)
	Membrane-associated guanylate kinase with inverted orientation-1 (MAGI-1/2/3)	JAMs, $\alpha$ -actinin-4	Scaffolding protein (Balbas <i>et al.</i> , 2014)
	Cingulin	JAMs, ZO-1/2/3, NMMII, F-actin, microtubules	Dispensable for TJ establishment; controls expression of transmembrane TJ proteins; regulates RhoA activity (Guillemot <i>et al.</i> , 2008; Guillemot <i>et al.</i> , 2012)
	JACOP/paracingulin	F-actin	Development of cell polarity; necessary for TJ establishment; prevents lateral diffusion of PAR3/PAR6/aPKC complex (Tanentzapf and Tepass, 2003)
	Pals-1	CRB3, PATJ, PAR6	
	PATJ	CRB3, Pals1, ZO-3	
	PAR3/ASIP	JAMs, PAR6	Development of cell polarity; apical localization of CRB3-Pals1-PATJ complex (Bilder <i>et al.</i> , 2003)
	PAR6	CRB3, PAR3, Cdc42, Rac1, Pals1	
Atypical-PKC	Occludin, PAR3, PAR6		

that function to bring apposing cell membranes into close proximity, and localize to cholesterol-rich lipid rafts (Sanchez-Pulido *et al.*, 2002), which are proposed to be sites for the nucleation of vesicles involved in membrane trafficking pathways, such as clathrin-coated pit invagination (Subtil *et al.*, 1999). Tricellulin and angulin-1/2/3 are found at tricellular tight junctions, where three adjacent epithelial cells come into contact, and play a role in epithelial barrier maintenance (Ikenouchi *et al.*, 2005). Angulins, in particular, are necessary for the formation of high resistance endothelial junctions. For example, knockout of angulin-1 impairs the formation of the impermeable blood-brain-barrier during embryogenesis (Sohet *et al.*, 2015). Despite being one of the first tight junction proteins described, the function of occludin is not well understood; however, it is dispensable for the formation of intact tight junctions, but plays a role in pathology (Feldman *et al.*, 2005; Runkle and Mu, 2013).

### **1.2.2 Role of claudins in defining tight junction permeability.**

The proteins most relevant to tight junction barrier function are the transmembrane claudins. Claudins are indispensable for the formation of the tight junction; however, they are primarily responsible for determining the ionic selectivity of the paracellular pathway. There are 27 known claudin genes in humans that can form homo- or hetero-oligomeric complexes and assemble with other transmembrane proteins including, tricellulin, occludin, and the JAMs, to form the tight junction strands. The strands are punctuated by ~3-7 Å pores in the intercellular space, which are proposed to be formed by claudins (Watson *et al.*, 2001; Guo *et al.*, 2003; Van Itallie *et al.*, 2008; Yu *et al.*, 2009a; Krug *et al.*, 2012). Claudins can be either cationic or anionic pore-formers or can act to occlude the paracellular space forming an impermeable barrier. In this way, the complement of claudins expressed in an epithelium confer a unique ionic conductance, charge and size selectivity, and solute permeability to the paracellular pathway. Of the known claudin isoforms only a few are known to form ion-specific pores in the intercellular space. These include

claudins -2, -10b, -15, -16, and -19 which are cationic pore-formers, and claudins -4, -10a, and -17, which form anion-specific pores (Gunzel and Yu, 2013).

Based off of the crystal structure of mouse claudin-15 it was proposed that the tight junction strands are formed by antiparallel double rows of individual claudin monomers (**Figure 2A**) with their transmembrane  $\alpha$ -helical domains embedded in the adjacent cell membranes (**Figure 2B**, cell membranes indicated by grey boxed areas) (Suzuki *et al.*, 2014; Suzuki *et al.*, 2015). The pore itself is formed by the five extracellular  $\beta$ -sheets connecting ECL 1 and 2 (**Figure 2A**) from four individual claudins. The  $\beta$ -sheet pore can be clearly seen when looking from the top down at the model of the claudin pore (see inset in **Figure 2B**, pore indicated with asterisks). The pore-forming claudins have a putative ion binding site present in the extracellular loop 1 (ECL1), which if mutated to an amino acid of the opposite charge reverses the ionic specificity of the pore. In the case of claudin-15, a negatively charged aspartic acid at position 55 mediates the cation selectivity of the pore (**Figures, 2A**, pink and **2B**, green) (Samanta *et al.*, 2018). From homology modeling of pore-forming claudins, based off of the claudin-15 crystal structure, it was proposed that the  $\beta$ -sheets form a “palm” region. The ionic selectivity of a particular claudin isoform is determined by a charged groove formed by the  $\beta$ 3- $\beta$ 4 strands, which includes the ECL1 and the ion binding site (Suzuki *et al.*, 2014). As one might expect, according to the proposed model, the charged “palm” region faces the inside of the pore, and the amino acid present in the ion binding site of claudin-15 (D55) protrudes into the theoretical lumen of the pore (**Figure 2B**, green).

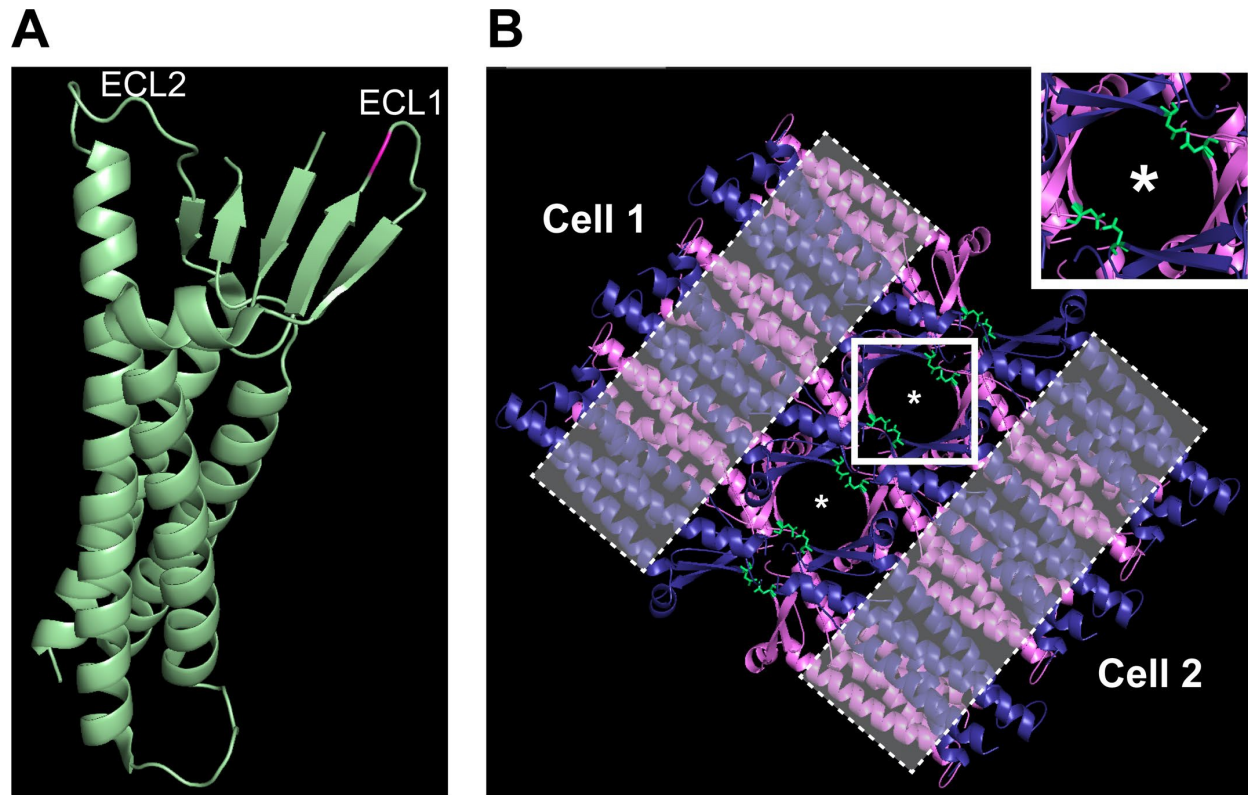


**Figure 2. Model of the claudin paracellular pore.**

(A) Cartoon representation of the mClaudin-15 crystal structure with the ion binding site (D55) within ECL1 highlighted in pink. (B) Top-down view of a computational model of the claudin-15 tight junction pore (indicated with asterisks) formed by the  $\beta$ -sheets from four individual claudin monomers that have their transmembrane domains embedded into the membranes of adjacent epithelial cells (putative membrane localization indicated by grey dashed boxes) with the ion binding site (D55) shown in stick representation (green) protruding into the lumen of the pore. A higher magnification image of the pore is shown in the inset in B. Model based on the mClaudin-15 PDB file 4P79 published by Suzuki *et al.*, 2015.

More recently, Alberini *et al.* proposed a refined model of the claudin-15 paracellular pore (Alberini *et al.*, 2017). They suggest that the claudin pore is highly dynamic and interactions between the extracellular domains can influence the size of the paracellular pore. The complexity of determining the ionic selectivity of individual claudins species is exacerbated by the fact that numerous claudins are expressed within a single epithelial cell, and they possess the ability to form heteromeric complexes. To this point, some claudins are reported to act as pores only when they interact with another claudin, e.g. claudins -16 and -19 are proposed to form a cation-specific pore mediating the reabsorption of divalent cations in the kidney (Hou *et al.*, 2008; Hou *et al.*,

2009), and claudins -4 and -8 are reported to associate in collecting duct cells of the kidney to form an anionic pore for the passive reabsorption of chloride (Hou *et al.*, 2010).

To further complicate our understanding of paracellular permeability, freeze fracture analysis of epithelia suggests a correlation between the number of strands and the “leakiness” of a tissue, i.e. epithelial tissues with more tight junction strands are less permeable and vice-versa (Claude and Goodenough, 1973). One notable exception is in the case of MDCKI/II cells (Stevenson *et al.*, 1988). MDCKI cells are reported to be much less permeable than MDCKII cells; despite this, the number of the tight junction strands and the complexity of the strand network appears almost identical in these two cell types. These findings indicate that there is not always a direct correlation between strand number and epithelial permeability.

Interestingly, in addition to being expressed at the apical-most tight junction, claudins -1, -4, and -7 are commonly found along the basolateral membrane of epithelial cells. Additionally, in stratified epithelia, such as the epidermis, or the urothelium, they are expressed not only in the uppermost layer of the epithelium, but along the plasma membranes of the intermediate and basal cell layers (Hagen, 2017). Although, claudin-1 is known to participate in forming the epithelial barrier in stratified epithelia, such as the skin (Furuse *et al.*, 2002), many of the claudins that are expressed in underlying cell layers associate with known signaling platforms that localize to the basal membrane of epithelial cells, such as the focal adhesion kinase complex (Hagen, 2017). This association suggests a role for these claudins outside of maintaining the paracellular barrier. However, the function of extra-tight junction claudins as signaling molecules is not well-understood and needs further investigation.

### **1.2.3 The adherens junction.**

The adherens junction lies just below the tight junction within the AJC and forms sites of cell-cell adhesion when plasma membranes from adjacent cells are bridged by single-pass

transmembrane cadherin proteins. Like the tight junction, by light microscopy the adherens junction appears as a continuous ring encircling polarized epithelial cells. Looking via TEM, the cytoplasmic side of the adherens junction is characterized by an electron dense plaque, where the associated actin filaments are anchored (**Figure 1A**). In epithelial cells cell-cell adhesion is maintained through homophilic interactions of epithelial cadherin (E-cadherin) (**Figure 3**). E-cadherin is a transmembrane protein with five extracellular repeats, or EC modules, containing calcium-binding sequences at the interface of these domains. Calcium binding causes a conformational change in the extracellular domain making it more rigid, thereby facilitating its binding to the extracellular domain of an E-cadherin molecule from the neighboring epithelial cell (Koch *et al.*, 1997). Classical cadherins form two conformationally distinct bonds which respond differently to tension: the X-dimer and the strand swap dimer. The X-dimer forms catch bonds, which are strengthened by mechanical tension; whereas, strand-swap dimers form slip bonds, which are weakened, or released, by pulling forces (Rakshit *et al.*, 2012). The cadherin cytoplasmic domains are highly conserved, and they bind cytoplasmic proteins called catenins. E-cadherin associates with  $\beta$ -catenin, or its homologue  $\gamma$ -catenin, through its cytoplasmic tail, which binds  $\alpha$ -E-catenin, which in turn forms a bridge between the cadherin complex and the actomyosin cytoskeleton (**Figure 3**).

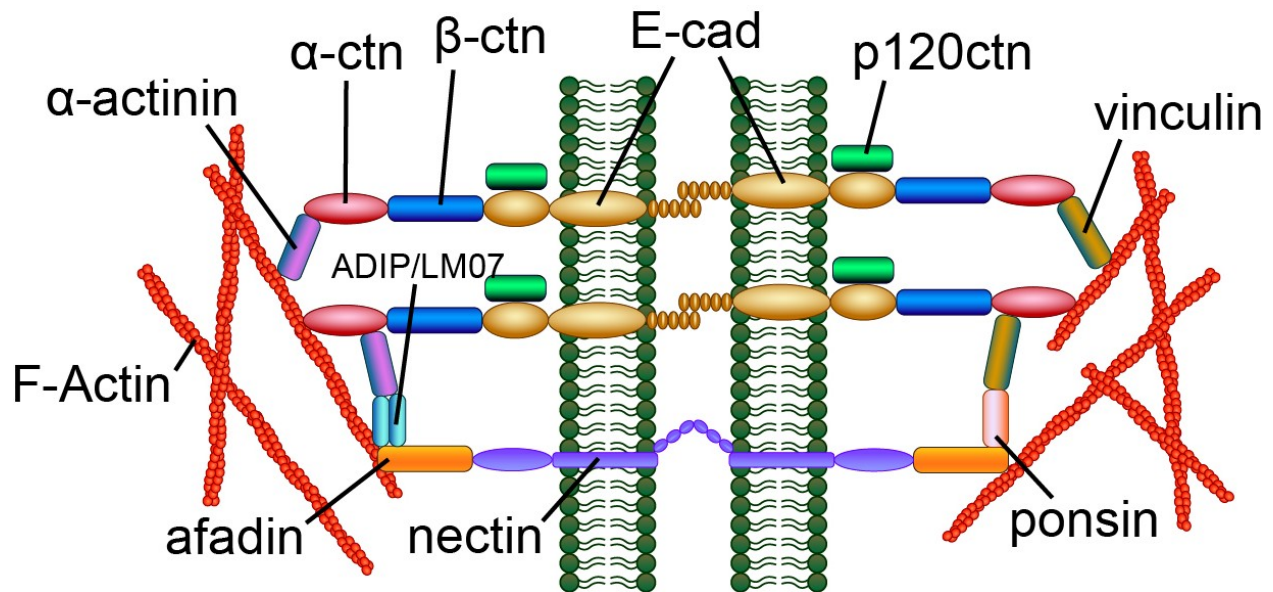


**Figure 3. Structure of the adherens junction.**

The transmembrane cadherins and nectins maintain cell-cell adhesion by forming bonds in the intercellular space. The cadherins are linked to the F-actin cytoskeleton via catenins, of which  $\alpha$ -catenin recruits other actin binding proteins, like vinculin and  $\alpha$ -actinin. The nectins are linked to the F-actin cytoskeleton via afadin, which indirectly binds  $\alpha$ -catenin via adaptor proteins including ponsin, LMO7, and ADIP.

The currently accepted model proposes that  $\alpha$ -catenin is only able to form a stable link between the E-cadherin/ $\beta$ -catenin heterodimer and the actin cytoskeleton if the protein is under constitutive tension (Buckley *et al.*, 2014). Additionally, under tension  $\alpha$ -catenin recruits a variety of other actin binding proteins including vinculin and  $\alpha$ -actinin-4 (Nieset *et al.*, 1997), which reinforce the adherens junction (**Table 2**). E-cadherin, also, interacts with p120-catenin, which regulates the amount of protein at the surface by controlling E-cadherin endocytosis (Miyashita and Ozawa, 2007).

In addition to the cadherins, nectins are transmembrane adherens junction proteins which form calcium-insensitive adhesions. The cytoplasmic domain of nectins interacts with the actin-binding protein afadin, providing a secondary method of adherens junction attachment to the actomyosin cytoskeleton (Takai and Nakanishi, 2003; Niessen and Gottardi, 2008). Additionally, afadin can indirectly bind to  $\alpha$ -catenin through a variety of adaptor proteins (**Figure 3** and **Table**

**2)** connecting the cadherin and nectin-based adhesion complexes (**Figure 3**) (Mandai *et al.*, 1999; Miyahara *et al.*, 2000; Asada *et al.*, 2003; Ooshio *et al.*, 2004; Sawyer *et al.*, 2009).

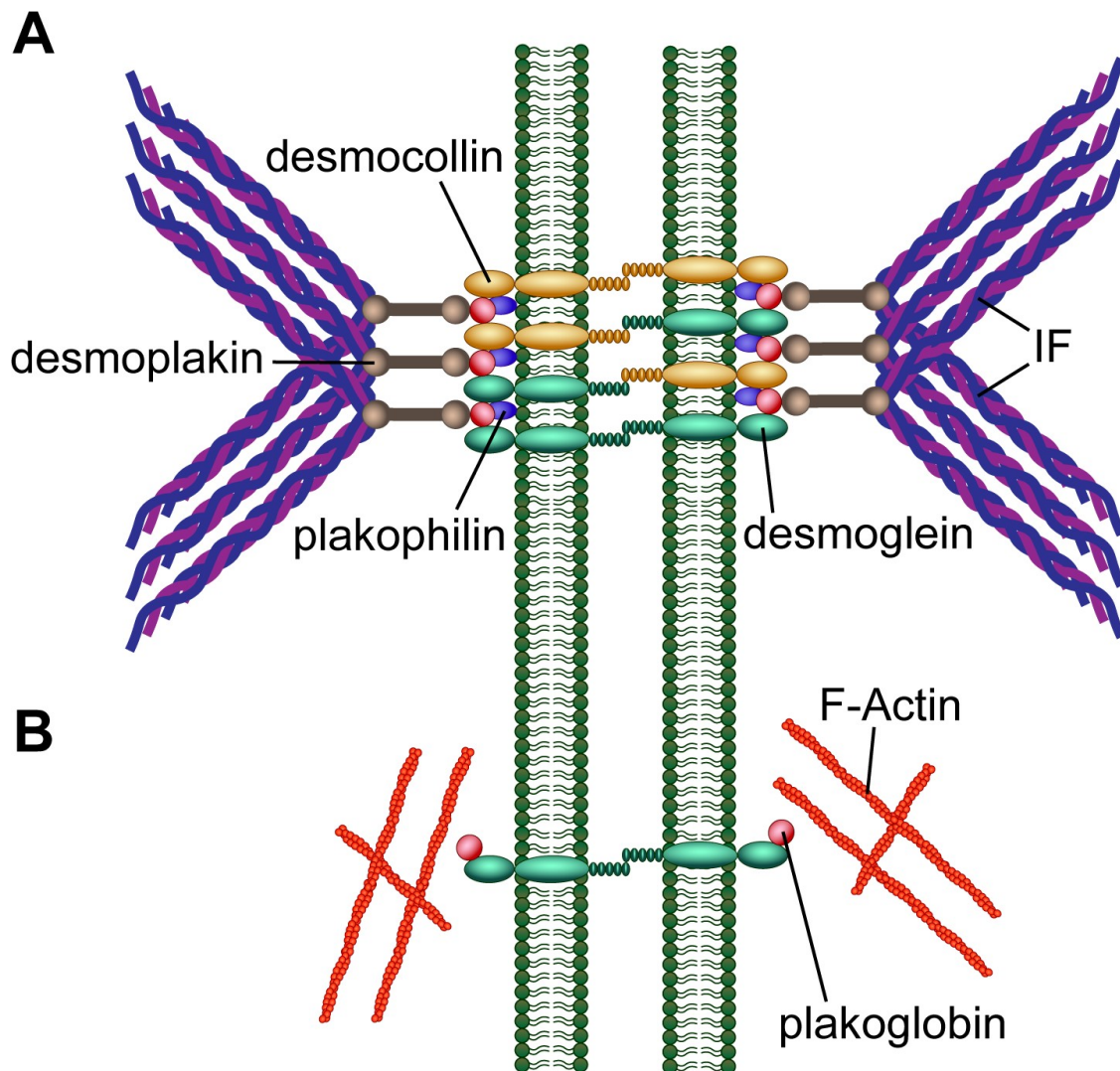
In addition to its function in cell-cell adhesion, the adherens junction plays a well-described role in cell signaling, in particular in the transcriptional regulation of gene expression. For example, E-cadherin can act both as a signaling receptor, and as a regulator of transcriptional activity. E-cadherin likely mediates cell signaling by acting as a docking site for recruitment of protein signaling complexes, such as Src (Serrels *et al.*, 2011), receptor tyrosine kinases (Andl and Rustgi, 2005), phosphoinositide-3-kinase (De Santis *et al.*, 2009), and Rho GTPases (Noren *et al.*, 2001). Additionally, E-cadherin can be cleaved intracellularly by  $\gamma$ -secretase, after which the C-terminal fragment translocates to the nucleus, binds directly to DNA, and upregulates pathways involved in cell proliferation, differentiation, and survival (Ferber *et al.*, 2008). The catenins, also, regulate gene transcription events. For example, p120-catenin is necessary for the translocation of E-cadherin into the nucleus and  $\beta$ -catenin can be activated by extracellular Wnt proteins leading to its translocation into the nucleus where it transcriptionally activates genes involved in cell proliferation and migration (MacDonald *et al.*, 2009).

Table 2. Adherens junction-associated proteins

Adherens junction protein		Interactors	Function
Transmembrane proteins	E-cadherin	$\beta$ -catenin, p120catenin	Ca <sup>2+</sup> -dependent cell-cell adhesion (Leckband and de Rooij, 2014)
	Nectins	Afadin	Ca <sup>2+</sup> -independent cell-cell adhesion (Takai and Nakanishi, 2003)
Cytoplasmic adaptor proteins	$\alpha$ -catenin	F-actin, $\alpha$ -actinin, $\beta$ -catenin, $\gamma$ -catenin, vinculin, afadin, ZO-1	Connects $\beta$ -catenin to the actin cytoskeleton; mechanically sensitive conformational change to recruit proteins and reinforce AJ (Yao <i>et al.</i> , 2014)
	$\beta$ -catenin/ $\gamma$ -catenin (plakoglobin)	E-cadherin, $\alpha$ -catenin	Connects transmembrane AJ proteins to the actin cytoskeleton (Leckband and de Rooij, 2014)
	p120 catenin	E-cadherin	Regulates E-cadherin endocytosis and Rho GTPase signaling (Niessen and Gottardi, 2008)
	Vinculin	$\alpha$ -catenin, ponsin	Recruited to $\alpha$ -catenin under tension; reinforces AJ (Yao <i>et al.</i> , 2014)
	$\alpha$ -actinin-4	$\alpha$ -catenin, ADIP, LMO7	Recruited to $\alpha$ -catenin under tension; reinforces AJ (Nieset <i>et al.</i> , 1997)
	Afadin	Nectins, $\alpha$ -catenin, ponsin, ZO-1	Recruited to $\alpha$ -catenin under tension (Miyahara <i>et al.</i> , 2000); reinforces AJ (Sawyer <i>et al.</i> , 2009); connects nectins to the actin cytoskeleton (Takai and Nakanishi, 2003)
	ZO-1	$\alpha$ -catenin, afadin	Connects TJ and AJ; formation of AJC (Rajasekaran <i>et al.</i> , 1996)
	Ponsin	Afadin, vinculin	Connects afadin to vinculin (Mandai <i>et al.</i> , 1999)
	Afadin dilute domain-interacting protein (ADIP)	Afadin, $\alpha$ -actinin-4	Connects and stabilizes cadherin and nectin adhesion complexes (Asada <i>et al.</i> , 2003)
	LIM domain only 7 (LMO7)	Afadin, $\alpha$ -actinin-4	Connects and stabilizes cadherin and nectin adhesion complexes (Ooshio <i>et al.</i> , 2004)

### 1.2.4 Desmosomes.

The most basal component of the AJC are the discontinuous, or punctate, desmosomes, which like the adherens junctions, are cadherin-based, multiprotein, adhesive complexes that mediate strong adhesion between adjacent cells (**Figure 4**); although less is known about desmosome structure, protein interactions, or functions outside of adhesion. At the ultrastructural



**Figure 4. Structure of the desmosome.**

(A) Transmembrane cadherins (desmoglein and desmocollin) maintain strong cell-cell adhesion and bind plakoglobin and plakophilin, which in turn links the desmosome complex to the intermediate filament cytoskeleton. (B) Extra-desmosomal desmogleins can be found associated with plakoglobin and the actin cytoskeleton.

level desmosomes appear as symmetrical, extremely electron dense plaques on either side of the plasma membrane (**Figure 1A**). Perhaps not surprisingly, desmosomes are often found in epithelial tissues that must withstand frequent mechanical perturbations, such as the skin or bladder (Broussard *et al.*, 2015); although somewhat surprisingly then, desmosomes are not present in endothelial cells which are continuously exposed to force as blood pumps through the body (Dejana, 2004). The desmosomal cadherins are the desmogleins and desmocollins, which can form both homo- and heterophilic interactions, and show tissue- and differentiation-specific distribution (**Table 3**) (Elias *et al.*, 2001; Eshkind *et al.*, 2002; Kljuic *et al.*, 2003; Getsios *et al.*, 2009). Similar to E-cadherin, the desmosomal cadherins have five calcium-sensitive EC modules and interact via their C-terminal tail with the Armadillo family protein and  $\beta$ -catenin homologue, plakoglobin ( $\gamma$ -catenin), and with another protein from the same family, plakophilin. However, unlike tight and adherens junctions the desmosomes are primarily associated with the intermediate filament cytoskeleton, rather than the actomyosin cytoskeleton. This interaction is mediated by desmoplakin which binds to both plakoglobin and plakophilin, and in this way integrates the intermediate filament cytoskeletons of adjacent epithelial cells (**Figure 4A**).

Like the other components of the AJC, the desmosomes are not just adhesion complexes, but are also recognized signaling scaffolds that regulate processes such as cell proliferation and differentiation (Johnson *et al.*, 2014). For example, the desmosomes signal through plakoglobin and plakophilin, which act to suppress  $\beta$ -catenin pro-proliferative transcriptional activity by directly competing for binding to DNA (Chen *et al.*, 2002). Another example is that “free” desmogleins can be found unattached to the desmosomal complex and are instead associated with a variety of signaling molecules such as Rho GTPases. Intriguingly, in the case of desmoglein-3 the extra-desmosomal pool associates with E-cadherin and the actin cytoskeleton where it regulates actin dynamics via Rac1/Cdc42 signaling, although the specifics of this interactions are not well understood (Tsang *et al.*, 2012a; Tsang *et al.*, 2012b).

Table 3. Desmosome-associated proteins.

<b>Desmosomal component</b>	<b>Expression</b>	<b>Function</b>	
<b>Transmembrane cadherins</b>	Desmoglein 1	Supra basal layers of stratified epithelia	Strong cell-cell adhesion; promotes epithelial differentiation and stratification (Getsios <i>et al.</i> , 2009); epidermal barrier function (Elias <i>et al.</i> , 2001)
	Desmoglein 2	Simple epithelia, basal cell layer of stratified epithelia	Strong cell-cell adhesion; basal stem cell proliferation (Eshkind <i>et al.</i> , 2002)
	Desmoglein 3	Basal cell layer of stratified epithelia	Strong cell-cell adhesion; epithelial cell proliferation (Mannan <i>et al.</i> , 2011); extra-desmosomal regulation of actin dynamics (Tsang <i>et al.</i> , 2012)
	Desmoglein 4	Stratified epithelia, hair	Strong cell-cell adhesion; promotes epithelial differentiation and stratification (Kljuic <i>et al.</i> , 2003)
	Desmocollin 1	Stratified epithelia	Strong cell-cell adhesion (Kowalczyk and Green, 2013)
	Desmocollin 2	Simple epithelia, basal cell layer of stratified epithelia	
	Desmocollin 3	Epithelia	
<b>Armadillo proteins</b>	Plakophilin 1	Suprabasal layers of stratified epithelia	Cytoplasmic scaffolding protein; <i>cis</i> cadherin interactions; connect cadherins to desmoplakin (Kowalczyk and Green, 2013)
	Plakophilin 2	Simple epithelia, stratified epithelia, cardiomyocytes	
	Plakophilin 3	Widespread	
	Plakoglobin	Widespread	Cytoplasmic scaffolding protein; <i>cis</i> cadherin interactions; connects cadherins to desmoplakin (Kowalczyk and Green, 2013)
<b>Plakin proteins</b>	Desmoplakin	Epithelia, cardiomyocytes	Connects transmembrane cadherins to the IF cytoskeleton (Kowalczyk and Green, 2013)

### 1.2.5 The peri-junctional cytoskeletal ring.

Polarized epithelial cells are completely circumscribed by cytoskeletal rings composed of both micro (actin) filaments and intermediate (keratin) filaments, which associate with the intercellular junctions, and in this way mechanically integrate adjacent epithelial cells. Both the tight junction and adherens junction physically associate with a perijunctional actin ring (PJAR) cross-linked by contractile non-muscle myosin II (NMMII) and other actin binding proteins including  $\alpha$ -actinins (**Figures 5, A-D**). The actomyosin cytoskeleton is the major force-generating machinery within the cell and can produce both pushing and pulling forces. Much of the junctional actin associated with NMMII is arranged in long filaments running tangential to the plasma membrane that generate pulling forces (Yonemura, 2011; Svitkina, 2018); however, orthogonal bundles are also observed in some settings (Mermelstein *et al.*, 1998; Gomez *et al.*, 2011; Efimova and Svitkina, 2018). In endothelial cells there are branched Arp2/3-positive actin filaments arranged roughly perpendicular to the tangential actin cables, which are proposed to produce pushing forces against adjacent adherens junctions that are essential to maintaining cell-cell adhesion (Efimova and Svitkina, 2018). Pushing forces can, additionally, be generated by the addition of g-actin-ATP monomers to a filament's barbed end by actin nucleation promoting factors, such as formins, and the simultaneous disassembly of f-actin-ADP monomers at the pointed end (Svitkina, 2018). In some cells, but not all the PJAR is arranged in a sarcomeric network similar to the contractile units found in muscle cells (Ebrahim *et al.*, 2013; Schwayer *et al.*, 2016).

The pulling forces generated on the actin cytoskeleton by NMMII contraction regulate a variety of processes including cell adhesion, migration, and proliferation. NMMII is a protein complex composed of a homodimer of two heavy chains (MYH9 in NMMIIA, MYH10 in NMMIIB, or MYH14 in NMMIIC), two essential light chains, and two regulatory chains. The heavy chain of

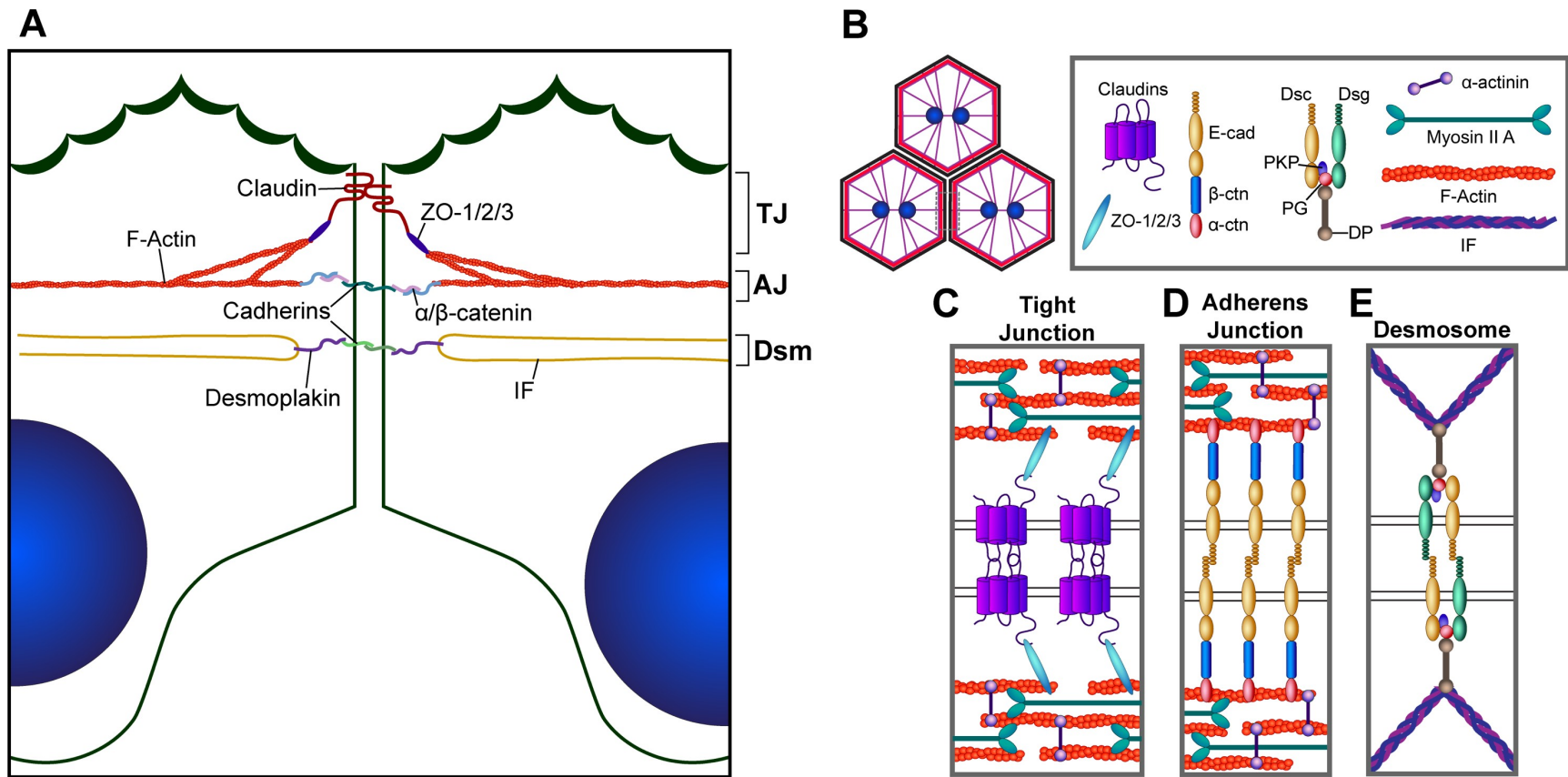


**Figure 5. Structure of the peri-junctional cytoskeletal ring.**

(A) Cross-sectional schematic of umbrella AJC. Umbrella cells, like all polarized epithelial cells, are completely circumscribed by a ring of F-actin at the height of their adherens junction, which is connected to the tight junction via oblique bundles of F-actin; and a ring of keratin intermediate filaments encircles epithelial cells at the height of the desmosomes. In reality the cytoskeletal rings would be running perpendicular to the plane of page around the entire circumference of the cell. (B) Top-down view of the cytoskeletal junctional rings and components, of which the peri-junctional actin ring is cross-linked by NMMIIA and  $\alpha$ -actinin-4 and associates with the (C) tight junctions via the ZO proteins and (D) adherens junctions via  $\alpha/\beta$ -catenins; whereas the peri-junctional keratin ring associates with the (E) desmosomes via desmoplakin.

NMMII is composed of a head domain, which contains the actin-binding domain and the motor domain, and a tail domain which mediates dimerization of the heavy chains. NMMII ATPase activity and contraction can be activated by phosphorylation of its regulatory light chain by Rho-associated coiled-coil kinase (ROCK), which is a downstream effector of RhoA, or myosin light-chain kinase (MLCK) (**Figure 6**). Alternatively, phosphatases, such as myosin light-chain phosphatase (MLCP), dephosphorylate the regulatory light chain, deactivating NMMII. The phosphatase domain of MLCP can, also, be phosphorylated by ROCK, preventing it from phosphorylating and deactivating NMMII. In addition to promoting NMMII ATPase activity, phosphorylation of the regulatory light chain favors the formation of bipolar NMMII dimers formed through interactions of the tail domains. In highly ordered actin structures, like the sarcomeres found in contractile muscle cells, these NMMII bipolar filaments are able to bind simultaneously to multiple cross-linked actin filaments with opposing polarity, which slide across each other in opposite directions upon NMMII contraction. NMMII, also, interacts with less ordered actin structures without any preferential orientation (Betapudi, 2014; Schwyer *et al.*, 2016).

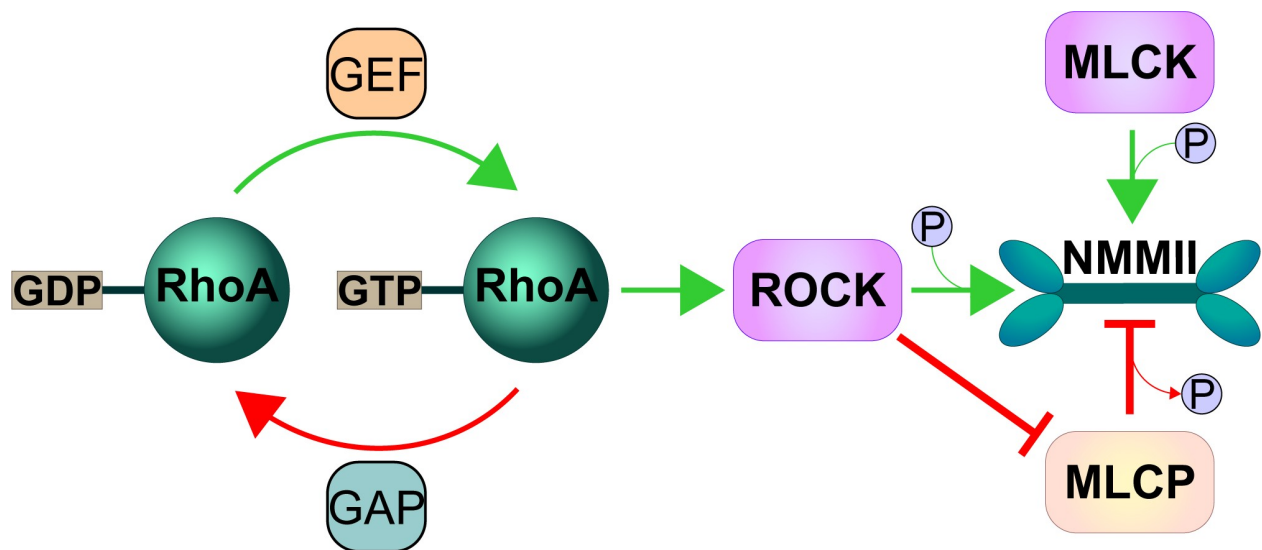


**Figure 6. RhoA-ROCK-NMMII signaling pathway.**

RhoA is inactivated by conversion of GTP to GDP by a Rho GAP and activated by conversion of GDP to GTP by a Rho GEF. RhoA-GTP activates ROCK. NMMII is activated by phosphorylation either by active ROCK or MLCK promoting contraction and formation of bipolar NMMII filaments. NMMII is inactivated by dephosphorylation by MLCP, which is inactivated itself by ROCK phosphorylation.

Some of the primary actin binding proteins associated with the AJR are the non-muscle isoforms of  $\alpha$ -actinin,  $\alpha$ -actinin-1 and  $\alpha$ -actinin-4, which can be found associated with actin filaments, but also localize to sites of cell-cell contact (**Figures 5, C and D**). The  $\alpha$ -actinins are made up of an actin-binding domain attached to four spectrin repeats, followed by a C-terminal calmodulin domain, which confers calcium sensitivity to the actin-binding properties of the non-muscle isoforms of  $\alpha$ -actinin. The  $\alpha$ -actinins associate via their spectrin repeats to form rod-shaped antiparallel homodimers with actin-binding domains at either end, which enables them to cross-link actin filaments. The actin-binding domain possesses a certain amount of inherent flexibility, so that it can bind not only antiparallel actin filaments, but also actin filaments arranged in diverse orientations. Additionally,  $\alpha$ -actinins are targeted to the plasma membrane via interactions with phospholipids and can link the actin cytoskeleton to junctional proteins. For example,  $\alpha$ -actinin-4 is known to bind to the cytoplasmic adherens junction protein  $\alpha$ -catenin (Otey and Carpen, 2004).

In addition to the PJAR, actomyosin rings have been reported in wide-ranging systems *in vivo*, at both the single-cell level, like during cytokinesis, and in multi-cellular tissues, such as during epithelial cell extrusion. Depending on the orientation of the actin filaments, the number and type of bundling proteins present, and the abundance of NMMII motors, actomyosin networks will assume unique contractile properties particularly suited for the diverse functions of different cells or tissues. Fascinatingly, contractile actomyosin ring-like structures of varying architecture and size have been present during single cell division dating back approximately one billion years ago, suggesting that the PJAR is a descendent of a conserved structure, the actomyosin ring, that has been evolutionarily adapted to serve a wide-variety of biological purposes across many species (Schwayer *et al.*, 2016).

Whereas, actomyosin rings are a well-described evolutionarily conserved structure, only relatively recently has it been appreciated that keratin filaments associated with desmosomes

organize into a “rim-and-spoke” structure which consists of a ring-like structure running around the circumference of epithelial cells forming the “rim”, which connects the “spokes” formed by the cytoplasmic network of radial keratin filaments anchored into individual desmosomes at the cell periphery (**Figures 5, A-B and E**) (Quinlan *et al.*, 2017). Keratin filament junctional rings or “rims” are observed in a wide-variety of cells and tissues that were known to possess radial keratin networks, including hepatocytes (Katsuma *et al.*, 1988; Baffet *et al.*, 1991), ciliated cells in the airway (Tateishi *et al.*, 2017), the exocrine cells of the duodenum (Iwatsuki and Suda, 2007) and the pancreas (Toivola *et al.*, 2000), the intestinal epithelium (Brunser and Luft, 1970), and bladder umbrella cells (Veranic and Jezernik, 2002). Intriguingly, like the PJAR the junctional intermediate filament ring is also evolutionarily conserved, suggesting an important function for this highly specialized structure (Coch and Leube, 2016). One example of this is in nematodes where a prominent circumferential keratin ring is found in the intestinal cells lining the endotube (Carberry *et al.*, 2012). However, the presence of a junctional intermediate filament ring is only newly recognized, and the function and regulation is poorly understood relative to the PJAR.

### **1.3 Formation, Maintenance, and Remodeling of the Apical Junctional Ring**

The formation of epithelial AJR during the establishment of epithelial polarity involves a complex interplay between cytoskeletal dynamics and membrane trafficking events. Initially, punctate nectin-based cell-cell adhesions are formed at nascent sites of cell-cell contacts (Sato *et al.*, 2006). Nectins then recruit cadherins resulting in the formation of discontinuous adherens junctions in parallel with the formation of thick bundles of actin filaments along the free cell border. This is followed by the formation of the belt-like adherens junctions characteristic of the mature AJC (Baum and Georgiou, 2011). Shortly after the establishment of discontinuous adherens junctions, desmosome precursors form punctate adhesions associated with intermediate

filaments at the sites of nascent adherens junctions (Green *et al.*, 2010). Over time the desmosomes remain punctate in structure but mature into Ca<sup>2+</sup>-insensitive “hyper-adhesive” complexes. During adherens junction and desmosomal maturation, the tight junctions are established more apically, and simultaneously the actin cytoskeleton is remodeled into a circumferential belt at the height of the AJC completing the formation of the AJR (Green *et al.*, 2010; Baum and Georgiou, 2011). The establishment of junctions occurs slightly differently during lumen formation, which initiates with cell division. Subsequently, Rab11-dependent membrane trafficking events are required to establish an apical membrane initiation site between the two daughter cells, followed by the formation of a pre-apical patch with a closed lumen that is delimited by tight junctions. Subsequently, diffusion of ions and water into the sealed lumen leads to luminal opening (Apodaca, 2010).

Critically, mature cell-cell junctions must be stable enough to maintain tissue integrity, but dynamic enough to accommodate changes in cell shape experienced during tissue morphogenesis, cell division, or when the cell experiences physiological forces like shear stress or stretch. Despite the importance of this function, it is not well understood how epithelia accomplish this, especially in mammalian tissues. An extreme example of dynamic epithelial junctions is during embryonic development when the entire AJC is disassembled and then reassembled during epithelial morphogenesis (Schock and Perrimon, 2002). Even at steady state the mature AJC is a highly dynamic structure, and both the tight junction and adherens junction, and even to a lesser degree the desmosomes, which engage in much stronger adhesion, are constantly being remodeled via coordinated mechanisms involving actomyosin dynamics and membrane trafficking.

### **1.3.1 Role of the actomyosin cytoskeleton in the formation and remodeling of the AJC.**

The junctional actomyosin cytoskeleton plays a crucial role in the assembly and disassembly of cell-cell junctions during the establishment of the AJC and, also in the maintenance of mature junctional complexes. Both the association of actin with the nascent adherens junction and active actin polymerization are necessary for the establishment of the adherens junction (Baum and Georgiou, 2011). It is also known that NMMII contractility is necessary for the recruitment of adherens junction components during junction formation and for the stabilization of the junctions after their initial assembly (Miyake *et al.*, 2006). Interestingly, both excessive activation and inhibition of NMMII-based cell contractility destabilizes mature adherens junctions, indicating that a delicate balance of NMMII activity is required for proper maintenance of the adherens junction. Additionally, the delivery of desmosomal precursors during the establishment of the desmosomes requires a reorganization of the actin cytoskeleton, as well as NMMII activity (Godsel *et al.*, 2005). Not surprisingly since the establishment of the adherens junction and desmosomes precedes the formation of the tight junction and is dependent on the actomyosin cytoskeleton, both inhibition of actin polymerization and inhibition of myosin light chain kinase (MLCK) (preventing NMMII contraction) impair the establishment of tight junctions after  $\text{Ca}^{2+}$  switch in intestinal cell monolayers (Ma *et al.*, 2000a; Ma *et al.*, 2000b). Taken together these data indicate that actin polymerization and NMMII contraction are necessary for the coordinated assembly of the entire AJC.

In mature adherens junctions, actin-NMMII bundles running parallel to the junction can be located more distal from the cadherin-rich zone and are connected to the adherens junctions by oblique bundles approaching the adherens junctions at various angles (Efimova and Svitkina, 2018). Regulators of both Arp2/3 branched actin networks, and of formin-mediated linear actin

filaments have been found localized at the AJC, more prominently at adherens junctions, but also at tight junctions. The Arp3 subunit of the Arp2/3 complex physically interacts with E-cadherin, indicating an importance for branched actin networks at the adherens junction (Kovacs *et al.*, 2002). Additionally, functional experiments have shown Arp2/3 to be necessary not only for adherens junction formation or morphogenesis, but also for the maintenance of mature adherens junctions (Sahai and Marshall, 2002; Ivanov *et al.*, 2005a; Furman *et al.*, 2007; Gates *et al.*, 2007; Kovacs *et al.*, 2011; O'Leary *et al.*, 2017; Efimova and Svitkina, 2018). There is less literature examining the role of Arp2/3 regulation at the tight junction, but loss of the ArpC3 subunit prevents the formation of functional tight junctions during establishment of the epidermal barrier in mouse embryos (Zhou *et al.*, 2013), indicating that Arp2/3 is involved in the assembly and maintenance of both the tight and adherens junctions.

Additionally, formin-mediated actin polymerization plays a role in the establishment and maintenance of the AJC. Similar to the Arp2/3 complex, E-cadherin is found colocalized with the formin mDia1 at adherens junctions in epithelial cells (Carramusa *et al.*, 2007; Acharya *et al.*, 2017). Using a FRET-based  $\alpha$ -catenin tension sensor, Acharya *et al.* report that mDia1 acts to maintain the integrity of the adherens junction by recruiting NMMII to the junction increasing junctional tension and stabilizing the junctional actin cytoskeleton (Acharya *et al.*, 2017). Other formins, including formin-1 in keratinocytes (Kobielak *et al.*, 2004) and formin-like 2 in mammary epithelial cells (Grikscheit *et al.*, 2015), are reported to regulate the assembly of adherens junctions, suggesting that this control is cell type specific. Acharya *et al.* (2017), also, found that mDia1 knockdown impairs the tight junction permeability barrier, indicating that formin-mediated actin polymerization, like Arp2/3-dependent actin polymerization, is required for the assembly and preservation of the entire AJC (Grikscheit and Grosse, 2016).

Less is known about the disassembly of the AJC, but actin cytoskeletal dynamics and NMMII contraction are necessary for this process, as well. Both stabilization of the actin cytoskeleton or inhibition of actin polymerization prevent the disassembly of the AJC after  $\text{Ca}^{2+}$

depletion. Interestingly, disassembly was Arp2/3-dependent suggesting a role for Arp2/3-mediated actin polymerization in the formation, stabilization, and disassembly of the AJC (Ivanov *et al.*, 2004a). Formin-mediated actin polymerization by Dia, the lone formin in the Dia family in fruit flies, is required for the clustering of E-cadherin prior to its endocytosis during the development of the fly embryo. This finding indicates that formin-mediated actin polymerization may, also, be involved in the disassembly of the adherens junction (Levayer *et al.*, 2011). Additionally, inhibiting NMMII contraction using blebbistatin prevented the reorganization of the actin cytoskeleton and the subsequent disassembly of the AJC (Ivanov *et al.*, 2004a). Taken together these data support the importance of both formin- and Arp2/3-mediated actin polymerization and NMMII contraction in the regulation of AJC dynamics.

### **1.3.2 Role of membrane trafficking during the formation and remodeling of the AJC.**

Asymmetrical membrane trafficking events are fundamental for the establishment and maintenance of distinct apical and basolateral membrane domains with unique functions in epithelial cells (Apodaca *et al.*, 2012). Directed transport of cargos to either the apical or basolateral domains involves movement through multiple distinct compartments prior to delivery to the cell surface. This passage is regulated by the Rab family of small GTPases, which regulate many aspects of membrane trafficking, such as cargo selection and vesicle transport along cytoskeletal tracks (Stenmark, 2009). Delivery of proteins to the plasma membrane can be direct along the biosynthetic or secretory route, where proteins are synthesized in the *trans*-Golgi network (TGN) and transported to either the apical or basolateral domains via distinct carriers. However, some cargoes are not targeted directly to the plasma membrane, but rather pass first through Rab11a or Rab8a-positive recycling endosomes (Goldenring, 2015). Alternatively, proteins and larger molecules can be transported via membrane-bound vesicles which are

internalized from either the apical or basolateral membrane and secreted by fusing with the opposite membrane domain in a process called transcytosis (Fung *et al.*, 2018).

Once at the surface proteins can be internalized via endocytosis into distinct Rab5-positive apical or basolateral early endosomes (Jovic *et al.*, 2010). The clathrin-mediated endocytic pathway is the most well-characterized and involves the adaptor protein AP2, and the large GTPase dynamin (Kaksonen and Roux, 2018), which pinches off the necks of vesicles from the plasma membrane; although, there are multiple pathways of clathrin-independent internalization, as well (Mayor *et al.*, 2014). At this point, cargo is either recycled back to the apical surface through the rapid Rab4-dependent pathway (Grant and Donaldson, 2009) or shuttled into the degradative pathway via Rab7-positive late endosomes (Parton *et al.*, 1989). Alternatively, cargo can be internalized and recycled to the surface via a Rab10 and Rab8-positive endosomal recycling pathway (Wang *et al.*, 2000). However, the Rab11-dependent slow recycling pathway is the most well-described, and is involved in the transport of cell surface receptors, junctional proteins, and ion channels back to the plasma membrane (Goldenring, 2015).

Not surprisingly, the establishment and maintenance of the AJC requires polarized membrane trafficking events. The AJC is a highly dynamic structure which undergoes constant remodeling, even within stable, confluent monolayers. This is highlighted by fluorescence recovery after photobleaching (FRAP) experiments showing that ZO-1 is highly mobile at steady state and exchanges with an intracellular pool, presumably via membrane trafficking (Shen *et al.*, 2008). Supporting this idea, the AJC is highly enriched in exocytic and endocytic proteins suggesting that the AJC is a signaling platform for trafficking events. Furthermore, fluorescently-tagged E-cadherin and claudins are constitutively internalized in MDCK cells (Le *et al.*, 1999) and in Eph4 murine epithelial cell monolayers (Matsuda *et al.*, 2004), highlighting the close association between membrane trafficking events and junctional dynamics.

Functional AJCs are initially assembled via Rab-dependent exocytosis (Marzesco *et al.*, 2002) that also requires the vesicle-associated protein, VAP-33 (Lapierre *et al.*, 1999), and the

Sec6/8 complex, which regulates secretory exocytosis (Grindstaff *et al.*, 1998). Junctions are then disassembled or remodeled via the endocytosis and recycling of AJC proteins, which is also in part regulated by Rab GTPases (Ivanov *et al.*, 2005b). There are a variety of endocytic recycling pathways that are implicated in junctional remodeling depending on the model system, suggesting that regulation differs by cell or tissue type. These include both clathrin-dependent (Ivanov *et al.*, 2004b) and -independent endocytosis (Paterson *et al.*, 2003), macropinocytosis (Bruewer *et al.*, 2005), and caveolin-dependent endocytosis (Shen and Turner, 2005).

The membrane trafficking of AJC proteins has been especially well studied in processes requiring dramatic morphogenesis of epithelial cell junctions while still maintaining the integrity of the epithelial sheet. For example, the recycling of E-cadherin is known to be necessary for junctional plasticity in a variety of epithelial remodeling events (Kowalczyk and Nanes, 2012; Takeichi, 2014). Studies looking at fruit fly development have shown that blocking dynamin-mediated endocytic redistribution of DE-cadherin (the fly homologue of E-cadherin) impairs proper cell-cell contact remodeling during germband extension (Levayer *et al.*, 2011). Additionally, during wing-packing in flies the adherens junction of epithelial cells shrinks due to E-cadherin turnover (Classen *et al.*, 2005; Warrington *et al.*, 2013). E-cadherin endocytosis is not only required for junctional morphogenesis during fly development, but is also required for morphogenesis during vertebrate development, indicating that these junctional remodeling mechanisms are conserved across species. For example in zebrafish, blocking E-cadherin endocytosis results in defects in epiboly (Ulrich *et al.*, 2005; Song *et al.*, 2013).

There is much less known about how the trafficking of tight junction proteins participates in cell-cell junctional morphogenesis; however JAM-A (Chatterjee *et al.*, 2013) and ZO-1 (Tornavaca *et al.*, 2015) are involved in endothelial remodeling during angiogenesis, and claudins are required for convergent extension during neural tube closure in mice (Baumholtz *et al.*, 2017). Whether or not membrane trafficking of tight junction proteins plays a role in these processes is still an open question, but presumably tight junction proteins must be redistributed during

processes involving junctional remodeling. It seems probable that a conserved mechanism involving membrane trafficking events could regulate both tight junction and adherens junction remodeling during morphogenesis, but this remains to be seen. It is critical to understand the mechanisms behind AJC trafficking under normal conditions because in a variety of pathological contexts including exposure to cytokines (Bruewer *et al.*, 2003), oxidative stress (Kevil *et al.*, 1998), and bacterial (McNamara *et al.*, 2001; Nusrat *et al.*, 2001; Singh *et al.*, 2001; Hopkins *et al.*, 2003) or viral infections (Obert *et al.*, 2000; Talavera *et al.*, 2004) AJC protein internalization is dramatically increased leading to a disruption of the epithelial barrier.

### **1.3.3 Role of Rab GTPases during the formation and remodeling of the AJC.**

The exocytic delivery and endocytic recycling of AJC proteins during assembly, disassembly, and remodeling of mature junctions is controlled by Rab GTPases. The AJC is enriched in a variety of Rab proteins including Rab3b (Weber *et al.*, 1994), Rab13 (Zahraoui *et al.*, 1994), Rab14 (Lu *et al.*, 2014), and Rab34 (Coyne *et al.*, 2007) and internalized AJC proteins have been detected in Rab5-positive early endosomes (Coyne *et al.*, 2007), Rab11- and Rab4-positive recycling endosomes (Hopkins *et al.*, 2003), Rab7-positive late endosomes (Xiao *et al.*, 2003; Matsuda *et al.*, 2004), and Rab8 (Lau and Mruk, 2003; Yamamura *et al.*, 2008) and Rab13-positive vesicles (Zahraoui *et al.*, 1994; Marzesco *et al.*, 2002; Marzesco and Zahraoui, 2005; Yamamura *et al.*, 2008).

In regards to the tight junction, Rab3b, Rab5, Rab13, Rab14, and Rab34 localize near the tight junction, or are found in vesicles containing tight junction proteins, and are implicated in the exocytosis and recycling of tight junction proteins during the formation and maintenance of the tight junction (Weber *et al.*, 1994; Zahraoui *et al.*, 1994; Marzesco *et al.*, 2002; Coyne *et al.*, 2007; Lu *et al.*, 2014). Rab13 is the Rab GTPase most often associated with the trafficking of transmembrane tight junction proteins in polarized epithelial cells. Rab13 was originally shown to

localize to cytosolic vesicles in non-polarized cells, however in polarized Caco-2 intestinal epithelial cells it colocalizes with ZO-1 at the tight junction (Zahraoui *et al.*, 1994). Since then, using dominant active (DA) and dominant negative (DN) mutants, it has been demonstrated that Rab13 regulates the endocytic recycling of occludin (Morimoto *et al.*, 2005) and the trafficking of claudin-1 during the formation of functional tight junctions in MDCK cells (Marzesco *et al.*, 2002; Marzesco and Zahraoui, 2005). On the other hand, Rab14 specifically regulates claudin-2 trafficking. Knockdown of Rab14 in MDCK cells leads to increased transepithelial resistance (TER) due to a decrease in Rab14-dependent sorting of claudin-2 out of the lysosomal degradation pathway (Lu *et al.*, 2014). Although, Rab3b localizes to the tight junction during the establishment of tight junctions after Ca<sup>2+</sup> switch, its role in tight junction regulation remains unclear (Weber *et al.*, 1994). Finally, Rab5 and Rab34 are involved in the internalization of occludin during *Coxsackievirus* entry across the tight junction of Caco-2 intestinal epithelial cells (Coyne *et al.*, 2007).

In the case of the adherens junction, the membrane trafficking of E-cadherin by Rab GTPases is especially well-studied (Bryant and Stow, 2004; Kowalczyk and Nanes, 2012). E-cadherin is found in Rab5-positive early endosomes (Bruser and Bogdan, 2017), and expression of a DN-Rab5 mutant prevents E-cadherin endocytosis during the disassembly of adherens junctions (Kamei *et al.*, 1999). Additionally, injecting embryos with a Rab5c morpholino during zebrafish gastrulation leads to a decrease in E-cadherin endocytosis (Ulrich *et al.*, 2005). After internalization E-cadherin is either recycled back to the surface in a Rab11-dependent manner (Lock and Stow, 2005), or targeted for lysosomal degradation. This is supported by the observation that inhibition of Rab11, or the exocyst complex, leads to intracellular accumulation of E-cadherin and junctional integrity is compromised (Langevin *et al.*, 2005; Bruser and Bogdan, 2017). More recently, a novel pathway of Rab11-dependent delivery of newly synthesized E-cadherin directly to the adherens junction has been suggested (Woichansky *et al.*, 2016).

Other Rabs that have been implicated in the regulation of adherens junction assembly and disassembly include Rab4 and Rab8. Rab4a associates with  $\alpha$ - and  $\beta$ -catenin during adherens junction disassembly in Sertoli cells (Mruk *et al.*, 2007), and there is, at least, one report of a rapid Rab4-dependent recycling pathway for E-cadherin (de Madrid *et al.*, 2015). Rab8b colocalizes with E-cadherin in the rat testis, and its expression is increased during the assembly of cell-cell junctions, suggesting that Rab8b may be involved in this process (Lau and Mruk, 2003). Additionally, Rab8 is reported to regulate the delivery of E-cadherin during the formation of adherens junctions in cultured epithelial cells (Yamamura *et al.*, 2008).

Despite the fact that many of the Rab-dependent membrane trafficking pathways that regulate the remodeling of tight junctions and adherens junctions appear to be distinct, there is some evidence of crosstalk between the two pathways. To this point, Junctional Rab13-Binding protein/Molecule Interacting with CasL-Like 2 (JRAB/MICAL-L2), an effector molecule shared by Rab8 and Rab13, was originally identified as a novel Rab13-binding protein (Terai *et al.*, 2006). JRAB/MICAL-L2 localizes to tight junctions in MTD-1A epithelial cells and binds specifically to Rab13-GTP via its C-terminal tail. Preventing the interaction between Rab13 and JRAB/MICAL-L2 inhibits the recycling of occludin and the establishment of functional tight junctions after  $Ca^{2+}$  switch (Terai *et al.*, 2006). Subsequently, it was discovered that JRAB/MICAL-L2, also, forms a complex with Rab8 via its C-terminal domain. Rab8 and Rab13 compete for binding to JRAB/MICAL-L2 and the association of JRAB/MICAL-L2 with either Rab8 or Rab13 appears to regulate the specificity of protein trafficking for the complex. Knockdown of JRAB/MICAL-L2 disrupts trafficking of both the tight junction proteins claudin-1 and occludin and the adherens junction protein E-cadherin. On the other hand, knockdown of Rab13 only affects the trafficking of claudin-1 and occludin, but not E-cadherin, and knockdown of Rab8 inhibits the Rab13-independent trafficking of E-cadherin (Yamamura *et al.*, 2008). Together, these data suggest that the competitive binding of Rab8 and Rab13 to JRAB/MICAL-L2 coordinates the trafficking of tight

junction and adherens junction components during the establishment of functional AJCs, at least, in cultured epithelial cells.

#### **1.3.4 Role of Rho GTPases in the formation and remodeling of the AJR.**

Polarized membrane trafficking events are fundamentally dependent on the cytoskeleton. The microtubule-based motors kinesin and dynein regulate transport of cargos to the apical domain; whereas, actin-based motors regulate short-range trafficking of vesicles within both the exocytic and endocytic pathways to and from the apical membrane domain, as well as to the basolateral domain depending on the particular motor (Apodaca *et al.*, 2012). The Rho family of small GTPases act as key regulators of membrane trafficking pathways by controlling actin cytoskeletal organization via binding to actin nucleating factors, and various kinases and phosphatases that regulate actin dynamics. The three main canonical Rho GTPases, RhoA, Rac1, and Cdc42 regulate a wide-variety of both exocytic and endocytic events including regulated and constitutive exocytosis and clathrin-dependent and -independent endocytosis (Croise *et al.*, 2014).

As discussed above, the assembly, disassembly, and remodeling of the AJC is highly dependent upon actin dynamics and NMMII contraction. This is illustrated by the observation that internalization of AJC proteins during junctional morphogenesis is generally accompanied by a rearrangement of the actin cytoskeleton (Akhtar and Hotchin, 2001; Singh *et al.*, 2001; Ivanov *et al.*, 2004a; Talavera *et al.*, 2004), and inhibition of actin polymerization or disruption of the actin cytoskeleton prevents the internalization of AJC proteins (Le *et al.*, 2002; Ivanov *et al.*, 2004a). Additionally, blocking NMMII ATPase activity with blebbistatin completely prevents the internalization of AJC proteins in T84 intestinal epithelial cells depleted of  $Ca^{2+}$  (Ivanov *et al.*, 2004a).

Not surprisingly since the Rho family of small GTPases regulate both actin cytoskeletal organization and NMMII contraction, and in this way indirectly control membrane trafficking events, they are also well-known regulators of the formation, disassembly, and remodeling of the AJR. On one hand, activation of Rho GTPases causes abnormal trafficking of AJC proteins leading to an increase in epithelial permeability. For example, expression of dominant-active (DA) mutants of RhoA, Rac1, and Cdc42 prevent epithelial cells from forming high resistance barriers, which coincides with a redistribution of the tight junction proteins occludin, ZO-1, claudin-1, claudin-2, and JAM-1 (Jou *et al.*, 1998; Rojas *et al.*, 2001; Wojciak-Stothard *et al.*, 2001; Bruewer *et al.*, 2004). The association of Rho GTPases with the regulation of membrane trafficking during the maintenance of the tight junction is further highlighted by experiments showing that direct activation of Rho GTPases by *Escherichia coli* (*E.coli*) cytotoxic necrotizing factor-1 (CNF-1) leads to internalization of tight junction proteins into early endosomal antigen-1 (EEA-1) and Rab11-positive endosomal structures and a subsequent loss of epithelial barrier function (Gerhard *et al.*, 1998; Hopkins *et al.*, 2003). Interestingly, inhibition of Rho GTPases using *Clostridium* toxins also results in an increase in paracellular permeability (Nusrat *et al.*, 1995), suggesting a complex interplay between the active and inactive forms of Rho proteins in maintaining the integrity of the tight junction barrier.

Rho GTPases are also fundamental in establishing and maintaining the adherens junction. To this point, the formation of nascent E-cadherin-mediated cell-cell contacts between adjacent epithelial cells requires local zones of Rac activation (Kovacs *et al.*, 2002; Lambert *et al.*, 2002). On the other hand, RhoA acts upstream of the formin mDia1 (Sahai and Marshall, 2002) and NMMII (Shewan *et al.*, 2005) to maintain the adherens junction after initial formation. RhoA is also implicated in the disassembly of cell-cell junctions during epithelial-to-mesenchymal transition (Takaishi *et al.*, 1994; Bhowmick *et al.*, 2001), again highlighting the delicate balance of Rho signaling in the regulation of the AJC. Rho regulation of the adherens junction is mainly accomplished by controlling endocytic recycling. Both Rac and Cdc42 are required for

internalization of E-cadherin in mammalian epithelial cells, which is associated with and altered actin cytoskeletal organization (Yap *et al.*, 2007). Cdc42 is particularly important in the control of adherens junction protein trafficking during active remodeling of mature adherens junctions, which is central to developmental or morphogenetic processes. For example, Cdc42 regulates E-cadherin trafficking during the development of the fruit fly ectoderm (Harris and Tepass, 2008). Ultimately, a tightly regulated balance between Rho GTPase activity in epithelial cells is necessary for the proper establishment and maintenance of the mature AJR.

### **1.4 Effects of Force on Epithelial Tissues**

Critically, epithelia must sense and respond to intrinsic (e.g., generated by contraction of the actomyosin cytoskeleton) and extrinsic (e.g., tension, compression, or shear stress) mechanical forces that occur during morphogenesis or that are generated during normal physiological functions such as lung inflation, fluid flow through the nephrons or vasculature, or bladder distension (Cavanaugh *et al.*, 2001; Thi *et al.*, 2004; Tzima *et al.*, 2005; Duan *et al.*, 2008; Carattino *et al.*, 2013; Rubsam *et al.*, 2018). Epithelia accomplish this via mechanotransduction, which is the process of translating a physical force into a biochemical signal to produce a downstream cellular response (Apodaca, 2002). The initial force sensing is mediated by molecular mechanosensors, which respond to mechanical stimuli by changing their conformation, or binding affinities for associated effector proteins (Hoffman *et al.*, 2011). These mechanosensitive proteins subsequently transduce force via the cytoskeleton, or by translating it into biochemical signals that activate pathways, leading to variable cellular responses (Apodaca, 2002; Janmey and McCulloch, 2007; Hoffman *et al.*, 2011). Numerous fundamental cellular changes occur in response to mechanical stimuli including cell division, signal transduction, apoptosis, and gene expression (Apodaca, 2002). Additionally, during development and tissue remodeling mechanical

forces direct epithelial morphogenesis (Heisenberg and Bellaiche, 2013; Gilmour *et al.*, 2017). It is important to understand the mechanically-regulated pathways within the cell because dysregulation of these various processes can lead to diverse pathologies, including atherosclerosis, hypertension, osteoporosis, muscular dystrophy, cardiomyopathies, and cancer (Hoffman *et al.*, 2011).

#### **1.4.1 Intrinsic mechanical forces.**

Many of the forces that act on epithelial cells and on cell-cell junctions, in particular, are generated by the cells themselves through contraction of the actomyosin cytoskeleton (Charras and Yap, 2018). These intrinsic forces were first observed during tissue morphogenesis during embryonic development (Levine *et al.*, 1994), but subsequently have been identified in mature, or quiescent tissues, especially in epithelia engaged in cell-cell adhesion (Acharya *et al.*, 2017), and during processes such as cell proliferation or division (Pan *et al.*, 2016). Since the AJC is physically attached to the PJAR, the intrinsic forces generated by the actomyosin cytoskeleton result in tension within the plasma membrane which is sensed at the AJC by mechanosensitive proteins that link the transmembrane junctional proteins to actin, such as  $\alpha$ -catenin (Yao *et al.*, 2014) and ZO-1 (Spadaro *et al.*, 2017). These proteins undergo conformational changes when exposed to a certain amount of tension, revealing cryptic binding domains, or sites for post-translational modification, in turn mediating the recruitment of downstream effectors, which can act to recruit proteins to reinforce cell adhesion (Yao *et al.*, 2014), or activate transcriptional regulation of processes such as cell proliferation (Spadaro *et al.*, 2017). In this way, internal forces generated by changes in the contractility of the actomyosin cytoskeleton associated with cell-cell junctions can regulate a wide variety of cellular events.

### **1.4.2 Extrinsic mechanical forces.**

In addition to the intrinsic forces generated by the actomyosin cytoskeleton, cells within epithelial tissues are also subject to a number of extrinsic forces under physiological conditions including tension or stretch, like in the epithelium lining the lumen of the bladder when urine accumulates; shear stress, for example in endothelial cells when blood flows through the vasculature; or, osmotic pressure, like in the intestinal epithelium when solutes pass from the stomach into the lumen of the gut drawing in water and increasing intraluminal pressure. There is very little known about how these extrinsic forces are accommodated, especially in mammalian epithelial tissues, but it is in part mediated through the AJC. This is supported by the observation that brain microvasculature endothelial monolayers orient in the direction of shear stress, which correlates with an increased localization of junctional proteins at sites of cell-cell contact and a tightening of the endothelial permeability barrier (Colgan *et al.*, 2007).

### **1.4.3 Effects of force on membrane trafficking in epithelia.**

One way that epithelia accommodate both intrinsic and extrinsic force is by altering membrane trafficking events in response to local changes in membrane tension (Morris and Homann, 2001; Apodaca, 2002; Gauthier *et al.*, 2012). Exocytosis involves the fusion of membrane-bound vesicles with the plasma membrane resulting in a net delivery of membrane, increasing cell surface area, and in turn decreasing plasma membrane tension (Apodaca, 2002). Not surprisingly, exocytosis is stimulated by processes that increase plasma membrane tension like during cell spreading (Gauthier *et al.*, 2011; Gauthier *et al.*, 2012), phagocytosis (Masters *et al.*, 2013), or extraction of cholesterol from the membrane (Hissa *et al.*, 2013). Exocytosis can also be stimulated in response to external mechanical stimuli (Carosi *et al.*, 1992; Grygorczyk and Hanrahan, 1997), such as when surfactant is secreted from alveolar cells after a single round of

stretching (Wirtz and Dobbs, 1990), or when chicken embryo fibroblasts are rapidly stretched via microcapillary action leading to a release of fluorescently-labeled vesicle contents (Hagmann *et al.*, 1992). In other instances, exocytosis is inhibited by extrinsic forces, for example when mast cell degranulation is prevented by cell inflation (Solsona *et al.*, 1998).

On the other hand, endocytosis involves the internalization of materials via invagination of plasma membrane. In contrast to exocytosis, endocytosis is stimulated by decreased membrane tension, and results in decreased plasma membrane surface area and increased plasma membrane tension (Apodaca, 2002; Gauthier *et al.*, 2012). One well-described example of this is integrin internalization via clathrin-mediated endocytosis, which is blocked when cells are cultured on glass to increase traction forces (Yu *et al.*, 2015). Additionally, endocytic rates decrease as plasma membrane tension increases when cells enter mitosis and endocytic rates increase as membrane tension decreases as cells exit mitosis (Raucher and Sheetz, 1999). Often, exocytosis and endocytosis are balanced, so that there is a no net change in plasma membrane surface area or tension. This is true in neuronal cells where synaptic vesicle fusion is closely followed by compensatory endocytosis to maintain plasma membrane tension and surface area (Boudier *et al.*, 1999), and in rat basophilic leukemia cells where exocytosis is coupled to rapid endocytosis which follows within seconds of secretion (Dai *et al.*, 1997).

Plasma membrane tension, which regulates exocytosis and endocytosis, is determined in large part by the adhesion of the plasma membrane to the actomyosin cytoskeleton. Therefore, not surprisingly, control of cytoskeletal dynamics by Rho GTPases is central to the regulation of tension-dependent membrane trafficking events (Morris and Homann, 2001; Gauthier *et al.*, 2012). Interestingly, the actin cytoskeleton is necessary for overcoming high levels of membrane tension during clathrin-mediated endocytosis (Boulant *et al.*, 2011). However, the clathrin-independent endocytic recycling pathways are most often linked to regulation of plasma membrane area, because the endocytic carriers have a much larger surface area, and these pathways typically require the actin cytoskeleton (Gauthier *et al.*, 2009; Howes *et al.*, 2010).

## 1.5 Effects of Force on the Apical Junctional Ring

Critically, the barrier created by the epithelial AJR must be maintained in the face of both intrinsic and extrinsic mechanical forces experienced during development, morphogenesis, and everyday physiological processes. There is a fair known about how the AJR senses and responds to intrinsic forces generated by the actomyosin cytoskeleton, such as during embryogenesis. However, there is much less known about how the AJR of epithelial cells accommodates extrinsic forces while maintaining the integrity of the tissue. There is a particular scarcity of knowledge about how vertebrate or mammalian epithelial tissues adapt to external forces while maintaining the epithelial permeability barrier, which is what I am addressing with my thesis research.

### 1.5.1 Effects of force on the tight junction.

It is known that the components of the tight junction are highly dynamic even at steady state and undergo structural and functional changes in response to a variety of stimuli (Nusrat *et al.*, 2000; Shen *et al.*, 2008; Yu and Turner, 2008; Weber, 2012); however, the mechanism of tight junction remodeling in response to mechanical stimuli remains poorly understood. There are reports that stretching alters the distribution of tight junction-associated proteins to reinforce the paracellular barrier; however, not surprisingly, excess force applied to epithelia causes a disruption of tight junctions, dissociation of tight junction components from the junctional complex, and ultimately a loss of barrier integrity (Cavanaugh *et al.*, 2001; Cohen *et al.*, 2010; Samak *et al.*, 2014; Song *et al.*, 2016).

This balance is exemplified in the vascular endothelium, which is constantly subject to fluid shear stress as blood pumps through the vessels of the body. In bovine aortic endothelial cells (BAECs) and human brain microvasculature endothelial cells exposed to physiological levels of shear stress over relatively long time periods, from 24 hours up to 5 days, there is an increased

association of tight junction proteins with the junctional complex and decreased epithelial permeability, indicating that the endothelial barrier is strengthened in response to normal shear stress (Collins *et al.*, 2006; Colgan *et al.*, 2007; Siddharthan *et al.*, 2007; Garcia-Polite *et al.*, 2017). However, in BAECs exposed to pathological levels of shear stress increases in endothelial permeability are observed after just 5 minutes and up to 3 hours which correlate with an increase in occludin phosphorylation and a subsequent decrease in occludin expression at the tight junction (DeMaio *et al.*, 2001). These findings demonstrate that endothelial tight junctions are reinforced by long-term exposure to physiological levels of shear stress, but exposure to acute pathological levels of shear stress leads to a downregulation of tight junction proteins and a loss of the epithelial barrier function. Redistribution of tight junction proteins and a compromised barrier are also observed in lung slices and alveolar and intestinal epithelial cell monolayers exposed to excess stretch (Cavanaugh *et al.*, 2001; Cavanaugh and Margulies, 2002; Samak *et al.*, 2010; Wang *et al.*, 2011; Samak *et al.*, 2014; Song *et al.*, 2016).

Stretch, also, affects tight junction strand number and distribution (Pitelka *et al.*, 1973; Hull and Staehelin, 1976; Metz *et al.*, 1977; Koga and Todo, 1978; Metz *et al.*, 1978; Greven and Robenek, 1980; Pitelka and Taggart, 1983; Akao *et al.*, 2000). Stretch-stimulated changes in strand organization is demonstrated by early studies showing that experimental distention of the tadpole large intestine (Hull and Staehelin, 1976), enlargement of the mammary gland (Pitelka *et al.*, 1973; Pitelka and Taggart, 1983), or swelling of the uterine epithelium (Greven and Robenek, 1980) causes a re-organization of tight junction strands. As, noted above, tight junction strands are formed in part by claudins, which act as pore-forming or resistive elements that are hypothesized to act in series when present in a network (Claude, 1978). This organization is proposed to produce a correlation between the number of strands and the tightness of the epithelial barrier (Claude and Goodenough, 1973), although this is not true in the case of MDCK cells (Stevenson *et al.*, 1988). A relationship between the mechanical regulation of strand number and the permeability of an epithelium is suggested by studies showing that ligating the pancreatic

or bile duct (increasing intraluminal pressure in the end organ) leads to fewer tight junction strands, discontinuities and irregularities in the strands, and increased paracellular permeability (Metz *et al.*, 1977; Koga and Todo, 1978; Metz *et al.*, 1978; Akao *et al.*, 2000).

In addition to these mechanically-induced structural and functional changes to the tight junction, there is emerging evidence that tight junctions are intimately involved in mechanotransduction (Balda and Matter, 2008; Tornavaca *et al.*, 2015; Balda and Matter, 2016; Sluysmans *et al.*, 2017). To this point, preventing ZO-1 from binding to the actin cytoskeleton disrupts the tight junction barrier (Yu *et al.*, 2010), indicating that the tight junction needs to be under actomyosin-generated tension for proper barrier function. This conclusion is supported by the recent observation that ZO-1 adopts an extended conformation in response to actomyosin-generated tension (Spadaro *et al.*, 2017). This conformational change allows the ZO-1-binding protein ZONAB to disengage from the tight junction and relocate to the nucleus where it functions as a transcription factor that triggers changes in gene expression, cell proliferation, and paracellular barrier function. The importance of the ZO proteins in mechanically-regulated cell signaling pathways, like those necessary for embryonic development, is further indicated by the requirement of ZO-1/2 for normal embryogenesis (Katsuno *et al.*, 2008; Xu *et al.*, 2008).

### **1.5.2 Effects of force on the adherens junction.**

Much more is understood about the mechanosensitive properties of the adherens junction, which like the tight junction undergoes structural and functional changes in response to mechanical forces (Charras and Yap, 2018; Pinheiro and Bellaiche, 2018; Rubsam *et al.*, 2018). For example, intrinsic forces generated by the contractile actomyosin ring stiffen junctional complexes formed by E-cadherin (le Duc *et al.*, 2010). Additionally, direct application of an external pulling force on endothelial cells increases the area of their adherens junctions (Liu *et al.*, 2010). The mechanism behind this mechanical reinforcement of the adherens junction was

revealed by experiments using magnetic tweezers to directly pull on  $\alpha$ -catenin. This causes  $\alpha$ -catenin to unfold, allowing it to bind more strongly to  $\beta$ -catenin, and recruit vinculin, thereby strengthening the junction (Yao *et al.*, 2014). Furthermore, this conformational change promotes further cell-cell contact remodeling through the recruitment of additional actin-binding proteins (Barry *et al.*, 2014; Leckband and de Rooij, 2014), altering actin and myosin dynamics (Muhamed *et al.*, 2016), and affecting cell events such as polarization (Takeichi, 2018).

Adherens junctions are also remodeled in response to morphogenetic forces, such as during cell division, cell intercalation in fruit flies, and cell extrusion (Pinheiro and Bellaiche, 2018). Additionally, physiological forces alter the organization and function of the adherens junction. One well-studied example of this is in endothelial cells, which appear to “sense” changes in shear forces and respond by remodeling their cytoskeleton, which, in turn, alters the tension forces on the junction proteins leading to a disruption and reassembly of the adherens junctions components, and ultimately to an aligning of the cells in the direction of the flow (Langille and Adamson, 1981; Noria *et al.*, 1999).

In addition to mediating intercellular adhesion, and maintaining epithelial integrity, adherens junction complexes initiate mechanotransduction pathways that regulate physiological processes (Leckband and de Rooij, 2014). For example, in fruit flies, Armadillo, the homologue of  $\beta$ -catenin, transduces mechanical signals from the adherens junction (Farge, 2003), and in mouse models for colon cancer,  $\beta$ -catenin gets phosphorylated after mechanical stimulation and translocates to nucleus leading to alter gene transcription (Whitehead *et al.*, 2008). In addition to the mechanosensitive properties of the catenins, externally applied force has been shown to increase tension across E-cadherin and activate downstream signaling pathways in cultured cells (Borghi *et al.*, 2012). Furthermore, changes in E-cadherin tension have been linked to adherens junction remodeling (Cai *et al.*, 2014).

### 1.5.3 Effects of force on desmosomes.

Even though the adherens junction is a well-established mechanosensitive complex which transduces forces into biological signals, and despite the structural similarities between the adherens junction and the desmosome, there is very little known about the mechanosensitive properties of desmosomes. Not surprisingly, since desmosomes are highly expressed in some tissues subjected to a large amount of mechanical stress, such as in the heart and skin, it has been hypothesized that their primary function is to dissipate mechanical stresses on tissues; however, there has been surprisingly little direct evidence supporting this idea. Until recently it had not been shown that desmosomes are under mechanical tension, at all. However, recent studies using FRET-based tension sensors have shown that desmosomal proteins indeed experience tensile force. Using a tension sensor integrated into the protein, desmoglein-2 was shown to be under mechanical tension, even under resting conditions, in both cardiomyocytes and cultured epithelial cells (Baddam *et al.*, 2018). Another group utilized a desmoplakin-based tension sensor to show that this protein is not under considerable tension under normal conditions but becomes loadbearing after exposure to external mechanical stimuli (Price *et al.*, 2018). Additionally, this increase in tensile loading on desmoplakin is magnitude and direction-dependent, which supports the idea that desmosomes are indeed loadbearing elements, and act to dissipate mechanical forces applied to the cell. This idea is further supported by observations that pathologies in tissues that experience significant mechanical loads, such as observed in the skin or heart, are often characterized by desmosomal anomalies (Hatzfeld *et al.*, 2017). For example, stretching keratinocytes expressing mutant keratins, characteristic of Epidermolysis Bullosa Simplex, leads to a progressive disassembly of desmosomes and loss of cell-cell adhesion (Russell *et al.*, 2004; Homberg *et al.*, 2015).

#### 1.5.4 Effects of force on the perijunctional cytoskeletal ring.

Not only is the AJC mechanosensitive, but the actomyosin cytoskeleton is itself intrinsically sensitive to force (Pinheiro and Bellaiche, 2018). Tension exerted on the AJC is transmitted to the PJAR where there are a variety of mechanosensitive proteins present. The mechanical characteristics of the actin cytoskeleton depend on the degree of crosslinking by NMMII and other proteins, such as  $\alpha$ -actinins (Schwayer *et al.*, 2016). Generally speaking, the higher degree of cross-linking the stiffer the actomyosin network will be. Interestingly, NMMII binding to actin filaments can be regulated by tension. Forces opposed to the power stroke of the myosin head delay its detachment from the actin cytoskeleton, thereby stabilizing the junctional localization of the protein (Greenberg *et al.*, 2016). Accordingly, tension at the junctional complex appears to stabilize NMMII (Pinheiro and Bellaiche, 2018), and extrinsically increasing plasma membrane tension by micropipette aspiration is sufficient to recruit NMMII; whereas, reducing junctional tension using laser ablation decreases NMMII levels proximal to the junctions (Fernandez-Gonzalez *et al.*, 2009).

Similar to NMMII other actin binding proteins such as formins, the Arp2/3 complex, and  $\alpha$ -actinin-4 are known to be mechanosensitive. For example, mDia1 (Jegou *et al.*, 2013) and the yeast formin Bni1 (Courtemanche *et al.*, 2013) undergo mechanically-stimulated conformational changes that allows them to recruit more actin monomers to the barbed end of the growing filament increasing the rate of polymerization. On the other hand, using atomic force microscopy, it was observed that Arp2/3 branched networks are reinforced after exposure to mechanical load (Bieling *et al.*, 2016). Finally,  $\alpha$ -actinin-4 undergoes a conformational change in response to force which increases its actin binding affinity (Shams *et al.*, 2012), which could explain the observation that applied mechanical force leads to accumulation of  $\alpha$ -actinin-4 (Schiffhauer *et al.*, 2016).

Relative to the actin cytoskeleton, there is much less literature looking at how the desmosome-associated keratin cytoskeleton is affected by force; however, it has been shown that stretching cultured keratinocytes leads to altered keratin expression, increased keratin phosphorylation, and ultimately to a reorganization of the keratin network and the associated cell-cell junctions (Yano *et al.*, 2004). Furthermore, in lung epithelial cells shear stress, but not stretch increases keratin phosphorylation leading to a reorganization of the keratin filaments and a change in the elastic properties of the cells (Sivaramakrishnan *et al.*, 2009). These findings indicate that both the intermediate filament cytoskeleton and the PJAR are mechanically regulated.

### **1.5.5 Apical junctional ring contraction.**

In response to the intrinsic mechanical forces such as those generated during cell-cell intercalation, wound closure, cell division, dorsal closure in fruit flies, cell extrusion, and epithelial invagination, the adherens junction (and presumably the entire AJR) undergoes contraction (i.e., reduction in circumference) (Schwayer *et al.*, 2016). The actomyosin cytoskeleton is necessary for orienting and driving these morphogenetic processes, which accordingly occur under tension. That tension fluctuations are a cause and not just an effect of morphogenesis is emphasized by the observations that in the amniosera cells of fruit flies a force imbalance caused by actomyosin contraction triggers dorsal closure (Saias *et al.*, 2015); and during nematode gastrulation apical membrane constriction only occurs when tension is generated across the adherens junctions via the actomyosin cytoskeleton (Roh-Johnson *et al.*, 2012).

This contraction of the AJR is driven by RhoA-dependent activation of the formin-mediated mDia1 pathway of actin polymerization (Homem and Peifer, 2008; Levayer *et al.*, 2011), and the RhoA- and ROCK-dependent activation of the NMMIIA complex (Kolesnikov and Beckendorf, 2007; Borges *et al.*, 2011; Itoh *et al.*, 2014; Sai *et al.*, 2014). In the case of neural tube closure in

mice, or the formation of the lens pit in chick embryos, additional regulators of apical constriction include Trio, a RhoA guanine nucleotide exchange factor (GEF), and Shroom3, which binds actin and recruits ROCK to the region of the AJR (Plageman *et al.*, 2011; Chu *et al.*, 2013; Das *et al.*, 2014).

Considering the close association between the actomyosin cytoskeleton and membrane traffic (Valentijn *et al.*, 1999; Apodaca, 2001a, 2002; Croise *et al.*, 2014; Kjos *et al.*, 2018), it should not be surprising that apical constriction in frogs and fruit flies, also, depends on endocytosis, which is modulated by dynamin, Rab5, Rab35, and other regulators of the actomyosin cytoskeleton (Lee and Harland, 2010; Levayer *et al.*, 2011; Mateus *et al.*, 2011; Jewett *et al.*, 2017). In the case of zebrafish gastrulation Rab5c-dependent endocytosis of E-cadherin is necessary for maintaining cohesion of the epithelial sheet (Ulrich *et al.*, 2005). However, if endocytosis plays a similar role in vertebrate AJR constriction is not known; although, the rate of internalization of adherens junction proteins is increased during physiological processes that involve contraction of the AJR in cultured mammalian cells, such as during cell division (Bauer *et al.*, 1998).

### **1.5.6 Apical junctional ring expansion.**

In contrast to AJR contraction, there is a very limited literature concerning the expansion of the AJR, or the mechanisms that regulate these events. Following cell intercalation, a new cell-cell contact is added perpendicular to the site of junction constriction (Mateus *et al.*, 2011). This addition requires pulling forces generated by myosin flows in adjacent border cells (Yu and Fernandez-Gonzalez, 2016), and likely depends on the insertion of new membrane by exocytosis in the intercalated cells (Shaye *et al.*, 2008); however, this has not been shown conclusively. In the development of the fruit fly pupal wing, junctional expansion requires the downregulation of NMMII activity, which is modulated by PTEN (Bardet *et al.*, 2013). Finally, in flies, Rab11-

dependent exocytosis promotes cell elongation, a process where the AJR increases in length along a single axis (Mateus *et al.*, 2011). At present, there are few insights into AJR expansion in vertebrate systems; although, as mentioned above, there is evidence that endothelial cells can increase the area of their adherens junction in response to externally applied stretch (Liu *et al.*, 2010).

## 1.6 Goals of this Dissertation

Epithelial tissues must accommodate intrinsic and extrinsic mechanical forces that occur during morphogenetic processes or that are experienced in the normal environment of the body while maintaining the integrity of the epithelial barrier. There is a fair amount known about how the AJR, especially the adherens junction, senses and responds to intrinsic forces, especially during developmental processes; however, there is still relatively little known about how this is accomplished in intact vertebrate or mammalian systems. Much less is known about how the AJR of epithelial cells maintain their integrity in the face of extrinsic forces generated under normal physiological conditions. In particular, there is very little known about how mammalian epithelial tissues adapt to these forces; however, their ability to sense and respond to external forces appears to be in part mediated through mechanically induced changes at the AJR.

In response to intrinsic forces generated by the actomyosin cytoskeleton during morphogenesis the adherens junction ring undergoes contraction; however, whether the entire AJR contracts in a coordinated fashion during these events has not been examined. Since the actomyosin cytoskeleton is involved in integrating membrane trafficking events, it is not surprising that apical contraction often depends on endocytosis. However, if endocytosis plays a similar role in mammalian AJR constriction is not known. Relative to AJR contraction, there is little known

about the mechanism of expansion of the AJR, especially in vertebrate systems; however, studies in non-mammalian systems suggest that it requires the addition of new membrane via exocytosis.

Despite many new discoveries over the past decade in the area of junctional biology, there is still relatively little understood about the mechanism behind structural and functional changes caused by external forces on the AJR, particularly in the context of mammalian systems. While many previous studies have focused on the effects of internal forces generated by the actomyosin cytoskeleton on mature, stable junctions, or on the remodeling of junctions during development or morphogenesis, there is limited understanding of how the AJR responds to the external forces that occur during normal physiological events.

To gain a better understanding of how extrinsic mechanical forces impact the AJR, we our lab uses rat bladder umbrella cells as a model. Umbrella cells form the luminal layer of the stratified urothelium and maintain a high-resistance barrier in the face of continuous cycles of bladder filling and voiding. This is made possible by several specializations. First, the umbrella cell transitions from an inverted parasol shape to one that is flat and squamous during filling, a change that is reversed upon voiding. Second, bladder filling stimulates a large subapical pool of vesicles to undergo Rab8a-, Rab11a-, and Rab27b-dependent exocytosis, dramatically increasing apical surface area. Upon voiding, the excess apical membrane is rapidly internalized by an integrin-triggered, dynamin-2-, RhoA-dependent, clathrin-independent endocytic pathway. Third, and most relevant to the current work, is our previous report that the umbrella cell tight junction and associated actin ring expand by ~150% during filling and return to their quiescent size after just five minutes of voiding. We hypothesized that the dynamic nature of the umbrella cell AJR likely serves as a mechanism to maintain umbrella cell barrier function in the face of large changes in bladder wall tension.

In the current study, we asked whether the adherens junction was similarly affected during the bladder cycle, if the organization and dynamics of the actomyosin cytoskeleton was affected by filling and voiding, and whether the mechanisms that regulate AJR contraction in other systems

are at work in the bladder, in particular the involvement of membrane trafficking events. Finally, we want to uncover the mechanisms behind AJR expansion, and see if membrane trafficking events contribute to this phenomenon as well as AJR contraction.

## 2.0 Effects of Filling and Voiding on the Umbrella Cell Apical Junctional Ring

### 2.1 Introduction

The AJR must maintain its integrity in the face of mechanical forces experienced under physiological conditions, but it is not well-understood how this is accomplished. Our lab uses the intact rat urinary bladder as a model for addressing this question. The bladder is an ideal model for examining how mammalian epithelial tissues respond to physiological forces without compromising the permeability barrier, because it is uniquely able to accommodate dramatic changes in luminal volume during repeated cycles of filling and voiding (**Figure 7**), while maintaining one of the least permeable epithelial barriers in the entire body.

When relaxed the entire urothelium and underlying lamina propria form large folds or “rugae”, similar to what is seen in the stomach. At the tissue level, the unfolding of these rugae allows the bladder to rapidly accommodate the increases in luminal volume during the initial stages of filling. Subsequently, the bladder umbrella cells, which line the luminal surface, accommodate changes in luminal volume by cycling between a roughly cuboidal cell shape in voided bladders to a much larger, flatter, and thinner cell during filling. This cell shape change is mediated by filling-stimulated exocytosis, which dramatically increases apical surface area. Subsequently, during voiding, the added apical membrane is rapidly internalized by endocytosis. Presumably, to accommodate changes in the apical surface area during filling and voiding, the umbrella cell AJR circumscribing each cell must, also, expand and contract with filling and voiding. Otherwise, the newly delivered apical membrane would likely expand into the lumen of the bladder, ultimately decreasing luminal capacity. Therefore, one would predict that a

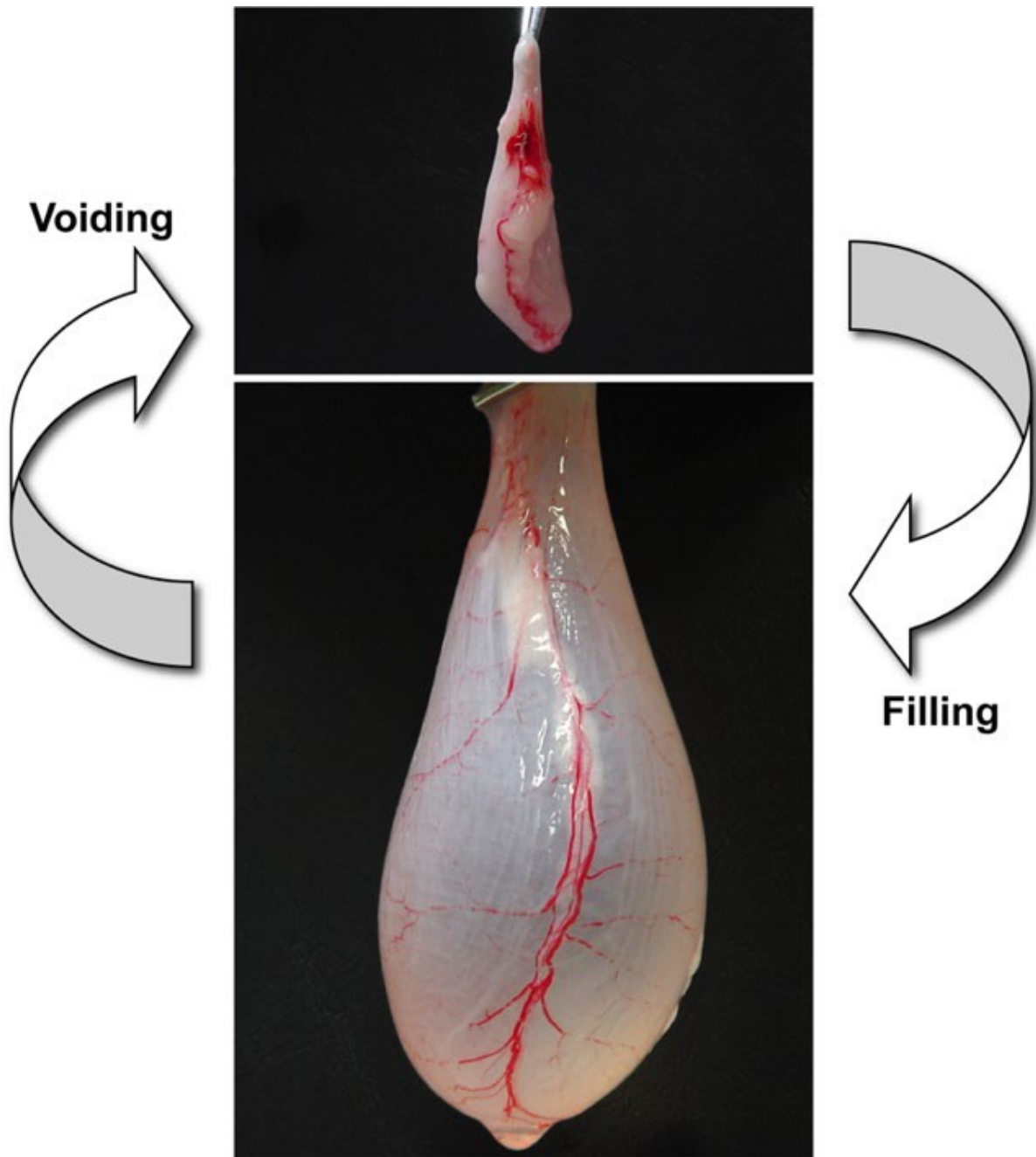


**Figure 7. Effects of filling and voiding on intact rat bladder.**

mechanism exists that coordinates the increase in apical surface area with the expansion of the AJR. Indeed, our previous observation that the umbrella cell tight junction and associated actin ring expand by ~150% during filling and returns to their quiescent size after just five minutes of voiding supports this idea (Carattino *et al.*, 2013). However, whether the entire AJR expands or

contracts as a unit with filling and voiding, and the mechanisms behind these changes remain unknown.

### **2.1.1 Hypothesis**

We hypothesize that external forces generated by bladder filling increases tension in the umbrella cell membrane, which promotes an active expansion and subsequently voiding decreases wall tension promoting contraction of the entire umbrella cell AJR. Furthermore, morphogenesis of the AJR in a variety of model systems requires trafficking of junctional proteins, leading us to predict that the remodeling of the umbrella cell AJR during the bladder cycle requires mechanically stimulated membrane trafficking of junctional proteins, as well.

### **2.1.2 Structure and function of the urothelium.**

The urothelium is a specialized, stratified epithelium found lining the renal pelvis, the ureters, the upper third of the urethra, and the luminal surface of the bladder. One of primary functions of the urothelium is the formation of a highly impermeably barrier between the extracellular toxic solutes and metabolites found in the urine, and the underlying bodily tissues. The urothelium is composed of an outer, or urine-contacting, layer of umbrella cells, a few layers of underlying intermediate cells, and a single layer of basal cells, which contact the underlying basement membrane (**Figure 8**). When relaxed the entire urothelium forms large rugae. Initially, the unfolding of these rugae acts as a rapid buffering system, allowing the bladder to accommodate changes in urine volume during the first stages of filling. However, the unfolding of the bladder folds, or rugae, only partially accounts for the bladders ability to accommodate large changes in urine volume during the bladder cycle without compromising its barrier function.

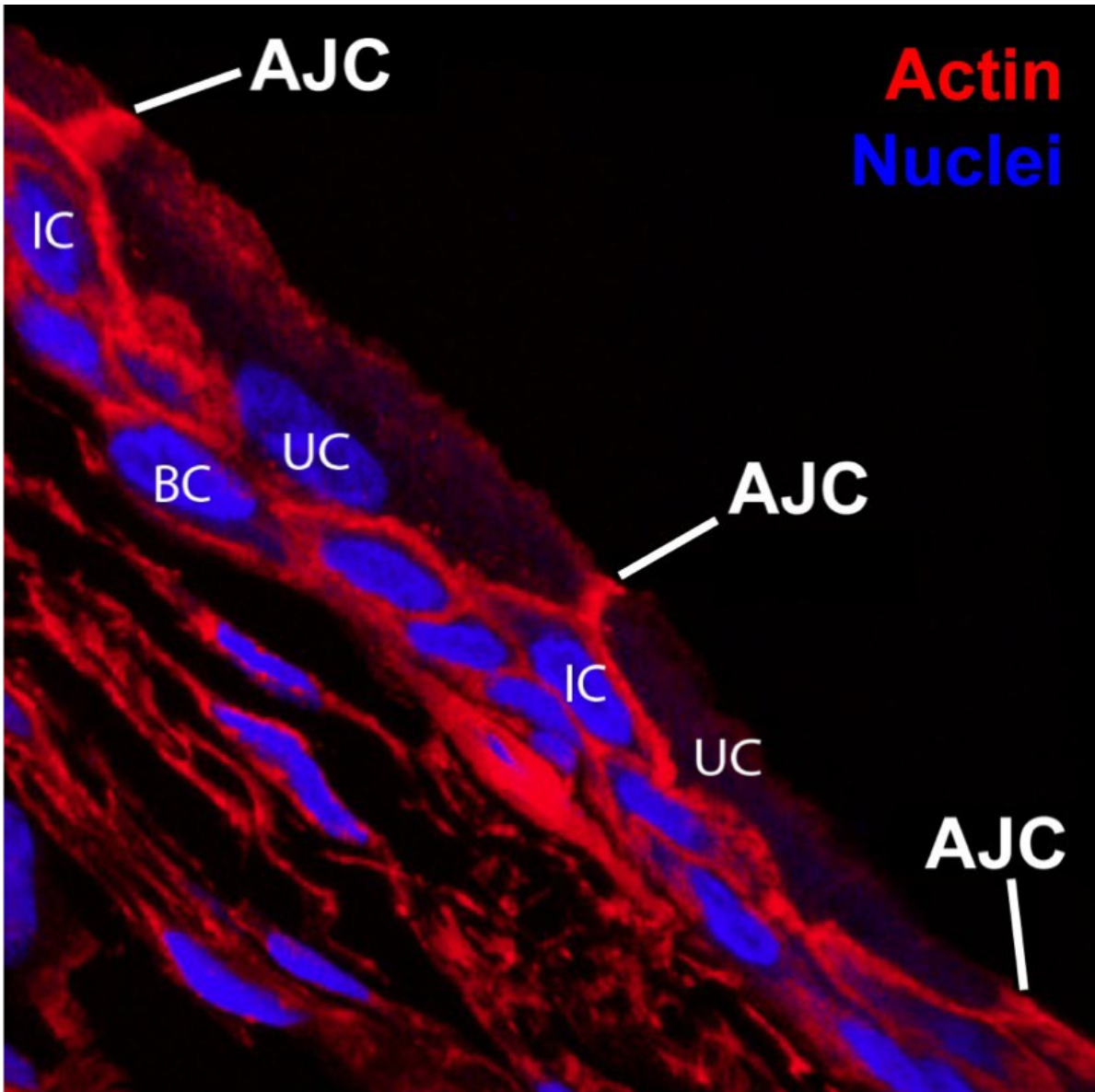


**Figure 8. Structure of the urothelium.**

Cross-section of quiescent rat bladder. F-actin is labeled with rhodamine-phalloidin (red) and nuclei with To-Pro-3 (blue).

### 2.1.3 Effects of filling and voiding on the structure and function of the umbrella cell layer.

The urothelial permeability barrier is primarily formed by the umbrella cells and depends on a specialized apical membrane that is almost entirely covered with rigid uroplakin-positive

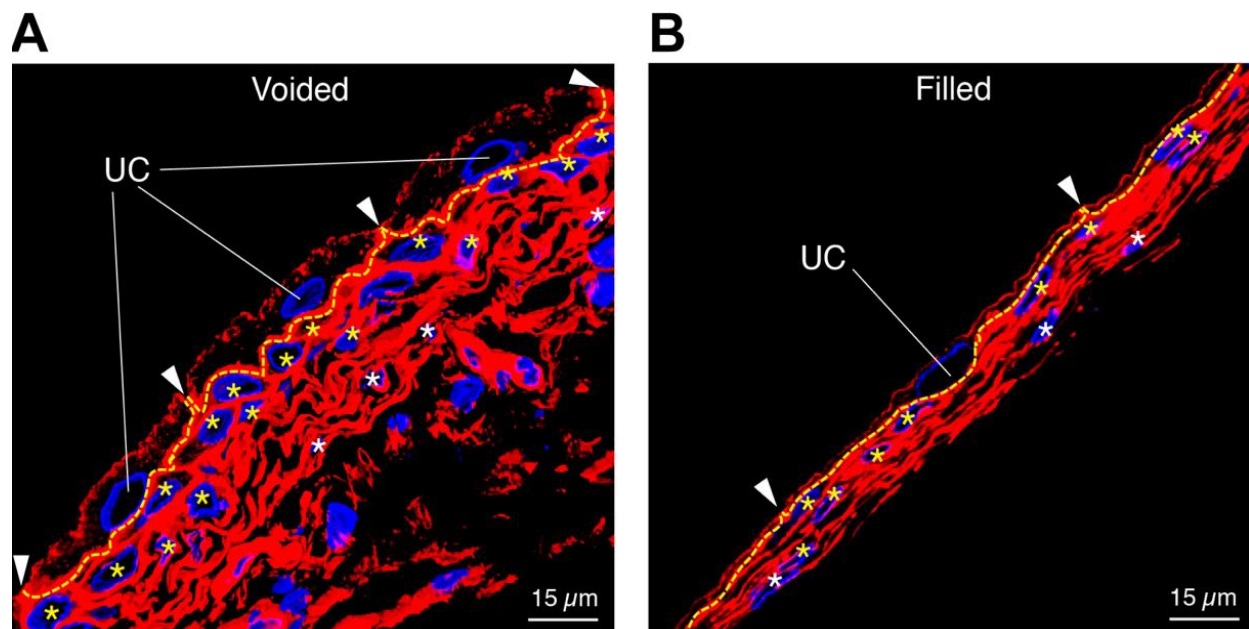


**Figure 9. Filling and voiding alter umbrella cell structure.**

Cross-sections of (A) voided and (B) filled rat bladders. F-actin is labeled with rhodamine-phalloidin (red) and nuclei are labeled with To-Pro-3 (blue). Umbrella cell borders are delineated with a dashed line (yellow), intermediate cells are indicated with yellow asterisks, basal cells are indicated with white asterisks, and the AJC is indicated with arrowheads. Used with the permission from Moulton *et al.*, 2016.

structures called plaques connected by more flexible regions termed hinges, and intact high-resistance junctional complexes between individual umbrella cells. Not surprisingly, the umbrella cells have molecular mechanisms in place to maintain their highly impermeable barrier in the face of mechanical forces experienced during the bladder cycle. These include the umbrella cell's ability to undergo a dramatic cell-shape change from a roughly cuboidal, or inverted paraboloid shape in voided or quiescent bladders (**Figure 9A**) to a much larger and flatter cell in filled

bladders (**Figure 9B**) (Truschel *et al.*, 2002; Moulton *et al.*, 2016). Our lab and others have shown that this cell shape change is mediated in part by a large amount of exocytosis of a subapical pool of discoidal and/or fusiform vesicles (DFV) during filling; subsequently, voiding stimulates endocytosis of the added umbrella cell plasma membrane (Hicks, 1975; Minsky and Chlapowski, 1978; Lewis and de Moura, 1982; Apodaca, 2001b; Balestreire and Apodaca, 2007; Khandelwal *et al.*, 2008; Khandelwal *et al.*, 2010; Khandelwal *et al.*, 2013; Gallo *et al.*, 2018).

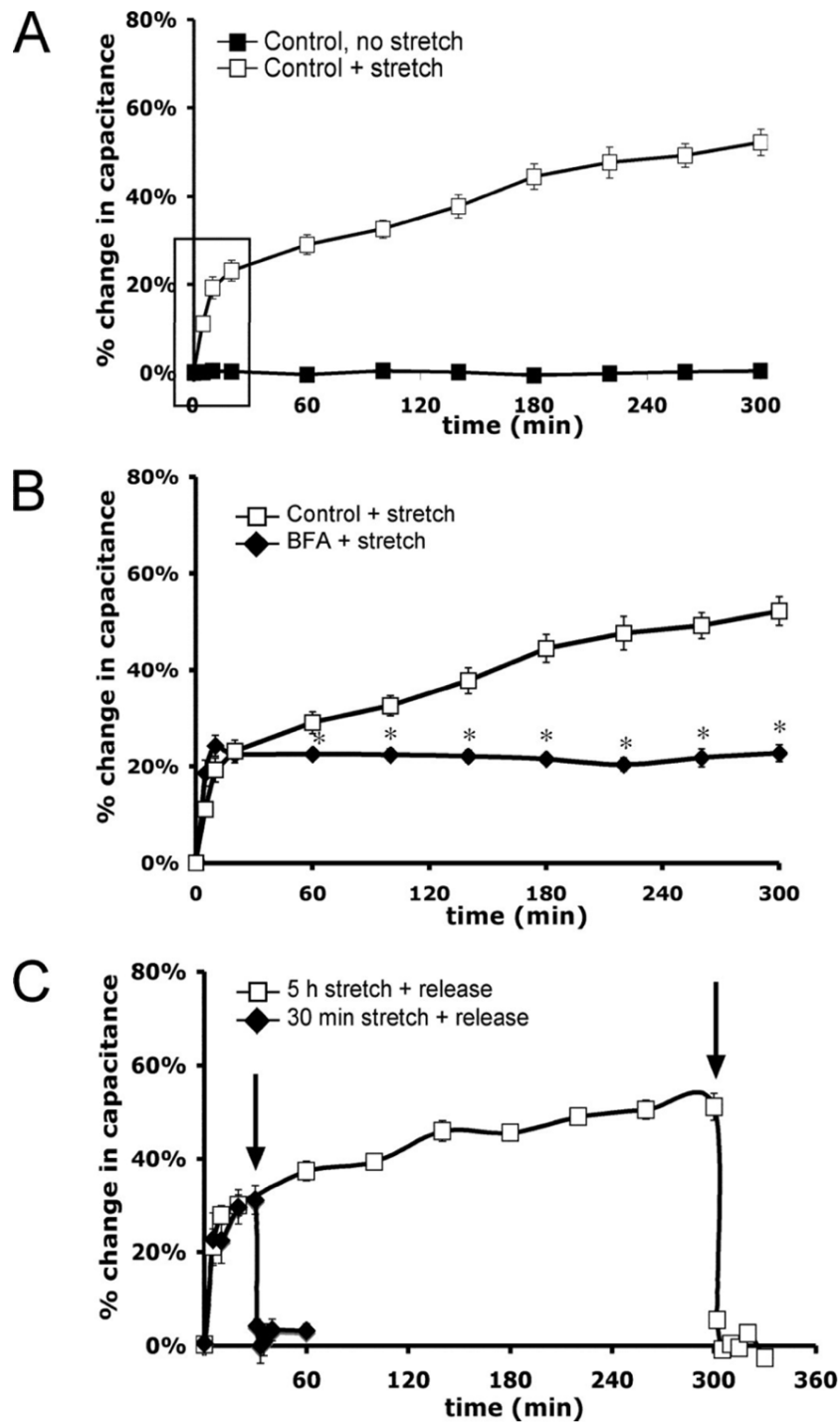


**Figure 10. Characterization of the response to urothelial stretch.**

(A) Isolated rabbit uroepithelium was left unstretched or exposed to  $\sim 1$  cm H<sub>2</sub>O pressure (+ stretch) in an Ussing stretch chamber, and changes in membrane capacitance were measured. The box indicates the early phase increase in surface area upon stretch. (B) Tissue was pretreated with 5  $\mu$ g/ml BFA for 10 min before stretching the tissue in the continued presence of BFA. \*, Statistically significant difference ( $p < 0.05$ ) relative to stretched samples. (C) Tissue was stretched for 30 min or 5 h and then the added Krebs' buffer was removed (indicated by arrows), releasing the stretch stimulus. Mean changes in capacitance  $\pm$  SEM ( $n \geq 3$ ) are shown. Figure used with permission from Balestreire and Apodaca, 2007.

Our lab has shown that when bladder filling is mimicked by stretching isolated urothelium in specialized Ussing chambers (**Appendix, Figure S1**) (Truschel *et al.*, 2002) the apical umbrella cell membrane area, estimated by measuring membrane capacitance, doubles in area with a corresponding decrease in cytoplasmic vesicle membrane area; whereas, if the bladder is left unstretched, or quiescent, there are no changes in the surface area of the apical membrane (**Figure 10A**). (Truschel *et al.*, 2002; Balestreire and Apodaca, 2007; Khandelwal *et al.*, 2008; Yu *et al.*, 2009b; Khandelwal *et al.*, 2013). The quiescent nature of unstretched umbrella cells is also reflected in the observation by Kreft *et al.* that there is very little endocytic traffic that occurs in highly differentiated umbrella cells under resting conditions (Kreft *et al.*, 2009). We confirmed that exocytosis was mediating the increase in apical surface area during filling using surface biotinylation assays and by measuring the release of secretory proteins (Truschel *et al.*, 2002; Khandelwal *et al.*, 2008; Khandelwal *et al.*, 2013). The increases in capacitance in response to stretch are partially inhibited by brefeldin A (BfA), a general inhibitor of the secretory route (Nebenfuhr *et al.*, 2002) (**Figure 10B**), and cyclohexamide (CHX), an inhibitor of new protein synthesis (Schneider-Poetsch *et al.*, 2010)(Balestreire and Apodaca, 2007). This suggests to us that the capacitance increase is due in part to the exocytosis of newly synthesized DFV along the biosynthetic route.

Ussing chamber experiments performed on rat bladders expressing dominant active (DA) or dominant negative (DN) mutants show that Rab11a acts upstream of Rab8a to promote stretch-stimulated exocytosis in rat bladder umbrella cells (Khandelwal *et al.*, 2008; Khandelwal *et al.*, 2013). Additionally, the actin-based motor protein myosin VB (Myo5B) is necessary for this exocytosis (Khandelwal *et al.*, 2013). In addition to this Rab11a/Rab8a cascade, our lab observes a distinct, but parallel pathway, of stretch-stimulated DFV exocytosis which requires Rab27b (Gallo *et al.*, 2018). Our lab's results indicate that there are multiple stretch-activated, Rab-dependent exocytic pathways that exist in umbrella cells. These findings conflict with reports from T.T. Sun's group that Rab8a, Rab11a, and Rab27b act along a singular exocytic pathway to the

apical umbrella cell membrane during bladder filling in mice (Wankel *et al.*, 2016). This conclusion is based upon the observations that Rab27b localizes to DFV (Chen *et al.*, 2003), colocalizes somewhat with Rab8a and Rab11a, and fewer DFV are observed in Rab27b knockout mice; however functional measurements of exocytosis were not performed. Another possibility is that the differences in these results could be attributed to species differences between rats and mice. Furthermore, the Sun group reports that apical fusion of DFV during filling requires the Rab27b effector, Slp2-a, the SNARE protein, VAMP8, and the hinge-associated myelin-and-lymphocyte (MAL) protein. Again, these conclusions were based solely on morphological data, and functional experiments looking at exocytosis were not performed. Perhaps not surprisingly, the filling stimulated exocytosis in bladder umbrella cells is dependent on an intact actin and keratin cytoskeleton, and pharmacologically disrupting either of these networks inhibits vesicle trafficking to and from the apical membrane (Lewis and de Moura, 1984; Sarikas and Chlapowski, 1989; Truschel *et al.*, 2002; Yu *et al.*, 2009b).

On the other hand, we show that simulating voiding by rapidly removing buffer added to the mucosal hemichamber triggers a rapid return of capacitance to baseline, unstretched levels (**Figure 10C**) (Balestreire and Apodaca, 2007; Khandelwal *et al.*, 2010), indicating that apical membrane is internalized via endocytosis upon voiding. This conclusion is further supported by the observation that an apically applied, fluorescently tagged endocytic tracer, FITC-conjugated wheat germ agglutinin (WGA), was internalized into cytoplasmic vesicles within 10 minutes of releasing the stretch stimulus in Ussing chambers. Of note, dynamin-2, the large GTPase mediating vesicle fission, is highly expressed at the apical pole of umbrella cells, and is shown to localize to the membrane of DFV using immunoelectron microscopy (Terada *et al.*, 2009). A role for dynamin-2 in endocytic internalization in umbrella cells is demonstrated by the observations that the levels of *E.coli*, which is found in DFV after being internalized by umbrella cells via endocytosis (Mulvey *et al.*, 2000), was reduced in DFV after treatment with the dynamin inhibitor dynasore (Terada *et al.*, 2009), and in intact rat bladders, WGA internalization is impaired by

expression of DN-dynamin-2 (Khandelwal *et al.*, 2010). Additionally, voiding-induced endocytosis requires the actin cytoskeleton, active RhoA, and integrins but is clathrin, caveolin, and flotillin independent (Khandelwal *et al.*, 2010).

Intriguingly, numerous labs have reported the presence of multiple populations of intracellular vesicles in umbrella cells, which suggests the presence of distinct trafficking

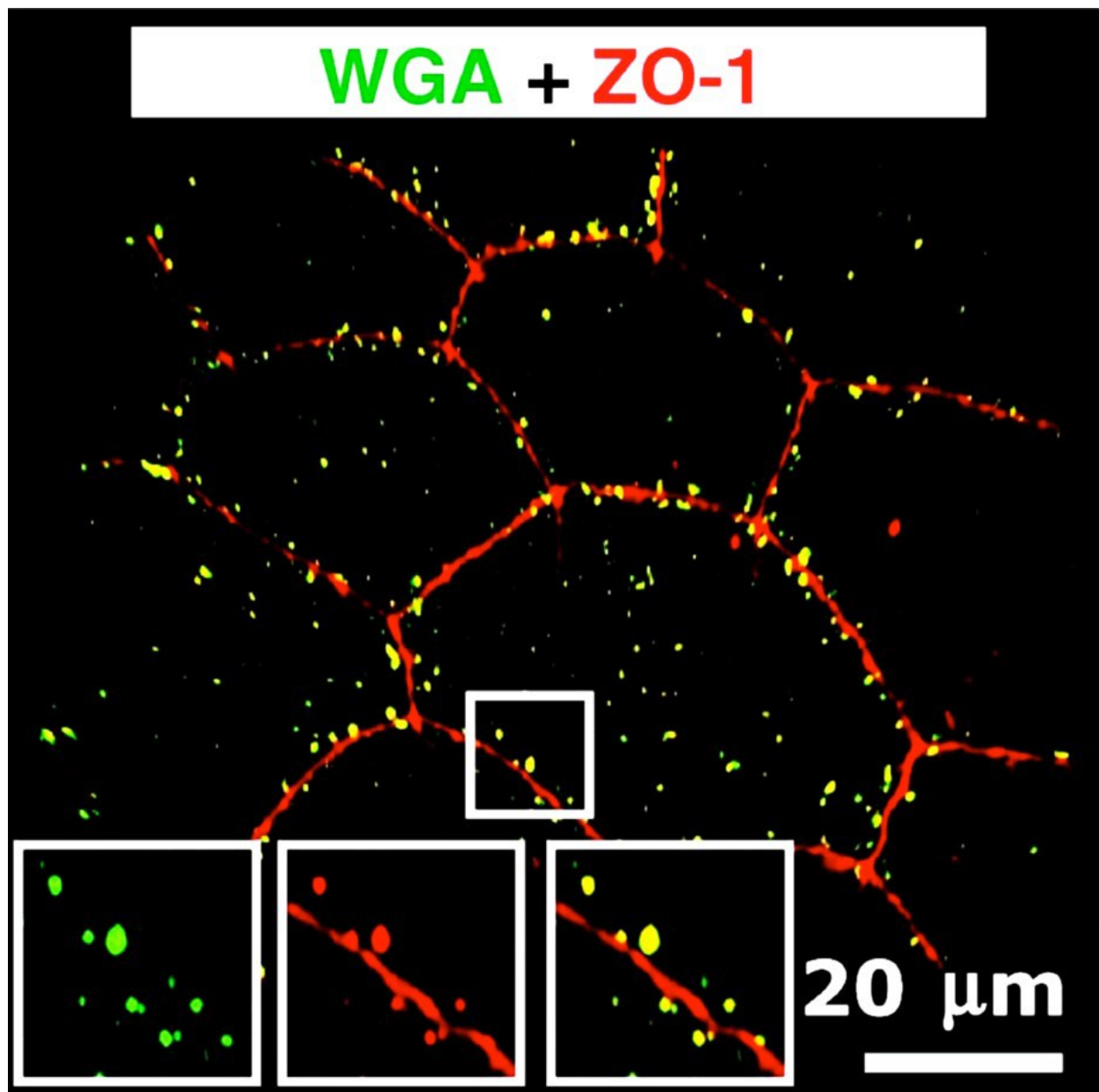


**Figure 11. ZO-1 is internalized upon voiding.** Co-localization of ZO-1 with FITC-WGA 10 m after experimental voiding. Used with permission from Khandelwal *et al.*, 2010.

pathways regulating the area and content of the umbrella cell plasma membrane (Kreft *et al.*, 2009; Khandelwal *et al.*, 2010; Grasso and Calderon, 2013). Of note, our lab observes that the majority of voiding-induced endocytosis occurs proximal to the umbrella cell AJR, therefore we call this population of vesicles: peripheral junction-associated endosomes (PJAEs). These vesicles are distinct from the population of early endosome antigen-1 (EEA-1)-positive vesicles, as well as from the pool of DFVs underlying the majority of the apical plasma membrane of the umbrella cell. Additionally, ZO-1 showed a high degree of colocalization with WGA in PJAEs after voiding (~70%) (Khandelwal *et al.*, 2010) (**Figure 11**), indicating that junctional proteins are internalized from the AJR into distinct endosomal compartments during voiding.

#### **2.1.4 Structure and function of the umbrella cell apical junctional ring.**

In addition to the barrier created by the specialized umbrella cell apical plasma membrane, an intact umbrella cell AJR is also critical to maintaining the urothelial barrier during the bladder cycle. Despite this, we have limited information about the composition of the umbrella cell AJR, or the structural and functional changes that allow it to accommodate cycles of filling and voiding without compromising the epithelial barrier.

When viewed *en face* the regions of cell-cell contact forming the AJR around the outermost layer of umbrella cells are easily visualized when the tissue is stained with rhodamine-phalloidin to label the f-actin cytoskeleton, which we have previously shown labels the PJAR (Acharya *et al.*, 2004) (**Figure 12A**). The tight junction protein, ZO-1, and the adherens junction protein, E-cadherin, both localize to the edges of the umbrella cells, and colocalize with f-actin at the umbrella cell AJR. E-cadherin is not only concentrated at the umbrella cell AJR but is also found in intracellular compartments (**Figure 12A**, top right panel). When the tissue is viewed in cross-section, it is readily apparent that the f-actin cytoskeleton labels the borders of the umbrella cells stopping just below the apical-most tight junction, which is identified by punctate ZO-1 staining

(Figure 12B). ZO-1 is also seen just below the basal cell layer of the urothelium, which we have previously reported is due to ZO-1 localization within the endothelial cells lining the capillaries underlying the urothelium (Acharya *et al.*, 2004) (Figure 12B). Also present at the umbrella cell tight junction are a variety of claudins, including claudin-10 (Figure 12B), although the expression of certain claudins is not restricted to the tight junction, as described below. Furthermore, viewed in cross-section it becomes readily apparent that the adherens junction, stained with E-cadherin, localizes basal to the f-actin positive tight junction (expanded and indicated with arrowhead in inset of lower right panel in Figure 12B). E-cadherin and is also found localized along the basolateral membranes of the umbrella cells, as is reported in other epithelial cells (Figure 12B).

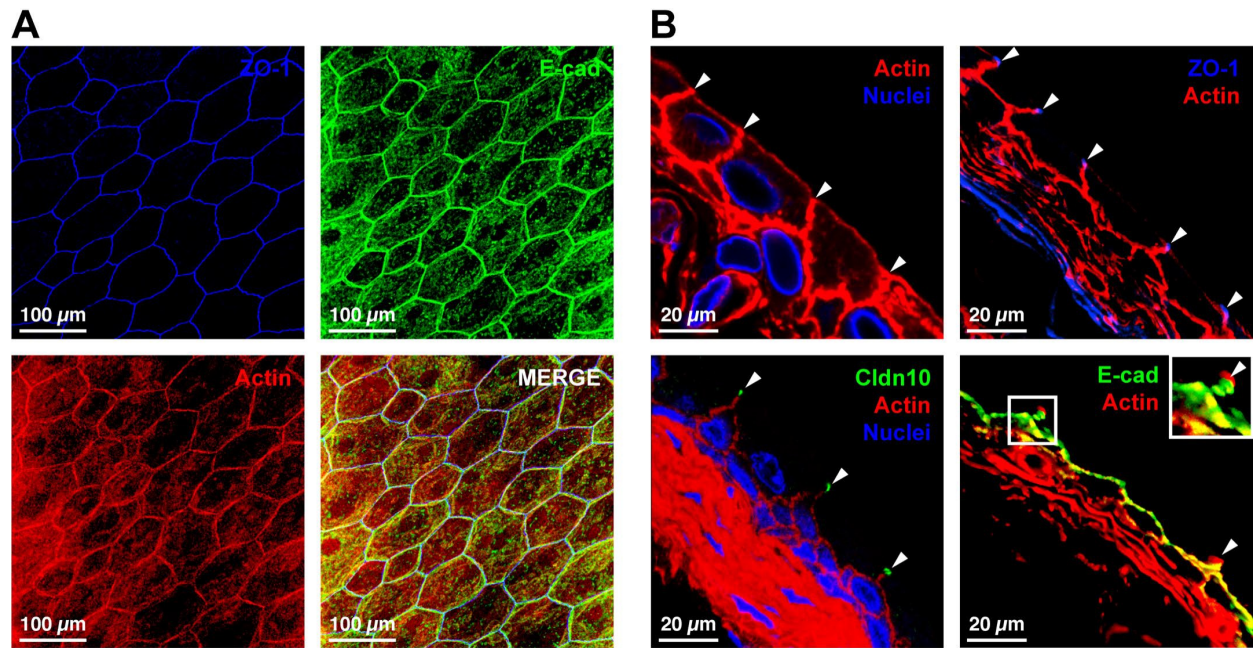


**Figure 12. Structure and composition of the umbrella cell AJR.**

(A) *En face* view of the umbrella cell layer in whole-mount preparations of quiescent rat bladders labeled with antibodies against ZO-1 (blue) and E-cadherin (green). F-actin is labeled with rhodamine-phalloidin (red). Images are 3D reconstructions of confocal Z-stacks. Scale bars = 100 µm. (B) Cross-sections of quiescent rat bladders with the apical-most tight junction indicated with arrowheads. The sections were labeled with antibodies against ZO-1 (blue), claudin-10 (green), and E-cadherin (green). F-actin is labeled with rhodamine-phalloidin (red) and nuclei with To-Pro-3 (blue). Images are 3D reconstructions of confocal Z-stacks. Scale bars = 20 µm.

### 2.1.5 Claudin expression within the rat urothelium.

Our lab, and others, have reported that numerous claudins are expressed in the urothelium, including claudins -1, -2, -3, -4, -5, -6, -7, -8, -11, -12, -13, -14, -15, -16, -20, -22 (Acharya *et al.*, 2004; Varley *et al.*, 2006; Southgate *et al.*, 2007; Nakanishi *et al.*, 2008; Rickard *et al.*, 2008; Keay *et al.*, 2011; Martin *et al.*, 2011; Moad *et al.*, 2013; Keay *et al.*, 2014). However, some of these were only detected *in vitro*, often in transformed cell lines, or only the mRNA was detectable. As of now, our lab has positively identified the expression of claudins -2, -3, -4, -6, -7, -8, -10 and -11 in the native rat urothelium using indirect immunofluorescence of fixed rat bladder and western blotting of urothelial rat bladder lysates (**Figures 13, A and B**). The specificity of the antibodies was confirmed by transfecting HEK cells, which do not express endogenous claudins, with cDNAs encoding individual claudin proteins, running the lysates on an SDS-PAGE gel, and probing the blot with a single claudin antibody. Antibodies were considered specific if the antibody only recognized the claudin encoded by the transfected DNA (**Figure 13C; Appendix, Figure S2**).

Of the claudins found within the rat urothelium, claudin-2 is a cationic pore-former (Yu *et al.*, 2009a), claudin-4 is an anionic pore-former (Hou *et al.*, 2010), and claudin-10 can form either a cationic, or anionic pore depending on the isoform expressed (Milatz and Breiderhoff, 2017). Whereas in rat claudins -2, -6, -8, and -10 were expressed exclusively at the apical-most tight junction of the umbrella cells, claudins -4, -7, and -11 not only localize to the apical-most umbrella cell tight junction, but also to the lateral and basal membranes of the umbrella cells and of the underlying urothelial cell layers, as well (**Figure 13A**). Intriguingly, claudin-3 appears to be

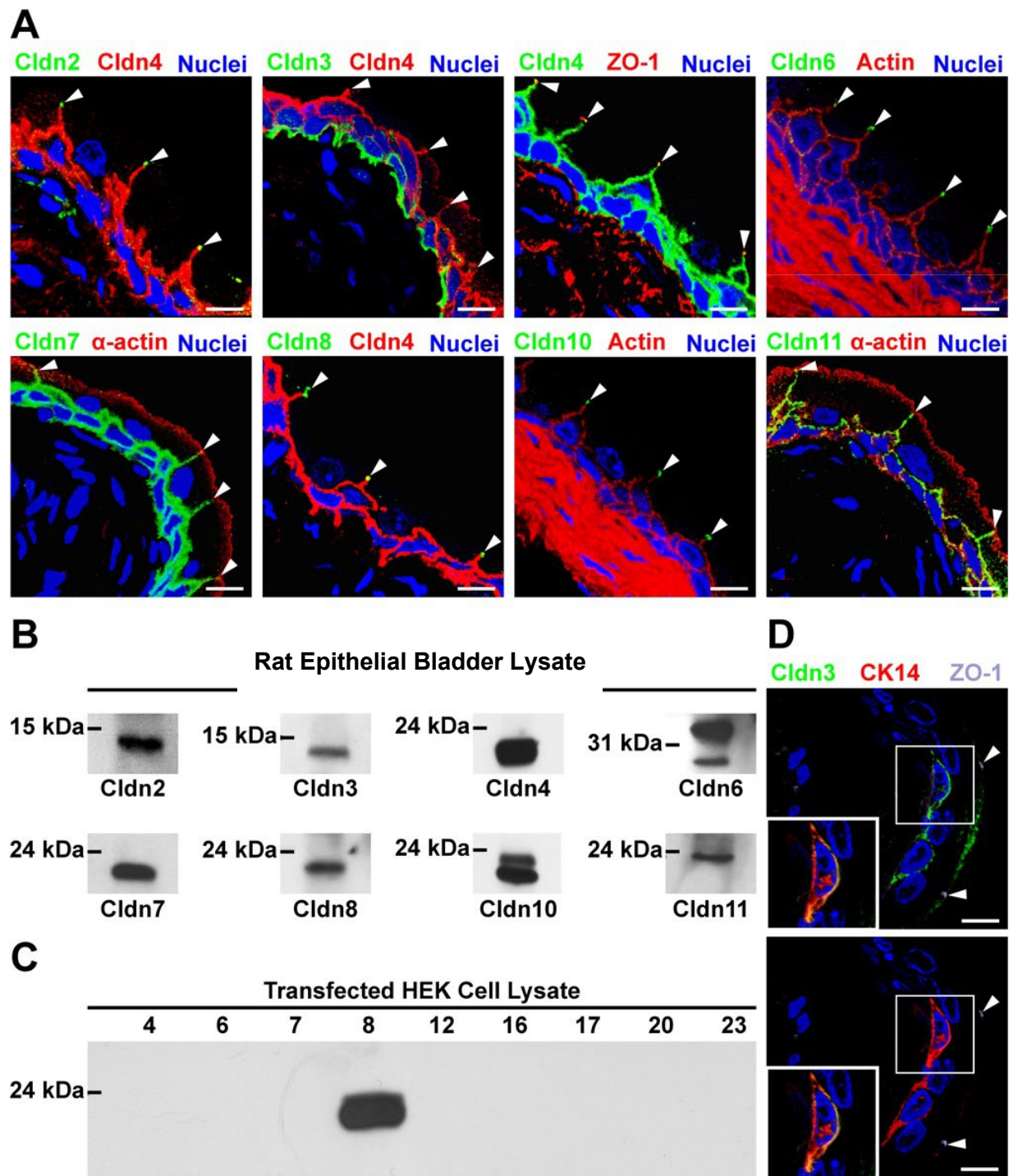


**Figure 13. Claudin expression in the urothelium.**

In the rat bladder we were able to confirm the expression of claudins -2, -3, -4, -6, -7, -8, -10, -11 using (A) immunofluorescence and (B) western blotting. (C) Antibody specificity was confirmed via western blot. (D) Claudin-3 expression in basal cells is confirmed by colocalization with CK14.

expressed solely in the basal cell layer (**Figure 13A**). We confirmed this by co-localizing claudin-3 and cytokeratin-14 (CK14), which is found exclusively in the basal cells of the rat urothelium (Papafotiou *et al.*, 2016) (**Figure 13D**). Of note, this differs from the reported localization of claudin-3 in the urothelium of the human ureter (Smith *et al.*, 2015), suggesting that there may be species differences in the localization and function of different claudins within the urothelium, or differences in the localization of certain claudins throughout the urinary tract.

Since umbrella cells have incredibly impermeable tight junctions, the urothelium is an ideal model to observe changes in paracellular permeability. However, there has been little investigation into the contribution of urothelial claudins to maintaining this “tight” epithelium, or how urothelial tight junctions maintain their permeability barrier in the face of mechanical deformation during cycles of bladder filling and voiding.

### **2.1.6 Effects of filling and voiding on the structure and function of the umbrella cell apical junctional ring.**

In addition to identifying the membrane trafficking-mediated structural changes to the umbrella cells that occur during the bladder cycle, our modified Ussing chambers allow us to mimic filling and voiding while simultaneously measuring electrophysiological responses of the urothelium. When performing these experiments, we input a known current pulse ( $I$ ), read out changes in voltage ( $V$ ) and then calculate resistance across the urothelium ( $R$ ) using Ohm’s Law ( $I = V/R$ ). Ohm’s Law tells us that resistance is inversely proportional to conductance, which is a measure of ionic permeability. Therefore, a decrease in resistance indicates an increase in conductance, or in other words, the epithelium is more permeable to ions, and vice-versa. When we simulate bladder filling, we observe a striking decrease in transepithelial resistance (TER)

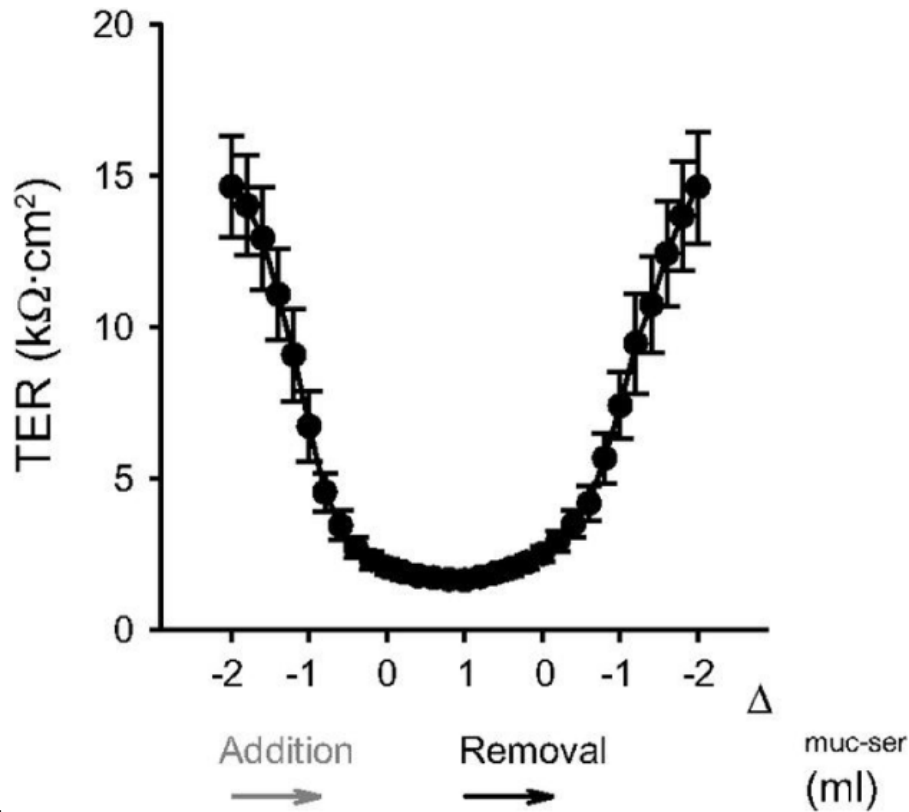


**Figure 14. Stretch augments urothelial ion transport.**

The rabbit bladder mucosa was mounted in Ussing chambers and equilibrated with a small, negative mucosal hydrostatic pressure, causing the tissue to bow inward. Urothelial TER was plotted as a function of the volume in the mucosal compartment. Values are mean  $\pm$  SE (n = 13 independent experiments). Used with permission from **Carattino *et al.*, 2013**.

which is completely reversible by removing the same amount of buffer from the mucosal hemichamber, thereby mimicking bladder voiding (**Figure 14**) (Carattino *et al.*, 2013). Surprisingly, these findings indicate that the urothelium is becoming selectively, and reversibly, more permeable to ions when it is stretched; however, the mechanism behind these changes remains unclear.

Previous studies from our group demonstrate that the perimeter of the tight junction and the PJAR circumscribing each umbrella cell doubles in size when the bladder is filled and these events are rapidly reversed upon voiding (Carattino *et al.*, 2013). As mentioned above, we also observe a decrease in TER with bladder filling, which recovers upon voiding (**Figure 14**). However, TER is a measure of both transcellular and paracellular ion movement across an

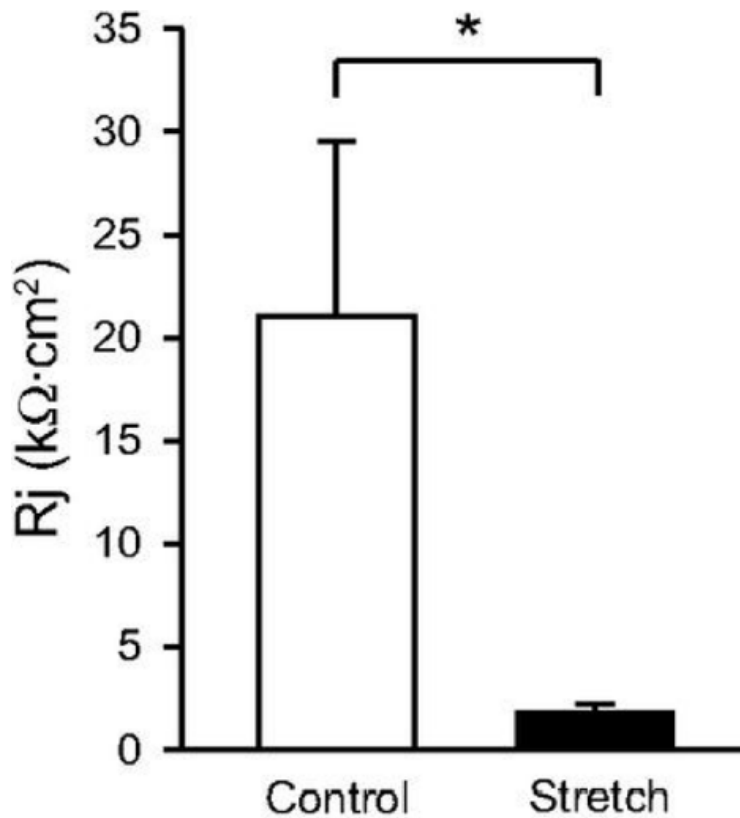


**Figure 15. Stretch increases the junctional permeability of the urothelium.**

Isolated rabbit uroepithelium was mounted in Ussing chambers and the junctional resistance ( $R_j$ ) was estimated.  $R_j$  of unstretched (control) and stretched uroepithelium. Values are mean  $\pm$  SE ( $n = 6-7$  independent experiments;  $P < 0.001$ , using a Mann-Whitney test). Used with permission from **Carattino et al., 2013**.

epithelium. To specifically assess changes in umbrella cell junctional resistance ( $R_j$ ), which is a measure of the permeability of the paracellular pathway alone, we used a method previously described by Lewis and Wills (Lewis and Wills, 1982), which indicates that the umbrella cell  $R_j$  significantly decreases during stretch (**Figure 15**) (Carattino *et al.*, 2013). Additionally, accumulations of intracellular claudin-8 puncta are observed in voided or quiescent bladders but are not seen in filled bladders (**Figure 16**). Looking more closely at the expanded AJC (**Figure 16**, bottom panels) it is apparent that many of these punctate structures localize proximal to the AJC. This result indicates that claudin localization is altered during filling and voiding, possibly providing a mechanism for the observed changes in  $R_j$ .

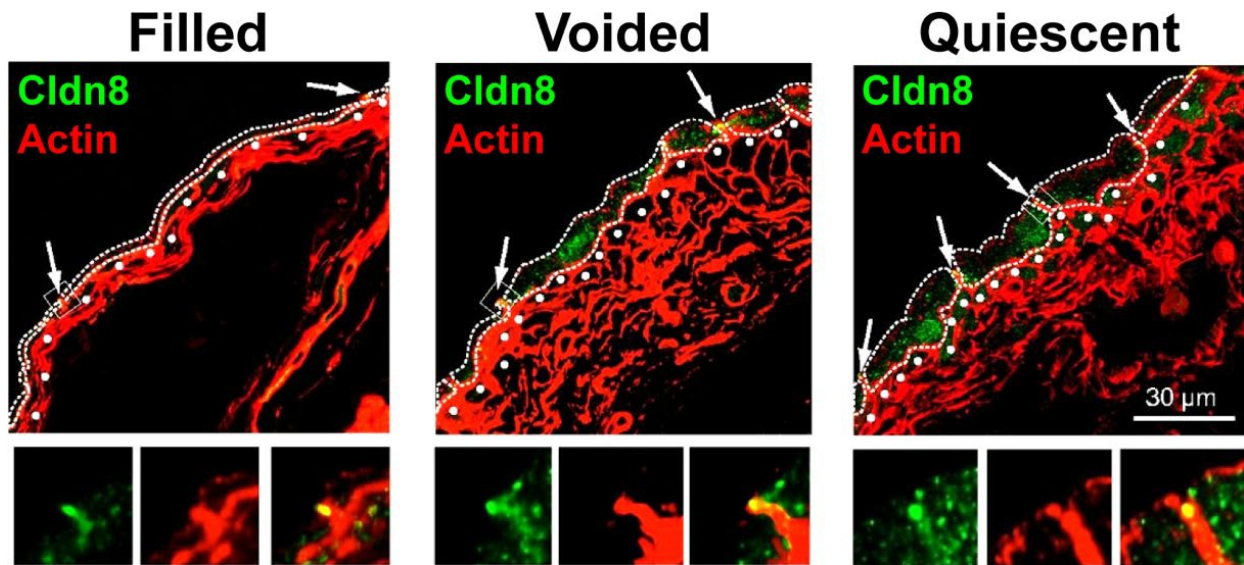


**Figure 16. Claudin-8 expression in full, voided, and quiescent rat bladders.**

Cross-sections of bladder tissue were labeled with an antibody against claudin-8 (green). F-actin was labeled with rhodamine-phalloidin (red). The apical-most tight junction is indicated with arrows. Umbrella cells are outlined with dashed lines. Bottom: higher-magnification views of the boxed region. Used with permission from **Carattino *et al.*, 2013**.

Thus, both the architecture and function of the tight junction are altered in response to filling and voiding. However, the mechanisms behind these changes are unknown. In the current study, we asked whether the adherens junction was similarly affected during the bladder cycle, if the organization and dynamics of the actomyosin cytoskeleton was affected by filling and voiding, and whether membrane traffic played a role in these events. We hypothesized that remodeling of the umbrella cell AJR depends on the membrane trafficking of junctional proteins, which then modulate AJR size, and permeability. Our studies indicate that both actomyosin dynamics and membrane trafficking events contribute to umbrella cell AJR expansion and contraction during the bladder cycle.

## 2.2 Results

### 2.2.1 The actomyosin cytoskeleton associated with the AJR of umbrella cells forms a non-sarcomeric network.

When viewed *en face*, the outermost umbrella cell layer of the stratified urothelium is composed of large (up to 100  $\mu\text{m}$  in diameter), typically binucleate, polyhedral cells that form an AJR at the apico-lateral borders of adjacent cells (**Figures 17, A and B**). We previously reported that the average perimeter of the AJR per umbrella cell increased in voided bladders from  $\sim 160$   $\mu\text{m}$  to  $\sim 250$   $\mu\text{m}$  in filled bladders (Carattino *et al.*, 2013). Using the tight junction-associated protein claudin-8, and the AJR-associated f-actin cytoskeleton (labeled with phalloidin) as markers, we confirmed that spontaneous bladder filling in anesthetized rats stimulated an expansion of the umbrella cell AJR, which was rapidly reversed within 5 min of voiding (compare filled bladders marked with an “F,” to those that were quiescent and never allowed to fill marked “Q”, or voided after filling and marked with a “V” in **Figure 17A**). The contracted AJR in voided bladders assumed a perimeter that was similar to that observed in quiescent bladders (compare “V” and “Q” in **Figure 17A**), indicating that the AJR contraction was complete within 5 min of bladder voiding. Using E-cadherin as a marker, we examined how the bladder cycle affected the adherens junction. Like the tight junction, the adherens junction ring expanded during bladder filling, and rapidly contracted upon voiding (**Figure 17B**).

We next sought to understand the organization of the AJR-associated actin cytoskeleton in the umbrella cell, and whether its organization was impacted by filling and voiding. Like the tight junction and adherens junction, the perimeter of the subapical actin ring expanded with filling and contracted after voiding (**Figures 17, A and B**). Furthermore, and reflecting their close proximity within the AJR, the tight junction and adherens junction completely matched the

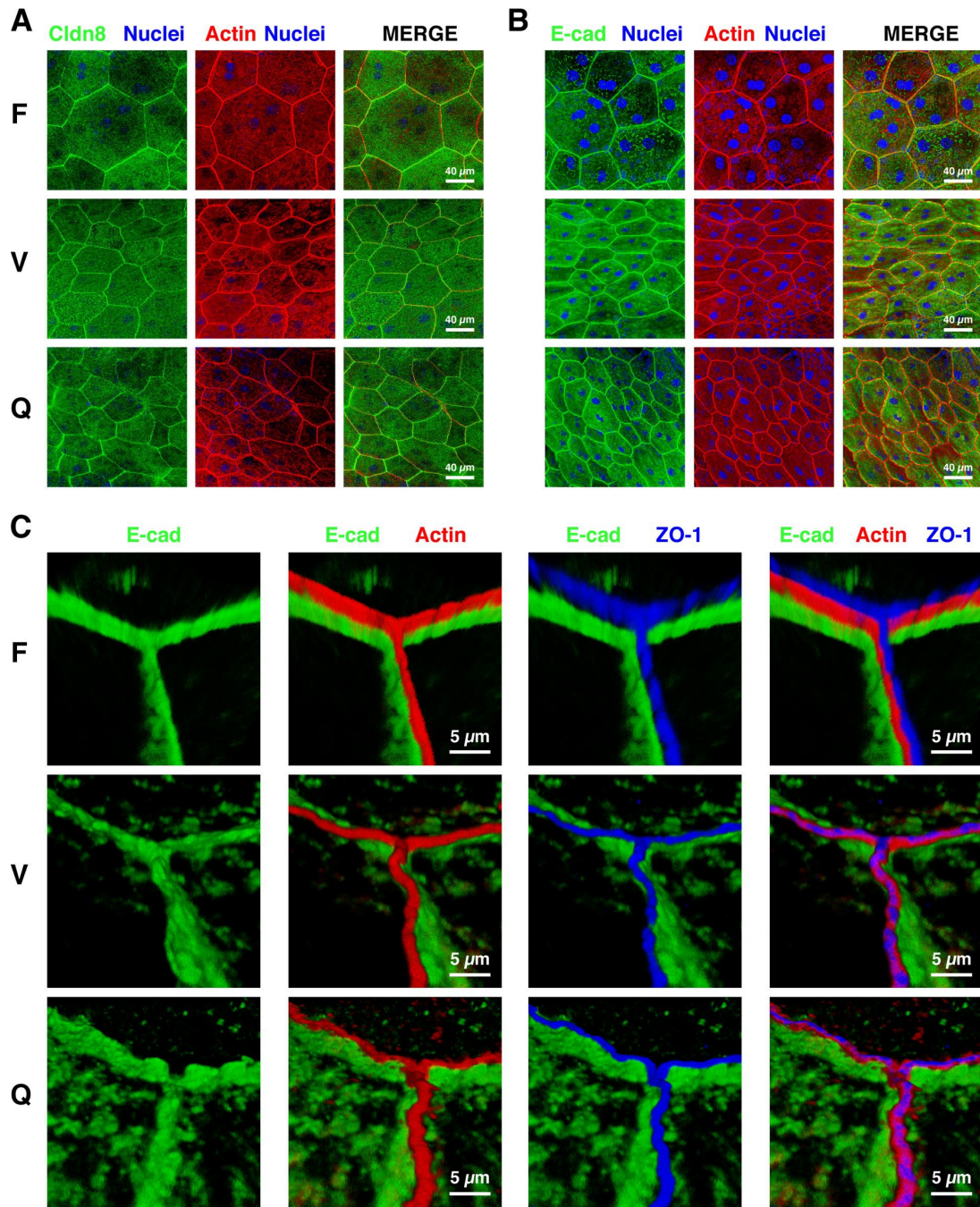


**Figure 17. The AJR expands and contracts as a unit during bladder filling and voiding.**

*En face* view of the umbrella cell layer in whole-mount preparations of filled (F), voided (V), or quiescent (Q) rat bladders. The apical junctional complex is labeled with (A) an antibody against the transmembrane tight-junction protein claudin-8 (green) or (B) an antibody against the transmembrane adherens-junction protein E-cadherin (green). F-actin is stained with rhodamine-phalloidin (red) and nuclei with To-Pro-3 (blue). Images are 3D reconstructions of confocal Z-stacks. Scale bars = 40 μm. Note that the AJR in the merged images does not appear to be completely “yellow,” as the intensity of the channels is not completely matched in these large cells. (C) Higher-magnification images of the AJR in filled (F), voided (V), or quiescent (Q) bladders labeled with antibodies against the adherens-junction protein E-cadherin (green) and the tight-junction protein ZO-1 (blue). F-actin is labeled with rhodamine-phalloidin (red). Images are 3D reconstructions of confocal Z-stacks. Scale bars = 5 μm.

contours of the actin ring during these transitions (**Figure 17**). At higher magnification, and within the limits of light microscopic resolution, the f-actin ring appeared as a single, continuous fine line between adjacent cells (**Figure 17C**), indicating that the plasma membranes of adjacent cells were very closely apposed in this region of the cell.

During filling and voiding, there were no obvious effects on the continuity of the actin ring, which always appeared smooth, unbroken, and not periodic in nature. However, when 3D reconstructions of the AJR at bicellular and tricellular junctions were examined, we noted the position of f-actin ring with respect to the tight junction changed. We observed that in filled bladders, the umbrella cell f-actin ring was readily resolved from the more apical tight junction, labeled with ZO-1, or the subjacent E-cadherin-labeled adherens junction (**Figure 17C**). In contrast, in voided and quiescent bladders, the actin ring was not easily resolved from the tight junction yet remained distinct from the adherens junction. Additionally, the AJR was slightly more tortuous and rounded in appearance in the voided and quiescent bladders, whereas it was very straight and wall-like in the filled bladders (**Figure 17C**). In the latter studies we used antibodies against ZO-1 because claudin-8 and E-cadherin antibodies were both made in rabbit and because of difficulties identifying antibodies made in non-rabbit species that label whole-mount rat tissues. However, we previously reported that ZO-1 and actin exhibit complete overlap in umbrella cells (Acharya *et al.*, 2004).

In the epithelial cells of the organ of Corti, the intestine, or the stomach, the AJR is organized as a highly-ordered sarcomeric network (Ebrahim *et al.*, 2013). In these cells, regularly spaced puncta of NMMIIB or NMMIIC, with a periodicity of ~450 nm, are interspersed between alternating, clusters of actin and  $\alpha$ -actinin-1. This is similar to what is seen in striated muscle cells, where  $\alpha$ -actinin-2 and  $\alpha$ -actinin-3 crosslink antiparallel actin filaments at the Z-line, which are engaged with muscle myosins tethered to the M-line. However, in umbrella cells the actomyosin cytoskeleton was not obviously organized in a sarcomeric network. First, rat umbrella cells expressed NMMIIA and NMMIIC, but not NMMIIB, which was instead expressed

in the interstitial cells below the urothelium (**Figure 18A, and Appendix, Figure S3**). NMMIIB expression in interstitial cells was confirmed by co-staining with platelet-derived growth factor- $\alpha$  (PDGFR $\alpha$ ), which is a marker of interstitial cells in the urothelium (**Appendix, Figure S3, D-F**) (Koh *et al.*, 2012). In the case of NMMIIA, the majority appeared in small vesicular structures and large “aggregates” that were dispersed across the apical pole of the umbrella cells (**Figures 18, A and C**). When the umbrella cell AJR of filled bladders was examined at higher magnification, NMMIIA formed very thin “railroad tracks” that overlapped with a continuous, unbroken ring of actin associated with the AJR (**Figure 18C**). Interestingly, the distribution of NMMIIA was not obviously periodic, but instead appeared stochastic, and was broken into small linear foci of staining. The highly folded nature of the umbrella cell apical membrane after voiding, coupled with the thin nature of the NMMIIA staining made it more difficult to image these tissues in the voided or quiescent state. However, areas of similarly distributed NMMIIA and actin were observed in these samples as well (**Figure 18C**). Although NMMIIC showed a prominent apical distribution in umbrella cells (**Appendix, Figure S3C**), it had no obvious association with the umbrella cell AJR in either cross-section or whole-mount preparations (**Appendix, Figures S3C and S4**).

We, also, examined the distribution of  $\alpha$ -actinin-4 in umbrella cells. Its association with the AJR was apparent even in relatively low-magnification images (**Figure 18B**). Like NMMIIA,  $\alpha$ -actinin-4 was closely apposed to the apical actin ring, again forming a “railroad track” pattern on either side of adjacent cell contacts (**Figure 18D**). However, its localization appeared more continuous, not obviously punctate, and thicker than the fine linear elements formed by NMMIIA (**Figure 18D**). Since  $\alpha$ -actinin-4 and NMMIIA antibodies were both made in rabbit, we could not colocalize NMMIIA with  $\alpha$ -actinin-4. We, also, observed that  $\alpha$ -actinin-4 was associated with a network of interlocking structures that had a mesh-like appearance (**Figure 18D**). The nature of these structures is unknown.

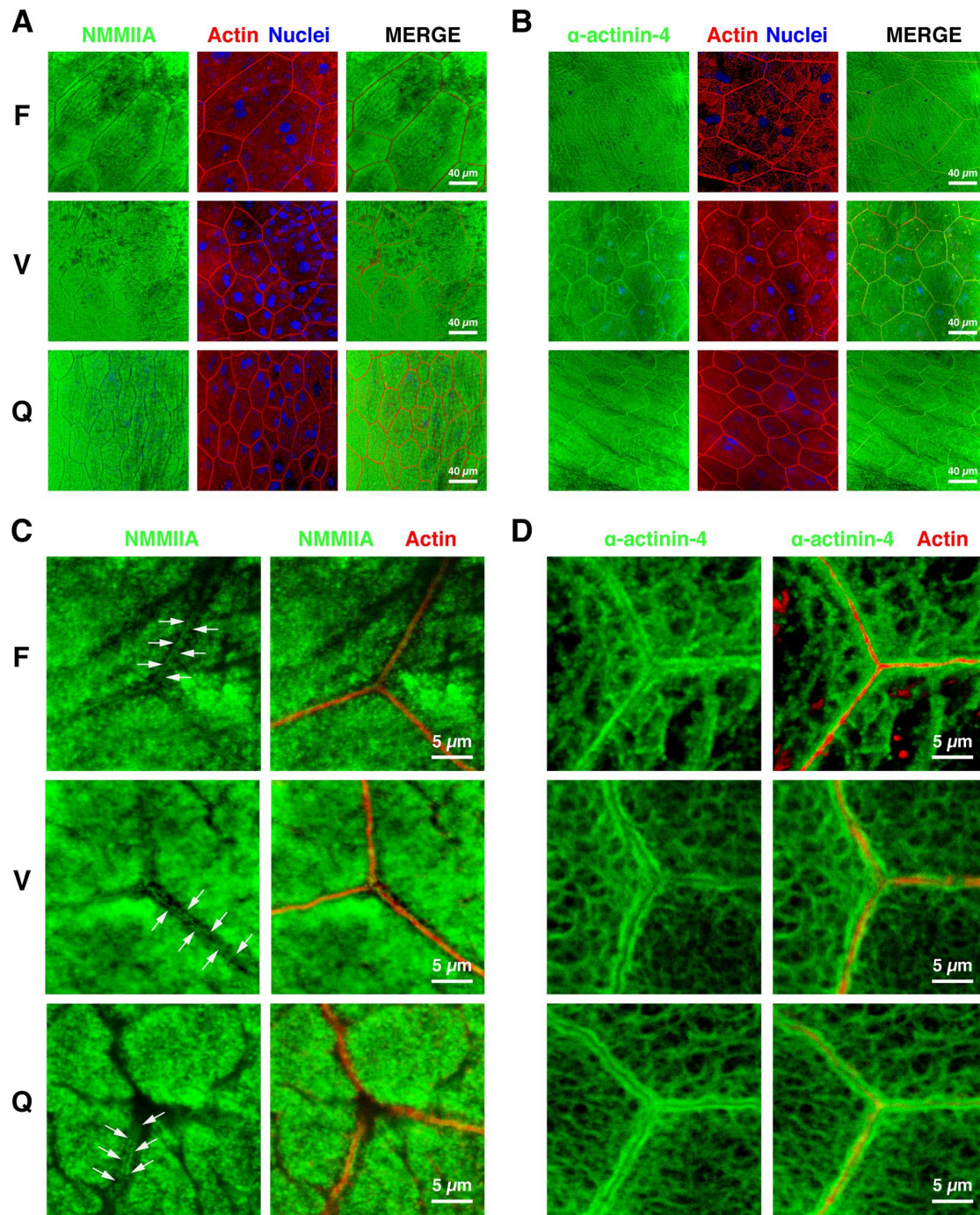


**Figure 18. The junctional actomyosin cytoskeleton expands and contracts with the apical junctional complex during bladder filling and voiding.**

*En face* view of the umbrella cell layer in whole-mount preparations of filled (F), voided (V), or quiescent (Q) rat bladders. The tissue is labeled with (A) an antibody against NMMIIA (MYH9 subunit; green) or (B) an antibody against  $\alpha$ -actinin-4 (green). F-actin is stained with rhodamine-phalloidin (red) and nuclei with To-Pro-3 (blue). Images are 3D projections of confocal Z-stacks. Scale bars = 40  $\mu$ m. (C, D) Higher-magnification images of the AJR in filled (F), voided (V), or quiescent (Q) bladders labeled with antibodies against (C) NMMIIA (MYH9 subunit; green; arrows indicate “railroad track” distribution of NMMIIA) or (D)  $\alpha$ -actinin-4 (green). F-actin is labeled with rhodamine-phalloidin (red). Images are 3D projections of confocal Z-stacks. Scale bars = 5  $\mu$ m.

Taken together, our studies indicate that the actomyosin cytoskeleton of the umbrella cell AJR is organized as a non-sarcomeric network with actin forming a thin continuous ring, bordered on either side by  $\alpha$ -actinin-4 and coincident with short linear arrays of NMMIIA. While filling and voiding did not impact this organization in an observable way, within the z-axis the actin ring appeared to segregate from the tight junction during filling, indicating some degree of reorganization of the AJR during the bladder cycle.

### 2.2.2 AJR expansion depends on the actin cytoskeleton.

In the studies above, we allowed urethane-anesthetized rats to fill their bladders spontaneously; however, to explore the changes in the AJR accompanying bladder filling and voiding in greater detail we needed an approach that would allow us to incorporate pharmacological treatments during the bladder cycle. Thus, we trans-urethrally catheterized the anesthetized rats, which

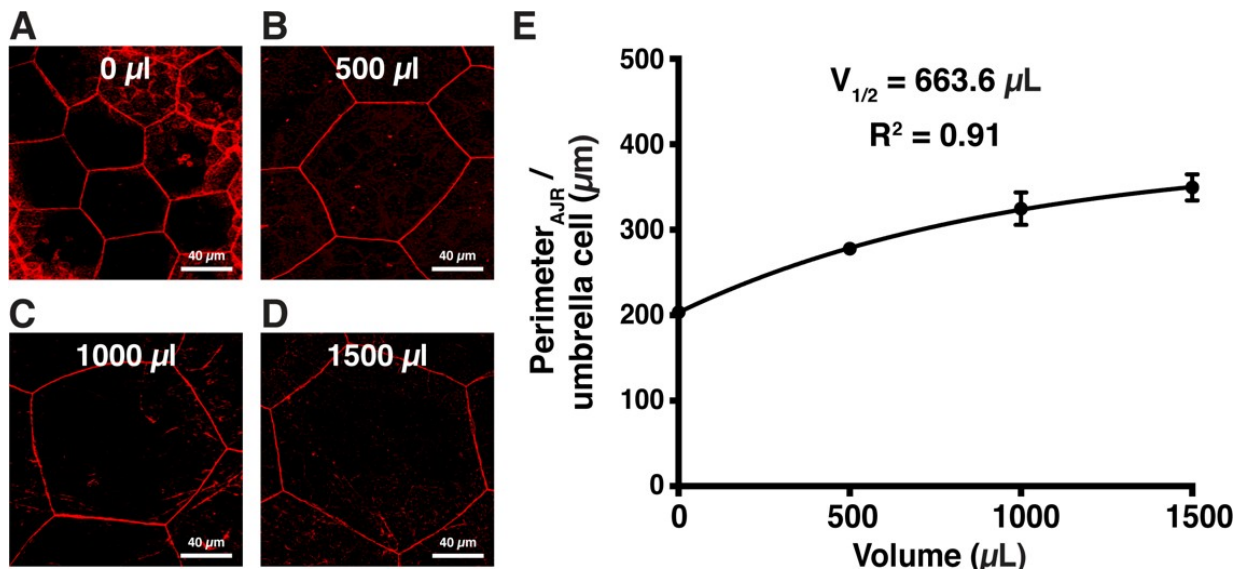


**Figure 19. Effect of filling on average perimeter<sub>AJR</sub> per umbrella cell.**

*En face* view of the umbrella cell layer in whole-mount preparations of rat bladders (A) left quiescent (0 µl) or filled with (B) 500, (C) 1000, or (D) 1500 µl of Kreb's buffer over 45 min (n = 3 for each group). F-actin is labeled with rhodamine-phalloidin (red). Images are 3D reconstructions of confocal Z-stacks. In some panels, the underlying intermediate cell layers are visible, but only the junctions associated with the uppermost umbrella cell layer were quantified. Scale bars = 40 µm. (E) Average perimeter<sub>AJR</sub> per umbrella cell (mean ± SEM; n = 3).

allowed us to fill their bladders using a syringe pump in a controlled manner to a specified volume over a given period of time. To assess the impact that filling had on the continuity of the urothelium and AJR perimeter per umbrella cell, we filled bladders to a volume of 500  $\mu\text{l}$  (the approximate volume achieved during spontaneous filling after 2.5 h (Carattino *et al.*, 2013)), 1000  $\mu\text{l}$ , or 1500  $\mu\text{l}$ . Using the f-actin ring as a surrogate for the AJR, we quantified the length of the umbrella cell AJR perimeter ( $\mu\text{m}$ ). Compared to unfilled, control bladders (0  $\mu\text{l}$ ), filled bladders exhibited an apparent volume-dependent increase in the AJR perimeter of umbrella cells (**Figures 19, A-D**). The increase in AJR perimeter was not linear, but instead fit a single exponential ( $R^2 = 0.91$ ) with a  $V_{1/2}$  of 663.6  $\mu\text{l}$  (95% CI = 304-1327  $\mu\text{l}$ ,  $n=3$ ), indicating that AJR approached its maximum size by 1500  $\mu\text{l}$  (**Figure 19E**). As 500  $\mu\text{l}$  was close to the measured  $V_{1/2}$ , we used this volume in our subsequent analyses.

To assess the actin requirements for AJR expansion, we preincubated the bladder by introducing a small volume (50  $\mu\text{l}$ ) of the actin disrupting agent cytochalasin D (Cyto D; 25  $\mu\text{g}/\text{ml}$ ) into the bladder and then allowed the bladder to remain in a quiescent state for 60 min. Subsequently, the bladder was filled to a final volume of 500  $\mu\text{l}$  in the continued presence of the drug. Under these conditions, Cyto D had a modest but significant inhibitory effect on filling-induced increases in AJR perimeter (**Figures 20, A-B and D**). In contrast, and relative to DMSO-treated control samples, preincubation with Cyto D in the absence of subsequent filling had no obvious effect on AJR perimeter ( $Q = 169 \pm 10 \mu\text{m}$  vs  $Q+\text{Cyto D} = 178 \pm 3 \mu\text{m}$ ;  $p > 0.05$ ). As we previously reported, the concentration of Cyto D used in our studies (25  $\mu\text{g}/\text{ml}$ ) caused the cytoplasmic accumulation of “focal aggregates” of actin (see arrows in **Figure 20B**), but did not obviously disrupt the AJR-associated actin cytoskeleton or the continuity of the umbrella cell layer (Khandelwal *et al.*, 2010). We, also, measured the effects of Cyto D on filled bladders not preincubated with this drug prior to analysis (**Figures 20, C and D**). In this case, AJRperimeter

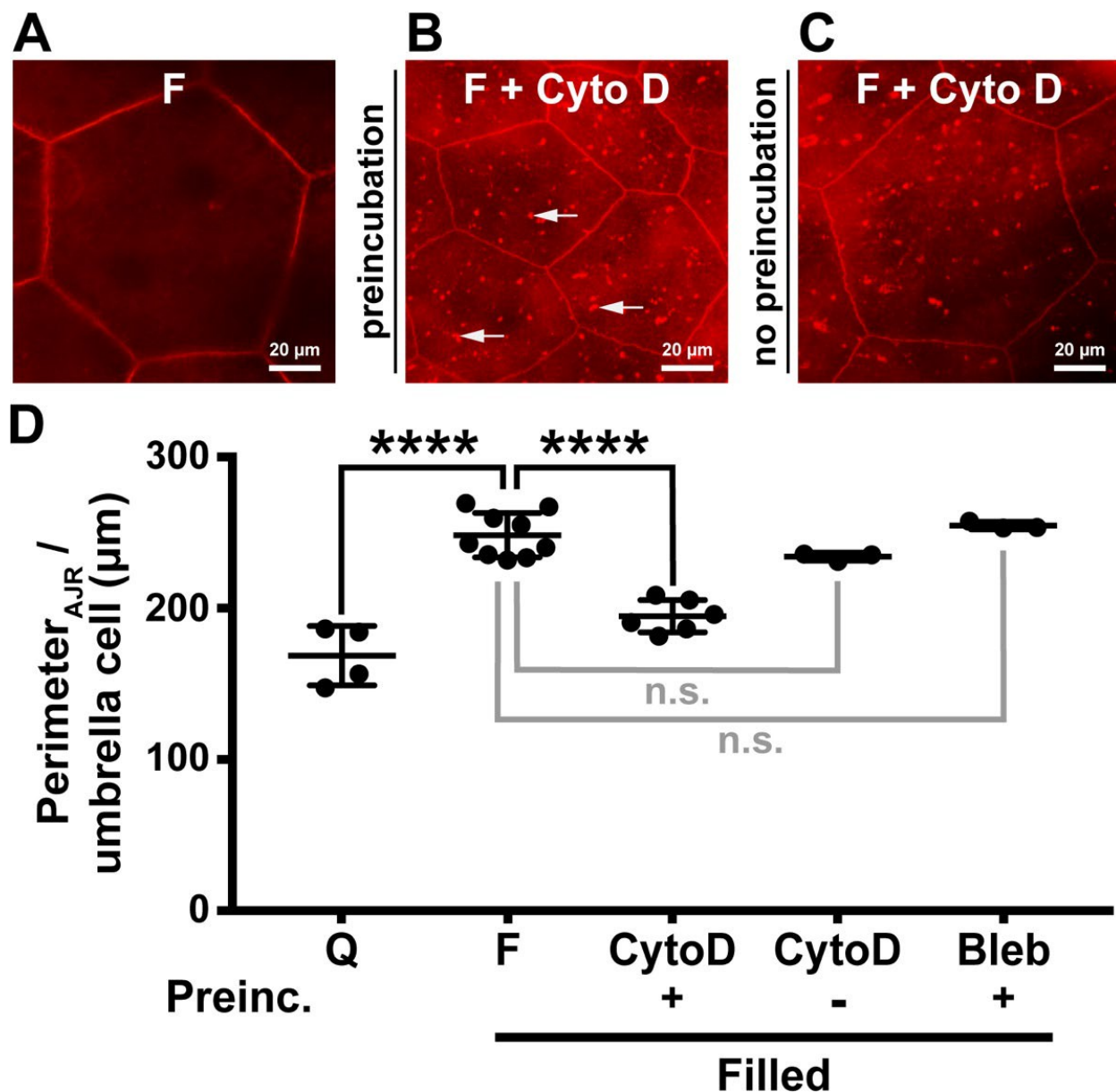


**Figure 20. F-actin disruption impairs AJR expansion during bladder filling.**

*En face* view of the umbrella cell layer in whole-mount preparations of rat bladders that were treated as follows: (A) preincubated with Krebs's buffer + 0.1% DMSO for 1 h, and filled in the presence of DMSO (F; control); (B) preincubated for 1 h with 25  $\mu$ g/ml Cyto D and then filled in the presence of the drug; (C) not preincubated, but filled in the presence of 25  $\mu$ g/ml Cyto D. F-actin is labeled with rhodamine-phalloidin (red). The "focal aggregates" of F-actin that resulted from Cyto D treatment (B) are indicated with arrows. Images were acquired using a wide-field microscope equipped with a digital camera. Scale bars = 20  $\mu$ m. (D) Average perimeter<sub>AJR</sub> per umbrella cell in quiescent bladders (Q; n = 4); control filled bladders preincubated with DMSO, and then filled in the presence of DMSO (F; n = 9); bladders preincubated with Cyto D, and then filled in the presence of the drug (n = 6); bladders not preincubated, but filled in the presence of Cyto D (n = 3); bladders preincubated with Bleb, and then filled in the presence of the drug (n = 3). Values are mean  $\pm$  SEM. Data were analyzed using ANOVA and p values  $\leq$  0.05 were considered significant, with \*\*\*\* denoting a p value  $\leq$  0.0001.

was not significantly different from filled bladders, indicating that preincubation was necessary to observe the effects of this drug.

Since we observed that general disruption of the actin cytoskeleton with Cyto D prevented the complete expansion of the AJR, we investigated what types of actin polymerization might be involved in this process. Both Arp2/3 and formins are involved in the formation and maintenance of the functional AJR (Park *et al.*, 2013; Zhou *et al.*, 2013). Therefore, we incubated bladders with either 100  $\mu$ M CK869, an Arp2/3 inhibitor (Nolen *et al.*, 2009), or 50  $\mu$ M SMIFH2, a formin polymerization inhibitor (Rizvi *et al.*, 2009), prior to and during filling. Whereas treatment with SMIFH2 prior to filling caused a significant decrease in AJR perimeter relative to DMSO-filled control bladders, CK869 treatment did not significantly affect AJR expansion (**Table 4**). Since Cdc42 can act upstream of formins (Grindstaff *et al.*, 1998; Vogler *et al.*, 2014), we examined the effects of 25  $\mu$ M ML141, a Cdc42 inhibitor (Surviladze *et al.*, 2010). However, ML141 treatment did not significantly affect AJR expansion in response to bladder filling (**Table 4**).

**Table 4. Effects of pharmacological inhibitors on AJR expansion.**

Experimental group	<i>n</i>	Function	Conc.	$P_{AJR/UC}$ ( $\mu$ m) $\pm$ SEM
Full DMSO control	4		0.1%	215 $\pm$ 16
CK869	4	Arp2/3 complex inhibitor	100 $\mu$ M	176 $\pm$ 9
Full DMSO control	6		0.1%	236 $\pm$ 12
SMIFH2	6	Formin FH2 domain inhibitor	50 $\mu$ M	<b>180 <math>\pm</math> 16*</b>
Full DMSO control	4		0.1%	204 $\pm$ 5
ML141	4	Cdc42 inhibitor	25 $\mu$ M	202 $\pm$ 10
Full DMSO control	3		0.1%	196 $\pm$ 31
GSK 269962	4	ROCK inhibitor	100 nM	203 $\pm$ 7

Rat bladders were preincubated with the indicated pharmacological agent for 1 h prior to filling. Average perimeter<sub>AJR</sub> per umbrella cell ( $P_{AJR/UC}$ ) of experimental bladders was compared with that of paired control bladders (mean  $\pm$  SEM). *p* values  $\leq 0.05$  were considered significant, with a \* denoting a *p* value  $\leq 0.05$ .

In many cells, the long, tangentially oriented actin filaments within the AJR are crosslinked by NMMIIA molecules to form a contractile unit (Schwayer *et al.*, 2016). To examine whether NMMII contraction played a role in AJR expansion during bladder filling, we preincubated bladders with blebbistatin (Bleb; 10  $\mu$ M), which specifically inhibits the ATPase activity of the myosin heavy chains associated with the vertebrate NMMIIA, NMMIIB, and NMMIIC complexes (Zhang *et al.*, 2017). However, there was no significant effect on filling induced AJR expansion after Bleb treatment (**Figure 20D**). Furthermore, bladders preincubated with Bleb, but left in a quiescent state showed no change in AJR perimeter relative to untreated control bladders ( $Q = 169 \pm 10 \mu\text{m}$  vs  $Q+\text{Bleb} = 166 \pm 0.4 \mu\text{m}$ ;  $p > 0.05$ ). As further evidence that NMMII may not play an active role during bladder filling we preincubated bladders with 100 nM GSK269962, a selective ROCK inhibitor, which should prevent ROCK-dependent activation of NMMII (Doe *et al.*, 2007). Again, GSK269962 did not affect expansion of the AJR (**Table 4**). Overall, our data indicate that active formin-mediated actin polymerization, but not NMMII contraction is required for the expansion of the umbrella cell AJR during bladder filling.

### **2.2.3 Apical junctional ring expansion depends on Rab13-dependent exocytosis.**

Many membrane trafficking events including exocytosis and endocytosis are actin-dependent (Valentijn *et al.*, 1999; Apodaca, 2001b, 2002; Croise *et al.*, 2014). In the case of the umbrella cell, the apical exocytosis stimulated by bladder filling is actin-dependent (Lewis and de Moura, 1982; Truschel *et al.*, 2002; Yu *et al.*, 2009b), as is voiding-induced apical endocytosis (Khandelwal *et al.*, 2010). This prompted us to determine if exocytosis is required for filling-induced expansion of the AJR. As a general inhibitor of the biosynthetic pathway, we preincubated bladders with BfA (5  $\mu\text{g/ml}$ ), which impairs exocytosis by preventing the exit of proteins from the Golgi (Klausner *et al.*, 1992). Compared with control bladders, BfA-treated bladders were unable

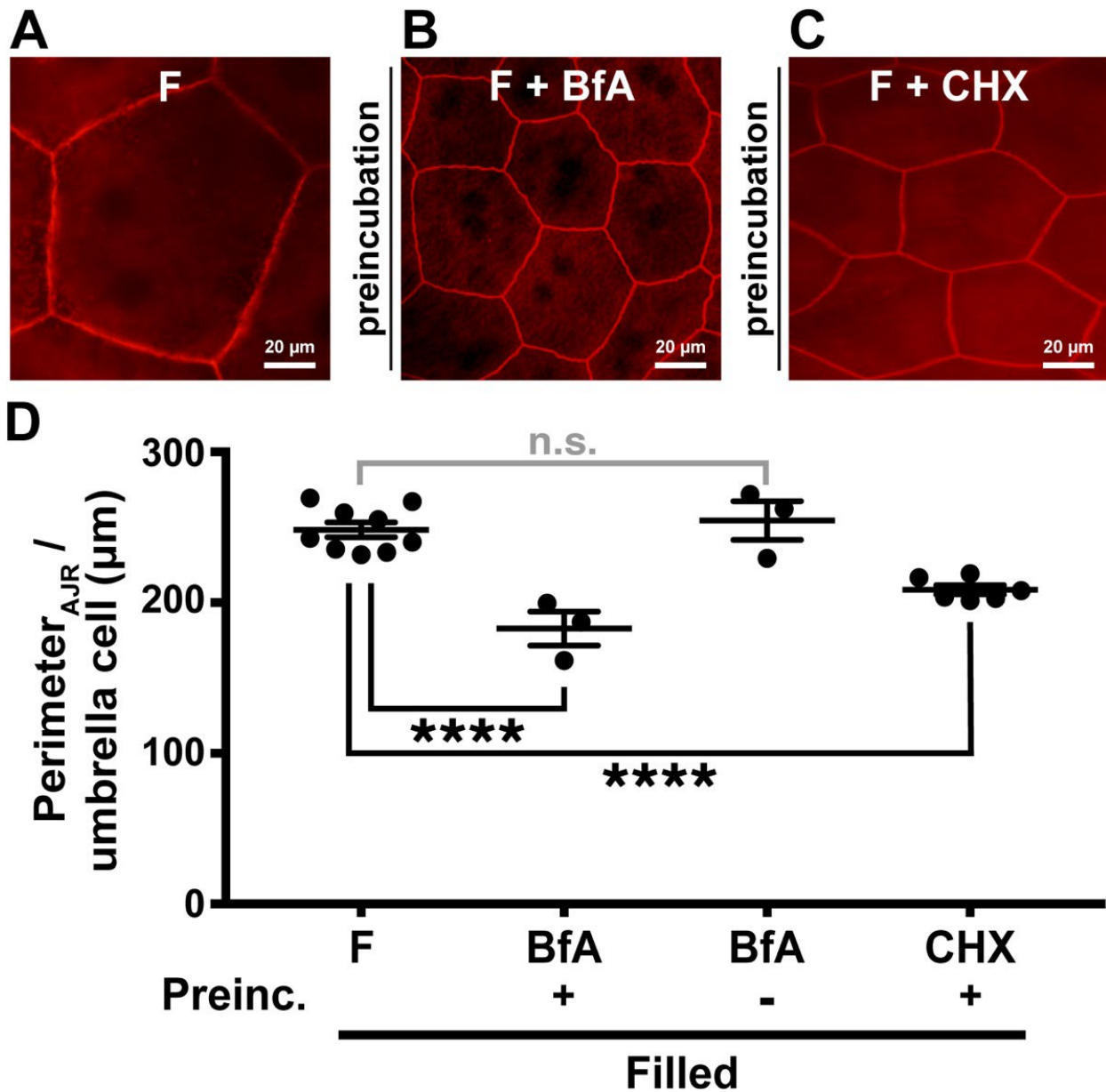


**Figure 21. Inhibition of exocytosis impairs AJR expansion during bladder filling.**

*En face* view of the umbrella cell layer in whole-mount preparations of rat bladders that were treated as follows: (A) preincubated for 1 h with 5  $\mu$ g/ml BfA and then filled in the presence of the drug; (B) not preincubated, but filled in the presence of 5  $\mu$ g/ml BfA; or (C) preincubated for 1 h with 100  $\mu$ g/ml CHX and then filled in the presence of the drug. F-actin is labeled with rhodamine-phalloidin (red). Images were acquired using a wide-field microscope equipped with a digital camera. Scale bars = 20  $\mu$ m. (D) Average perimeter<sub>AJR</sub> per umbrella cell in control filled bladders preincubated with DMSO, and then filled in the presence of DMSO (F; n = 9); bladders preincubated with BfA and then filled in the presence of the drug (n = 3); bladders not preincubated, but filled in the presence of BfA (n = 3); or bladders preincubated with CHX and then filled in the presence of the drug (n = 6). Control data for filled bladders are reproduced from Figure 15D. Values are mean  $\pm$  SEM. Data were analyzed using ANOVA and p values  $\leq$  0.05 were considered significant, with \*\*\*\* denoting a p value  $\leq$  0.0001.

to fully expand their AJR (**Figures 21, A and B**), and exhibited a significant decrease in AJR perimeter relative to control bladders (**Figure 21D**). However, in the absence of preincubation, the AJRs of BfA-treated umbrella cells were able to expand to a similar size as measured in control filled bladders (**Figure 21D**). We, also, preincubated bladders with the protein synthesis inhibitor CHX (Schneider-Poetsch *et al.*, 2010) (100 µg/ml), which also significantly inhibited the increase in AJR perimeter that normally accompanies bladder filling (**Figures 21, A, C, and D**).

To more specifically target the exocytic machinery that could be involved in the expansion of the AJR, we used adenoviral transduction to express DN-mutants of Rab8a, Rab11a, and Rab13, or GFP alone as a control. A critical step in this approach is a brief treatment with N-dodecyl-β-D-maltoside (DDM), which makes the umbrella cells permissive for adenoviral infection (Ramesh *et al.*, 2004; Khandelwal *et al.*, 2008). While this treatment has no effect on the TER of the urothelium or the expression and distribution of differentiation markers (Khandelwal *et al.*, 2010; Carattino *et al.*, 2013), it does cause a reduction in the perimeter of the umbrella cells, a phenotype that slowly reverses over several days. Nonetheless, DDM-treated umbrella cells were still capable of expanding and contracting their AJR in response to filling and voiding (**Appendix, Figure S5**). We first explored the impact of expressing DN-Rab8a-GFP or DN-Rab11a-GFP, as these mutant GTPases inhibit the pathways for apical exocytosis that expand the umbrella cell apical surface area in response to filling (Khandelwal *et al.*, 2008; Khandelwal *et al.*, 2013). To ensure that we only quantified effects in transduced umbrella cells, we exclusively measured the perimeter of AJR per umbrella cell in GFP-positive cells. Relative to GFP alone, expression of either DN-Rab8a-GFP or DN-Rab11a-GFP did not significantly affect the perimeter of AJR per umbrella cell in filled bladders (**Figures 22, A-C and E**). Interestingly, umbrella cells transduced with DN-Rab8a-GFP exhibited profound changes in the morphology of their AJR, which became highly convoluted, even in filled bladders (**Figure 22B**, arrowheads).

Of the known Rabs, Rab13 is the one most often associated with trafficking events that occur at the tight junction (Marzesco *et al.*, 2002; Kohler *et al.*, 2004; Marzesco and Zahraoui,

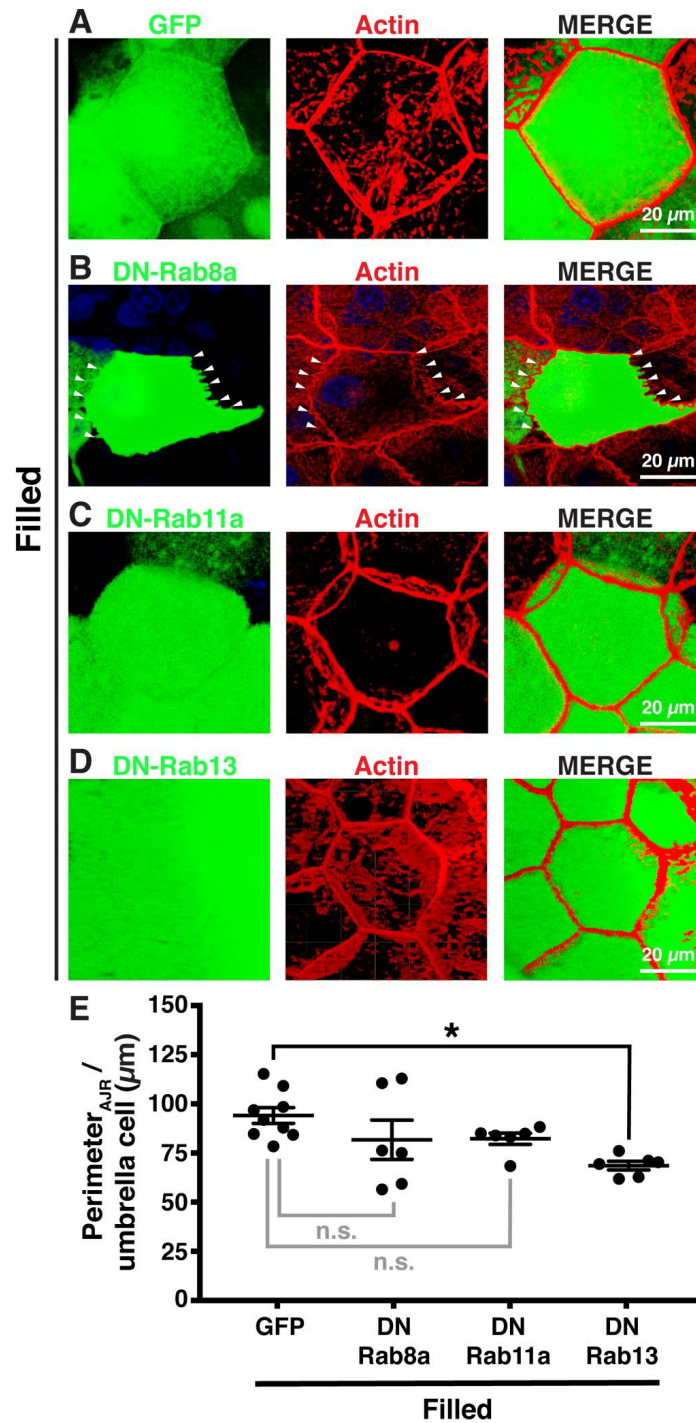


**Figure 22. Expression of DN-RAB13-GFP impairs AJR expansion during bladder filling.**

*En face* view of the umbrella cell layer in whole-mount filled rat bladders transduced with adenoviruses encoding (A) GFP (control), (B) DN-Rab8a-GFP (arrowheads indicate altered AJR morphology in cells expressing this protein), (C) DN-Rab11a-GFP, or (D) DN-Rab13-GFP. F-actin was labeled with rhodamine-phalloidin (red). Images are 3D reconstructions of confocal Z-stacks. Scale bars = 20  $\mu\text{m}$ . (E) Average perimeter<sub>AJR</sub> per umbrella cell in bladders transduced with GFP (n = 9), DN-Rab8a-GFP (n = 6), DN-Rab11a-GFP (n = 6), or DN-Rab13-GFP (n = 6). Values are mean  $\pm$  SEM. Data were analyzed using ANOVA, with \* denoting a p value  $\leq$  0.05.

2005; Yamamura *et al.*, 2008). We confirmed that rat umbrella cells expressed Rab13 by western blot and immunofluorescence (**Appendix, Figure S6**). Whereas, expression of DN-Rab8a-GFP or DN-Rab11a-GFP had no significant effect on expansion of the AJR, expression of DN-Rab13-GFP resulted in a significant decrease in AJR perimeter relative to GFP-expressing umbrella cells in filled bladders (**Figure 22, A, D and E**). We compared the expression levels of exogenously expressed DN-Rab mutants versus their endogenous counterparts and confirmed that relative expression levels were similar and thus could not account for the observed inhibitory effect of DN-Rab13 versus the other Rabs tested (**Appendix, Figure S7**). Collectively, these data indicate that expansion of the AJR requires new protein synthesis and Rab13-dependent exocytosis.

#### **2.2.4 Apical junctional ring contraction depends on the actomyosin cytoskeleton.**

We next explored the requirements for AJR contraction during voiding, focusing on the role of the actomyosin cytoskeleton in these events. As noted in **Figure 20D**, if the bladder was filled in the presence of Cyto D, but without preincubation, there was no significant effect on AJR expansion. However, when this treatment protocol was followed by voiding, Cyto D reduced the voiding-induced contraction of the AJR (**Figures 23, A-B, and D**). Thus, the actin cytoskeleton is involved in both the expansion and contraction of the umbrella cell AJR during bladder filling and voiding. To examine if there was also a role for NMMII in AJR contraction, we preincubated bladders with Bleb, filled the bladders, and then induced voiding. Under these conditions, Bleb impaired the contraction of the AJR, resulting in a significant increase in AJR perimeter relative to control voided bladders (**Figure 23, A, C and D**).

An upstream activator of NMMIIA contraction is RhoA (Amano *et al.*, 1996). Thus, we also tested whether expression of DN-RhoA-GFP impacted AJR contraction. We observed that expression of DN-RhoA-GFP caused a moderate, but significant, increase in AJR perimeter per umbrella cell versus umbrella cells transduced with GFP (**Figures 24, A-B, and D**). We also

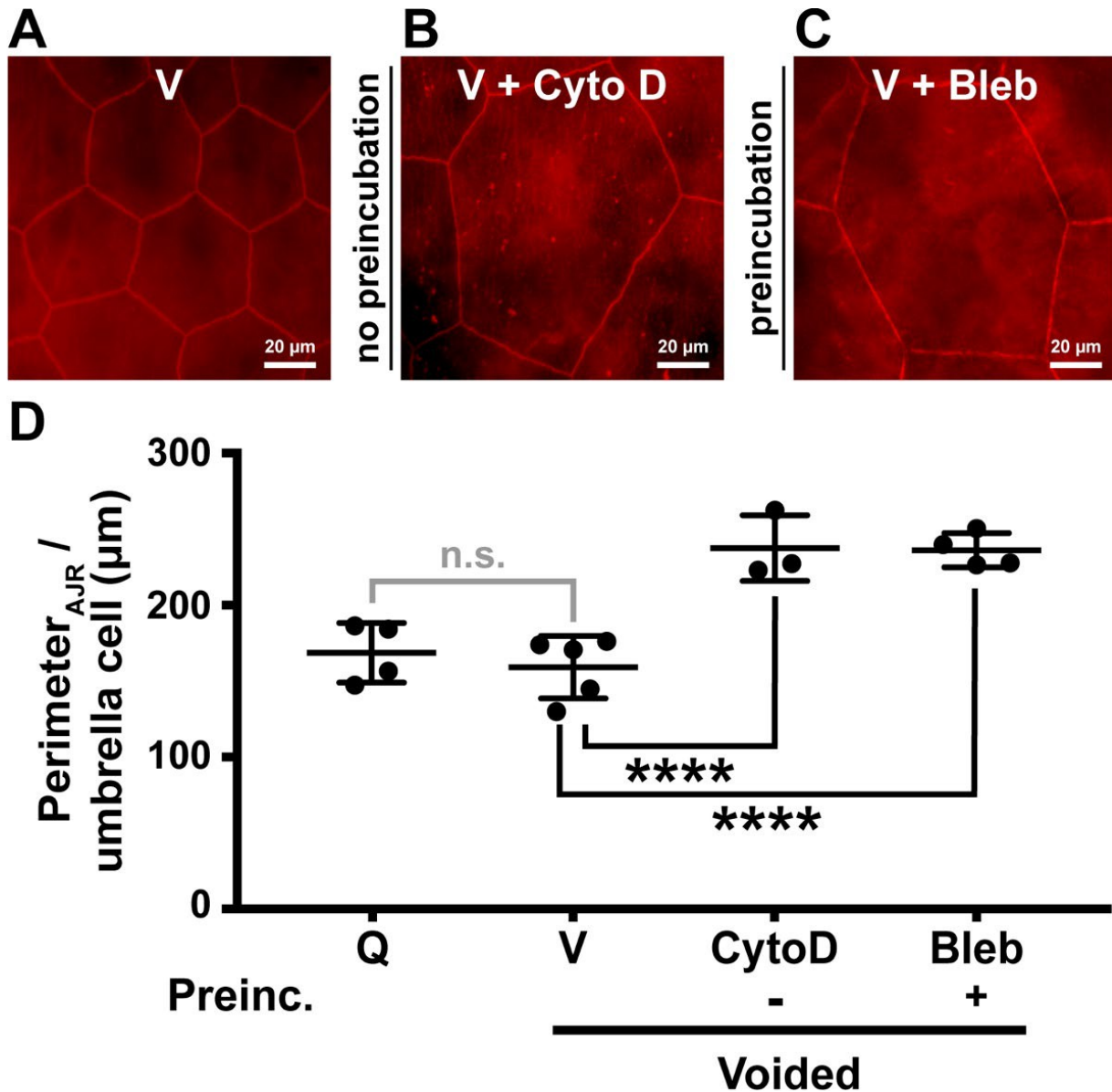


**Figure 23. Disruption of the actin cytoskeleton or inhibition of NMMIIA contractility impairs AJR contraction during bladder voiding.**

*En face* view of the umbrella cell layer of whole-mount rat bladders that were (A) preincubated with Krebs' buffer + 0.1% DMSO for 1 h, filled in the presence of DMSO, and then voided (V; control); (B) not preincubated, but filled in the presence of 25  $\mu$ g/ml CytoD and then voided; (C) preincubated for 1 h with 10  $\mu$ M Bleb, filled in the presence of the drug, and then voided. F-actin was stained with rhodamine-phalloidin (red). Images were acquired using a wide-field microscope fitted with a digital camera. Scale bars = 20  $\mu$ m. (D) Average perimeter<sub>AJR</sub> per umbrella cell in quiescent bladders (Q; n = 4); control voided bladders preincubated with DMSO, filled in the presence of DMSO, and then voided (V; n = 5); bladders not preincubated, but filled in the presence of 25  $\mu$ g/ml CytoD, and then voided (n = 3); bladders preincubated for 1 h with 10  $\mu$ M Bleb, filled in the presence of the drug, and then voided (n = 4). Control data from quiescent and filled bladders are reproduced from Figure 15D. Values are mean  $\pm$  SEM. Data were analyzed using ANOVA and p values  $\leq$  0.05 were considered significant, with \*\*\*\* denoting a p value  $\leq$  0.0001.

confirmed that DN-RHOA-GFP had no effect on expansion of the AJR (**Figure 24D**). Taken together, these data indicate that RhoA-dependent contraction of the actomyosin cytoskeleton is required for the constriction of the umbrella cell AJR upon bladder voiding.

### **2.2.5 Apical junctional ring contraction depends on the dynamin-2-dependent endocytosis.**

Like exocytosis, endocytosis is also intimately linked to the actomyosin cytoskeleton (Apodaca, 2001a). For example, we previously showed that voiding-induced apical endocytosis in umbrella cells is dependent on RhoA and actin, as well as dynamin-2 (Truschel *et al.*, 2002; Khandelwal *et al.*, 2010). This suggested to us that contraction of the AJR may also involve endocytosis. To examine this possibility, we preincubated bladders with 30  $\mu$ M Pitstop2, which was originally identified in a screen for inhibitors of clathrin-mediated endocytosis (von Kleist *et al.*, 2011), but was later shown to be a general inhibitor of clathrin-dependent and -independent endocytosis (Dutta *et al.*, 2012). While preincubation with Pitstop2 had no effect on filling-induced expansion of the AJR, it impaired contraction of the AJR, resulting in an increase in AJR perimeter (**Figures 25, A-C and D**). We, also, determined whether AJR contraction was dependent on dynamin, a GTPase required for clathrin-dependent and -independent forms of endocytosis (Mayor *et al.*, 2014; Kaksonen and Roux, 2018). While we previously reported that umbrella cells express dynamin-2 (Khandelwal *et al.*, 2010), we chose to use a DN mutant of dynamin-1 (HA-tagged dynamin-1-K44A), because of reports that dynamin-2 can trigger apoptosis when overexpressed (Soulet *et al.*, 2006). Expression of DN-dynamin-1-HA had no impact on the expansion of the AJR (**Figure 24D**); however, it caused a significant increase in AJR perimeter per umbrella cell in voided bladders as compared to voided bladders expressing GFP (**Figure 24, A, C, and D**). Taken as a whole, these data indicate that the contraction of the AJR during bladder

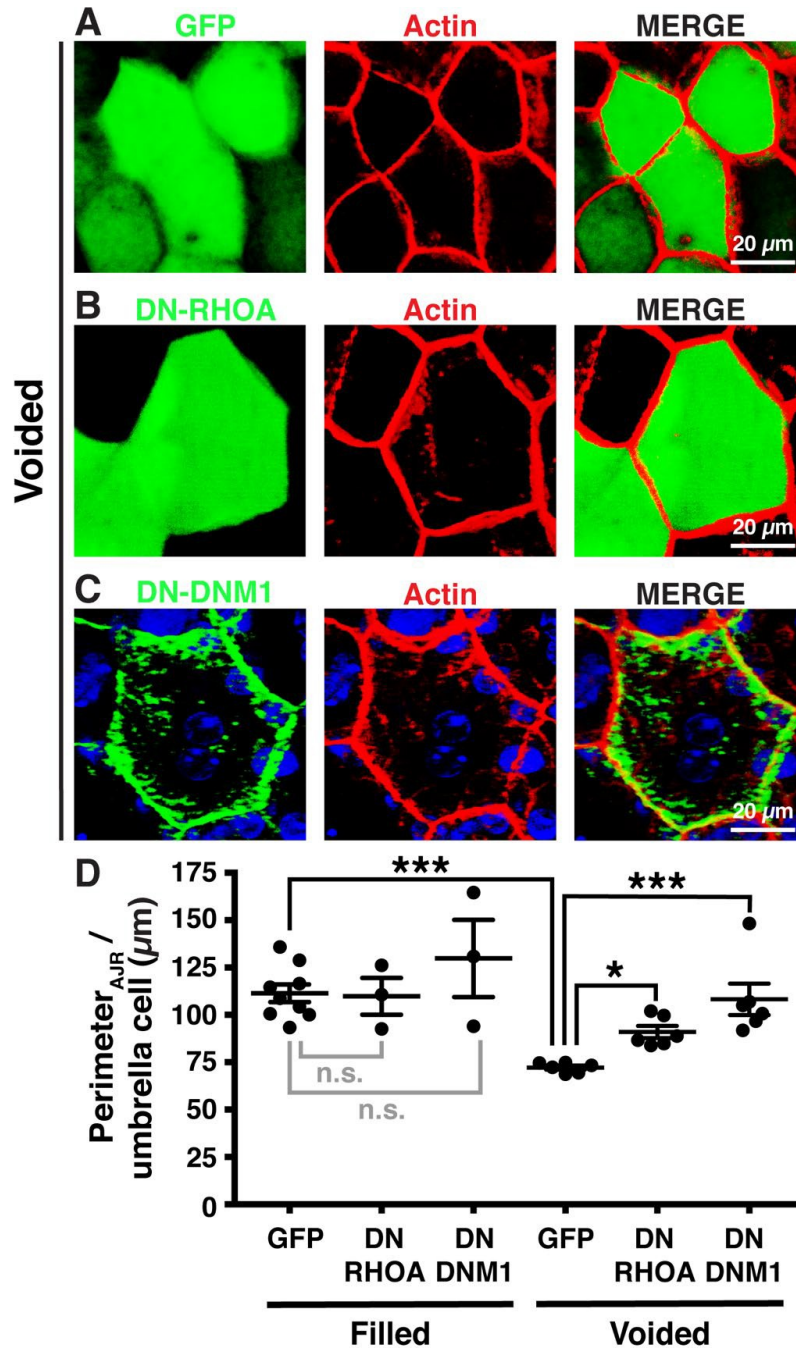


**Figure 24. Expression of DN-RhoA or DN-dynamin-1 impairs AJR contraction during bladder voiding.**

*En face* view of the umbrella cell layer of whole-mount voided rat bladders transduced with adenoviruses encoding (A) GFP (control), (B) DN-RhoA-GFP, or (C) DN-dynamin-1-HA. F-actin was labeled with rhodamine-phalloidin (red) and nuclei with To-Pro-3 (blue). Images are 3D reconstructions of confocal Z-stacks. Scale bars = 20 μm. (D) Average perimeter<sub>AJR</sub> per umbrella cell in filled bladders transduced with GFP (n = 9), DN-RhoA-GFP (n = 3), or DN-dynamin-1-HA (n = 3), or voided bladders transduced with GFP (n = 6), DN-RhoA-GFP (n = 6), or DN-dynamin-1-HA (n = 6). Control data from GFP filled bladders are reproduced from Figure 17E. Values are mean ± SEM. Data were analyzed using ANOVA and p values ≤ 0.05 were considered significant, with \*\*\* denoting a p value ≤ 0.001.

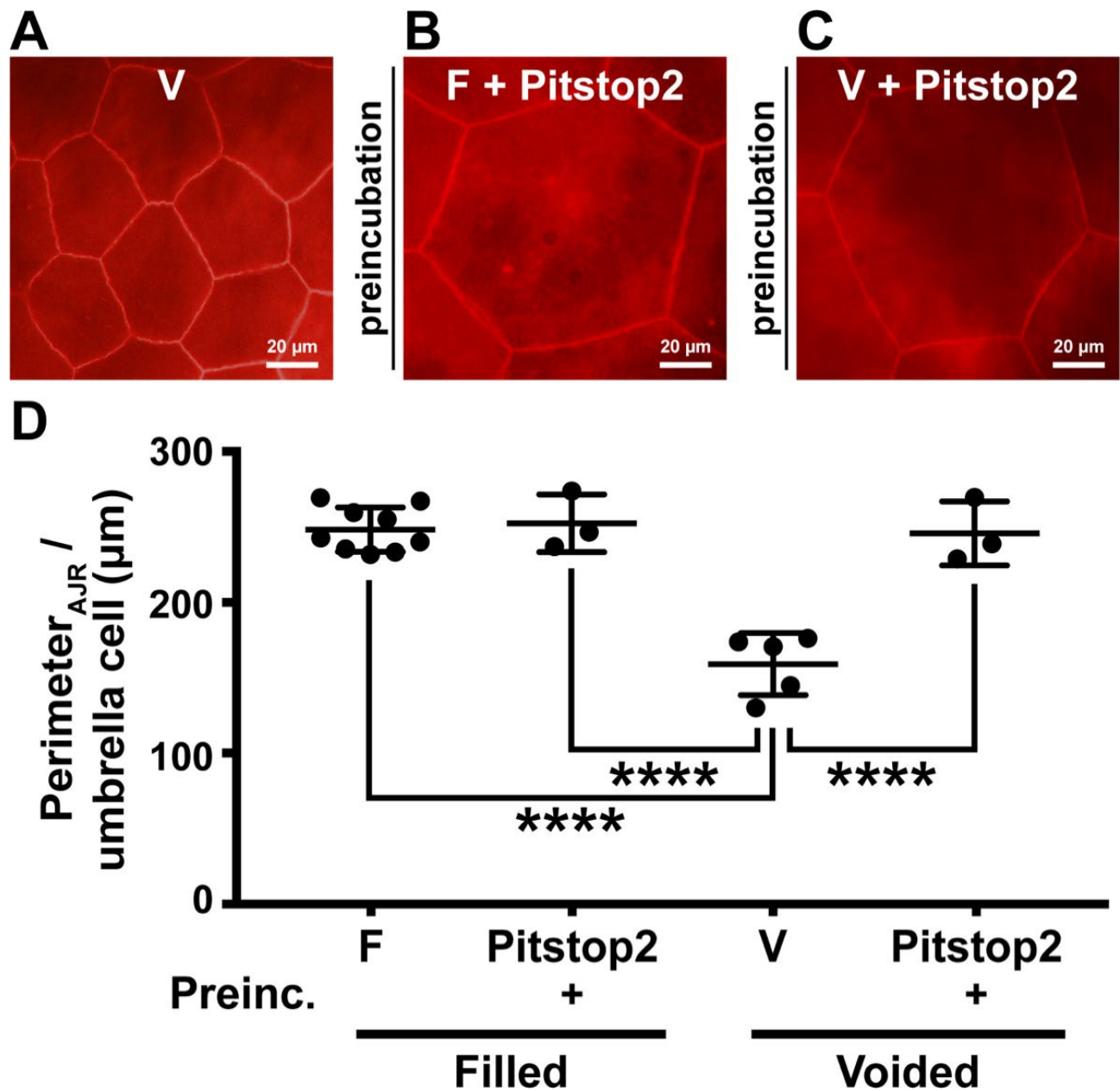


**Figure 25. Inhibition of endocytosis impairs AJR contraction during bladder voiding.**

*En face* view of the umbrella cell layer of whole-mount rat bladders that were (A) preincubated with Kreb's buffer + 0.1% DMSO for 1 h, filled in the presence of DMSO, and then voided (V; control); (B) preincubated for 1 h with 30 µM Pitstop2 and filled in the presence of the drug (C) preincubated for 1 h with 30 µM Pitstop2, filled in the presence of the drug, and then voided. F-actin was stained with rhodamine-phalloidin (red). Images were acquired using a wide-field microscope fitted with a digital camera. Scale bars = 20 µm. (D) Average perimeter<sub>AJR</sub> per umbrella cell in control filled bladders preincubated with DMSO and filled in the presence of DMSO (F; n = 9); bladders preincubated with Pitstop2, and filled in the presence of the drug (n = 3); control voided bladders preincubated with DMSO, filled in the presence of DMSO, and then voided (V; n = 5); bladders preincubated with Pitstop2, filled in the presence of the drug, and then voided. Control data from filled bladders are reproduced from Figure 15D, and control data from voided bladders are reproduced from Figure 18D. Values are mean ± SEM. Data were analyzed using ANOVA and p values ≤ 0.05 were considered significant, with \*\*\*\* denoting a p value ≤ 0.0001.

voiding is not only dependent on the actomyosin cytoskeleton, but on dynamin-dependent endocytosis as well.

## **2.3 Discussion**

While many previous studies have focused on the internal forces generated by the actomyosin cytoskeleton on mature, stable junctions or on the remodeling of junctions during development or morphogenesis, there is limited understanding of how the AJR responds to the external forces that occur during normal physiological events. In the case of umbrella cells, we previously reported that they expanded and contracted their AJR as the bladder underwent cycles of filling and voiding (Carattino *et al.*, 2013). How this is accomplished was unknown, but it is unlikely to result from simple folding and unfolding of the AJR as even at the ultrastructural level there is little evidence of AJR pleating (Carattino *et al.*, 2013). Instead, our current studies indicate that expansion of the umbrella cell AJR, which has a non-sarcomeric organization, requires active formin-mediated actin polymerization and membrane trafficking events, likely exocytosis, while constriction of the umbrella cell AJR requires NMMII-dependent contraction coupled with endocytosis. The importance of these findings is discussed below.

### **2.3.1 Organization and dynamics of the AJR-associated actomyosin cytoskeleton in umbrella cells.**

While the AJR and its components have been known for decades (Farquhar and Palade, 1963), the past few years have revealed important insights into the details of its organization, particularly that of the associated actomyosin ring. In the epithelial cells that line the Organ of Corti, the intestine, and the stomach, the actomyosin ring forms a sarcomeric belt comprised of

bipolar NMMIIB/C filaments, arranged in puncta, that are periodically interspersed between puncta of  $\alpha$ -actinin-1-tethered actin filaments; an organization that would be ideal to promote contraction (Ebrahim *et al.*, 2013) (**Appendix, Figure S8**). In contrast, in nematodes, the actomyosin cytoskeleton of the hypodermis is organized at right angles to the apical junctions (Costa *et al.*, 1998), and in cultured MDCK cells, punctate NMMIIB staining overlaps considerably with a continuous ring of f-actin at the AJR (Fanning *et al.*, 2012). Interestingly, when MDCK cells are depleted of ZO-1/2, the bicellular junctions become more linear, the f-actin staining becomes more prominent, and NMMIIB assumes a periodic distribution, somewhat like that observed in cells with a sarcomeric AJR, such as in muscle, the gut, or the stomach (Fanning *et al.*, 2012).

In the case of umbrella cells, our studies indicate that the f-actin ring is continuous, and NMMIIA and  $\alpha$ -actinin-4 are arranged in linear tracts on either side. The unique mechanical properties of a cell are in large part determined by the organization of the actin cytoskeleton and the degree of cross-linking by contractile NMMII proteins. As mentioned above, the contractile units of muscle cells, as well as, the AJR of certain epithelial cells are organized in a sarcomeric pattern. This organization is likely designed to promote contractions, like are characteristic of muscle cells. Somewhat surprisingly, this sarcomeric organization of the AJR was similarly observed in stomach and intestinal epithelial cells. Unlike muscle cells, the intestine, stomach, and the bladder undergo dramatic changes in luminal volume, and are characterized by extensive folding of the epithelium and lamina propria into rugae. We hypothesize that the increase in luminal volume that occurs in the gut or the stomach is primarily accommodated through the unfolding of the rugae, and the sarcomeric AJR promotes the contractions involved in passing chyme from the stomach to the duodenum, or peristalsis through the gut. On the other hand, the bladder must accommodate larger changes in urine volume, but over a more gradual time period; thus, the unfolding of the rugae is likely not sufficient to accommodate these dramatic changes. Additionally, the contraction of the umbrella cell AJR during voiding is much greater (in terms of

a decrease in AJR perimeter) and occurs much more rapidly than in the intestine or stomach, which undergo more pulsatile contractions, as described above. The unusual organization of the umbrella cell PJAR most likely reflects the necessities for AJR expansion to accommodate extreme increases in luminal volume, followed by a very rapid and large-scale contraction of the AJR.

As mentioned above, we observe that the umbrella cell f-actin ring is continuous, and is likely comprised of long, formin-generated cables of actin filaments. Consistent with this possibility, we observe that expansion of the umbrella cell AJR in response to stretch is sensitive to an inhibitor of formin-dependent actin polymerization. Interestingly, it has been shown that the formin mDia1 is mechanosensitive and pulling force applied to individual actin filaments is sufficient to promote an increased rate of filament elongation. Additionally, mDia1 is able to respond to an opposing pulling force by promoting barbed end polymerization thereby generating mechanical tension on actin filaments (Jegou *et al.*, 2013). Thus, formins could potentially both sense increased tension generated by bladder filling and respond to this increased force by generating tension on cortical actin filaments. We, also, tested the effects of the Arp2/3 inhibitor CK869, but we observed no significant impact on AJR expansion after treatment with this drug. However, it is possible that other more targeted inhibitors of Arp2/3 may reveal a requirement for this form of actin polymerization in future studies. We, also, observed that NMMIIA forms short linear structures that, similar to MDCK cells, overlap with the f-actin ring.  $\alpha$ -actinin-4, also forms a ring on either side of the f-actin ring, but they were thicker, more continuous tracts compared to those formed by NMMIIA. While we were unable to resolve changes in the actomyosin network in filled bladders versus those fixed five minutes after voiding, it is possible that during the actual voiding event actin,  $\alpha$ -actinin-4, and NMMIIA undergo a rapid and reversible re-arrangement, promoting contraction. Intriguingly, in the pupal wing of the fruit fly, junctional expansion requires the downregulation of NMMII activity (Bardet *et al.*, 2013). This could explain why inhibition of

NMMIII with Bleb has no effect on AJR expansion during bladder filling, but that voiding-triggered AJR contraction is sensitive to Bleb treatment.

Another difference in the AJR of filled versus voided bladders is the position of the f-actin ring with respect to the tight junction in the Z-axis. While the f-actin ring is easily resolved from the tight junction in filled bladders, this is not true of voided (or quiescent) bladders. Additionally, the AJR appears very narrow and tall in filled bladders, while it looks shorter and more rounded in voided and quiescent bladders. Whether these differences reflect changes in the folding of the cells or molecular rearrangements of the junctional complex is difficult to determine in these highly deformable cells and using the techniques we employed. In this regard, electron microscopy, similar to that performed by Efimova and Svitkina (Efimova and Svitkina, 2018), is likely to be highly revealing if it could be adapted to non-coverslip grown umbrella cells. Coupled with our previous observations that filling increases paracellular conductance of ions without altering barrier function (Carattino *et al.*, 2013), our current studies indicate that the filling/voiding cycle not only impacts the structure and function of the tight junction, also it apparently impacts the organization of the entire umbrella cell AJR.

### **2.3.2 Expansion of the umbrella cell apical junctional ring.**

Other than cell intercalation and cell extension in fruit flies (Butler *et al.*, 2009; Kong *et al.*, 2017), there are few reports of AJR expansion, particularly in response to external mechanical stimuli. Intriguingly, cultured endothelial cells increase the area of their adherens junction in response to applied stretch (Liu *et al.*, 2010), but also if they increase the perimeter of their AJR around each cell is unknown. In the case of the umbrella cell, we report that expansion of the AJR not only depends on the actin cytoskeleton, but also membrane trafficking events, likely exocytosis. In support of this latter possibility, we observe that AJR expansion is inhibited by treatment with BfA. This drug is a general inhibitor of biosynthetic traffic along the ER-to-Golgi

route (Klausner *et al.*, 1992), but can also impact cargo sorting events in endosomes (Wang *et al.*, 2001). The inhibition of AJR expansion by CHX is consistent with the possibility that biosynthetic traffic, possibly of newly synthesized junctional components, is involved; however, it is feasible that CHX is instead preventing the synthesis of a regulatory protein(s) that is necessary for AJR expansion to occur.

We, also, explored the role of trafficking pathways modulated by Rab11a, Rab8a, and Rab13 in AJR expansion. Our investigation was driven in part by a long-standing interest in the abundant population of subapical discoidal and/or fusiform vesicles that undergo regulated exocytosis in response to bladder filling (Apodaca, 2001b; Truschel *et al.*, 2002). Our previous studies, and those of others, established that these events were dependent on a Rab11a-Rab8a-Myo5b network (Khandelwal *et al.*, 2008; Khandelwal *et al.*, 2013), as well as on Rab27b-dependent exocytosis (Chen *et al.*, 2003; Gallo *et al.*, 2018). Although one would predict that a mechanism exists that coordinates the large increase in apical surface area with expansion of the AJR, in our current analysis we observe no significant role for Rab11a or Rab8a in AJR expansion. Instead, the expansion of the AJR is dependent on Rab13, a well-described regulator of tight junction protein trafficking (Marzesco *et al.*, 2002; Kohler *et al.*, 2004; Marzesco and Zahraoui, 2005; Yamamura *et al.*, 2008). Interestingly, in cultured epithelial cells, knockdown of Rab13 specifically reduces the trafficking of claudin-1 and occludin to the surface, but not E-cadherin (Yamamura *et al.*, 2008), whereas Rab8 (Yamamura *et al.*, 2008) and Rab11a (Lock and Stow, 2005; Desclozeaux *et al.*, 2008; Chung *et al.*, 2014; Woichansky *et al.*, 2016) are primarily associated with the membrane trafficking of cadherins. These findings are at odds with our analysis, as all components of the umbrella cell AJR appear to move synchronously. These differences may reflect cell specific Rab function. For example, in umbrella cells Rab11a primarily operates along the secretory pathway (Khandelwal *et al.*, 2008; Khandelwal *et al.*, 2013), whereas in many other cell types Rab11a functions within the endocytic system (Welz *et al.*, 2014). Another possible explanation for the observed differences is that we were exploring responses to external

mechanical forces, whereas the studies in cultured cells examined junction dynamics when extracellular  $\text{Ca}^{2+}$  was depleted and then replenished (Yamamura *et al.*, 2008).

### **2.3.3 Contraction of the umbrella cell apical junctional ring.**

Not only does the umbrella cell AJR expand during filling, but it contracts rapidly upon voiding. How quickly this occurs is unclear, although we know from studies of voiding-induced endocytosis in *ex vivo* preparations of bladder that apical membrane can be recovered on the order of several seconds (Khandelwal *et al.*, 2010). Presumably, the same is true of the AJR. Like expansion of the AJR, its contraction also depends on the actin cytoskeleton and membrane traffic; however, the specific molecules and pathways involved are different. During voiding, contraction of the AJR likely depends on the actin cytoskeleton and NMMII contraction as treatment with Cyto D or Bleb, an inhibitor of NMMIIA, NMMIIB, and NMMIIC (Allingham *et al.*, 2005; Zhang *et al.*, 2017), impairs AJR contraction. The lack of expression of NMMIIB in umbrella cells, would indicate that either NMMIIA or NMIIC is chiefly responsible for this contraction. However, the accumulation of NMMIIA on either side of the AJR, forming “railroad tracks,” suggests that it may be the primary regulator of AJR contraction in umbrella cells. We, also, noted that AJR contraction, but not its expansion, is dependent on RhoA, an important regulator of both actomyosin contraction upstream of NMMIIA and membrane internalization, including voiding-induced apical endocytosis in umbrella cells (Lamaze *et al.*, 2001; Doherty and McMahon, 2009; Khandelwal *et al.*, 2010; Mateus *et al.*, 2011).

Consistent with analyses of dorsal closure and cell intercalation in fruit flies (Levayer *et al.*, 2011), as well as the apical constriction that accompanies *Xenopus* gastrulation (Lee and Harland, 2010), we observe that endocytosis plays a critical role in the contraction of the umbrella cell AJR. Here, we observe that Pitstop2 and expression of DN-dynamin-1 both inhibit AJR contraction. Intriguingly, we previously reported that ZO-1 and actin are associated at the

cytoplasmic face of endocytic structures near to the AJR (PJAEs) (Khandelwal *et al.*, 2010). PJAEs accumulated near the AJR immediately upon voiding, indicating that the AJR may be a site for nucleation of endocytic structures. If other components of the AJR, including claudins, E-cadherin, or NMMIIA are also localized to these structures is unknown. We, also, previously reported that voiding-induced endocytosis was triggered by  $\beta$ 1-integrins and their downstream pathways (Khandelwal *et al.*, 2010). Again, it will be interesting to determine if similar pathways are involved in contraction of the umbrella cell AJR.

#### **2.3.4 Summary.**

Under normal physiological conditions, epithelial cells are exposed to mechanical forces as gases, fluids, and solids pass over their surfaces and push against them. How these external mechanical forces affect AJR activity (e.g., adhesion and permeability), remodeling, and stability has only received passing attention. Our studies demonstrate that as tension within the bladder wall builds during filling, the umbrella cell actively dissipates these forces by expanding its AJR, which depends on actin dynamics and Rab13-mediated trafficking events. Upon voiding, the decrease in wall tension likely triggers NMMIIA-dependent actomyosin contraction, which along with endocytosis returns the umbrella cell AJR back to its pre-tension state, ready for the next cycle of filling (**Figure 26**).

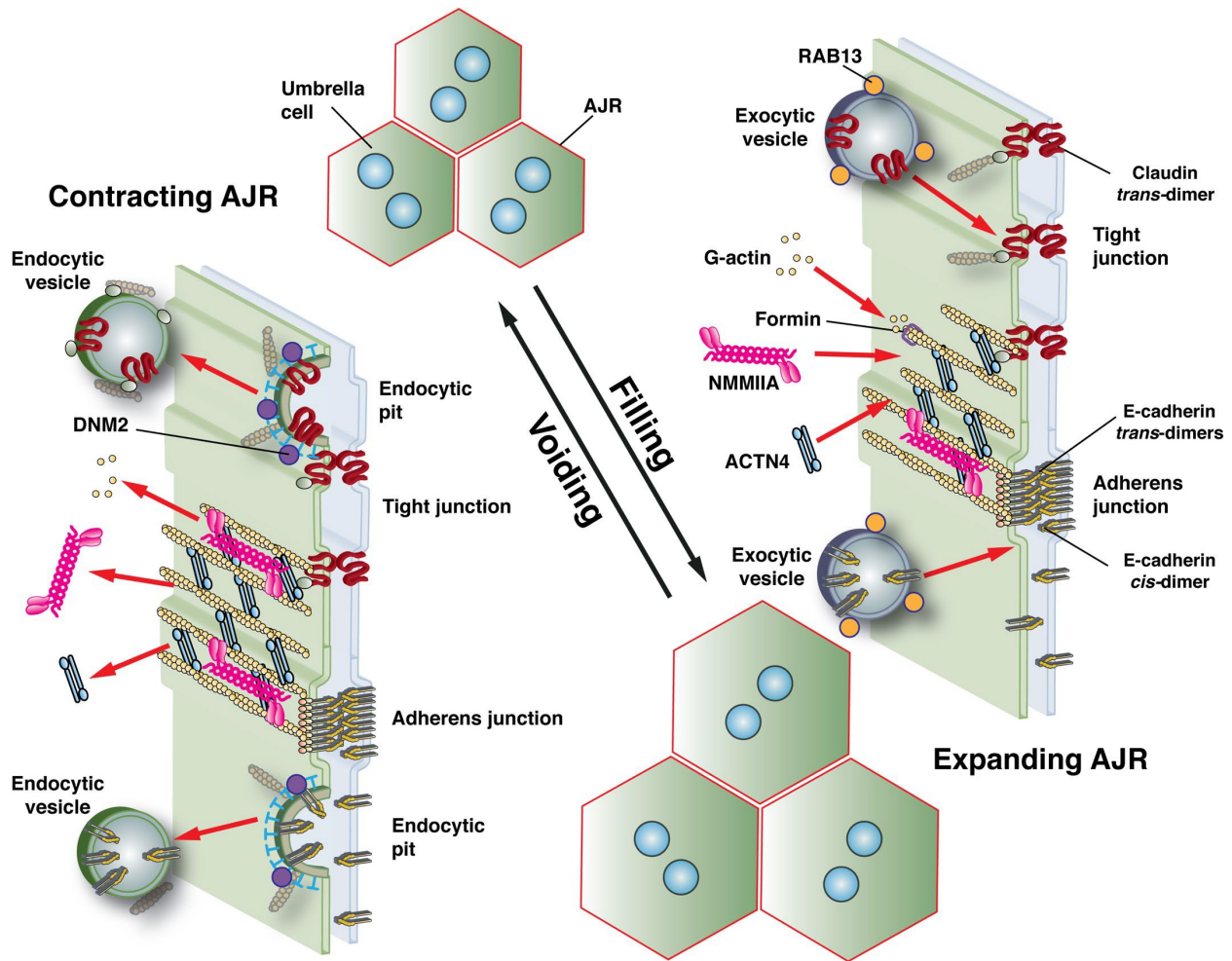


**Figure 26. Model for AJR dynamics during bladder filling and voiding.**

During bladder filling the AJR expands in a process that requires formin-dependent actin polymerization. AJR expansion also requires Rab13-dependent exocytosis, likely of tight and adherens junction-associated proteins. Although shown traveling in distinct vesicles, the tight and adherens-junction proteins may travel in the same exocytic vesicles. Upon voiding, the AJR contracts in a process that requires NMMIIA contraction of the PJAR. Contraction also depends on dynamin-2-dependent endocytosis of AJR-associated proteins. It is unknown whether endocytosis is clathrin-dependent or -independent, or whether endocytic vesicles contain both tight and adherens junction-associated proteins.

### **3.0 Perspectives and Future Directions**

Dramatic changes in luminal volume during the bladder cycle is, in part, accommodated by mechanically-stimulated membrane trafficking events which alter the umbrella cell's apical surface area (Minsky and Chlapowski, 1978; Lewis and de Moura, 1982, 1984; Apodaca, 2001b; Truschel *et al.*, 2002; Balestreire and Apodaca, 2007; Khandelwal *et al.*, 2008; Yu *et al.*, 2009b; Khandelwal *et al.*, 2010; Khandelwal *et al.*, 2013; Gallo *et al.*, 2018). Our current studies indicate that an additional mechanism of accommodation is the expansion and contraction of the umbrella cell AJR during filling and voiding, which also depends on membrane trafficking events (Carattino *et al.*, 2013; Eaton *et al.*, 2019). Despite these observations, there are still many questions that remain to be answered, such as how do the umbrella cells sense filling and what triggers voiding, how are distinct mechanosensitive events coordinated across such a large cell, and what are the molecular components that define umbrella cell paracellular permeability and how are they affected by stretch. We have some insights into these questions, as discussed below, but further work is needed to fully understand the umbrella cell's response to stretch and the role of the AJR in this response.

#### **3.1 Umbrella cell mechanotransduction.**

Our lab has shown that in bladder umbrella cells increasing tension in the umbrella cell plasma membrane during filling stimulates membrane trafficking events that result in a net addition of apical membrane. Subsequently, increased basolateral tension during voiding promotes endocytosis of the added apical membrane (Yu *et al.*, 2009b). Likely, changes in umbrella cell plasma membrane tension also promote the membrane trafficking events that

regulate the expansion and contraction of the AJR (Carattino *et al.*, 2013; Eaton *et al.*, 2019); however, we did not show this directly in our current studies. Despite these observations, the molecular mechanosensors that allow the bladder to sense filling and that promote voiding remain largely unknown.

### **3.1.1 Role of ENaC and a Nonselective Cation Channel.**

The presence of an apical mechanosensor in the umbrella cell is indicated by experiments showing that the exocytosis during filling is stimulated by increases in apical membrane tension (Yu *et al.*, 2009b). Stretch-regulated ion channels are a type of mechanosensor that is common to the majority of cells. In umbrella cells, the epithelial sodium channel (ENaC), which is expressed at the apical umbrella cell membrane (Smith *et al.*, 1998), and a nonselective cation channel (NSCC) are implicated as potential apical mechanosensors (Yu *et al.*, 2009b). Both types of channels are mechanosensitive, and NSCCs are known to facilitate  $\text{Ca}^{2+}$  entry into cells, thereby stimulating exocytosis (Hamill, 2006).

In support of a role for ENaC as an apical mechanosensor in umbrella cells, an increase in amiloride-sensitive current is observed when bladder filling is simulated in Ussing chambers (Lewis and de Moura, 1982), likely due to increased delivery of ENaC to the apical surface. Additionally, more recent studies have identified a requirement for ENaC in stretch-stimulated exocytosis during bladder filling (Yu *et al.*, 2009b). Interestingly, we observe that the expansion of the AJR during bladder filling is also significantly impaired by treatment with benzamil, a highly specific ENaC inhibitor (our unpublished data). These findings indicate that mechanically stimulated ENaC-mediated  $\text{Na}^+$  transport may be required for both the expansion of the apical domain and the AJR during bladder filling.

In addition to increasing  $\text{Na}^+$  transport, stretch promotes increased ion transport by an apically expressed NSCC (Wang *et al.*, 2003; Yu *et al.*, 2009b). This may facilitate  $\text{Ca}^{2+}$  entry into

the umbrella cell stimulating exocytosis either directly, or indirectly via  $\text{Ca}^{2+}$ -dependent  $\text{Ca}^{2+}$  release. To this point,  $\text{Ca}^{2+}$  depletion prevents the exocytic response in umbrella cells during filling (Yu *et al.*, 2009b). Although the identity of the NSCC is unknown, possible candidates include the Piezo channels (Miyamoto *et al.*, 2014; Dalghi *et al.*, 2019), the transient receptor potential (TRP) channels, or the P2X receptors, all of which are expressed in the urothelium and have been suggested as mechanosensors regulating filling-stimulated exocytosis in umbrella cells (Khandelwal *et al.*, 2009). To this point, knockdown of Piezo-1 or TRPV4 abrogates the stretch-stimulated  $\text{Ca}^{2+}$ -dependent ATP release in primary urothelial cultures (Mochizuki *et al.*, 2009; Miyamoto *et al.*, 2014). Similarly, TRPV1, TRPV4, or P2X<sub>3</sub> knockout mice show reduced ATP release upon bladder distention (Vlaskovska *et al.*, 2001; Yu *et al.*, 2011). However, further experiments will be needed to determine the role of stretch-regulated ion channels in the umbrella cell during the bladder cycle.

### **3.1.2 Junctional proteins as mechanosensors.**

Intercellular junctional complexes are well-described hubs for mechanotransduction, especially in the case of the adherens junction; however, the role that junctional proteins may play in the mechanotransduction pathways triggered by bladder filling and voiding remains unexamined. Both  $\alpha$ -catenin and ZO-1 are known to adopt extended conformations upon application of external stretch in cultured cells (Yao *et al.*, 2014; Spadaro *et al.*, 2017). However, the types of extrinsic forces that could lead to these conformational changes and the resulting cellular outcomes have not been studied in intact epithelial tissues to our knowledge.

It was originally shown that pulling on single  $\alpha$ -catenin molecules *in vitro* using magnetic tweezers causes  $\alpha$ -catenin to adopt an extended conformation (Yao *et al.*, 2014). This conformational change reveals a cryptic binding site, which recruits vinculin and reinforces the

adherens junction. Subsequently, it has been observed *in vivo* that acutely applied external force is sufficient to trigger this conformational change. Studies using a FRET-based  $\alpha$ -catenin tension sensor, in cultured MDCK cells, show that force-loading E-cadherin by twisting E-cadherin-coated beads causes  $\alpha$ -catenin to adopt its extended conformation and recruit vinculin (Kim *et al.*, 2015). Alternatively, when intercellular tension is reduced by disrupting cadherin-based adhesion with an E-cadherin blocking antibody or by  $\text{Ca}^{2+}$  depletion, or by disrupting the actin cytoskeleton using Cyto D, higher levels of FRET are observed indicating that  $\alpha$ -catenin adopts its relaxed or folded conformation under conditions of low tensile force. These observations support a model in which  $\alpha$ -catenin functions *in vivo* as a reversible mechanosensor downstream of force-loading on E-cadherin or the actin cytoskeleton.

Despite these insights, there is still very little known about whether  $\alpha$ -catenin adopts an extended conformation in response to intrinsic forces, like those generated during morphogenetic processes, or in response to external forces generated during everyday physiological processes. The internal mechanical forces generated during morphogenetic processes are transduced via mechanosensitive junctional proteins attached to the cytoskeleton and in this way trigger the apical contraction that is characteristic of epithelial remodeling events (Roh-Johnson *et al.*, 2012). Although the molecular mechanism of this response is not well understood, one recent report finds that proper dorsal closure in fruit flies is impaired by expression of  $\alpha$ -catenin mutants that are unable to bind the actin cytoskeleton due to a slowed rate of apical contraction (Jurado *et al.*, 2016). These results indicate that tension generated across  $\alpha$ -catenin via the actomyosin cytoskeleton, which would promote its extended conformation, is necessary for apical contraction during morphogenesis.

Even less is known about how  $\alpha$ -catenin's conformational state is affected by external forces, such as those generated during the bladder cycle. It would be interesting to use an antibody against the open conformation of  $\alpha$ -catenin (Biswas *et al.*, 2016), or an  $\alpha$ -catenin FRET

tension sensor (Kim *et al.*, 2015) to examine whether the external forces generated during bladder filling and voiding promote a conformational change in  $\alpha$ -catenin. Additionally,  $\alpha$ -catenin mutants that either lack the  $\beta$ -catenin binding site, and are therefore unable to adopt the open conformation (Kim *et al.*, 2015), or have a mutation that promotes unfolding in the  $\alpha$ 1 helix of the actin binding domain (Ishiyama *et al.*, 2018), could be used to determine the role the conformational switch plays in AJR remodeling during bladder filling and voiding.

Another protein that is reported to be a junctional mechanosensor is ZO-1, which adopts an extended conformation in response to externally applied force thereby regulating cell proliferation and barrier function (Spadaro *et al.*, 2017). These experiments provided the first evidence for a tight junction-associated mechanosensor; however, there has been no investigation into whether the extended conformation of ZO-1 plays a role in mechanically stimulated junctional remodeling, such as during morphogenesis or in response to physiological forces, such as during bladder filling. A proximity ligation assay, like used by Spadaro *et al.* (Spadaro *et al.*, 2017), or antibodies against the N-terminal and C-terminal of ZO-1 could be used to determine whether bladder filling causes ZO-1 to adopt its extended conformation.

Although we know from TEM studies that desmosomes are present in the umbrella cell AJC (C) (**Figure 1A**), there is very little literature looking at the molecular composition of the umbrella cell desmosome, or if it is affected by filling or voiding. It would be informative to use immunofluorescence to identify which desmosomal proteins are differentially expressed in the layers of the urothelium, like is reported in other stratified epithelia, such as the skin (C). It would be revealing in the future to specifically knockdown desmosomal proteins that are expressed in the different layers of the urothelium to uncover distinct functions for these proteins. Likely, the desmosomal proteins found in the basal cell layers of the urothelium play a role in differentiation, like is observed in the skin (C). This could be investigated using models that look at urothelial differentiation after desquamation, such as occurs after spinal cord injury (C). On the other hand,

the desmosomal proteins expressed in the suprabasal layers are likely central to adhering adjacent cells to each other and defining the mechanical properties of the urothelium (C). It would be interesting to use atomic force microscopy to investigate whether knocking down desmosomal proteins expressed in the intermediate or superficial cell layers affects the stiffness, or adhesive properties of the cells (Fung *et al.*, 2011; Vielmuth *et al.*, 2015).

Interestingly, it has been shown that desmosomal proteins experience tensile force when cells are exposed to mechanical stimuli (Baddam *et al.*, 2018; Price *et al.*, 2018); however, there is very little direct evidence in support of desmosomes acting as mechanosensors, or transducers. Although structurally similar to the adherens junction, the desmosome does not have a direct homologue of  $\alpha$ -catenin, which is the best characterized mechanosensitive protein present in the AJC. However, like  $\alpha$ -catenin for the adherens junctions, desmoplakin links the desmosome to the cytoskeleton and is composed of spectrin-like repeats, which are known to unfold under tension (Rief *et al.*, 1999). This indicates that desmoplakin could undergo a force-dependent conformational change. Intriguingly, a number of disease-causing mutations are found within this spectrin-repeat domain, which act to destabilize the helices (Ortega *et al.*, 2016). These findings indicate that this region plays an important role in proper desmosomal function, possibly by undergoing a mechanosensitive conformational change; however, future investigation will be necessary to explore this possibility. In the current studies, we did not investigate whether the desmosomal or keratin junctional rings expand with the rest of the AJR, however this would be an interesting line of future inquiry, as well.

### **3.1.3 The actomyosin cytoskeleton is mechanosensitive.**

In addition to the known mechanosensory properties of proteins associated with the AJC, the actomyosin cytoskeleton and many of the affiliated proteins are also mechanosensitive. Two

well-known mechanosensitive proteins which cross link actin filaments within the AJR are NMMIIA and  $\alpha$ -actinin-4. We observed that both of these proteins localize to either side of the continuous umbrella cell PJAR in a “railroad track” distribution (**Figure 18**). Intriguingly, both of these proteins have been reported to accumulate at the plasma membrane in response to an externally applied force (Fernandez-Gonzalez *et al.*, 2009; Schiffhauer *et al.*, 2016). At the resolution that we imaged our whole mount tissues in the current studies, we were unable to discern whether there were changes in the localization of either of these proteins during filling or voiding. In the future it would be revealing to employ a high-resolution, or quantitative, imaging technique which would allow us to determine whether there is an accumulation of these proteins at the junction as plasma membrane tension increases during filling in preparation for the coordinated NMMII-dependent contraction of the AJR during voiding. A line intensity scan of the AJR in quiescent and voided versus filled bladders could identify whether there is an increase in  $\alpha$ -actinin-4 or NMMIIA fluorescence intensity at the AJR. Alternatively, using real time fluorescence recovery after photobleaching (FRAP) on isolated urothelium could be used to determine whether new  $\alpha$ -actinin-4 or NMMIIA is recruited to the AJR when the bladder is stretched.

### **3.2 Coordination of umbrella cell mechanotransduction.**

Umbrella cells are exceptionally large epithelial cells, reaching up to 100  $\mu\text{m}$  in diameter. This raises the question of how such dynamic, and rapid (in the case of voiding) changes are coordinated over the space of such a large cell. The umbrella cell AJR mechanically integrates adjacent cells through indirect interactions of transmembrane junctional proteins with the cell's cytoskeleton. We suggest that the AJR, and its associated cytoskeletal network, acts as a master regulator of the umbrella cell's response to the forces experienced during filling and voiding.

Intriguingly, the umbrella cell cytoskeleton is organized into a “rim-and-spoke” structure with f-actin and keratin networks traversing the cytoplasm and inserting into actin and keratin rings which completely circumscribe umbrella cells at their apico-lateral borders. This organization may enable the umbrella cell AJR and its associated cytoskeleton to coordinate multiple signaling pathways. For example, those regulating the surface area of the apical domain and the perimeter of the AJR during filling and voiding, or events occurring at the apical and basolateral membrane domains.

### **3.2.1 Role of the umbrella cell cytoskeleton.**

The umbrella cell is characterized by a dense cytoplasmic cytoskeletal network with a highly specialized organization that most likely reflects the umbrella cell’s function. As mentioned above, when looking at the umbrella cell layer *en face* it is apparent that the network of cytoplasmic actin and cytokeratin filaments terminate at ring-like structures that completely circumscribe the apico-lateral membrane of the cell (**Figures 18 and 27**). In the case of the actin cytoskeleton the ring is formed by large tangential bundles of f-actin running parallel to the lateral membrane; whereas the cytokeratin ring is proposed to be formed by the lateral-most walls of the “trajectories” within the network (Veranic and Jezernik, 2002).

In addition to this “rim-and-spoke” organization, in the plane of the membrane, the components of the umbrella cell’s cytoskeleton are also segregated into zones in an apical-to-basal orientation. Most apically, a thin layer of cortical actin is present just below the umbrella cell plasma membrane. Underlying the actin network, a few hundred nanometers below the apical membrane, begins a thicker belt of cytokeratin 20 (CK20) which forms a mesh-like network of “trajectories” encasing the uroplakin-positive DFV (Minsky and Chlapowski, 1978; Veranic and Jezernik, 2002). Most apically, and closest to the cortical actin layer, the “trajectories” within the cytokeratin meshwork have smaller diameter openings that gradually become larger moving

towards the basal surface of the umbrella cell (Veranic and Jezernik, 2002). When the DFV are examined using deep etch electron microscopy it becomes apparent that they are bound to short branched actin filaments on their cytoplasmic face, and these actin filaments are indirectly associated with cytokeratin intermediate filaments (Terada *et al.*, 2009). This organization indicates that there is an, as of yet, unidentified protein or protein complex that mediates the association of the actin and cytokeratin cytoskeletal networks. A possible candidate is plectin, which is highly expressed at the apical surface of the umbrella cells (Veranic and Jezernik, 2002), and is a member of the plakin family of proteins, which mediate cross-linking between different components of the cytoskeleton (Jefferson *et al.*, 2004).

The elastic properties of the cytokeratin network (Charrier and Janmey, 2016) likely provide mechanical support for the umbrella cells as they stretch, while allowing the umbrella cells to contract back to their smaller, quiescent size and shape extremely rapidly upon voiding. It would not be surprising if the unique elastic properties of the cytokeratin network also facilitate the rapid contraction of the AJR that occurs with bladder voiding. Although, the contraction of actomyosin rings is reported in a variety of cellular processes, the contraction of the umbrella cell AJR occurs on a much faster time scale. For example, cytokinesis occurs over hours (Bryant and Francis, 2008), whereas the contraction of the umbrella cell AJR can occur in just minutes, or even seconds (Carattino *et al.*, 2013; Eaton *et al.*, 2019). For the cytokeratin and actin rings and their associated cytoplasmic networks to contract in a coordinated manner they would need to be physically associated. It is known that there are junctional proteins that bind to components of both the actin and cytokeratin cytoskeletons, such as plectin (mentioned above), or plakoglobin which can bind both adherens junction and desmosomal proteins. These linker proteins could serve as a mechanism to integrate the AJR and its associated cytoplasmic cytoskeletal networks into a functionally unified complex.

A number of labs have reported a requirement for the actin cytoskeleton during the expansion of the apical domain and the AJR during bladder filling and during the voiding-induced

internalization of the apical membrane and contraction of the AJR (Lewis and de Moura, 1982; Yu *et al.*, 2009b). Additionally, a necessity for the cytokeratin network in the membrane trafficking events regulating the expansion and contraction of the apical domain is indicated by experiments using the keratin disrupting agent, thioglycolic acid, which appears to block DFV exocytosis with bladder filling (Sarikas and Chlapowski, 1989). A requirement for the cytokeratin network is further supported by Veranic and Jezernik's observation that bladder filling promotes a 70% increase in the diameter of the "trajectories" within the cytokeratin network, which they propose facilitates the movement of DFV towards the apical pole of the umbrella cell (Veranic and Jezernik, 2002). Interestingly, bladder filling leads to a physical reorganization of the cytokeratin network from a random orientation of filaments in voided bladders to filaments that are aligned parallel to the umbrella cell apical plasma membrane in filled bladders. This reorganization may correlate with the increasing diameter of the "trajectories" within the network and thereby promote the apical movement of DFV. However, further investigation is needed to fully understand the interplay between the actomyosin and cytokeratin networks and their association with the AJR in umbrella cells.

### **3.2.2 Role of $\alpha$ -actinin-4.**

A protein that is a particularly compelling candidate as a coordinator of mechanically stimulated events in the umbrella cell is  $\alpha$ -actinin-4. The reasons include: its calcium sensitivity, and its mechanosensitive conformational change (which both regulate its actin binding affinity), its role in the regulation of force transmission through  $\beta$ 1-integrins (Otey and Carpen, 2004), and its unique distribution in umbrella cells. Intriguingly, when rat bladder is viewed in cross-section  $\alpha$ -actinin-4 forms a lacey web that is strikingly similar to the CK20 network (**Figure 27A**). Additionally, looking at the umbrella cell layer *en face* it becomes readily apparent that the CK20

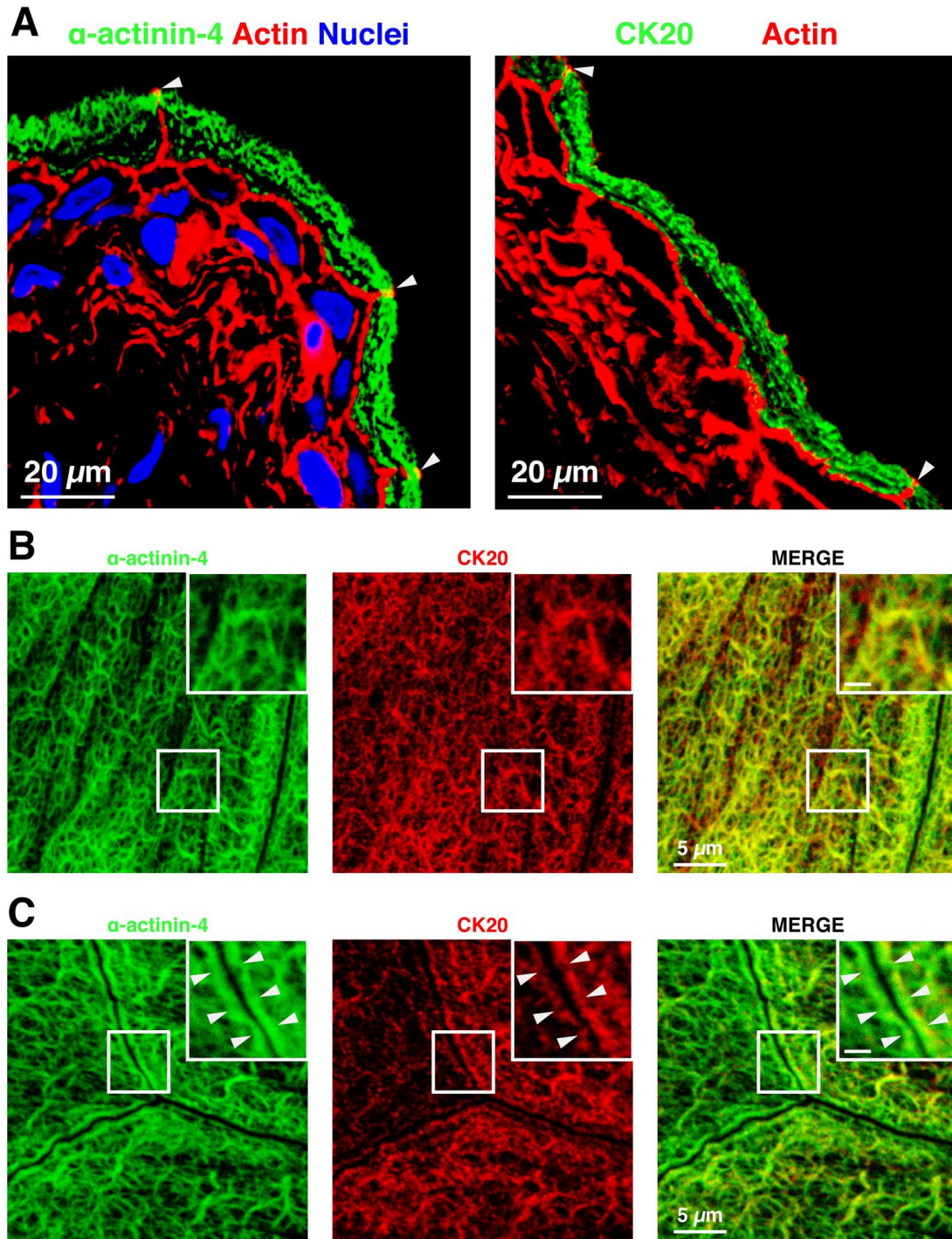


**Figure 27.  $\alpha$ -actinin-4 colocalizes with the cytokeratin network.**

(A) Cross section views of rat bladders with the apical-most tight junction indicated with arrowheads. Sections are labeled with antibodies against  $\alpha$ -actinin-4, left (green) and CK20, right (green). The F-actin cytoskeleton is labeled with Rhodamine-phalloidin (red) and nuclei with To-Pro-3 (blue). Images are 3D reconstructions of confocal images. Scale bars = 20  $\mu$ m. (B-C) *En face* view of the umbrella cell layer of whole-mount rat bladders with the AJR indicated with arrowheads and labeled with antibodies against  $\alpha$ -actinin-4 (green) and CK20 (red). Insets are magnifications of the boxed regions. Images are 3D reconstructions of confocal Z-stacks. Scale bars = 5  $\mu$ m.

network colocalizes prominently with  $\alpha$ -actinin-4 at the apical pole of the umbrella cell (**Figure 27B**). These results indicate that these two structures may be physically and functionally associated.

As mentioned above,  $\alpha$ -actinin-4 which colocalizes with CK20 along the cytoplasmic edge of the umbrella cell PJAR (**Figures 18 and 27C**, see arrowheads in inset), also, colocalizes with the CK20 network that runs throughout the entire cytoplasm. This suggests that  $\alpha$ -actinin-4 is either directly or indirectly associated with the cyokeratin network and may act to coordinate events happening at the junctions and throughout the rest of the umbrella cell. For example, the Rab13-dependent expansion of the AJR, and events happening below the apical membrane, like expansion of the cyokeratin trajectories to allow for DFV exocytosis. It is possible that an increase in the actin binding affinity of  $\alpha$ -actinin-4, due to increased plasma membrane tension during bladder filling, acts to recruit the protein priming the umbrella cell for rapid contraction during voiding. Recruitment of  $\alpha$ -actinin-4 during filling may, also, promote AJR expansion by recruiting additional proteins, such as Rab13, proximal to the AJR. This possibility will be discussed further below (**Section 3.2.4**).

In addition to being expressed at the AJR and in a network underlying the apical umbrella cell membrane, both the CK20 and  $\alpha$ -actinin-4 can be found along the basal membrane of the umbrella cells (**Figure 27A**). Our lab observes that apical endocytosis during voiding requires activation of basolateral  $\beta$ 1-integrins, phosphoinositide 3-kinase (PI3K), and RhoA (Khandelwal *et al.*, 2010). These observations highlight the need to coordinate signaling events happening at the basolateral surface and trafficking events occurring at the apical surface of the umbrella cell. Intriguingly,  $\alpha$ -actinin-4 is reported to bind directly to both  $\beta$ 1-integrins and PI3K, where it regulates force transmission and cytoskeletal organization (Otey and Carpen, 2004). This indicates a possible role for  $\alpha$ -actinin-4 in coordinating the responses to filling and voiding at the apical and basal membrane domains. In the future it would be interesting to perform biochemical

experiments to examine whether  $\alpha$ -actinin-4 binds to  $\beta$ 1-integrins, PI3K, or CK20 in umbrella cells and whether this interaction plays a role in regulating umbrella cell mechanotransduction during filling and voiding. Additionally, novel binding partners of  $\alpha$ -actinin-4 may be revealed, which could bring to light new functions of this protein.

### **3.2.3 Role of Rab GTPases.**

Presumably, if the AJR and apical domain of the umbrella cell did not expand concertedly during filling, then the added apical membrane would be forced to protrude into the lumen of the bladder, ultimately decreasing its capacity. Therefore, one would predict that a mechanism exists that coordinates the increase in apical surface area with the expansion of the AJR. However, in our current analysis we observe no significant role for Rab11a or Rab8a, which regulate the expansion of the apical domain, in AJR expansion. Instead, the expansion of the AJR is dependent on Rab13, a well-described regulator of tight junction protein trafficking.

The movement of DFV from the cyokeratin network to the actin network corresponds with a conversion from Rab11a-positive DFV to Rab8a-positive DFV. To this point, Rab11a is primarily found associated with DFV within the cyokeratin network, whereas Rab8a-DFV are concentrated within the thin band of cortical actin proximal to umbrella cell apical membrane, although there are Rab8a positive vesicles found in the basolateral cytoplasm of the umbrella cell, as well (Khandelwal *et al.*, 2013). Interestingly, Rab27b, which is reported to regulate DFV exocytosis independently of Rab8a and Rab11a, localizes primarily to the cortical actin network (Gallo *et al.*, 2018). Due to antibody limitations, we were unable to localize Rab13-positive vesicles within the cytoskeletal networks. It would be interesting in the future to exogenously express a fluorescently tagged form of Rab13 and see where it localizes within the cyokeratin or actin networks, and if there is any colocalization among the different populations of Rab-positive vesicles.

Presumably the different Rab species associate with adaptor proteins that expedite vesicle trafficking through the different cytoskeletal components. Intriguingly, not only is Rab-dependent trafficking regulated by the actin cytoskeleton and its effectors, but conversely Rabs and their effectors are known regulators of the actin cytoskeleton. For example, many Rab13 effectors localize to the actin cytoskeleton, and all of its known effectors can promote actin polymerization (Ioannou and McPherson, 2016). Although Rab13 is especially well-characterized in this respect, both Rab8 and Rab11 also are known to indirectly regulate the actin cytoskeleton via activation of Rho GTPases (Bravo-Cordero *et al.*, 2016; Bouchet *et al.*, 2018). Interestingly, in umbrella cells Rab8a is found co-localizing with the actin-based motor, Myo5B, which promotes movement of DFV through the cortical actin network (Khandelwal *et al.*, 2013). On the other hand, Rab11a, although it, also, partially colocalizes with Myo5B, most likely associates with additional, as of yet unidentified adaptor proteins. Possible roles for these adaptor proteins include facilitating DFV movement through the cyokeratin network, most likely some kind of motor protein, and promoting the conversion of DFV from Rab11a to Rab8a-positive vesicles, probably a Rab11 GTPase-Activating Protein (GAP) that may, also, act as a Rab8 recruitment factor or GEF. However, the identity of further Rab8a, or Rab11a, or Rab13 adaptor proteins remains unknown, and will require further investigation.

#### **3.2.4 Role of Rab13/JRAB-MICAL-L2/ $\alpha$ -actinin-4 signaling cascade.**

As mentioned above, instead of observing a common membrane trafficking pathway regulating both the increase in apical surface area and AJR expansion, we identified a unique Rab13-dependent pathway that controls AJR expansion (Eaton *et al.*, 2019). Intriguingly, Rab13 has been reported to form a tripartite complex with  $\alpha$ -actinin-4 via a cytoplasmic linker protein, JRAB/MICAL-L2. This interaction is promoted by Rab13-GTP binding to JRAB/MICAL-L2,

causing a conformational change in JRAB, which reveals a cryptic  $\alpha$ -actinin-4 binding site (Sakane *et al.*, 2016). By concurrently binding to  $\alpha$ -actinin-4, at the plasma membrane, and to Rab13, JRAB/MICAL-L2 is able to recruit Rab13-positive vesicles to the membrane, priming them for fusion. Co-sedimentation experiments have shown that  $\alpha$ -actinin-4 is able to bind f-actin and the Rab13-JRAB/MICAL-L2 complex simultaneously (Sakane *et al.*, 2012), so it is possible that Rab13 vesicles could be tethered via  $\alpha$ -actinin-4 to the umbrella cell AJR prior to or during filling-stimulated exocytosis. However,  $\alpha$ -actinin-4 is also known to interact directly with junctional proteins, such as  $\alpha$ -catenin or ZO-1, so it may be that  $\alpha$ -actinin-4 is tethering the Rab13-JRAB/MICAL-L2 complex directly to the umbrella cell AJC in preparation for fusion during filling. In addition to the biochemical and morphological data showing the formation of the tripartite complex at the plasma membrane, functional experiments have shown that the formation of this complex does indeed promote exocytosis. One well-described stimulus that triggers the formation of the tripartite complex is insulin, which ultimately leads to insertion of the glucose transporter type 4 (GLUT4) into the plasma membrane via exocytosis (Sun *et al.*, 2016). Supporting the conclusion that the formation of this complex promotes GLUT4 exocytosis, knockdown of  $\alpha$ -actinin-4, or inhibition of the Rab13-JRAB/MICAL-L2 complex binding to  $\alpha$ -actinin-4, prevents the delivery of GLUT4.

In the context of cell-cell junctions, knocking down  $\alpha$ -actinin-4 slowed the localization of occludin to the AJC after  $\text{Ca}^{2+}$  switch (Terai *et al.*, 2006). Like after insulin stimulation, inhibiting the Rab13-dependent conformational change of JRAB/MICAL-L2, or preventing JRAB/MICAL-L2 from binding to Rab13 or  $\alpha$ -actinin-4, impairs the maturation of cell-cell junctions after  $\text{Ca}^{2+}$  switch in cultured epithelial cells (Marzesco *et al.*, 2002; Yamamura *et al.*, 2008; Sakane *et al.*, 2012). This indicates that the formation of the tripartite complex regulates delivery of junctional proteins during the establishment of the AJC, most likely by docking Rab13-positive vesicles containing junctional proteins proximal to the AJC in preparation for fusion.

In our current studies we show that Rab13, as well as new protein synthesis, are required for the expansion of the AJR with filling (**Figures 21 and 22**). Additionally,  $\alpha$ -actinin-4 localizes prominently on either side of the PJAR associated with the umbrella cell AJC (**Figure 18**). Based on these observations, and the established literature, we hypothesize that expansion of the AJR during filling requires the formation of the tripartite complex, which promotes the delivery of junctional proteins via Rab13-dependent exocytosis (**Figure 28**). Briefly, we propose that initially, newly synthesized vesicles exit the TGN, possibly bound to Rab13-GDP. Alternatively, another Rab may facilitate vesicle exit from the TGN, and Rab13-GDP may be a passive cargo, or become associated with the vesicles as they mature. Unlike many other Rab proteins, Rab13 is able to traffic on vesicles in its GDP-bound form (Ioannou and McPherson, 2016). Subsequently, Rab13-GDP is converted to Rab13-GTP by an unknown Rab13 GEF, which may also act to recruit JRAB/MICAL-L2. Rab13-GTP binds to JRAB/MICAL-L2, promoting its conformational switch, and allowing it to bind to  $\alpha$ -actinin-4. The formation of this complex effectively recruits the Rab13-GTP vesicles, presumably containing AJR proteins, to the umbrella cell AJR prior to fusion.

It would be conceptually straight forward to assess whether the tripartite complex is formed during filling using both biochemical and imaging techniques. CoIP and indirect immunofluorescence experiments on filled, voided, and quiescent bladders could reveal whether the Rab13/JRAB-MICAL-L2/ $\alpha$ -actinin-4 complex formation is promoted by filling. However, the way that we prepare the bladders only gives us a snapshot of what is happening after the bladder is completely full. If the purpose of the complex is to promote fusion and allow the umbrella cells to accommodate filling, then the complex may form and subsequently disassociate after fusion, but prior to the completion of filling. If this is the case, it may be hard to detect the formation of the complex at the timepoints used in our current studies by immunofluorescence or CoIP. One solution to this would be to utilize FRET-based sensors and live-imaging to track the movement and possible association of the different components of the complex. Alternatively, mutants of

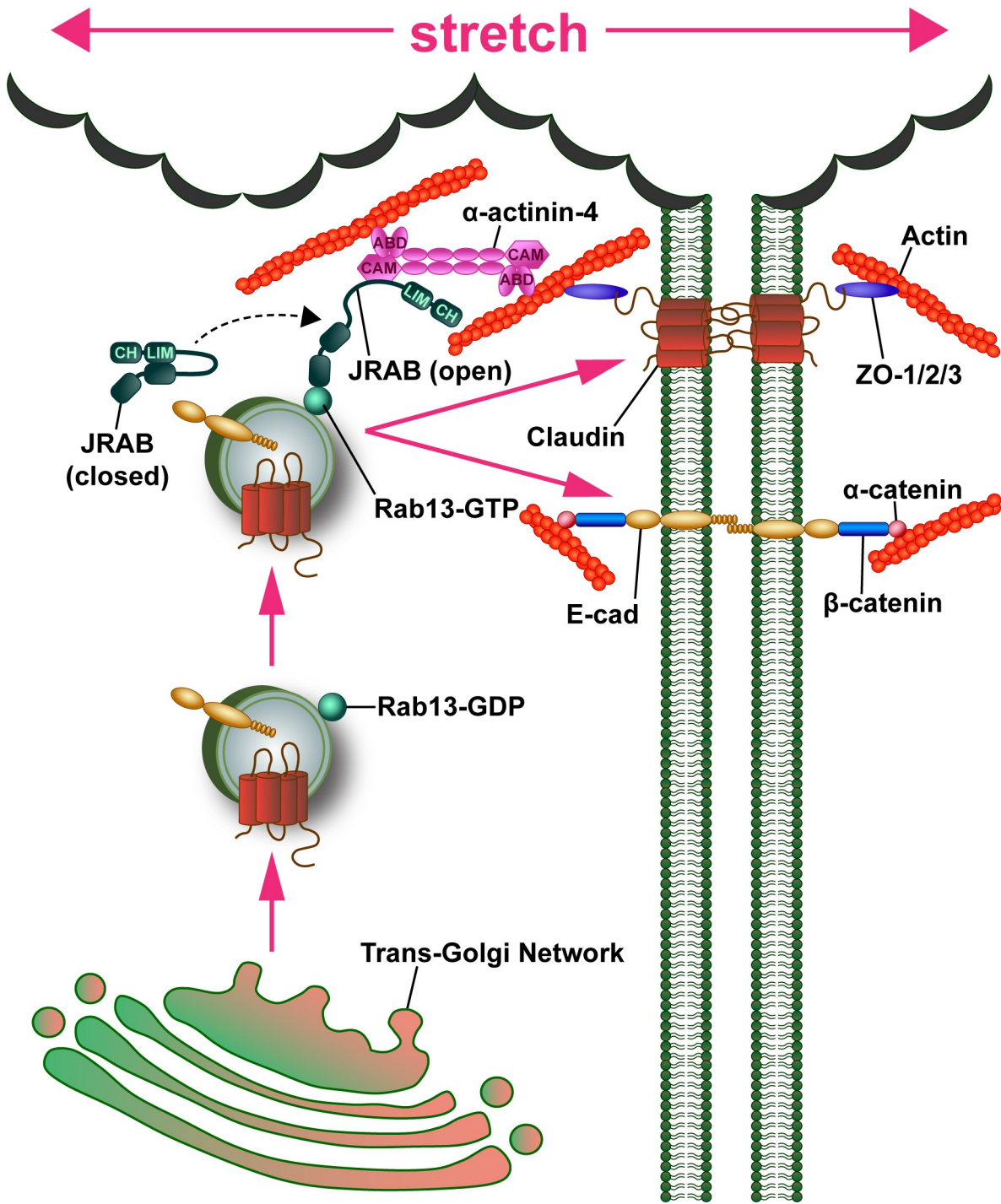


**Figure 28. Proposed model of Rab13-JRAB/MICAL-L2- $\alpha$ -actinin-4 signaling cascade.**

Newly synthesized vesicles exit the TGN, where they associate with Rab13-GDP. Rab13-GDP recruits an unknown Rab13 GEF, which promotes conversion of Rab13-GDP to Rab13-GTP. Subsequently, JRAB/MICAL-L2 is recruited and converted to its open conformation by Rab13-GTP binding and tethers the Rab13-GTP vesicles close to the AJC via interaction with PJAR-associated  $\alpha$ -actinin-4 prior to fusion. It is, also, possible that  $\alpha$ -actinin-4 directly links the Rab13-JRAB complex to the AJC via interactions with junctional proteins such as,  $\alpha$ -catenin or ZO-1.

Rab13, JRAB/MICAL-L2, or  $\alpha$ -actinin-4 that prevent or promote the formation of the complex could be used to assess its role during filling and voiding.

### 3.3 Umbrella cell paracellular permeability.

The primary function of the umbrella cell is the maintenance of the highly impermeable barrier between the internal environment and the extracellular toxic solutes and metabolites found in the urine. This barrier is formed by an intact apical plasma membrane and high-resistance tight junctions within the AJC. Intriguingly, when bladder filling is mimicked by stretching isolated urothelium in our specialized Ussing chambers (**Appendix, Figure S1**) we observe a dramatic decrease in TER, which is fully reversible after removing the stretch stimulus (**Figure 14**) (Carattino *et al.*, 2013). By definition TER is a measure of both transcellular, and paracellular resistances. The components that contribute to transcellular resistance are the resistance of the apical and basolateral plasma membranes; whereas, the contributions to paracellular resistance include the resistances across the tight junction and the lateral intercellular space (LIS) (Claude, 1978). We know that transcellular ion transport is increased in umbrella cells by stretch, leading to a decrease in TER (Lewis *et al.*, 1976; Lewis and de Moura, 1982; Wang *et al.*, 2003; Yu *et al.*, 2009b). More recently, we observed that paracellular resistance is also decreased by simulating bladder filling (**Figure 15**) (Carattino *et al.*, 2013). However, the mechanisms behind the force-induced increase in paracellular permeability are not well-understood. There are several possibilities which may contribute. The first is that the organization and/or number of tight junction strands is altered by filling and voiding. The second possibility is that there are reversible changes in the LIS between adjacent cell membranes, which would affect paracellular permeability. Finally, there is a third possibility: pore-forming claudins are delivered to the tight junction via exocytosis during bladder filling, and then recovered by endocytosis upon voiding. Our empirical

observations of these different parameters and their theoretical contributions to umbrella cell paracellular permeability during the bladder cycle are discussed below.

### **3.3.1 Tight junction strands.**

Tight junction strands act as a series of resistive elements; therefore, not surprisingly, experimental data generally supports a correlation between the number of strands and the permeability of the AJC (Claude and Goodenough, 1973). Furthermore, stretch-stimulated changes in strand organization are indicated by a large number of studies showing that experimental stretch leads to a re-organization of tight junction strands (Pitelka *et al.*, 1973; Hull and Staehelin, 1976; Metz *et al.*, 1977; Koga and Todo, 1978; Metz *et al.*, 1978; Greven and Robenek, 1980; Pitelka and Taggart, 1983; Akao *et al.*, 2000). We hypothesize that bladder filling stimulates a reduction in the number of umbrella cell tight junction strands, which could partially explain the increase in paracellular permeability we observe. Freeze fracture studies examining the ultrastructure of the tight junction in filled versus voided bladders would offer insight into this possibility. Additionally, the permeability of the tight junction could be affected by changes in claudin expression within the strands during the bladder cycle. Performing immuno-electron microscopy in conjunction with freeze fracture studies would identify whether the relative expression of certain claudin species is affected by filling or voiding.

### **3.3.2 Lateral intercellular space.**

Changes in LIS also affect permeability of the AJC. Theoretically, if the width of the LIS increases, then  $R_J$  will decrease, and vice versa (Claude, 1978). Interestingly, we observe a significant increase in the width of the LIS in filled bladders, relative to voided or quiescent bladders, using TEM (**Figure 29**). This data indicates that a widening of the LIS between umbrella

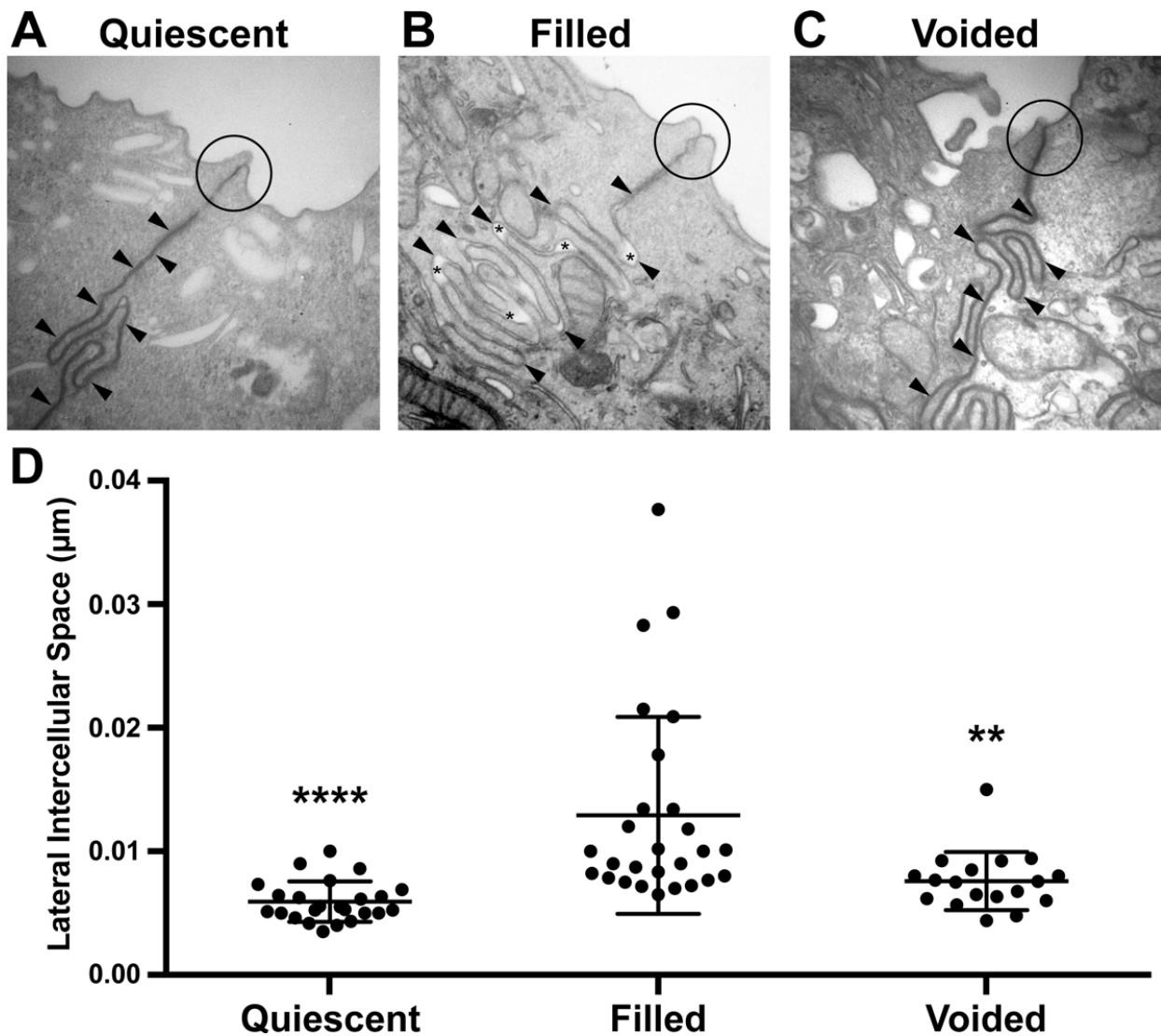


**Figure 29. Stretch increases umbrella lateral intercellular space.**

(A-C) Cross-section SEM images of (A) quiescent, (A) filled, and (C) voided rat bladders with the apical-most tight junction circled and the lateral intercellular space of adjacent umbrella cells indicated with arrowheads. Areas of increased LIS in filled bladders are indicated with asterisks.

cells may contribute to the increase in paracellular permeability with stretch. Additionally, we observe that the lateral junctions became more compressed when the bladders are filled, and the increases in LIS appear to occur primarily at the bends in the lateral junction (see arrowheads in **Figure 29**). Increases in lateral folding of the junctions have been previously reported in filled bladders across a variety of different species (Minsky and Chlapowski, 1978). Despite these observations, it is difficult to quantify what impact this increase in LIS has on the overall

permeability of the umbrella cell paracellular pathway, although presumably it would facilitate an increase in permeability, which agrees with our electrophysiological data (Carattino *et al.*, 2013).

### 3.3.3 Membrane trafficking of junctional proteins.

Taking these other factors into account, it still seems likely that the increase in paracellular permeability observed with bladder filling is, at least in part, due to the membrane trafficking of tight junction proteins. We propose that the exocytic delivery of pore-forming claudins increases paracellular permeability with filling, whereas voiding stimulates the endocytic internalization of pore-forming claudins allowing the umbrella cell tight junction to return to its higher-resistance state. It seems likely that other junctional proteins are trafficked synchronously with claudins, although not necessarily in the same vesicles, promoting the physical expansion and contraction of the entire AJR, in addition to changes in permeability.

Indeed, our data indicates that tight junction proteins are trafficked during bladder filling and voiding. For one thing, intracellular, punctate accumulations of claudin-8 were observed in voided or quiescent bladders but were not present in filled bladders (**Figure 16**) (Carattino *et al.*, 2013). Additionally, ZO-1, which links the AJC to the PJAR, was observed in endosomes adjacent to the AJR (PJAEs) within ten minutes of voiding (**Figure 11**) (Khandelwal *et al.*, 2010). However, neither of these tight junction proteins are reported to form pores in the intercellular space. Although the increase in permeability could be explained by the internalization of a sealing claudin from the apical tight junction during filling, such as claudin-8, this is not what we observe using indirect immunofluorescence (**Figure 16**), although it is difficult to determine what is happening at the apical-most tight junction itself.

On the other hand, claudin-4 has been reported to act as an anion-specific pore in collecting duct cells of the kidney (Hou *et al.*, 2010), and when we knockdown claudin-4 in umbrella cells using shRNA (**Figure 30A**) the paracellular pathway becomes relatively less

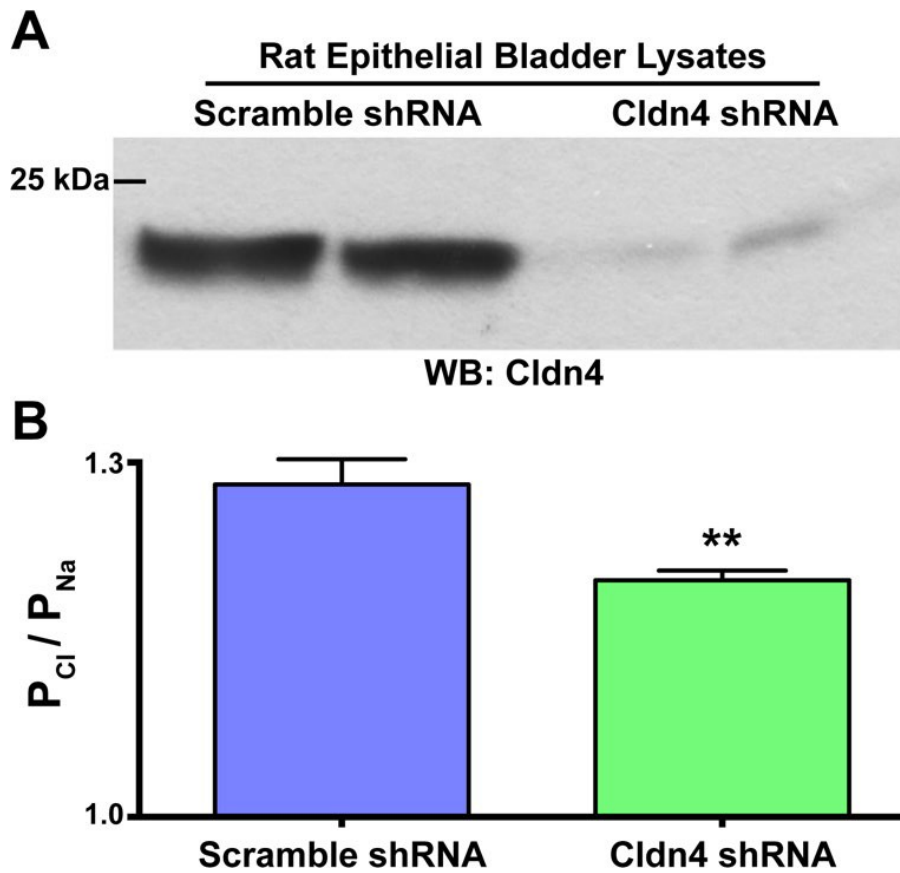


**Figure 30. Claudin-4 knockdown decreases paracellular permeability to anions.**

(A) Claudin-4 shRNA causes a 91% decrease in total protein expression. (B) Relative Cl:Na permeability in control shRNA and cld4 shRNA expressing rat bladders (n=3).

permeable to anions (**Figure 30B**). This result indicates that claudin-4 may act as an anionic pore-former throughout the entire urinary system. Intriguingly, in the urothelium of quiescent bladders, claudin-4 is expressed at the apical tight junction (marked with ZO-1, indicated with arrowheads, and expanded in bottom panels), along the umbrella cell basolateral membranes, and throughout the plasma membranes of the intermediate and basal cell layers (**Figure 31A**). Subsequently, when the bladder is full, claudin-4 expression is decreased in the umbrella cell lateral membranes (**Figure 31B**) and after voiding its expression in the umbrella cell layer appears restricted exclusively to the apical-most tight junction (**Figure 31C**). Thus, claudin-4 may form an anion-specific pore in umbrella cells and undergoes a dramatic redistribution in umbrella cells during

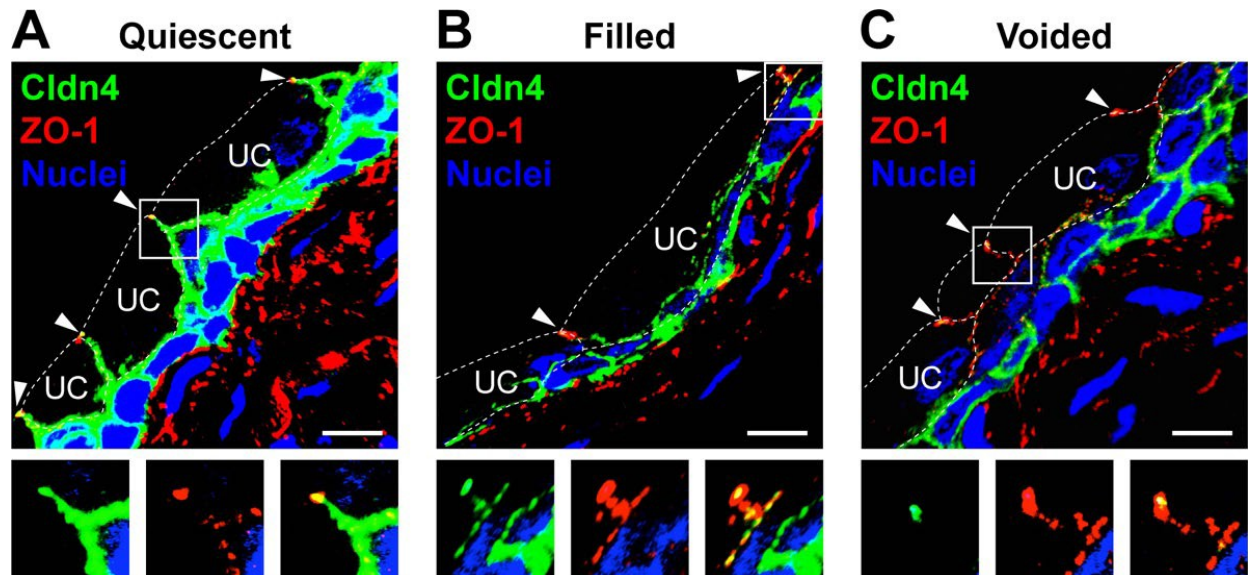


**Figure 31. Claudin-4 localization is altered by filling and voiding.**

Cross section views of (A) quiescent, (B) filled, or (C) voided rat bladders with the apical-most tight junction indicated with arrowheads and umbrella cell borders outlined with dashed lines. Sections are labeled with antibodies against claudin-4 (green) and ZO-1 (red). Nuclei are labeled with To-Pro-3 (blue). Images are 3D reconstructions of confocal images. Scale bars = 20  $\mu\text{m}$ .

filling and voiding. These results demonstrate that filling and voiding alter the localization of, at least one, pore-forming claudin.

Claudin-specific knockout mice or claudin shRNAs could help us understand which claudins act as pore-formers in the bladder, and how the paracellular permeability of the bladder is determined. Ultimately, whether the movement of claudins during the bladder cycle is mediated by membrane trafficking events or contribute to the increase in paracellular permeability remains unclear. However, we could establish that exocytosis is mediating the expansion of the AJR during filling by identifying and targeting the SNARE that mediates vesicle fusion, using techniques similar to the DN-dynamin experiments we performed in the current studies. Furthermore, identifying that claudins that are delivered to, or removed from, the apical-most tight junction during filling and voiding would provide evidence that membrane trafficking of junctional proteins is, indeed, regulating the expansion and contraction of the AJR.

Finally, knowing which claudins are differentially expressed at the tight junction in filled or voided bladders might provide clues to the mechanism of the permeability changes. However, this data may be difficult to interpret since a number of pore-forming claudins are expressed at the umbrella cell tight junction, not to mention the various other claudins that are also expressed and may contribute to umbrella cell paracellular permeability. Potential methods to identify changes in claudin localization during the bladder cycle include examining the internalization of antibodies against the extracellular domains of claudins, using a cell-surface biotinylation approach, or biochemically isolating the tight junction fraction in filled and voided bladders. An alternate approach would be to use live imaging to visualize the movement of fluorescently tagged claudins to and from the AJR when the isolated urothelium is stretched on a biaxial stretching device, to mimic filling and voiding. If we identify a particular set of claudins whose localization is affected by filling or voiding we can establish that they are being redistributed via membrane trafficking by using BfA, expressing DN-Rab13, or expressing a DN mutant of the SNARE responsible for fusion to inhibit exocytosis. Finally, if the trafficking of claudins is responsible for the permeability changes seen with filling and voiding, then inhibiting membrane trafficking should prevent these changes.

### **3.4 Perspectives.**

#### **3.4.1 The AJR: A mechanotransduction signaling complex.**

Epithelial cell-cell junctions are adhesive structures that physically integrate neighboring cells into a cohesive tissue by opposing the mechanical forces that would otherwise pull the tissue apart. Thus, not surprisingly, the biology of junctions has evolved to fulfill the mechanical nature of their function. It has become increasingly clear that the AJR itself is able to sense mechanical

forces and transduce these forces into cellular signals. As such, mechanical forces sensed at cell-cell junctions define a mechanism of cellular communication in addition to the classical modes of signal transmission, such as via gap junctions or endocrine or exocrine secretion. Although many of the downstream mechanisms are conserved between biochemical and biomechanical signal transduction, such as post-translational modifications, transcriptional regulation, or the use of second messengers, the initial mechanosensing, where a physical force exerted on a protein is transduced into a cellular output, is unique to mechanotransduction, and the molecular mechanisms are less well understood.

Many of the forces generated on epithelial cells are concentrated at points of intercellular adhesion; consequently, mechanotransduction is frequently initiated at the multi-protein complexes found at these adhesion sites. It is well-established that cell-cell junctions have a large plaque of signaling molecules, trafficking machinery, and ion channels associated with their cytoplasmic domain, which are directly or indirectly modulated by physical stimuli applied to the junction. The AJR couples adjacent cell's cytoskeletons, allowing for tissue scale tension to be generated. In this way the AJR is able to regulate a variety of downstream mechanosensitive processes such as ion transport and membrane trafficking events. Thus, the AJR in epithelial cells acts as a mechanosensitive signaling hub that controls everything from adhesion, to calcium signaling.

As the initial site of mechanotransduction, focus should be put on understanding the mechanosensitive aspects of junctional biology, which may offer therapeutic insights into pathologies that are characterized by an altered physical environment, such as tumor growth and metastasis. Perhaps not surprisingly, given that physical forces are disproportionately sensed at intercellular junctions, cancer cells are characterized by abnormal expression of junctional proteins, such as claudins and E-cadherin, and junctional regulatory proteins, such as Rab13 and its effectors (Onder *et al.*, 2008; Ioannou and McPherson, 2016; Tabaries and Siegel, 2017). Mechanosensitive adhesion complexes have emerged as key regulators of signaling during tissue

development, normal physiological function, and in disease states. Therefore, increasing our understanding of the molecular machineries involved in junctional mechanotransduction, as our current studies aim to do, will provide knowledge of their relevance *in vivo*, and insights into their use as therapeutic targets.

### **3.4.2 Paracellular permeability in health and disease.**

It seems counterintuitive that the highly impermeable umbrella cell AJC should become more permeable to ions when the bladder is full, particularly after the kidney has expended so much energy establishing the appropriate solute concentration of the urine. However, the permeability of the umbrella cell AJC is still exponentially lower than most other cell-cell junctions found within the body, perhaps only exceeded by the tightness of the blood-brain-barrier. Intriguingly, a population of large, afferent nerve processes terminate just below the umbrella cell layer, suggesting that nervous signals may be regulated by changes at the level of the umbrella cell. We propose that the increase in paracellular permeability that accompanies filling acts as a signal to the sub-adjacent nerves that the bladder is full. Accordingly, an increase in paracellular permeability, which is characteristic of many bladder pathologies, could act as a nervous signal, and account for the pain that accompanies these bladder diseases. This hypothesis is supported by our observations that increasing paracellular permeability by exogenously expressing the cationic pore former claudin-2, which is overexpressed in patients with interstitial cystitis, is sufficient to sensitize the bladder's sensory neurons (Montalbetti *et al.*, 2017). These findings indicate that paracellular ion movement is sufficient to trigger nervous signals, like might happen when the bladder senses fullness.

Intriguingly, not only does exogenous claudin-2 expression increase the responsiveness of the sensory neurons, but it is sufficient to trigger the downstream inflammation associated with bladder diseases such as interstitial cystitis (Montalbetti *et al.*, 2015). It was already known that

urothelial permeability is increased in cases of interstitial cystitis, but whether this was a cause of the inflammation, or a result was unknown. Our results demonstrate that increases in paracellular permeability can act upstream of the inflammatory responses that are observed in a wide variety of diseases that are characterized by a compromised junctional barrier, such as multiple sclerosis (Forster, 2008) and inflammatory bowel disease (Bruewer *et al.*, 2006), and including bladder pathologies, such as bladder outlet obstruction, bacterial or interstitial cystitis, or the bladder dysfunction that accompanies spinal cord injury (Birder *et al.*, 2012). Taken together these observations illustrate the delicate balance between normal changes in paracellular permeability, which may act as a signaling mechanism, and excessive increases in permeability, which create a pathological environment. This highlights the importance of understanding the mechanisms controlling paracellular permeability under normal conditions, so that we can identify what goes wrong during pathological conditions. Overall, our current studies aim to provide a greater understanding of epithelial junctional mechanotransduction, and how this might affect paracellular permeability, which could provide insight into how epithelial tissues accommodate physiological forces without losing their integrity.

## **4.0 Materials and Methods**

### **4.1 Animals**

Urinary bladders were obtained from female Sprague-Dawley rats (250–300 g; Envigo, Harlan Laboratories, Frederick, MD). Following perfusion fixation (see below), rats were euthanized by inhalation of 100% v/v CO<sub>2</sub> and euthanasia was confirmed by a thoracotomy. All animal studies were performed in accordance with relevant guidelines/regulations of the Public Health Service Policy on Humane Care and Use of Laboratory Animals and the Animal Welfare Act, and under the approval of the University of Pittsburgh Institutional Animal Care and Use Committee.

### **4.2 Antibodies and reagents**

Unless otherwise specified, all reagents were purchased from MilliporeSigma (St. Louis, MO). CK869, SMIFH2, ML141, and GSK269962 were purchased from Tocris Bioscience, Biotechne Corporation (Minneapolis, MN). Chemicals stocks were prepared in DMSO as 1000-fold stocks and stored at -20°C: cytochalasin D, 25 mg/ml; blebbistatin, 10 mM; brefeldin A, 5 mg/ml; cycloheximide, 100 mg/ml; Pitstop2, 30 mM; CK869, 100 mM; SMIFH2, 50 mM; ML141, 25 mM; GSK269962, 100 µM. They were diluted 1000-fold immediately prior to use. Primary antibodies used in this study: rabbit polyclonal claudin-8 (cat# 400700, Thermofisher Scientific, Waltham, MA), mouse monoclonal E-cadherin (cat# 610181, BD Transduction Laboratories, San Jose, CA), rabbit polyclonal non-muscle myosin IIA (cat# 909801, Biolegend, San Diego, CA), rabbit polyclonal non-muscle myosin IIB (cat# 909901, Biolegend), rabbit polyclonal non-muscle

myosin IIC (cat# PA5-66483, Thermofisher Scientific), rabbit polyclonal  $\alpha$ -actinin-4 (cat# ALX-210-356, Enzo Life Sciences Inc., New York, NY), rabbit polyclonal zonula occludens-1 (cat# 61-7300, Thermofisher Scientific), goat polyclonal platelet-derived growth factor- $\alpha$  (cat# AF1062, R&D Systems, Minneapolis, MN), rabbit polyclonal RAB13 (cat# NBP1-85799, Novus Biologicals, Centennial, CO) was used for western blot, rabbit polyclonal RAB13 (cat# 07-794, Millipore Sigma) was used for immunofluorescence, mouse monoclonal RAB8A (cat# 610844, BD Transduction Laboratories), rabbit polyclonal RAB11A (cat# 71-5300, Thermofisher Scientific) and rabbit polyclonal HA (cat# SAB4300603, Millipore Sigma). Minimal cross-reacting Alexa488, Cy5, or HRP-conjugated goat anti-mouse and goat-anti-rabbit and Alexa488-conjugated goat-anti-mouse secondary antibodies were purchased from Jackson ImmunoResearch (West Grove, PA). Rhodamine-phalloidin, Alexa594-phalloidin, and To-Pro-3 were purchased from Thermofisher Scientific.

### **4.3 Preparation of filled, voided, and quiescent bladders.**

Rats were sedated by inhalation of 3% (v/v) isoflurane and then injected subcutaneously with 1.35 g/kg urethane prepared fresh in dH<sub>2</sub>O and sterile filtered through a 0.22  $\mu$ m STERIFLIP-GP filter (Millipore Sigma) prior to use. Animals were allowed to reach proper anesthetic depth over a period of 2.5 h, which was confirmed by lack of a response to a toe pinch. Anesthetized rats allowed to undergo spontaneous filling were separated into three groups: filled, voided, and quiescent. All three groups were catheterized by inserting a 22-gauge Jelco IV catheter (trimmed to ~1cm in length) (Smiths-Medical, Minneapolis, MN) into the urethra. A three-way port was attached to the Luer fitting and, if necessary, the animals were subjected to Credé's maneuver to void their bladders prior to the start of the experiment. Subsequently, animals in the filled and voided groups had their catheter ports closed, and their bladders were allowed to fill over 2.5 h to

an approximate final volume of 500  $\mu\text{L}$ . After the 2.5-h filling period, animals in the voided group had their catheter ports re-opened and were allowed to void for 5 min. The animals with quiescent bladders remained catheterized for the full 2.5-h time period, so the bladders remained in a relaxed state.

For drug filling/voiding assays, animals were anesthetized (**Appendix, Figure S9A**), as described above. A small incision was made in the lower portion of the abdomen revealing the peritoneal cavity. The ureters were identified, cut, and sutured closed using 6-0, 13-mm Unify Silk Surgical Sutures (AD Surgical, Sunnyvale, CA). The peritoneal incision was closed using the BD Autoclip Wound Closing System (Becton, Dickinson and Company, Parsippany, NJ). Subsequently, the animals were trans-urethrally catheterized, and the Jelco IV catheter was secured using a surgical suture inserted below and then around the catheter. Animals were subject to Credé's maneuver to void their bladders prior to the start of the experiment. Again, anesthetized rats were separated into three groups: filled, voided, and quiescent. The catheters were attached via their Luer fittings to 5 ml syringes mounted on a multi-syringe pump (NE-1600, World Precision Instruments, Sarasota, FL). Syringes were either loaded with Kreb's buffer (110 mM NaCl, 25 mM  $\text{NaHCO}_3$ , 5.8 mM KCl, 1.2 mM  $\text{MgSO}_4$ , 4.8 mM  $\text{KH}_2\text{PO}_4$ , 11 mM glucose, 2 mM  $\text{CaCl}_2$ , gassed with 5% v/v  $\text{CO}_2$ ) containing 0.1% (v/v) DMSO for controls, or with Kreb's buffer + drug for experimental groups. For groups with preincubation, 50  $\mu\text{L}$  was pumped into the bladders over 5 min at a rate of 10  $\mu\text{L}/\text{min}$  and incubated for 1 h (**Appendix, Figure S9B**). After the 1-h preincubation, the filled and voided groups had an additional 450  $\mu\text{L}$  of Kreb's buffer  $\pm$  drug pumped into the bladder over 45 min at a rate of 10  $\mu\text{L}/\text{min}$  to a final volume of 500  $\mu\text{L}$ . After the 45-min filling period, animals in the voided group had their catheter ports re-opened and were allowed to void for 5 min (**Appendix, Figure S9C**). After the 1-h preincubation, the quiescent group had the syringe attached to the catheter port removed from the pump during the 45-min filling period, so that there was no additional liquid instilled into the bladder and the animals ended the experiment with a total volume of 50  $\mu\text{L}$  in the bladder lumen (**Appendix, Figure S9D**). For

filled and voided groups without preincubation, 500  $\mu$ L of Kreb's + DMSO or Kreb's + drug was pumped into the bladder over 30 min at a rate of 16.67  $\mu$ l/min. After the 30-min filling period, animals in the voided group had their catheter ports re-opened and were allowed to void for 5 min (**Appendix, Figure S9E**). The quiescent group had the syringe attached to the catheter port removed from the pump during the 30-min filling period, so that there was no liquid instilled into the bladder (**Appendix, Figure S9F**).

At the end of the experiment animals were perfusion fixed. A thoracotomy was performed, the caudal vena cava was cut, and 50 ml of 100 mM sodium-phosphate buffer (pH 7.4) at 37°C, was perfused through the left ventricle using an 18-gauge needle. Subsequently, the perfusate was switched to 100 mM sodium-phosphate buffer (pH 7.4) containing 4% (w/v) paraformaldehyde. The bladders were excised, placed in Kreb's buffer containing 2% paraformaldehyde (w/v), cut open down their midline and pinned out on a rubber mat, with minimal stretching, to expose the apical-most umbrella cell layer. The tissues were stored at 4°C in 2% (w/v) paraformaldehyde until ready for processing for whole-mount microscopy. Alternatively, the fixed bladder was cut into quarters, cryoprotected by incubating in 35% (w/v) sucrose in PBS until the tissue sank, embedded in optimal cutting temperature (OCT) compound (Scigen Inc., Gardena, CA), and frozen in 10mm x 10mm x 5mm Tissue-Tek Cryomolds (Sakura Finetek, Torrance, CA) on dry ice. Frozen tissue blocks were stored at -80°C in water-tight plastic bags prior to sectioning.

## **4.4 Indirect immunofluorescence and image capture.**

### **4.4.1 Indirect immunofluorescent tissue labeling.**

Frozen tissue blocks were sectioned at 5  $\mu\text{m}$  thick using a CM1950 cryostat (Leica Biosystems, Wetzlar, Germany) and collected on Fisherbrand Superfrost Plus Microscope Slides (ThermoFisher Scientific). Immunofluorescent labeling of whole-mount and cryosectioned bladder tissue was performed at room temperature, unless otherwise indicated. Tissue was washed three times with PBS for 5 min. Unreacted paraformaldehyde was quenched and the tissue was permeabilized by washing tissue for 10 min with PBS containing 0.1% (v/v) Triton X-100, 20 mM glycine (pH 8.0), and 75 mM ammonium chloride. Tissue was washed three times with PBS for 5 min, and then three times quickly with block solution (which contained 0.7% (w/v) fish-skin gelatin, 0.025% (w/v) saponin, and 0.02% (w/v) sodium azide, all dissolved in PBS). Tissue was then incubated for 30 min in block solution, and then incubated overnight at 4°C in block solution containing the primary antibody. After incubation with the primary antibody, the tissue was washed three times with block solution, and then three times for 5 min with block solution. Subsequently, the tissue was incubated for 1 h with secondary antibody diluted in block solution. Tissue was then washed three times with block solution, three times for 5 min with block solution, and then three times with PBS. The antibodies were post-fixed with 4% (w/v) paraformaldehyde in 100 mM sodium-phosphate buffer (pH 7.4) for 10 min (tissue sections) or 20 min (whole-mount), after which the tissue was washed three times with PBS. Finally, the paraformaldehyde was quenched, as described above, and washed three times with PBS. After labeling, tissue sections were covered with a drop of Slowfade Diamond Antifade Mountant (Thermo Fisher Scientific), covered with a Gold Seal Cover Glass (number 1.5, Thermo Fisher Scientific), and sealed around the edges with a thin layer of nail polish (Electron Microscopy Sciences, Hatfield, PA). Whole-mount tissue was placed, apical surface facing up, within a square well created with nail polish in which

a drop of Slowfade Diamond Antifade Mountant was added. An additional drop of mountant was added to the top of the tissue. A cover glass was placed over the tissue and sealed around its edges with a thin layer of nail polish.

#### **4.4.2 Image capture.**

Confocal images were captured using a Leica HCX PL APO 40X 1.25 NA oil objective, a Leica HCX PL APO 63X 1.3 NA glycerol objective, or a Leica 100X 1.4 NA oil objective on a Leica TCS SP5 CW-STED confocal microscope (in normal confocal mode). The HyD detectors were set at their maximal values, laser output used to control image “brightness,” and 8-bit images were collected using 8 line averages in combination with 6 frame averages. For tissue sections, serial 0.2  $\mu\text{m}$  Z-sections were acquired. For whole-mounted tissues, serial 0.5  $\mu\text{m}$  Z-sections were acquired. Maximum intensity projections of each sample were generated using Volocity 4-D software (Perkin Elmers, Waltham, MA) and exported as TIFF files. Alternatively, single widefield images were captured using a Leica HCX PL APO 40X 1.25 NA oil objective on a Leica DM6000 B widefield fluorescence microscope. Images were captured using a Retiga 4000R digital camera (Q Imaging, Surrey, CA). Images were contrast corrected in Adobe Photoshop CC2017 (Adobe Inc, Mountain View, CA), and composite images created using Adobe Illustrator CC2017.

### **4.5 Production of adenoviruses and summary of viral constructs.**

#### **4.5.1 Preparation of chemically competent AdEasier-1 cells.**

AdEasier-1 cells (Addgene, Watertown, MA; bacterial strain #16399, deposited by Bert Vogelstein) were grown in 5 ml Luria-Bertani (LB) broth with 1:1000 streptomycin (30  $\mu\text{g}/\text{ml}$ ) and

1:1000 ampicillin (100 µg/ml). overnight on a shaker at 37°C. Subsequently, the 5 ml culture was diluted into 100 ml LB broth with streptomycin and ampicillin and shaken at 37°C for 1.5 h, or until the culture reached an OD<sub>600</sub> of 0.5. The culture was spun for 10 min at 2057 RCF at 4°C in a 5810R centrifuge outfitted with an F-34-6-38 fixed-angle rotor (Eppendorf, Hamburg, DE), and the pellet was resuspended in 20 ml, ice-cold 100 mM MgCl<sub>2</sub> and incubated on ice for 20 min. The resuspension was centrifuged for an additional 10 min at 2057 RCF at 4°C and the pellet was resuspended in 2 ml sterile, ice-cold CaCl<sub>2</sub> in 15% v/v glycerol. Cells were aliquoted into tubes prechilled to -80°C and stored until use at -80°C.

#### **4.5.2 Production of DN-Rab13-GFP adenovirus.**

DN-Rab13-GFP adenovirus was produced using the AdEasy system. A gBlock (Integrated DNA Technologies, Coralville, IA) encoding GFP-tagged rat Rab13 flanked by XhoI and HINDIII restriction sites was cloned into pShuttleCMV (Addgene; plasmid #16403, deposited by Bert Vogelstein). DN-Rab13-GFP (T22N) was generated by mutating pShuttleCMV-Rab13-GFP using Qiagen QuikChange II Site-Directed Mutagenesis kit (Agilent Technologies, Santa Clara, CA) using the primer 5'-TCG GGG GTG GGC AAG AAT TGT CTC ATC ATT CGC TT-3'. The construct was confirmed by sequencing. DN-Rab13-GFP was linearized with PmeI and recombined with the adenoviral backbone in chemically competent Adeasier-1 cells, described above. Recombined pShuttleCMV-DN-Rab13-GFP cDNA was extracted from AdEasier-1 cells using a QIAprep Spin Miniprep Kit (Qiagen, Hilden, DE). This cDNA was transformed into recA-deficient XL10-Gold Ultracompetent Cells (Agilent Technologies). Recombined cDNA was extracted with a NucleoBond Xtra Endotoxin-Free Midiprep kit (Macherey-Nagel, Bethlehem, PA) and linearized with PacI. Adenovirus encoding DN-Rab13-GFP was produced by transfection of AD293 cells with the linearized cDNA (Agilent Technologies). After ~3 wk, cells were harvested

and the virus was extracted by repeated freeze/thaw cycles in liquid nitrogen and in a 37°C water bath, respectively. The crude adenovirus was subsequently purified by loading it on a CsCl step gradient made of low-density CsCl (323 g/l) layered on top of high-density CsCl (530 g/l) prepared in sterile 100 mM Tris/10 mM EDTA (pH 7.4), and by spinning for 1 h at 151,263 RCF at 4°C in an Optima L-80 XP ultracentrifuge outfitted with an SW41 Ti rotor (Beckman Coulter Life Sciences, Indianapolis, IN). The viral band found at the interface of the low-density and high-density CsCl layers was extracted using a 12-gauge needle and loaded onto a Sephadex G-25 PD10 Desalting Column (GE Healthcare Life Sciences, Pittsburgh, PA), pre-equilibrated with sterile 10% glycerol in PBS. Ten, 500- $\mu$ l fractions were collected. The virus was found in fractions 9, 10, and 11 at concentrations ranging from 25-35 million IVP/ $\mu$ l.

#### **4.5.3 DN-Rab8a and DN-Rab11a adenoviruses.**

DN-Rab8a-GFP (T22N) adenovirus was produced and purified in house, as described previously (Khandelwal et al., 2013). DN-Rab11a-GFP (S25N) adenovirus was a kind gift from Dr. Bruce Baum and was amplified and purified in house, as described previously (Khandelwal et al., 2008b). Crude adenovirus encoding DN-Dynamin1-HA (K44A) was a kind gift from Dr. Sandra Schmid and was amplified and purified in house. DN-RhoA-GFP (V19N) adenovirus was a kind gift from Dr. James Bamburg and Dr. James Casanova, as described previously (Khandelwal et al., 2010).

#### **4.5.4 *In situ* adenoviral transduction.**

*In situ* transduction was performed as described previously (Khandelwal et al., 2008a). Briefly, rats were sedated with 3% (v/v) isofluorane and a 22-gauge Jelco IV catheter (Smith Medicals), trimmed to ~ 1-cm in length, was inserted into the bladder via the urethra. The bladder

was rinsed with PBS and filled with 400  $\mu$ l of 0.1% w/v dodecyl- $\beta$ -D-maltoside dissolved in PBS. The urethra was clamped, and after 5 min unclamped to allow the detergent to void. The latter step was facilitated by performing Credé's maneuver. Subsequently, the bladder was filled with 400  $\mu$ l PBS containing adenoviruses expressing the constructs described above ( $2.0 \times 10^8$  infectious virus particles, typically in a volume of 2-10  $\mu$ l for each virus). The urethra was clamped, and after 30 min unclamped and the virus solution was allowed to void. The bladder was rinsed with PBS, anesthesia was discontinued, and the rats were allowed to revive. The rats were euthanized 3 days post transduction to allow time for the umbrella cells to regain their normal morphology.

#### **4.5.5 Lysate preparation and western blotting.**

To obtain rat epithelial bladder lysates, rat bladders were excised, cut down the midline, and pinned open on a rubber mat to expose the apical umbrella cell layer. Fifty  $\mu$ l 0.5% (w/v) SDS-lysis buffer (100 mM NaCl, 50 mM tetraethylammonium, 5 mM EDTA, 0.2% w/v NaN<sub>3</sub>, and 0.5% w/v SDS) containing 0.5 mM phenyl-methylsulfonylfluoride (PMSF) and 1:100 dilution of a protease inhibitor cocktail (PIC, MilliporeSigma) was pipetted onto the apical surface of the tissue. Epithelial cells were gently scraped with a rubber cell scraper (Sarstedt, Nümbrecht, DE) and deposited in a 1.5 ml microcentrifuge tube. This process was repeated once more for a final volume of 100  $\mu$ l of lysate. For HeLa cell lysates, cells were grown to confluence on 6-well tissue culture dishes (Corning Inc., Corning, NY). 500  $\mu$ l 0.5% SDS-lysis buffer containing 0.5 mM PMSF and 1:100 dilution of PIC (MilliporeSigma) was pipetted onto the apical surface of the cells. The cells were gently scraped with a rubber cell scraper (Sarstedt) and deposited in a 1.5 ml microcentrifuge tube. All lysates were shaken at 4°C in a MixMate benchtop mixer (Eppendorf, Hamburg, DE) at 3000 RPM for 15 min. Fifty  $\mu$ g of rat bladder lysates and 10  $\mu$ g of HeLa cell lysates were diluted 1:1 with 2X Laemmli Sample Buffer (Bio-Rad, Hercules, CA) supplemented

with 0.05% v/v  $\beta$ -mercapto-ethanol and incubated at 95°C for 5 min. The proteins were resolved on a 12% Criterion TGX SDS-polyacrylamide gel (Bio-Rad) and transferred for 30 min in 100 mM CAPS buffer (pH 11) at 400 mA onto an Immobilon-P membrane (MilliporeSigma). The membrane was blocked with 5% w/v bovine serum albumin (BSA) in tris-buffered saline + Tween (TBST, 2.68 mM KCl, 0.5 M NaCl, 25 mM Tris-HCl pH 8.0, and 0.05% v/v Tween 20) for 45 min at room temperature, washed three times with TBST, and incubated overnight at 4°C with 1:1000 anti-Rab8a, Rab11a, or Rab13 antibody diluted in TBST containing 1% w/v BSA. After the overnight incubation, the membrane was washed three times with TBST, incubated for 1 h with rotation at room temperature with the appropriate HRP-conjugated goat anti-mouse or goat anti-rabbit secondary antibody diluted 1:5000 in TBST containing 1% w/v BSA, and then washed three times with TBST. Immunoreactive protein species were visualized using Pierce SuperSignal West Pico PLUS Chemiluminescent Substrate (ThermoFisher Scientific) and image capture was performed using a Chemidoc Touch Imaging System (Bio-Rad).

## **4.6 Data and statistical analysis.**

### **4.6.1 Quantitation of AJR perimeter.**

Whole-mount tissue from filled, voided, and quiescent bladders was processed and imaged as described above. Twenty random images, 5 images per bladder quadrant, were collected. Each image was opened in FIJI and the “set scale” command was selected from the “analyze” drop-down menu. The distance in pixels per known distance was entered and the “global” check box was selected. The “set measurements” command was selected from the “analyze” drop-down menu and the “perimeter” option was selected. For images that contained five or fewer umbrella cells (e.g., those from filled bladders) the perimeter of the AJR

( $\text{perimeter}_{\text{AJR}}$ ) of each cell was measured by following the contours of the AJR using the “polygon” tool and selecting “measure” from the “analyze” drop-down menu.  $\text{Perimeter}_{\text{AJR}}$  values for each image were averaged. For images than contained more than five umbrella cells (e.g., those from voided bladders), we employed a random number generator to choose five representative cells to measure. In this case, each of the cells in the image were numbered using the “text tool.” The “Sequence Generator” option on [www.Random.org](http://www.Random.org) was chosen and the number of cells in the image input. Using the first five numbers of the random sequence generated, the perimeters of the corresponding cells were measured using the technique described above. Again, an average of all five measurements was made. The average umbrella cell  $\text{perimeter}_{\text{AJR}}$  for an individual bladder was calculated by determining the mean of the  $\text{perimeter}_{\text{AJR}}$  for each of the 20 random images.

#### **4.6.2 Non-linear regression analysis of filling data.**

Bladders were filled with a syringe pump (as described above) with 0  $\mu\text{L}$ , 500  $\mu\text{L}$ , 1000  $\mu\text{L}$ , or 1500  $\mu\text{L}$  ( $n=3$  for each group) over 45 min. Average  $\text{perimeter}_{\text{AJR}}$  per umbrella cell was estimated for each bladder, as described above, and these values were fitted to a single exponential using Prism’s (Graphpad, San Diego, CA) non-linear regression curve fit analysis.

#### **4.6.3 Data analysis.**

Data are reported as mean  $\pm$  SEM. Statistically significant differences were determined using one-way Analysis of Variance (ANOVA) with Dunnett’s correction. A  $p$  value  $\leq 0.05$  was considered statistically significant. Alternatively, we used a paired two-tailed  $t$ -test with a  $p$  value  $\leq 0.05$  considered statistically significant.

Appendix: Supplemental Material for Chapter 2.0

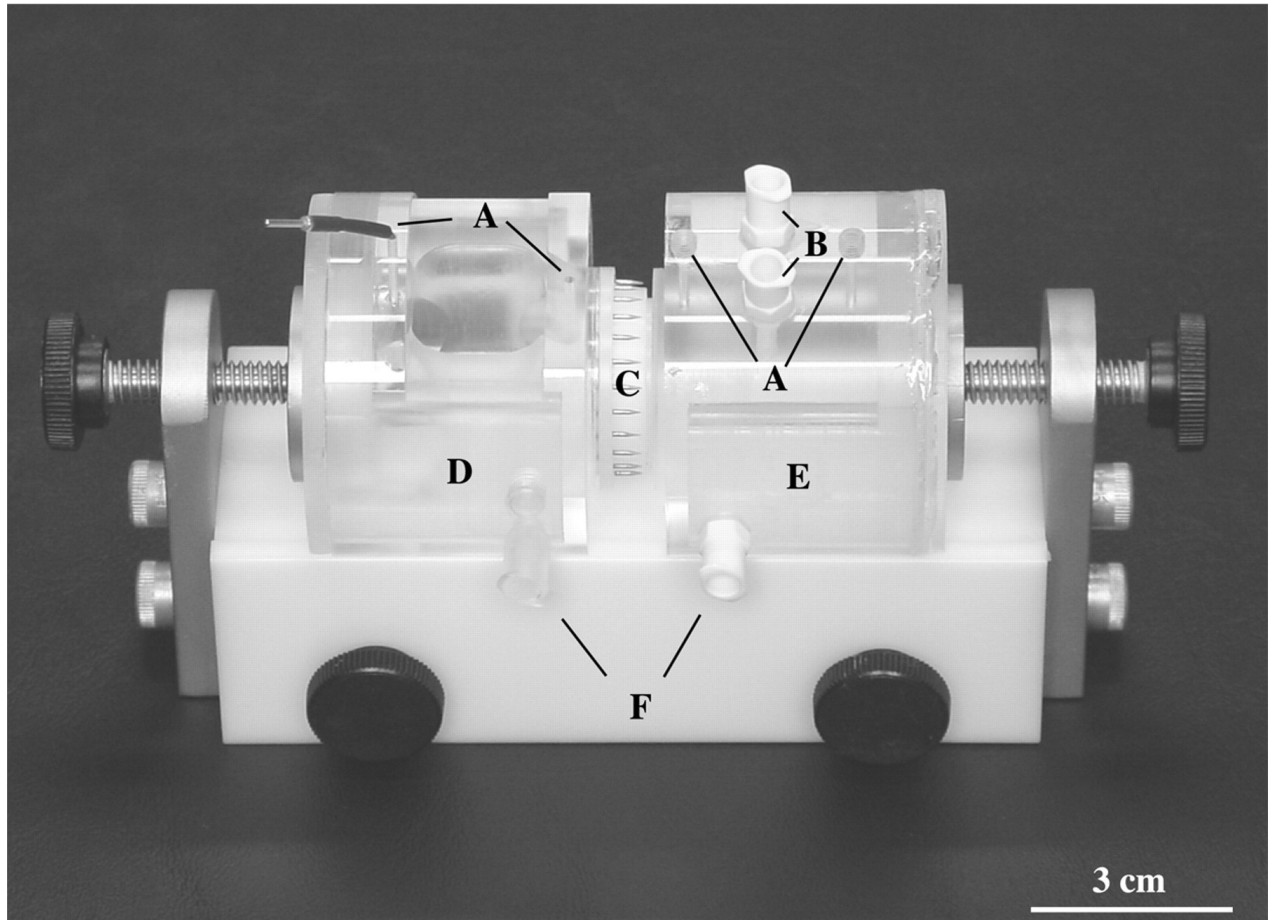


**Figure S1. Modified Ussing chambers used to stretch bladder tissue.**

Electrode ports (A), Luer ports (B), plastic ring containing excised tissue (C), basal (serosal) chamber (D), apical (mucosal) chamber (E), and water jacket ports (F). Figure used with permission from Truschel *et al.*, 2002.

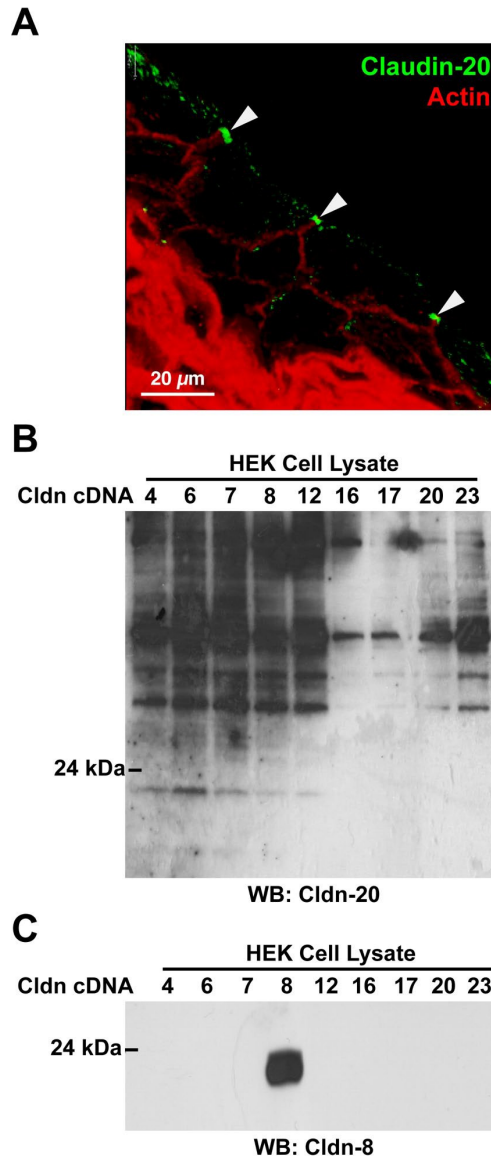


**Figure S2. Claudin Antibody Specificity Assay.**

To confirm the specificity of the antibodies, we transfected human embryonic kidney (HEK) cells, which do not express endogenous claudins, with claudin cDNAs, resolved the lysates by SDS-PAGE, and probed Western blots with nominally isoform-specific, commercially available claudin antibodies. Antibodies are considered specific if: (1) they show no reactivity to untransfected HEK cells; (2) they only recognize lysates from cells transfected with the claudin cDNA of the antibodies intended target; and (3) by IF, they detect antigen localized to the ZO-1-labeled tight junction. (A-B) Example of non-specific antibody (claudin-20). (A) Cross-section of rat bladder stained with an antibody against claudin-20, which appears to specifically stain the apical-most tight junction. F-actin is labeled with rhodamine-phalloidin (red). (B) Western blot using the same claudin-20 antibody as in (A) showing that it reacts with HEK lysates from cells expressing a variety of claudin species with higher affinity than it recognizes HEK lysates from cells expressing claudin-20. (C) Example of specific antibody (claudin-8), which only recognizes HEK lysates from cells expressing claudin-8.

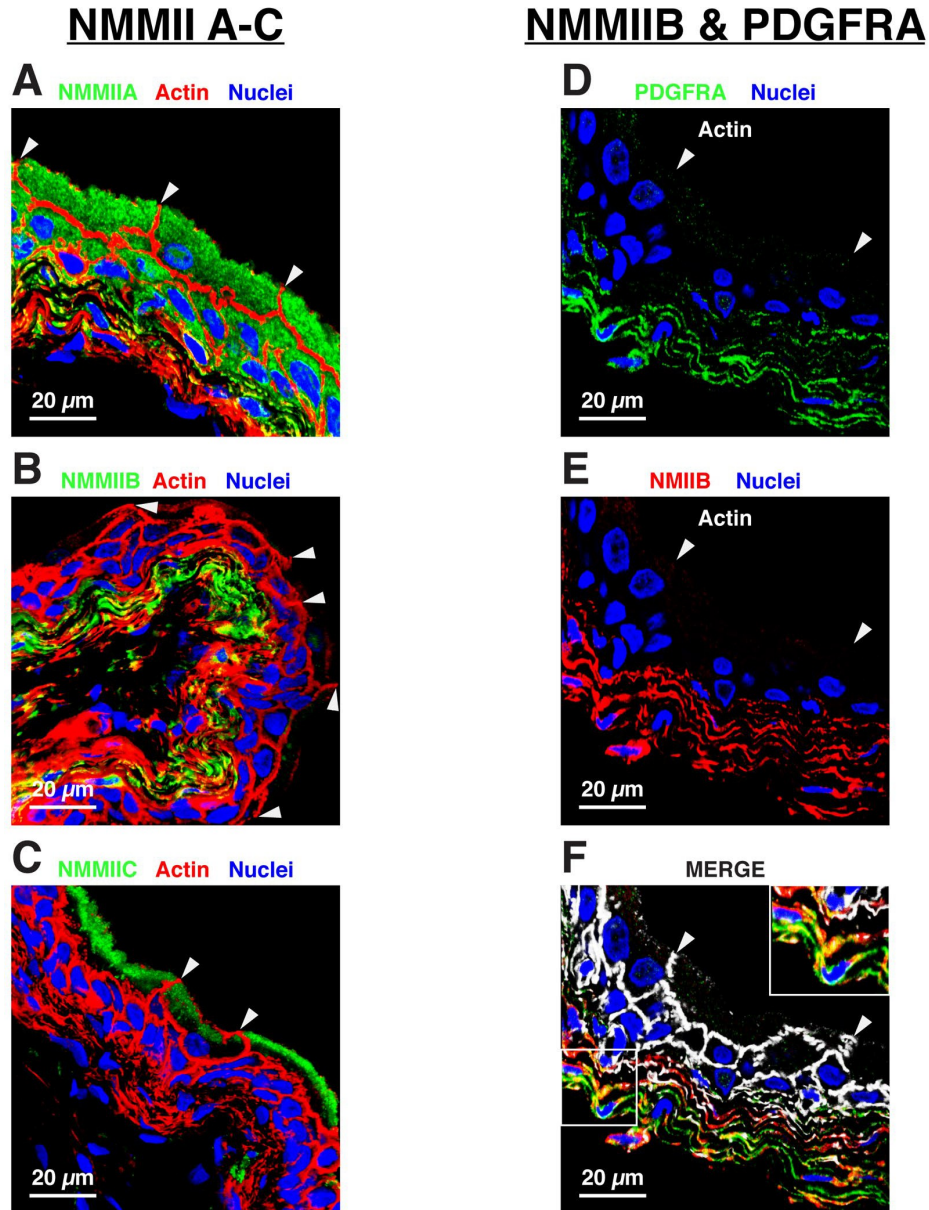


**Figure S3. NMMII distribution within the bladder mucosa.**

Cross-sections of *quiescent* rat bladders with the apical-most tight junction of the AJR indicated with arrowheads. The sections were labeled with antibodies against (A) NMMIIA (MYH9 subunit; green), (B) NMMIIB (MYH10 subunit; green), (C), NMMIIC (MYH14 subunit; green). F-actin is labeled with rhodamine-phalloidin (red) and nuclei with To-Pro-3 (blue). Images are 3D-reconstructions of confocal Z-stacks. Scale bars = 20  $\mu\text{m}$ . Panels (D-F) show the distribution of NMMIIB and PDGFRA-labeled interstitial cells. (D) Distribution of PDGFRA (green) and nuclei (blue) in the lamina propria underlying the urothelium. (E) NMMIIB (red) expression and nuclei (blue) in the lamina propria. (F) Merged image showing the distribution of NMMIIB (red), PDGFRA (green). F-actin is stained with Alexa594-phalloidin (white) and nuclei with To-Pro-3 (blue). Images are 3D-reconstructions of confocal Z-stacks. Scale bars = 20  $\mu\text{m}$ .

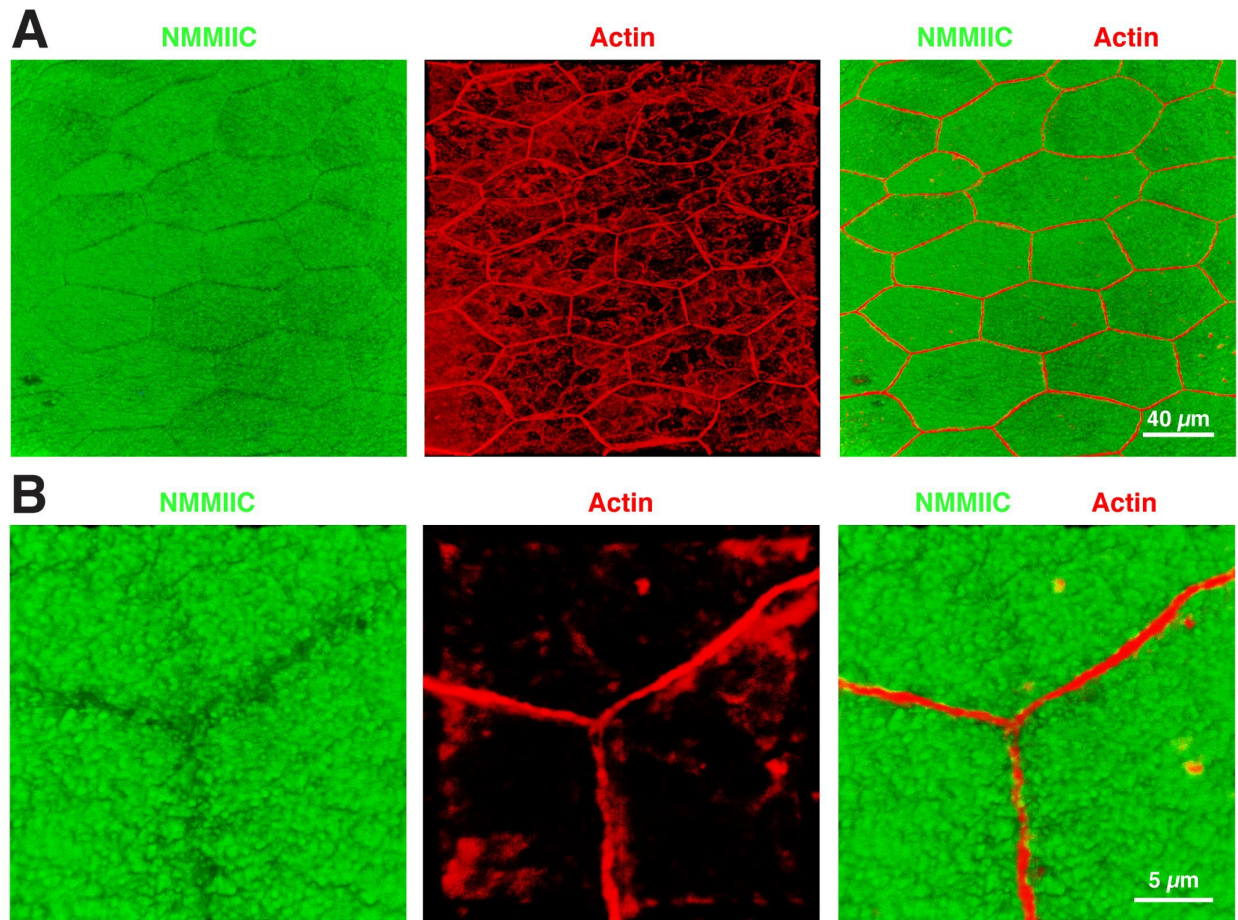


**Figure S4. NMMIIC distribution in the umbrella cell layer.**

*En face* view of the umbrella cell layer of whole-mounted preparations of *quiescent* rat bladders. Bladders were labeled with an antibody against (A) NMMIIC (MYH14 subunit; green). F-actin is labeled with rhodamine-phalloidin (red). Images are 3D-reconstructions of confocal Z-stacks. Scale bars = 40 μm. (B) Higher magnification images of the AJR in *quiescent* bladders labeled with an antibody against NMMIIC (MYH14 subunit; green). F-actin is labeled with rhodamine-phalloidin (red). Images are 3D-reconstructions of confocal Z-stacks. Scale bars = 5 μm.

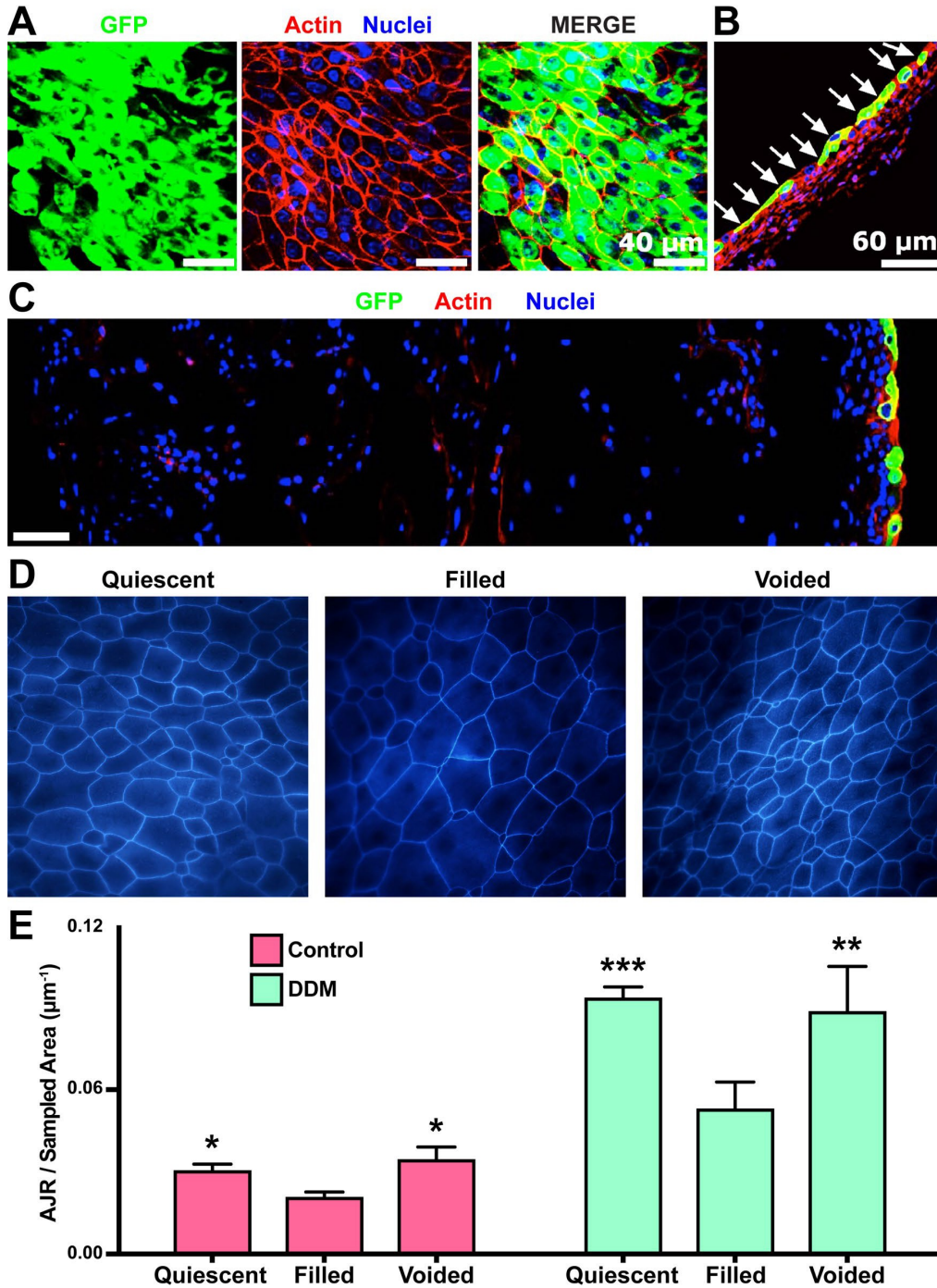


**Figure S5. The umbrella cell AJR can expand after DDM treatment.**

(A) En face and (B-C) cross section view of rat bladders transduced with GFP showing high-efficiency of expression that primarily affects the umbrella cell layer. (D) En face view of the umbrella cell layer in quiescent, filled, and voided rat bladders treated with DDM. (E) AJR/sampled area in quiescent, filled, and voided control (untreated) and DDM treated rat bladders.

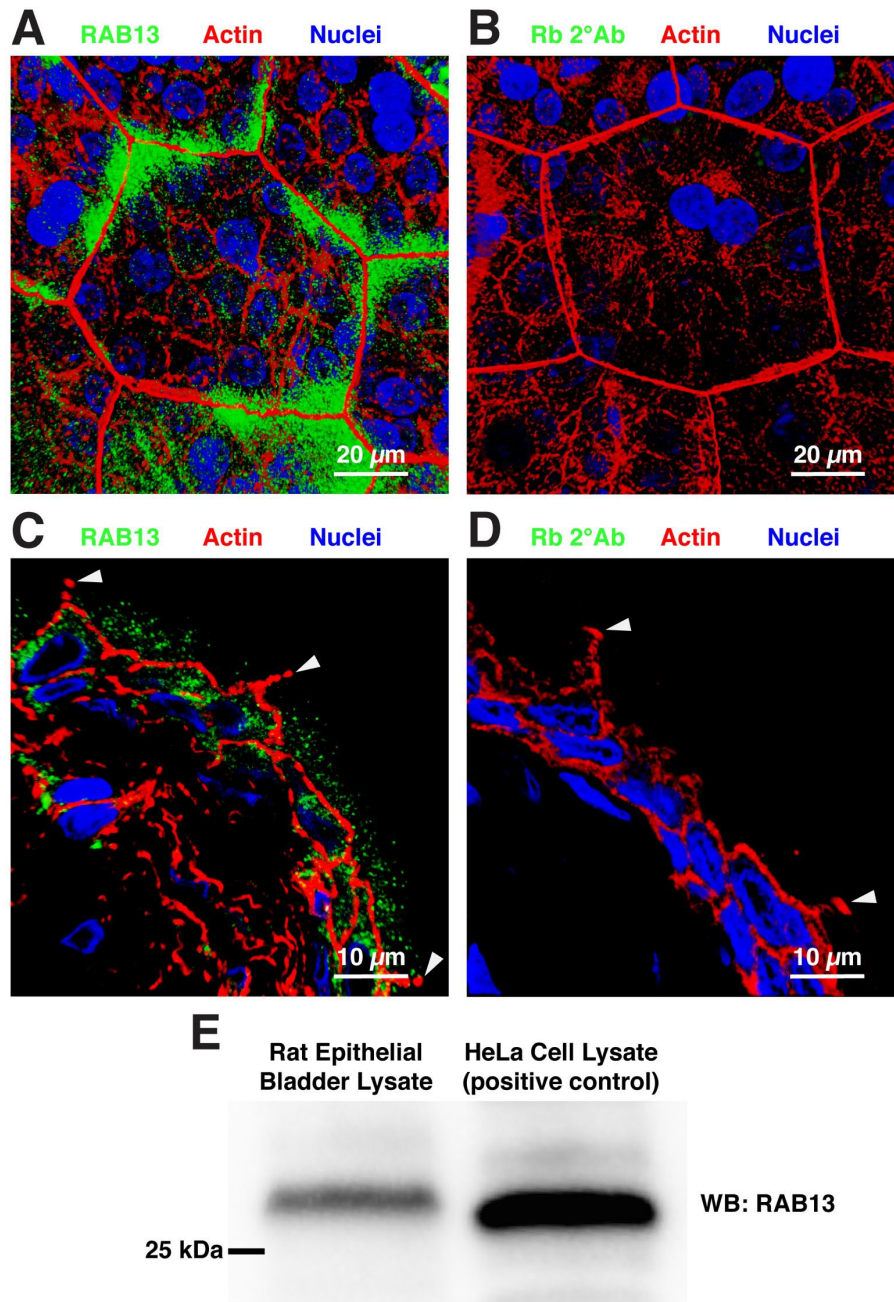


**Figure S6. RAB13 expression in umbrella cells.**

*En face* (A-B) or cross-sectional (C-D) view of urothelium obtained from *quiescent* rat bladders first labeled with (A and C) an antibody against RAB13 (green) or (B and D) no primary antibody, followed by incubation with an Alexa488-conjugated goat-anti-rabbit secondary antibody (green). F-actin is labeled with rhodamine-phalloidin (red) and nuclei with To-Pro-3 (blue). Images are 3D-reconstructions of confocal Z-stacks. Scale bars = 20  $\mu\text{m}$  (A-B) or 10  $\mu\text{m}$  (C-D). (E) Rat urothelial cell or cultured HeLa cell (used as a positive control for RAB13 expression) lysates were resolved by SDS-PAGE, and RAB13 detected by Western blot using antibodies against RAB13.

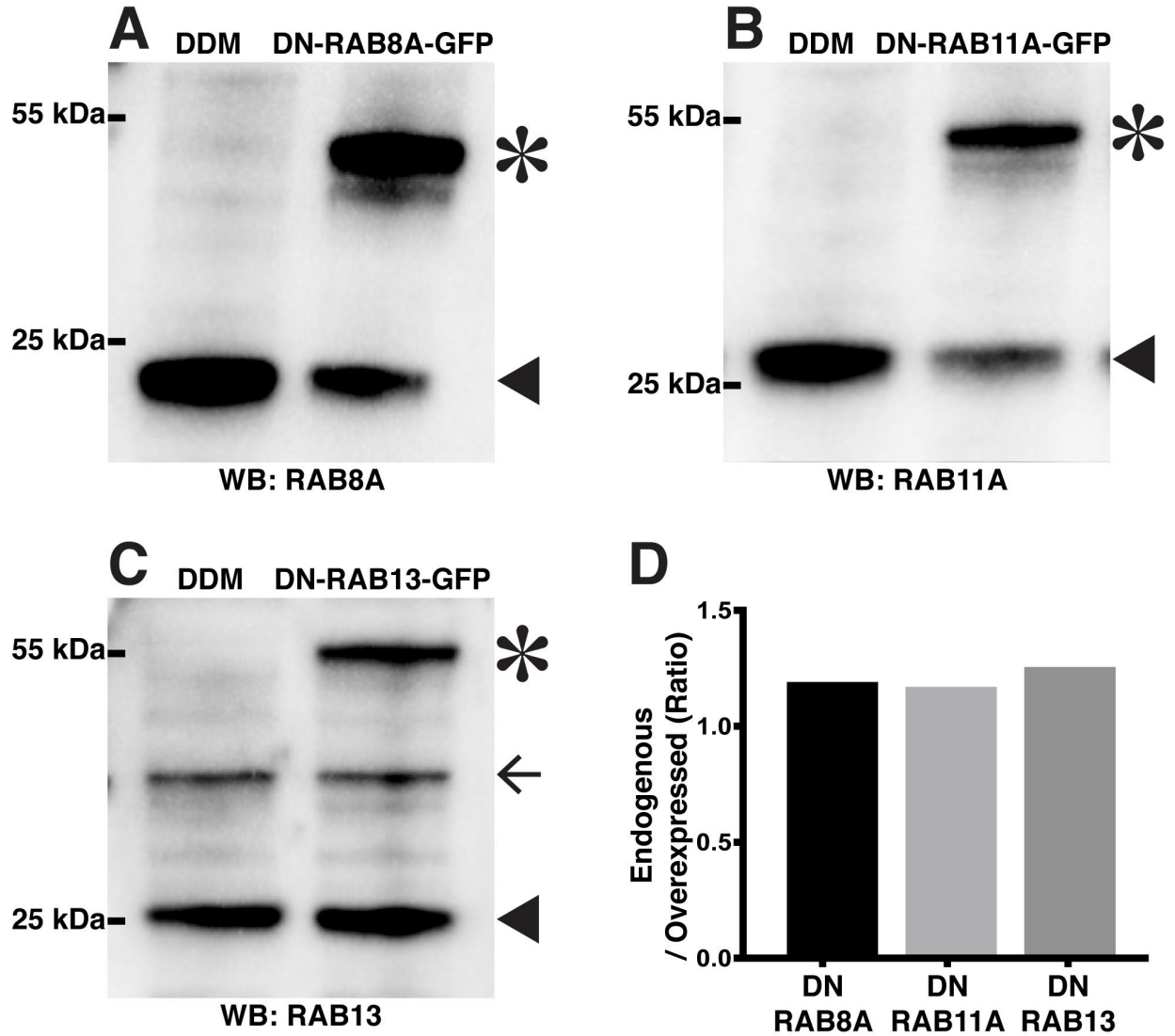


**Figure S7. Expression levels of endogenous Rab proteins relative to exogenously expressed DN-Rab mutants.**

(A-C) Rat urothelial cells from bladders subjected to DDM treatment (control) or DDM-treated bladders transduced with (A) DN-RAB8A, (B) DN-RAB11A, or (C) DN-RAB13 were lysed, resolved by SDS-PAGE, and detected by Western blot using antibodies against (A) RAB8A, (B) RAB11A, or (C) RAB13. Arrowheads indicate endogenous Rab proteins, asterisks indicate DN-GFP-tagged Rab mutants, and the arrow in C indicates a non-specific protein species. (D) Ratio of endogenous levels of RAB8A, RAB11A, and RAB13 in DDM-treated bladders versus levels of exogenously expressed DN-RAB8A, DN-RAB11A, and DN-RAB13 in DDM-treated and transduced bladders.

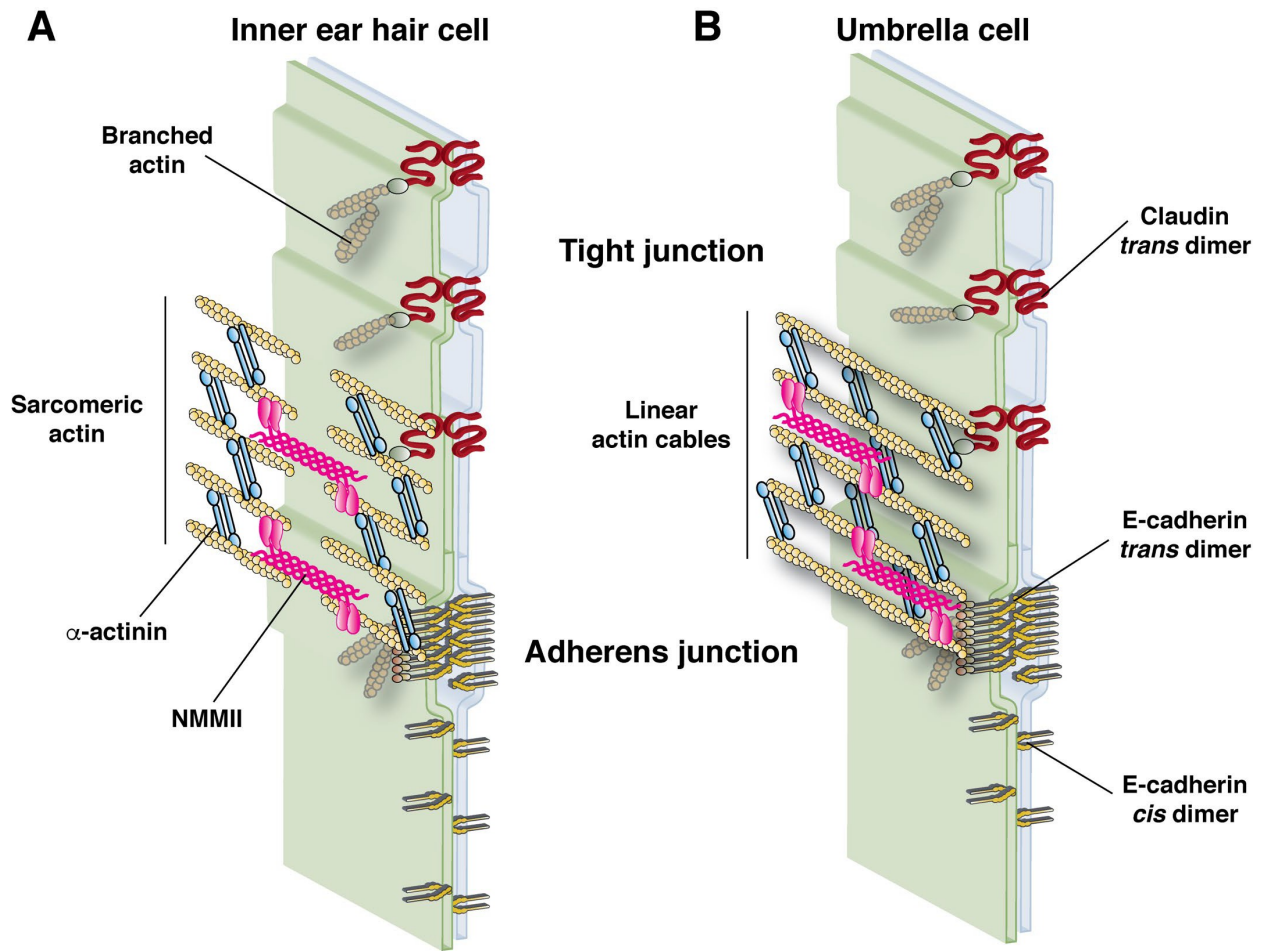


**Figure S8. Comparison of ear hair cell AJR organization versus that of umbrella cells.** (A) Hair cell AJR. (B) Umbrella cell AJR. Note that the actomyosin organization of the former is sarcomeric, with clusters of NMMII alternating with clusters of  $\alpha$ -actinin/f-actin, while that of the umbrella cell has a more continuous ring of  $\alpha$ -actinin/f-actin, and a more stochastic distribution of NMMII.

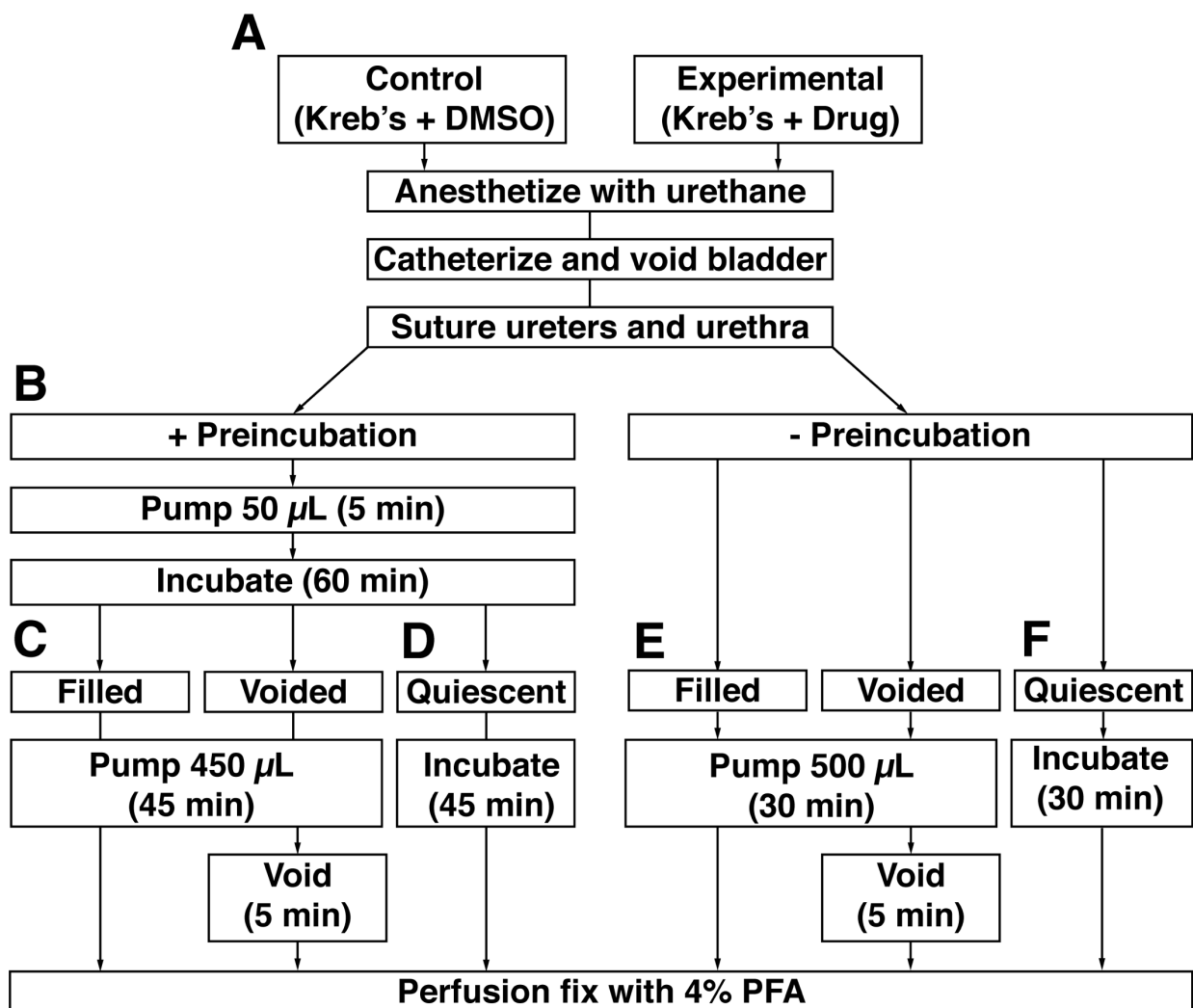


**Figure S9. Drug filling/voiding assay schematic.**

(A) Urethane-anesthetized rats were trans-urethrally catheterized, manually voided, and their ureters sutured and cut. The animals were separated into three groups: *filled*, *voided*, and *quiescent*. For groups *with preincubation* (B), 50  $\mu\text{L}$  of Kreb's buffer + 0.1% DMSO or Kreb's buffer + drug was pumped into the bladders at 10  $\mu\text{L}/\text{min}$  over 5 min period and incubated for 1 h. After the 1-h preincubation, the *filled* and *voided* groups (C) had an additional 450  $\mu\text{L}$  of Kreb's buffer  $\pm$  drug pumped into the bladder over 45 min at a rate of 10  $\mu\text{L}/\text{min}$  to a final volume of 500  $\mu\text{L}$ . After the 45-min filling period, animals in the *voided* group had their catheter ports re-opened and were allowed to void for 5 min. After the 1-h preincubation, the *quiescent* group (D) had the syringe attached to the catheter port removed from the pump during the 45-min filling period, so that there was no additional liquid instilled into the bladder and the animals ended the experiment with a total volume of 50  $\mu\text{L}$  in the bladder lumen. For *filled* and *voided* groups *without preincubation* (E), 500  $\mu\text{L}$  of Kreb's buffer + 0.1% DMSO or Kreb's buffer + drug was pumped into the bladder over 30 min at a rate of 16.67  $\mu\text{L}/\text{min}$ . After the 30-min filling period, animals in the *voided* group had their catheter ports re-opened and were allowed to void for 5 min. (F) The *quiescent* group had the syringe attached to the catheter port removed from the pump during the 30-min filling period, so that there was no liquid instilled into the bladder. At the end of the experiment, animals were perfusion fixed with 4% w/v paraformaldehyde.

## Bibliography

- Acharya, B.R., Wu, S.K., Lieu, Z.Z., Parton, R.G., Grill, S.W., Bershadsky, A.D., Gomez, G.A., and Yap, A.S. (2017). Mammalian Diaphanous 1 Mediates a Pathway for E-cadherin to Stabilize Epithelial Barriers through Junctional Contractility. *Cell Rep* 18, 2854-2867.
- Acharya, P., Beckel, J., Ruiz, W.G., Wang, E., Rojas, R., Birder, L., and Apodaca, G. (2004). Distribution of the tight junction proteins ZO-1, occludin, and claudin-4, -8, and -12 in bladder epithelium. *Am J Physiol Renal Physiol* 287, F305-318.
- Adachi, M., Hamazaki, Y., Kobayashi, Y., Itoh, M., Tsukita, S., Furuse, M., and Tsukita, S. (2009). Similar and distinct properties of MUPP1 and Patj, two homologous PDZ domain-containing tight-junction proteins. *Mol Cell Biol* 29, 2372-2389.
- Akao, S., Oya, M., Akiyama, H., and Ishikawa, H. (2000). The tight junction of pancreatic exocrine cells is a morphometrically dynamic structure altered by intraductal hypertension. *J Gastroenterol* 35, 758-767.
- Akhtar, N., and Hotchin, N.A. (2001). RAC1 regulates adherens junctions through endocytosis of E-cadherin. *Mol Biol Cell* 12, 847-862.
- Alberini, G., Benfenati, F., and Maragliano, L. (2017). A refined model of claudin-15 tight junction paracellular architecture by molecular dynamics simulations. *PLoS One* 12, e0184190.
- Allingham, J.S., Smith, R., and Rayment, I. (2005). The structural basis of blebbistatin inhibition and specificity for myosin II. *Nat Struct Mol Biol* 12, 378-379.
- Amano, M., Ito, M., Kimura, K., Fukata, Y., Chihara, K., Nakano, T., Matsuura, Y., and Kaibuchi, K. (1996). Phosphorylation and activation of myosin by Rho-associated kinase (Rho-kinase). *J Biol Chem* 271, 20246-20249.
- Andl, C.D., and Rustgi, A.K. (2005). No one-way street: cross-talk between e-cadherin and receptor tyrosine kinase (RTK) signaling: a mechanism to regulate RTK activity. *Cancer Biol Ther* 4, 28-31.
- Apodaca, G. (2001a). Endocytic traffic in polarized epithelial cells: role of the actin and microtubule cytoskeleton. *Traffic* 2, 149-159.
- Apodaca, G. (2001b). Stretch-regulated exocytosis of discoidal vesicles in urinary bladder epithelium. *Urology* 57, 103-104.
- Apodaca, G. (2002). Modulation of membrane traffic by mechanical stimuli. *Am J Physiol Renal Physiol* 282, F179-190.
- Apodaca, G. (2010). Opening ahead: early steps in lumen formation revealed. *Nat Cell Biol* 12, 1026-1028.

- Apodaca, G., Gallo, L.I., and Bryant, D.M. (2012). Role of membrane traffic in the generation of epithelial cell asymmetry. *Nat Cell Biol* 14, 1235-1243.
- Apodaca, G., Kiss, S., Ruiz, W., Meyers, S., Zeidel, M., and Birder, L. (2003). Disruption of bladder epithelium barrier function after spinal cord injury. *Am J Physiol Renal Physiol* 284, F966-976.
- Asada, M., Irie, K., Morimoto, K., Yamada, A., Ikeda, W., Takeuchi, M., and Takai, Y. (2003). ADIP, a novel Afadin- and alpha-actinin-binding protein localized at cell-cell adherens junctions. *J Biol Chem* 278, 4103-4111.
- Baddam, S.R., Arsenovic, P.T., Narayanan, V., Duggan, N.R., Mayer, C.R., Newman, S.T., Abutaleb, D.A., Mohan, A., Kowalczyk, A.P., and Conway, D.E. (2018). The Desmosomal Cadherin Desmoglein-2 Experiences Mechanical Tension as Demonstrated by a FRET-Based Tension Biosensor Expressed in Living Cells. *Cells* 7.
- Baffet, G., Loyer, P., Glaise, D., Corlu, A., Etienne, P.L., and Guguen-Guillouzo, C. (1991). Distinct effects of cell-cell communication and corticosteroids on the synthesis and distribution of cytokeratins in cultured rat hepatocytes. *J Cell Sci* 99 ( Pt 3), 609-615.
- Balbas, M.D., Burgess, M.R., Murali, R., Wongvipat, J., Skaggs, B.J., Mundel, P., Weins, A., and Sawyers, C.L. (2014). MAGI-2 scaffold protein is critical for kidney barrier function. *Proc Natl Acad Sci U S A* 111, 14876-14881.
- Balda, M.S., and Matter, K. (2008). Tight junctions at a glance. *J Cell Sci* 121, 3677-3682.
- Balda, M.S., and Matter, K. (2016). Tight junctions as regulators of tissue remodelling. *Curr Opin Cell Biol* 42, 94-101.
- Balestreire, E.M., and Apodaca, G. (2007). Apical epidermal growth factor receptor signaling: regulation of stretch-dependent exocytosis in bladder umbrella cells. *Mol Biol Cell* 18, 1312-1323.
- Bardet, P.L., Guirao, B., Paoletti, C., Serman, F., Leopold, V., Bosveld, F., Goya, Y., Mirouse, V., Graner, F., and Bellaiche, Y. (2013). PTEN controls junction lengthening and stability during cell rearrangement in epithelial tissue. *Dev Cell* 25, 534-546.
- Barry, A.K., Tabdili, H., Muhamed, I., Wu, J., Shashikanth, N., Gomez, G.A., Yap, A.S., Gottardi, C.J., de Rooij, J., Wang, N., and Leckband, D.E. (2014). alpha-catenin cytomechanics--role in cadherin-dependent adhesion and mechanotransduction. *J Cell Sci* 127, 1779-1791.
- Bauer, A., Lickert, H., Kemler, R., and Stappert, J. (1998). Modification of the E-cadherin-catenin complex in mitotic Madin-Darby canine kidney epithelial cells. *J Biol Chem* 273, 28314-28321.
- Baum, B., and Georgiou, M. (2011). Dynamics of adherens junctions in epithelial establishment, maintenance, and remodeling. *J Cell Biol* 192, 907-917.

- Baumholtz, A.I., Simard, A., Nikolopoulou, E., Oosenbrug, M., Collins, M.M., Piontek, A., Krause, G., Piontek, J., Greene, N.D.E., and Ryan, A.K. (2017). Claudins are essential for cell shape changes and convergent extension movements during neural tube closure. *Dev Biol* 428, 25-38.
- Betapudi, V. (2014). Life without double-headed non-muscle myosin II motor proteins. *Front Chem* 2, 45.
- Bhowmick, N.A., Ghiassi, M., Bakin, A., Aakre, M., Lundquist, C.A., Engel, M.E., Arteaga, C.L., and Moses, H.L. (2001). Transforming growth factor-beta1 mediates epithelial to mesenchymal transdifferentiation through a RhoA-dependent mechanism. *Mol Biol Cell* 12, 27-36.
- Bieling, P., Li, T.D., Weichsel, J., McGorty, R., Jreij, P., Huang, B., Fletcher, D.A., and Mullins, R.D. (2016). Force Feedback Controls Motor Activity and Mechanical Properties of Self-Assembling Branched Actin Networks. *Cell* 164, 115-127.
- Bilder, D., Schober, M., and Perrimon, N. (2003). Integrated activity of PDZ protein complexes regulates epithelial polarity. *Nat Cell Biol* 5, 53-58.
- Birder, L.A., Ruggieri, M., Takeda, M., van Koeveringe, G., Veltkamp, S., Korstanje, C., Parsons, B., and Fry, C.H. (2012). How does the urothelium affect bladder function in health and disease? ICI-RS 2011. *Neurourol Urodyn* 31, 293-299.
- Biswas, K.H., Hartman, K.L., Zaidel-Bar, R., and Groves, J.T. (2016). Sustained alpha-catenin Activation at E-cadherin Junctions in the Absence of Mechanical Force. *Biophys J* 111, 1044-1052.
- Borges, R.M., Lamers, M.L., Forti, F.L., Santos, M.F., and Yan, C.Y. (2011). Rho signaling pathway and apical constriction in the early lens placode. *Genesis* 49, 368-379.
- Borghi, N., Sorokina, M., Shcherbakova, O.G., Weis, W.I., Pruitt, B.L., Nelson, W.J., and Dunn, A.R. (2012). E-cadherin is under constitutive actomyosin-generated tension that is increased at cell-cell contacts upon externally applied stretch. *Proc Natl Acad Sci U S A* 109, 12568-12573.
- Bouchet, J., McCaffrey, M.W., Graziani, A., and Alcover, A. (2018). The functional interplay of Rab11, FIP3 and Rho proteins on the endosomal recycling pathway controls cell shape and symmetry. *Small GTPases* 9, 310-315.
- Boudier, J.A., Martin-Moutot, N., Boudier, J.L., Iborra, C., Takahashi, M., and Seagar, M.J. (1999). Redistribution of presynaptic proteins during alpha-latrotoxin-induced release of neurotransmitter and membrane retrieval at the frog neuromuscular junction. *Eur J Neurosci* 11, 3449-3456.
- Boulant, S., Kural, C., Zeeh, J.C., Ubelmann, F., and Kirchhausen, T. (2011). Actin dynamics counteract membrane tension during clathrin-mediated endocytosis. *Nat Cell Biol* 13, 1124-1131.

- Bravo-Cordero, J.J., Cordani, M., Soriano, S.F., Diez, B., Munoz-Agudo, C., Casanova-Acebes, M., Boullosa, C., Guadamillas, M.C., Ezkurdia, I., Gonzalez-Pisano, D., Del Pozo, M.A., and Montoya, M.C. (2016). A novel high-content analysis tool reveals Rab8-driven cytoskeletal reorganization through Rho GTPases, calpain and MT1-MMP. *J Cell Sci* *129*, 1734-1749.
- Broussard, J.A., Getsios, S., and Green, K.J. (2015). Desmosome regulation and signaling in disease. *Cell Tissue Res* *360*, 501-512.
- Bruwer, M., Hopkins, A.M., Hobert, M.E., Nusrat, A., and Madara, J.L. (2004). RhoA, Rac1, and Cdc42 exert distinct effects on epithelial barrier via selective structural and biochemical modulation of junctional proteins and F-actin. *Am J Physiol Cell Physiol* *287*, C327-335.
- Bruwer, M., Luegering, A., Kucharzik, T., Parkos, C.A., Madara, J.L., Hopkins, A.M., and Nusrat, A. (2003). Proinflammatory cytokines disrupt epithelial barrier function by apoptosis-independent mechanisms. *J Immunol* *171*, 6164-6172.
- Bruwer, M., Samarin, S., and Nusrat, A. (2006). Inflammatory bowel disease and the apical junctional complex. *Ann N Y Acad Sci* *1072*, 242-252.
- Bruwer, M., Utech, M., Ivanov, A.I., Hopkins, A.M., Parkos, C.A., and Nusrat, A. (2005). Interferon-gamma induces internalization of epithelial tight junction proteins via a macropinocytosis-like process. *FASEB J* *19*, 923-933.
- Brunser, O., and Luft, H.J. (1970). Fine structure of the apex of absorptive cell from rat small intestine. *J Ultrastruct Res* *31*, 291-311.
- Bruser, L., and Bogdan, S. (2017). Adherens Junctions on the Move-Membrane Trafficking of E-Cadherin. *Cold Spring Harb Perspect Biol* *9*.
- Bryant, D.M., and Stow, J.L. (2004). The ins and outs of E-cadherin trafficking. *Trends Cell Biol* *14*, 427-434.
- Bryant, J., and Francis, D. (2008). The eukaryotic cell cycle. Preface. *SEB Exp Biol Ser* *59*, xvii-xviii.
- Buckley, C.D., Tan, J., Anderson, K.L., Hanein, D., Volkmann, N., Weis, W.I., Nelson, W.J., and Dunn, A.R. (2014). Cell adhesion. The minimal cadherin-catenin complex binds to actin filaments under force. *Science* *346*, 1254-1259.
- Butler, L.C., Blanchard, G.B., Kabla, A.J., Lawrence, N.J., Welchman, D.P., Mahadevan, L., Adams, R.J., and Sanson, B. (2009). Cell shape changes indicate a role for extrinsic tensile forces in *Drosophila* germ-band extension. *Nat Cell Biol* *11*, 859-864.
- Cai, D., Chen, S.C., Prasad, M., He, L., Wang, X., Choesmel-Cadamuro, V., Sawyer, J.K., Danuser, G., and Montell, D.J. (2014). Mechanical feedback through E-cadherin promotes direction sensing during collective cell migration. *Cell* *157*, 1146-1159.
- Carattino, M.D., Prakasam, H.S., Ruiz, W.G., Clayton, D.R., McGuire, M., Gallo, L.I., and Apodaca, G. (2013). Bladder filling and voiding affect umbrella cell tight junction organization and function. *Am J Physiol Renal Physiol* *305*, F1158-1168.

- Carberry, K., Wiesenfahrt, T., Geisler, F., Stocker, S., Gerhardus, H., Uberbach, D., Davis, W., Jorgensen, E., Leube, R.E., and Bossinger, O. (2012). The novel intestinal filament organizer IFO-1 contributes to epithelial integrity in concert with ERM-1 and DLG-1. *Development* 139, 1851-1862.
- Carosi, J.A., Eskin, S.G., and McIntire, L.V. (1992). Cyclical strain effects on production of vasoactive materials in cultured endothelial cells. *J Cell Physiol* 151, 29-36.
- Carramusa, L., Ballestrem, C., Zilberman, Y., and Bershadsky, A.D. (2007). Mammalian diaphanous-related formin Dia1 controls the organization of E-cadherin-mediated cell-cell junctions. *J Cell Sci* 120, 3870-3882.
- Cavanaugh, K.J., Jr., and Margulies, S.S. (2002). Measurement of stretch-induced loss of alveolar epithelial barrier integrity with a novel in vitro method. *Am J Physiol Cell Physiol* 283, C1801-1808.
- Cavanaugh, K.J., Jr., Oswari, J., and Margulies, S.S. (2001). Role of stretch on tight junction structure in alveolar epithelial cells. *Am J Respir Cell Mol Biol* 25, 584-591.
- Charras, G., and Yap, A.S. (2018). Tensile Forces and Mechanotransduction at Cell-Cell Junctions. *Curr Biol* 28, R445-R457.
- Charrier, E.E., and Janmey, P.A. (2016). Mechanical Properties of Intermediate Filament Proteins. *Methods Enzymol* 568, 35-57.
- Chatterjee, S., Wang, Y., Duncan, M.K., and Naik, U.P. (2013). Junctional adhesion molecule-A regulates vascular endothelial growth factor receptor-2 signaling-dependent mouse corneal wound healing. *PLoS One* 8, e63674.
- Chen, X., Bonne, S., Hatzfeld, M., van Roy, F., and Green, K.J. (2002). Protein binding and functional characterization of plakophilin 2. Evidence for its diverse roles in desmosomes and beta -catenin signaling. *J Biol Chem* 277, 10512-10522.
- Chen, Y., Guo, X., Deng, F.M., Liang, F.X., Sun, W., Ren, M., Izumi, T., Sabatini, D.D., Sun, T.T., and Kreibich, G. (2003). Rab27b is associated with fusiform vesicles and may be involved in targeting uroplakins to urothelial apical membranes. *Proc Natl Acad Sci U S A* 100, 14012-14017.
- Chu, C.W., Gerstenzang, E., Ossipova, O., and Sokol, S.Y. (2013). Lulu regulates Shroom-induced apical constriction during neural tube closure. *PLoS One* 8, e81854.
- Chung, Y.C., Wei, W.C., Huang, S.H., Shih, C.M., Hsu, C.P., Chang, K.J., and Chao, W.T. (2014). Rab11 regulates E-cadherin expression and induces cell transformation in colorectal carcinoma. *BMC Cancer* 14, 587.
- Classen, A.K., Anderson, K.I., Marois, E., and Eaton, S. (2005). Hexagonal packing of *Drosophila* wing epithelial cells by the planar cell polarity pathway. *Dev Cell* 9, 805-817.
- Claude, P. (1978). Morphological factors influencing transepithelial permeability: a model for the resistance of the zonula occludens. *J Membr Biol* 39, 219-232.
- Claude, P., and Goodenough, D.A. (1973). Fracture faces of zonulae occludentes from "tight" and "leaky" epithelia. *J Cell Biol* 58, 390-400.

- Coch, R.A., and Leube, R.E. (2016). Intermediate Filaments and Polarization in the Intestinal Epithelium. *Cells* 5.
- Cohen, T.S., Gray Lawrence, G., Khasgiwala, A., and Margulies, S.S. (2010). MAPK activation modulates permeability of isolated rat alveolar epithelial cell monolayers following cyclic stretch. *PLoS One* 5, e10385.
- Colgan, O.C., Ferguson, G., Collins, N.T., Murphy, R.P., Meade, G., Cahill, P.A., and Cummins, P.M. (2007). Regulation of bovine brain microvascular endothelial tight junction assembly and barrier function by laminar shear stress. *Am J Physiol Heart Circ Physiol* 292, H3190-3197.
- Collins, N.T., Cummins, P.M., Colgan, O.C., Ferguson, G., Birney, Y.A., Murphy, R.P., Meade, G., and Cahill, P.A. (2006). Cyclic strain-mediated regulation of vascular endothelial occludin and ZO-1: influence on intercellular tight junction assembly and function. *Arterioscler Thromb Vasc Biol* 26, 62-68.
- Costa, M., Raich, W., Agbunag, C., Leung, B., Hardin, J., and Priess, J.R. (1998). A putative catenin-cadherin system mediates morphogenesis of the *Caenorhabditis elegans* embryo. *J Cell Biol* 141, 297-308.
- Courtemanche, N., Lee, J.Y., Pollard, T.D., and Greene, E.C. (2013). Tension modulates actin filament polymerization mediated by formin and profilin. *Proc Natl Acad Sci U S A* 110, 9752-9757.
- Coyne, C.B., Shen, L., Turner, J.R., and Bergelson, J.M. (2007). Coxsackievirus entry across epithelial tight junctions requires occludin and the small GTPases Rab34 and Rab5. *Cell Host Microbe* 2, 181-192.
- Croise, P., Estay-Ahumada, C., Gasman, S., and Ory, S. (2014). Rho GTPases, phosphoinositides, and actin: a tripartite framework for efficient vesicular trafficking. *Small GTPases* 5, e29469.
- Dai, J., Ting-Beall, H.P., and Sheetz, M.P. (1997). The secretion-coupled endocytosis correlates with membrane tension changes in RBL 2H3 cells. *J Gen Physiol* 110, 1-10.
- Dalghi, M.G., Clayton, D.R., Ruiz, W.G., Al-Bataineh, M.M., Satlin, L.M., Kleyman, T.R., Ricke, W.A., Carattino, M.D., and Apodaca, G. (2019). Expression and distribution of PIEZO1 in the mouse urinary tract. *Am J Physiol Renal Physiol* 317, F303-F321.
- Das, D., Zalewski, J.K., Mohan, S., Plageman, T.F., VanDemark, A.P., and Hildebrand, J.D. (2014). The interaction between Shroom3 and Rho-kinase is required for neural tube morphogenesis in mice. *Biol Open* 3, 850-860.
- de Madrid, B.H., Greenberg, L., and Hatini, V. (2015). RhoGAP68F controls transport of adhesion proteins in Rab4 endosomes to modulate epithelial morphogenesis of *Drosophila* leg discs. *Dev Biol* 399, 283-295.
- De Santis, G., Miotti, S., Mazzi, M., Canevari, S., and Tomassetti, A. (2009). E-cadherin directly contributes to PI3K/AKT activation by engaging the PI3K-p85 regulatory subunit to adherens junctions of ovarian carcinoma cells. *Oncogene* 28, 1206-1217.

- Dejana, E. (2004). Endothelial cell-cell junctions: happy together. *Nat Rev Mol Cell Biol* 5, 261-270.
- DeMaio, L., Chang, Y.S., Gardner, T.W., Tarbell, J.M., and Antonetti, D.A. (2001). Shear stress regulates occludin content and phosphorylation. *Am J Physiol Heart Circ Physiol* 281, H105-113.
- Desclozeaux, M., Venturato, J., Wylie, F.G., Kay, J.G., Joseph, S.R., Le, H.T., and Stow, J.L. (2008). Active Rab11 and functional recycling endosome are required for E-cadherin trafficking and lumen formation during epithelial morphogenesis. *Am J Physiol Cell Physiol* 295, C545-556.
- Doe, C., Bentley, R., Behm, D.J., Lafferty, R., Stavenger, R., Jung, D., Bamford, M., Panchal, T., Grygielko, E., Wright, L.L., Smith, G.K., Chen, Z., Webb, C., Khandekar, S., Yi, T., Kirkpatrick, R., Dul, E., Jolivet, L., Marino, J.P., Jr., Willette, R., Lee, D., and Hu, E. (2007). Novel Rho kinase inhibitors with anti-inflammatory and vasodilatory activities. *J Pharmacol Exp Ther* 320, 89-98.
- Doherty, G.J., and McMahon, H.T. (2009). Mechanisms of endocytosis. *Annu Rev Biochem* 78, 857-902.
- Duan, Y., Gotoh, N., Yan, Q., Du, Z., Weinstein, A.M., Wang, T., and Weinbaum, S. (2008). Shear-induced reorganization of renal proximal tubule cell actin cytoskeleton and apical junctional complexes. *Proc Natl Acad Sci U S A* 105, 11418-11423.
- Dutta, D., Williamson, C.D., Cole, N.B., and Donaldson, J.G. (2012). Pitstop 2 is a potent inhibitor of clathrin-independent endocytosis. *PLoS One* 7, e45799.
- Eaton, A.F., Clayton, D.R., Ruiz, W.G., Griffiths, S.E., Rubio, M.E., and Apodaca, G. (2019). Expansion and contraction of the umbrella cell apical junctional ring in response to bladder filling and voiding. *Mol Biol Cell* 30, 2037-2052.
- Ebnet, K., Suzuki, A., Ohno, S., and Vestweber, D. (2004). Junctional adhesion molecules (JAMs): more molecules with dual functions? *J Cell Sci* 117, 19-29.
- Ebrahim, S., Fujita, T., Millis, B.A., Kozin, E., Ma, X., Kawamoto, S., Baird, M.A., Davidson, M., Yonemura, S., Hisa, Y., Conti, M.A., Adelstein, R.S., Sakaguchi, H., and Kachar, B. (2013). NMII forms a contractile transcellular sarcomeric network to regulate apical cell junctions and tissue geometry. *Curr Biol* 23, 731-736.
- Efimova, N., and Svitkina, T.M. (2018). Branched actin networks push against each other at adherens junctions to maintain cell-cell adhesion. *J Cell Biol* 217, 1827-1845.
- Elias, P.M., Matsuyoshi, N., Wu, H., Lin, C., Wang, Z.H., Brown, B.E., and Stanley, J.R. (2001). Desmoglein isoform distribution affects stratum corneum structure and function. *J Cell Biol* 153, 243-249.
- Eshkind, L., Tian, Q., Schmidt, A., Franke, W.W., Windoffer, R., and Leube, R.E. (2002). Loss of desmoglein 2 suggests essential functions for early embryonic development and proliferation of embryonal stem cells. *Eur J Cell Biol* 81, 592-598.

- Fanning, A.S., Van Itallie, C.M., and Anderson, J.M. (2012). Zonula occludens-1 and -2 regulate apical cell structure and the zonula adherens cytoskeleton in polarized epithelia. *Mol Biol Cell* **23**, 577-590.
- Farge, E. (2003). Mechanical induction of Twist in the *Drosophila* foregut/stomodaeal primordium. *Curr Biol* **13**, 1365-1377.
- Farquhar, M.G., and Palade, G.E. (1963). Junctional complexes in various epithelia. *J Cell Biol* **17**, 375-412.
- Feldman, G.J., Mullin, J.M., and Ryan, M.P. (2005). Occludin: structure, function and regulation. *Adv Drug Deliv Rev* **57**, 883-917.
- Ferber, E.C., Kajita, M., Wadlow, A., Tobiansky, L., Niessen, C., Ariga, H., Daniel, J., and Fujita, Y. (2008). A role for the cleaved cytoplasmic domain of E-cadherin in the nucleus. *J Biol Chem* **283**, 12691-12700.
- Fernandez-Gonzalez, R., Simoes Sde, M., Roper, J.C., Eaton, S., and Zallen, J.A. (2009). Myosin II dynamics are regulated by tension in intercalating cells. *Dev Cell* **17**, 736-743.
- Forster, C. (2008). Tight junctions and the modulation of barrier function in disease. *Histochem Cell Biol* **130**, 55-70.
- Fromter, E., and Diamond, J. (1972). Route of passive ion permeation in epithelia. *Nat New Biol* **235**, 9-13.
- Fung, C.K., Xi, N., Yang, R., Seiffert-Sinha, K., Lai, K.W., and Sinha, A.A. (2011). Quantitative analysis of human keratinocyte cell elasticity using atomic force microscopy (AFM). *IEEE Trans Nanobioscience* **10**, 9-15.
- Fung, K.Y.Y., Fairn, G.D., and Lee, W.L. (2018). Transcellular vesicular transport in epithelial and endothelial cells: Challenges and opportunities. *Traffic* **19**, 5-18.
- Furman, C., Sieminski, A.L., Kwiatkowski, A.V., Rubinson, D.A., Vasile, E., Bronson, R.T., Fassler, R., and Gertler, F.B. (2007). Ena/VASP is required for endothelial barrier function in vivo. *J Cell Biol* **179**, 761-775.
- Furuse, M., Hata, M., Furuse, K., Yoshida, Y., Haratake, A., Sugitani, Y., Noda, T., Kubo, A., and Tsukita, S. (2002). Claudin-based tight junctions are crucial for the mammalian epidermal barrier: a lesson from claudin-1-deficient mice. *J Cell Biol* **156**, 1099-1111.
- Furuse, M., and Tsukita, S. (2006). Claudins in occluding junctions of humans and flies. *Trends Cell Biol* **16**, 181-188.
- Gallo, L.I., Dalghi, M.G., Clayton, D.R., Ruiz, W.G., Khandelwal, P., and Apodaca, G. (2018). RAB27B requirement for stretch-induced exocytosis in bladder umbrella cells. *Am J Physiol Cell Physiol* **314**, C349-C365.

- Garcia-Polite, F., Martorell, J., Del Rey-Puech, P., Melgar-Lesmes, P., O'Brien, C.C., Roquer, J., Ois, A., Principe, A., Edelman, E.R., and Balcells, M. (2017). Pulsatility and high shear stress deteriorate barrier phenotype in brain microvascular endothelium. *J Cereb Blood Flow Metab* 37, 2614-2625.
- Gates, D.H., Lee, J.S., Hultman, C.S., and Cairns, B.A. (2007). Inhibition of rho-kinase impairs fibroblast stress fiber formation, confluence, and contractility in vitro. *J Burn Care Res* 28, 507-513.
- Gauthier, N.C., Fardin, M.A., Roca-Cusachs, P., and Sheetz, M.P. (2011). Temporary increase in plasma membrane tension coordinates the activation of exocytosis and contraction during cell spreading. *Proc Natl Acad Sci U S A* 108, 14467-14472.
- Gauthier, N.C., Masters, T.A., and Sheetz, M.P. (2012). Mechanical feedback between membrane tension and dynamics. *Trends Cell Biol* 22, 527-535.
- Gauthier, N.C., Rossier, O.M., Mathur, A., Hone, J.C., and Sheetz, M.P. (2009). Plasma membrane area increases with spread area by exocytosis of a GPI-anchored protein compartment. *Mol Biol Cell* 20, 3261-3272.
- Gerhard, R., Schmidt, G., Hofmann, F., and Aktories, K. (1998). Activation of Rho GTPases by Escherichia coli cytotoxic necrotizing factor 1 increases intestinal permeability in Caco-2 cells. *Infect Immun* 66, 5125-5131.
- Getsios, S., Simpson, C.L., Kojima, S., Harmon, R., Sheu, L.J., Dusek, R.L., Cornwell, M., and Green, K.J. (2009). Desmoglein 1-dependent suppression of EGFR signaling promotes epidermal differentiation and morphogenesis. *J Cell Biol* 185, 1243-1258.
- Gilmour, D., Rembold, M., and Leptin, M. (2017). From morphogen to morphogenesis and back. *Nature* 541, 311-320.
- Godsel, L.M., Hsieh, S.N., Amargo, E.V., Bass, A.E., Pascoe-McGillicuddy, L.T., Huen, A.C., Thorne, M.E., Gaudry, C.A., Park, J.K., Myung, K., Goldman, R.D., Chew, T.L., and Green, K.J. (2005). Desmoplakin assembly dynamics in four dimensions: multiple phases differentially regulated by intermediate filaments and actin. *J Cell Biol* 171, 1045-1059.
- Goldenring, J.R. (2015). Recycling endosomes. *Curr Opin Cell Biol* 35, 117-122.
- Gomez, G.A., McLachlan, R.W., and Yap, A.S. (2011). Productive tension: force-sensing and homeostasis of cell-cell junctions. *Trends Cell Biol* 21, 499-505.
- Grant, B.D., and Donaldson, J.G. (2009). Pathways and mechanisms of endocytic recycling. *Nat Rev Mol Cell Biol* 10, 597-608.
- Grasso, E.J., and Calderon, R.O. (2013). Urothelial endocytic vesicle recycling and lysosomal degradative pathway regulated by lipid membrane composition. *Histochem Cell Biol* 139, 249-265.
- Green, K.J., Getsios, S., Troyanovsky, S., and Godsel, L.M. (2010). Intercellular junction assembly, dynamics, and homeostasis. *Cold Spring Harb Perspect Biol* 2, a000125.
- Greenberg, M.J., Arpag, G., Tuzel, E., and Ostap, E.M. (2016). A Perspective on the Role of Myosins as Mechanosensors. *Biophys J* 110, 2568-2576.

- Greven, H., and Robenek, H. (1980). Intercellular junctions in the uterine epithelium of *Salamandra salamandra* (L.) (Amphibia, Urodela). A freeze-fracture study. *Cell Tissue Res* 212, 163-172.
- Grikscheit, K., Frank, T., Wang, Y., and Grosse, R. (2015). Junctional actin assembly is mediated by Formin-like 2 downstream of Rac1. *J Cell Biol* 209, 367-376.
- Grikscheit, K., and Grosse, R. (2016). Formins at the Junction. *Trends Biochem Sci* 41, 148-159.
- Grindstaff, K.K., Yeaman, C., Anandasabapathy, N., Hsu, S.C., Rodriguez-Boulan, E., Scheller, R.H., and Nelson, W.J. (1998). Sec6/8 complex is recruited to cell-cell contacts and specifies transport vesicle delivery to the basal-lateral membrane in epithelial cells. *Cell* 93, 731-740.
- Grygorczyk, R., and Hanrahan, J.W. (1997). CFTR-independent ATP release from epithelial cells triggered by mechanical stimuli. *Am J Physiol* 272, C1058-1066.
- Guillemot, L., Paschoud, S., Jond, L., Foglia, A., and Citi, S. (2008). Paracingulin regulates the activity of Rac1 and RhoA GTPases by recruiting Tiam1 and GEF-H1 to epithelial junctions. *Mol Biol Cell* 19, 4442-4453.
- Guillemot, L., Schneider, Y., Brun, P., Castagliuolo, I., Pizzuti, D., Martines, D., Jond, L., Bongiovanni, M., and Citi, S. (2012). Cingulin is dispensable for epithelial barrier function and tight junction structure, and plays a role in the control of claudin-2 expression and response to duodenal mucosa injury. *J Cell Sci* 125, 5005-5014.
- Gunzel, D., and Yu, A.S. (2013). Claudins and the modulation of tight junction permeability. *Physiol Rev* 93, 525-569.
- Guo, P., Weinstein, A.M., and Weinbaum, S. (2003). A dual-pathway ultrastructural model for the tight junction of rat proximal tubule epithelium. *Am J Physiol Renal Physiol* 285, F241-257.
- Hagen, S.J. (2017). Non-canonical functions of claudin proteins: Beyond the regulation of cell-cell adhesions. *Tissue Barriers* 5, e1327839.
- Hagmann, J., Dagan, D., and Burger, M.M. (1992). Release of endosomal content induced by plasma membrane tension: video image intensification time lapse analysis. *Exp Cell Res* 198, 298-304.
- Hamill, O.P. (2006). Twenty odd years of stretch-sensitive channels. *Pflugers Arch* 453, 333-351.
- Han, M.K., Hoijman, E., Noel, E., Garric, L., Bakkers, J., and de Rooij, J. (2016). alphaE-catenin-dependent mechanotransduction is essential for proper convergent extension in zebrafish. *Biol Open* 5, 1461-1472.
- Harris, K.P., and Tepass, U. (2008). Cdc42 and Par proteins stabilize dynamic adherens junctions in the *Drosophila* neuroectoderm through regulation of apical endocytosis. *J Cell Biol* 183, 1129-1143.
- Hatzfeld, M., Keil, R., and Magin, T.M. (2017). Desmosomes and Intermediate Filaments: Their Consequences for Tissue Mechanics. *Cold Spring Harb Perspect Biol* 9.

- Heisenberg, C.P., and Bellaiche, Y. (2013). Forces in tissue morphogenesis and patterning. *Cell* 153, 948-962.
- Hernandez, S., Chavez Munguia, B., and Gonzalez-Mariscal, L. (2007). ZO-2 silencing in epithelial cells perturbs the gate and fence function of tight junctions and leads to an atypical monolayer architecture. *Exp Cell Res* 313, 1533-1547.
- Hicks, R.M. (1975). The mammalian urinary bladder: an accommodating organ. *Biol Rev Camb Philos Soc* 50, 215-246.
- Hissa, B., Pontes, B., Roma, P.M., Alves, A.P., Rocha, C.D., Valverde, T.M., Aguiar, P.H., Almeida, F.P., Guimaraes, A.J., Guatimosim, C., Silva, A.M., Fernandes, M.C., Andrews, N.W., Viana, N.B., Mesquita, O.N., Agero, U., and Andrade, L.O. (2013). Membrane cholesterol removal changes mechanical properties of cells and induces secretion of a specific pool of lysosomes. *PLoS One* 8, e82988.
- Hoffman, B.D., Grashoff, C., and Schwartz, M.A. (2011). Dynamic molecular processes mediate cellular mechanotransduction. *Nature* 475, 316-323.
- Homberg, M., Ramms, L., Schwarz, N., Dreissen, G., Leube, R.E., Merkel, R., Hoffmann, B., and Magin, T.M. (2015). Distinct Impact of Two Keratin Mutations Causing Epidermolysis Bullosa Simplex on Keratinocyte Adhesion and Stiffness. *J Invest Dermatol* 135, 2437-2445.
- Homem, C.C., and Peifer, M. (2008). Diaphanous regulates myosin and adherens junctions to control cell contractility and protrusive behavior during morphogenesis. *Development* 135, 1005-1018.
- Hopkins, A.M., Walsh, S.V., Verkade, P., Boquet, P., and Nusrat, A. (2003). Constitutive activation of Rho proteins by CNF-1 influences tight junction structure and epithelial barrier function. *J Cell Sci* 116, 725-742.
- Hou, J., Renigunta, A., Gomes, A.S., Hou, M., Paul, D.L., Waldegger, S., and Goodenough, D.A. (2009). Claudin-16 and claudin-19 interaction is required for their assembly into tight junctions and for renal reabsorption of magnesium. *Proc Natl Acad Sci U S A* 106, 15350-15355.
- Hou, J., Renigunta, A., Konrad, M., Gomes, A.S., Schneeberger, E.E., Paul, D.L., Waldegger, S., and Goodenough, D.A. (2008). Claudin-16 and claudin-19 interact and form a cation-selective tight junction complex. *J Clin Invest* 118, 619-628.
- Hou, J., Renigunta, A., Yang, J., and Waldegger, S. (2010). Claudin-4 forms paracellular chloride channel in the kidney and requires claudin-8 for tight junction localization. *Proc Natl Acad Sci U S A* 107, 18010-18015.
- Howes, M.T., Kirkham, M., Riches, J., Cortese, K., Walser, P.J., Simpson, F., Hill, M.M., Jones, A., Lundmark, R., Lindsay, M.R., Hernandez-Deviez, D.J., Hadzic, G., McCluskey, A., Bashir, R., Liu, L., Pilch, P., McMahon, H., Robinson, P.J., Hancock, J.F., Mayor, S., and Parton, R.G. (2010). Clathrin-independent carriers form a high capacity endocytic sorting system at the leading edge of migrating cells. *J Cell Biol* 190, 675-691.

- Hull, B.E., and Staehelin, L.A. (1976). Functional significance of the variations in the geometrical organization of tight junction networks. *J Cell Biol* 68, 688-704.
- Ikenouchi, J., Furuse, M., Furuse, K., Sasaki, H., Tsukita, S., and Tsukita, S. (2005). Tricellulin constitutes a novel barrier at tricellular contacts of epithelial cells. *J Cell Biol* 171, 939-945.
- Ioannou, M.S., and McPherson, P.S. (2016). Regulation of Cancer Cell Behavior by the Small GTPase Rab13. *J Biol Chem* 291, 9929-9937.
- Ishiyama, N., Sarpal, R., Wood, M.N., Barrick, S.K., Nishikawa, T., Hayashi, H., Kobb, A.B., Flozak, A.S., Yemelyanov, A., Fernandez-Gonzalez, R., Yonemura, S., Leckband, D.E., Gottardi, C.J., Tepass, U., and Ikura, M. (2018). Force-dependent allostery of the alpha-catenin actin-binding domain controls adherens junction dynamics and functions. *Nat Commun* 9, 5121.
- Itoh, K., Ossipova, O., and Sokol, S.Y. (2014). GEF-H1 functions in apical constriction and cell intercalations and is essential for vertebrate neural tube closure. *J Cell Sci* 127, 2542-2553.
- Ivanov, A.I., Hunt, D., Utech, M., Nusrat, A., and Parkos, C.A. (2005a). Differential roles for actin polymerization and a myosin II motor in assembly of the epithelial apical junctional complex. *Mol Biol Cell* 16, 2636-2650.
- Ivanov, A.I., McCall, I.C., Parkos, C.A., and Nusrat, A. (2004a). Role for actin filament turnover and a myosin II motor in cytoskeleton-driven disassembly of the epithelial apical junctional complex. *Mol Biol Cell* 15, 2639-2651.
- Ivanov, A.I., Nusrat, A., and Parkos, C.A. (2004b). Endocytosis of epithelial apical junctional proteins by a clathrin-mediated pathway into a unique storage compartment. *Mol Biol Cell* 15, 176-188.
- Ivanov, A.I., Nusrat, A., and Parkos, C.A. (2005b). Endocytosis of the apical junctional complex: mechanisms and possible roles in regulation of epithelial barriers. *Bioessays* 27, 356-365.
- Iwatsuki, H., and Suda, M. (2007). Keratin 20 expressed in the endocrine and exocrine cells of the rabbit duodenum. *Acta Histochem Cytochem* 40, 123-130.
- Jang, A.S. (2014). The apical junctional complex in respiratory diseases. *Chonnam Med J* 50, 1-5.
- Janmey, P.A., and McCulloch, C.A. (2007). Cell mechanics: integrating cell responses to mechanical stimuli. *Annu Rev Biomed Eng* 9, 1-34.
- Jefferson, J.J., Leung, C.L., and Liem, R.K. (2004). Plakins: goliaths that link cell junctions and the cytoskeleton. *Nat Rev Mol Cell Biol* 5, 542-553.
- Jegou, A., Carlier, M.F., and Romet-Lemonne, G. (2013). Formin mDia1 senses and generates mechanical forces on actin filaments. *Nat Commun* 4, 1883.

- Jewett, C.E., Vanderleest, T.E., Miao, H., Xie, Y., Madhu, R., Loerke, D., and Blankenship, J.T. (2017). Planar polarized Rab35 functions as an oscillatory ratchet during cell intercalation in the *Drosophila* epithelium. *Nat Commun* 8, 476.
- Jiang, Y.H., and Kuo, H.C. (2014). Urothelial dysfunction and increased suburothelial inflammation of urinary bladder are involved in patients with upper urinary tract urolithiasis--clinical and immunohistochemistry study. *PLoS One* 9, e110754.
- Johnson, J.L., Najor, N.A., and Green, K.J. (2014). Desmosomes: regulators of cellular signaling and adhesion in epidermal health and disease. *Cold Spring Harb Perspect Med* 4, a015297.
- Jou, T.S., Schneeberger, E.E., and Nelson, W.J. (1998). Structural and functional regulation of tight junctions by RhoA and Rac1 small GTPases. *J Cell Biol* 142, 101-115.
- Jovic, M., Sharma, M., Rahajeng, J., and Caplan, S. (2010). The early endosome: a busy sorting station for proteins at the crossroads. *Histol Histopathol* 25, 99-112.
- Jurado, J., de Navascues, J., and Gorfinkiel, N. (2016). alpha-Catenin stabilises Cadherin-Catenin complexes and modulates actomyosin dynamics to allow pulsatile apical contraction. *J Cell Sci* 129, 4496-4508.
- Kaksonen, M., and Roux, A. (2018). Mechanisms of clathrin-mediated endocytosis. *Nat Rev Mol Cell Biol* 19, 313-326.
- Kamei, T., Matozaki, T., Sakisaka, T., Kodama, A., Yokoyama, S., Peng, Y.F., Nakano, K., Takaishi, K., and Takai, Y. (1999). Coendocytosis of cadherin and c-Met coupled to disruption of cell-cell adhesion in MDCK cells--regulation by Rho, Rac and Rab small G proteins. *Oncogene* 18, 6776-6784.
- Katsuma, Y., Marceau, N., Ohta, M., and French, S.W. (1988). Cytokeratin intermediate filaments of rat hepatocytes: different cytoskeletal domains and their three-dimensional structure. *Hepatology* 8, 559-568.
- Katsuno, T., Umeda, K., Matsui, T., Hata, M., Tamura, A., Itoh, M., Takeuchi, K., Fujimori, T., Nabeshima, Y., Noda, T., Tsukita, S., and Tsukita, S. (2008). Deficiency of zonula occludens-1 causes embryonic lethal phenotype associated with defected yolk sac angiogenesis and apoptosis of embryonic cells. *Mol Biol Cell* 19, 2465-2475.
- Keay, S., Kaczmarek, P., Zhang, C.O., Koch, K., Szekely, Z., Barchi, J.J., Jr., and Michejda, C. (2011). Normalization of proliferation and tight junction formation in bladder epithelial cells from patients with interstitial cystitis/painful bladder syndrome by d-proline and d-pipecolic acid derivatives of antiproliferative factor. *Chem Biol Drug Des* 77, 421-430.
- Keay, S.K., Birder, L.A., and Chai, T.C. (2014). Evidence for bladder urothelial pathophysiology in functional bladder disorders. *Biomed Res Int* 2014, 865463.
- Kevil, C.G., Ohno, N., Gute, D.C., Okayama, N., Robinson, S.A., Chaney, E., and Alexander, J.S. (1998). Role of cadherin internalization in hydrogen peroxide-mediated endothelial permeability. *Free Radic Biol Med* 24, 1015-1022.

- Khandelwal, P., Abraham, S.N., and Apodaca, G. (2009). Cell biology and physiology of the uroepithelium. *Am J Physiol Renal Physiol* 297, F1477-1501.
- Khandelwal, P., Prakasam, H.S., Clayton, D.R., Ruiz, W.G., Gallo, L.I., van Roekel, D., Lukianov, S., Peranen, J., Goldenring, J.R., and Apodaca, G. (2013). A Rab11a-Rab8a-Myo5B network promotes stretch-regulated exocytosis in bladder umbrella cells. *Mol Biol Cell* 24, 1007-1019.
- Khandelwal, P., Ruiz, W.G., and Apodaca, G. (2010). Compensatory endocytosis in bladder umbrella cells occurs through an integrin-regulated and RhoA- and dynamin-dependent pathway. *EMBO J* 29, 1961-1975.
- Khandelwal, P., Ruiz, W.G., Balestreire-Hawryluk, E., Weisz, O.A., Goldenring, J.R., and Apodaca, G. (2008). Rab11a-dependent exocytosis of discoidal/fusiform vesicles in bladder umbrella cells. *Proc Natl Acad Sci U S A* 105, 15773-15778.
- Kim, T.J., Zheng, S., Sun, J., Muhamed, I., Wu, J., Lei, L., Kong, X., Leckband, D.E., and Wang, Y. (2015). Dynamic visualization of alpha-catenin reveals rapid, reversible conformation switching between tension states. *Curr Biol* 25, 218-224.
- Kjos, I., Vestre, K., Guadagno, N.A., Borg Distefano, M., and Progida, C. (2018). Rab and Arf proteins at the crossroad between membrane transport and cytoskeleton dynamics. *Biochim Biophys Acta Mol Cell Res* 1865, 1397-1409.
- Klausner, R.D., Donaldson, J.G., and Lippincott-Schwartz, J. (1992). Brefeldin A: insights into the control of membrane traffic and organelle structure. *J Cell Biol* 116, 1071-1080.
- Kljuic, A., Bazzi, H., Sundberg, J.P., Martinez-Mir, A., O'Shaughnessy, R., Mahoney, M.G., Levy, M., Montagutelli, X., Ahmad, W., Aita, V.M., Gordon, D., Uitto, J., Whiting, D., Ott, J., Fischer, S., Gilliam, T.C., Jahoda, C.A., Morris, R.J., Panteleyev, A.A., Nguyen, V.T., and Christiano, A.M. (2003). Desmoglein 4 in hair follicle differentiation and epidermal adhesion: evidence from inherited hypotrichosis and acquired pemphigus vulgaris. *Cell* 113, 249-260.
- Kobiela, A., Pasolli, H.A., and Fuchs, E. (2004). Mammalian formin-1 participates in adherens junctions and polymerization of linear actin cables. *Nat Cell Biol* 6, 21-30.
- Koch, A.W., Pokutta, S., Lustig, A., and Engel, J. (1997). Calcium binding and homoassociation of E-cadherin domains. *Biochemistry* 36, 7697-7705.
- Koga, A., and Todo, S. (1978). Morphological and functional changes in the tight junctions of the bile canaliculi induced by bile duct ligation. *Cell Tissue Res* 195, 267-276.
- Koh, B.H., Roy, R., Hollywood, M.A., Thornbury, K.D., McHale, N.G., Sergeant, G.P., Hatton, W.J., Ward, S.M., Sanders, K.M., and Koh, S.D. (2012). Platelet-derived growth factor receptor-alpha cells in mouse urinary bladder: a new class of interstitial cells. *J Cell Mol Med* 16, 691-700.
- Kohler, K., Louvard, D., and Zahraoui, A. (2004). Rab13 regulates PKA signaling during tight junction assembly. *J Cell Biol* 165, 175-180.

- Kolesnikov, T., and Beckendorf, S.K. (2007). 18 wheeler regulates apical constriction of salivary gland cells via the Rho-GTPase-signaling pathway. *Dev Biol* 307, 53-61.
- Kong, D., Wolf, F., and Grosshans, J. (2017). Forces directing germ-band extension in *Drosophila* embryos. *Mech Dev* 144, 11-22.
- Kovacs, E.M., Goodwin, M., Ali, R.G., Paterson, A.D., and Yap, A.S. (2002). Cadherin-directed actin assembly: E-cadherin physically associates with the Arp2/3 complex to direct actin assembly in nascent adhesive contacts. *Curr Biol* 12, 379-382.
- Kovacs, E.M., Verma, S., Ali, R.G., Ratheesh, A., Hamilton, N.A., Akhmanova, A., and Yap, A.S. (2011). N-WASP regulates the epithelial junctional actin cytoskeleton through a non- canonical post-nucleation pathway. *Nat Cell Biol* 13, 934-943.
- Kowalczyk, A.P., and Nanes, B.A. (2012). Adherens junction turnover: regulating adhesion through cadherin endocytosis, degradation, and recycling. *Subcell Biochem* 60, 197-222.
- Kreft, M.E., Romih, R., Kreft, M., and Jezernik, K. (2009). Endocytotic activity of bladder superficial urothelial cells is inversely related to their differentiation stage. *Differentiation* 77, 48-59.
- Krug, S.M., Gunzel, D., Conrad, M.P., Rosenthal, R., Fromm, A., Amasheh, S., Schulzke, J.D., and Fromm, M. (2012). Claudin-17 forms tight junction channels with distinct anion selectivity. *Cell Mol Life Sci* 69, 2765-2778.
- Lamaze, C., Dujeancourt, A., Baba, T., Lo, C.G., Benmerah, A., and Dautry-Varsat, A. (2001). Interleukin 2 receptors and detergent-resistant membrane domains define a clathrin-independent endocytic pathway. *Mol Cell* 7, 661-671.
- Lambert, M., Choquet, D., and Mege, R.M. (2002). Dynamics of ligand-induced, Rac1-dependent anchoring of cadherins to the actin cytoskeleton. *J Cell Biol* 157, 469-479.
- Langevin, J., Morgan, M.J., Sibarita, J.B., Aresta, S., Murthy, M., Schwarz, T., Camonis, J., and Bellaiche, Y. (2005). *Drosophila* exocyst components Sec5, Sec6, and Sec15 regulate DE-Cadherin trafficking from recycling endosomes to the plasma membrane. *Dev Cell* 9, 365-376.
- Langille, B.L., and Adamson, S.L. (1981). Relationship between blood flow direction and endothelial cell orientation at arterial branch sites in rabbits and mice. *Circ Res* 48, 481-488.
- Lapierre, L.A., Tuma, P.L., Navarre, J., Goldenring, J.R., and Anderson, J.M. (1999). VAP-33 localizes to both an intracellular vesicle population and with occludin at the tight junction. *J Cell Sci* 112 ( Pt 21), 3723-3732.
- Lau, A.S., and Mruk, D.D. (2003). Rab8B GTPase and junction dynamics in the testis. *Endocrinology* 144, 1549-1563.
- le Duc, Q., Shi, Q., Blonk, I., Sonnenberg, A., Wang, N., Leckband, D., and de Rooij, J. (2010). Vinculin potentiates E-cadherin mechanosensing and is recruited to actin-anchored sites within adherens junctions in a myosin II-dependent manner. *J Cell Biol* 189, 1107-1115.

- Le, T.L., Joseph, S.R., Yap, A.S., and Stow, J.L. (2002). Protein kinase C regulates endocytosis and recycling of E-cadherin. *Am J Physiol Cell Physiol* 283, C489-499.
- Le, T.L., Yap, A.S., and Stow, J.L. (1999). Recycling of E-cadherin: a potential mechanism for regulating cadherin dynamics. *J Cell Biol* 146, 219-232.
- Leckband, D.E., and de Rooij, J. (2014). Cadherin adhesion and mechanotransduction. *Annu Rev Cell Dev Biol* 30, 291-315.
- Lee, J.Y., and Harland, R.M. (2010). Endocytosis is required for efficient apical constriction during *Xenopus* gastrulation. *Curr Biol* 20, 253-258.
- Levayer, R., Pelissier-Monier, A., and Lecuit, T. (2011). Spatial regulation of Dia and Myosin-II by RhoGEF2 controls initiation of E-cadherin endocytosis during epithelial morphogenesis. *Nat Cell Biol* 13, 529-540.
- Levine, E., Lee, C.H., Kintner, C., and Gumbiner, B.M. (1994). Selective disruption of E-cadherin function in early *Xenopus* embryos by a dominant negative mutant. *Development* 120, 901-909.
- Lewis, S.A., and de Moura, J.L. (1982). Incorporation of cytoplasmic vesicles into apical membrane of mammalian urinary bladder epithelium. *Nature* 297, 685-688.
- Lewis, S.A., and de Moura, J.L. (1984). Apical membrane area of rabbit urinary bladder increases by fusion of intracellular vesicles: an electrophysiological study. *J Membr Biol* 82, 123-136.
- Lewis, S.A., Eaton, D.C., and Diamond, J.M. (1976). The mechanism of Na<sup>+</sup> transport by rabbit urinary bladder. *J Membr Biol* 28, 41-70.
- Lewis, S.A., and Wills, N.K. (1982). Electrical properties of the rabbit urinary bladder assessed using gramicidin D. *J Membr Biol* 67, 45-53.
- Liu, Z., Tan, J.L., Cohen, D.M., Yang, M.T., Sniadecki, N.J., Ruiz, S.A., Nelson, C.M., and Chen, C.S. (2010). Mechanical tugging force regulates the size of cell-cell junctions. *Proc Natl Acad Sci U S A* 107, 9944-9949.
- Lock, J.G., and Stow, J.L. (2005). Rab11 in recycling endosomes regulates the sorting and basolateral transport of E-cadherin. *Mol Biol Cell* 16, 1744-1755.
- Lu, R., Johnson, D.L., Stewart, L., Waite, K., Elliott, D., and Wilson, J.M. (2014). Rab14 regulation of claudin-2 trafficking modulates epithelial permeability and lumen morphogenesis. *Mol Biol Cell* 25, 1744-1754.
- Ma, T.Y., Hoa, N.T., Tran, D.D., Bui, V., Pedram, A., Mills, S., and Merryfield, M. (2000a). Cytochalasin B modulation of Caco-2 tight junction barrier: role of myosin light chain kinase. *Am J Physiol Gastrointest Liver Physiol* 279, G875-885.
- Ma, T.Y., Tran, D., Hoa, N., Nguyen, D., Merryfield, M., and Tarnawski, A. (2000b). Mechanism of extracellular calcium regulation of intestinal epithelial tight junction permeability: role of cytoskeletal involvement. *Microsc Res Tech* 51, 156-168.

- MacDonald, B.T., Tamai, K., and He, X. (2009). Wnt/beta-catenin signaling: components, mechanisms, and diseases. *Dev Cell* 17, 9-26.
- Mandai, K., Nakanishi, H., Satoh, A., Takahashi, K., Satoh, K., Nishioka, H., Mizoguchi, A., and Takai, Y. (1999). Ponsin/SH3P12: an I-afadin- and vinculin-binding protein localized at cell-cell and cell-matrix adherens junctions. *J Cell Biol* 144, 1001-1017.
- Martin, T.A., and Jiang, W.G. (2009). Loss of tight junction barrier function and its role in cancer metastasis. *Biochim Biophys Acta* 1788, 872-891.
- Martin, T.A., Mason, M.D., and Jiang, W.G. (2011). Tight junctions in cancer metastasis. *Front Biosci (Landmark Ed)* 16, 898-936.
- Marzesco, A.M., Dunia, I., Pandjaitan, R., Recouvreur, M., Dauzonne, D., Benedetti, E.L., Louvard, D., and Zahraoui, A. (2002). The small GTPase Rab13 regulates assembly of functional tight junctions in epithelial cells. *Mol Biol Cell* 13, 1819-1831.
- Marzesco, A.M., and Zahraoui, A. (2005). Assay of Rab13 in regulating epithelial tight junction assembly. *Methods Enzymol* 403, 182-193.
- Masters, T.A., Pontes, B., Viasnoff, V., Li, Y., and Gauthier, N.C. (2013). Plasma membrane tension orchestrates membrane trafficking, cytoskeletal remodeling, and biochemical signaling during phagocytosis. *Proc Natl Acad Sci U S A* 110, 11875-11880.
- Mateus, A.M., Gorfinkiel, N., Schamberg, S., and Martinez Arias, A. (2011). Endocytic and recycling endosomes modulate cell shape changes and tissue behaviour during morphogenesis in *Drosophila*. *PLoS One* 6, e18729.
- Matsuda, M., Kubo, A., Furuse, M., and Tsukita, S. (2004). A peculiar internalization of claudins, tight junction-specific adhesion molecules, during the intercellular movement of epithelial cells. *J Cell Sci* 117, 1247-1257.
- Mayor, S., Parton, R.G., and Donaldson, J.G. (2014). Clathrin-independent pathways of endocytosis. *Cold Spring Harb Perspect Biol* 6.
- McNamara, B.P., Koutsouris, A., O'Connell, C.B., Nougayrede, J.P., Sonnenberg, M.S., and Hecht, G. (2001). Translocated EspF protein from enteropathogenic *Escherichia coli* disrupts host intestinal barrier function. *J Clin Invest* 107, 621-629.
- McNeil, E., Capaldo, C.T., and Macara, I.G. (2006). Zonula occludens-1 function in the assembly of tight junctions in Madin-Darby canine kidney epithelial cells. *Mol Biol Cell* 17, 1922-1932.
- Mehta, S., Nijhuis, A., Kumagai, T., Lindsay, J., and Silver, A. (2015). Defects in the adherens junction complex (E-cadherin/ beta-catenin) in inflammatory bowel disease. *Cell Tissue Res* 360, 749-760.
- Mermelstein, C.S., Rodrigues, A.P., Einicker-Lamas, M., Navarrete, R.E., Farina, M., and Costa, M.L. (1998). Distribution of F-actin, alpha-actinin, tropomyosin, tubulin and organelles in *Euglena gracilis* by immunofluorescence microscopy. *Tissue Cell* 30, 545-553.

- Metz, J., Aoki, A., Merlo, M., and Forssmann, W.G. (1977). Morphological alterations and functional changes of interhepatocellular junctions induced by bile duct ligation. *Cell Tissue Res* 182, 299-310.
- Metz, J., Merlo, M., Billich, H., and Forssmann, W.G. (1978). Exocrine pancreas under experimental conditions. IV. Alterations of intercellular junctions between acinar cells following pancreatic duct ligation. *Cell Tissue Res* 186, 227-240.
- Meyer, T.N., Schwesinger, C., and Denker, B.M. (2002). Zonula occludens-1 is a scaffolding protein for signaling molecules.  $\alpha(12)$  directly binds to the Src homology 3 domain and regulates paracellular permeability in epithelial cells. *J Biol Chem* 277, 24855-24858.
- Milatz, S., and Breiderhoff, T. (2017). One gene, two paracellular ion channels-claudin-10 in the kidney. *Pflugers Arch* 469, 115-121.
- Minsky, B.D., and Chlapowski, F.J. (1978). Morphometric analysis of the translocation of luminal membrane between cytoplasm and cell surface of transitional epithelial cells during the expansion-contraction cycles of mammalian urinary bladder. *J Cell Biol* 77, 685-697.
- Miyahara, M., Nakanishi, H., Takahashi, K., Satoh-Horikawa, K., Tachibana, K., and Takai, Y. (2000). Interaction of nectin with afadin is necessary for its clustering at cell-cell contact sites but not for its cis dimerization or trans interaction. *J Biol Chem* 275, 613-618.
- Miyake, Y., Inoue, N., Nishimura, K., Kinoshita, N., Hosoya, H., and Yonemura, S. (2006). Actomyosin tension is required for correct recruitment of adherens junction components and zonula occludens formation. *Exp Cell Res* 312, 1637-1650.
- Miyamoto, T., Mochizuki, T., Nakagomi, H., Kira, S., Watanabe, M., Takayama, Y., Suzuki, Y., Koizumi, S., Takeda, M., and Tominaga, M. (2014). Functional role for Piezo1 in stretch-evoked  $Ca^{2+}$  influx and ATP release in urothelial cell cultures. *J Biol Chem* 289, 16565-16575.
- Miyashita, Y., and Ozawa, M. (2007). Increased internalization of p120-uncoupled E-cadherin and a requirement for a dileucine motif in the cytoplasmic domain for endocytosis of the protein. *J Biol Chem* 282, 11540-11548.
- Moad, M., Pal, D., Hepburn, A.C., Williamson, S.C., Wilson, L., Lako, M., Armstrong, L., Hayward, S.W., Franco, O.E., Cates, J.M., Fordham, S.E., Przyborski, S., Carr-Wilkinson, J., Robson, C.N., and Heer, R. (2013). A novel model of urinary tract differentiation, tissue regeneration, and disease: reprogramming human prostate and bladder cells into induced pluripotent stem cells. *Eur Urol* 64, 753-761.
- Mochizuki, T., Sokabe, T., Araki, I., Fujishita, K., Shibasaki, K., Uchida, K., Naruse, K., Koizumi, S., Takeda, M., and Tominaga, M. (2009). The TRPV4 cation channel mediates stretch-evoked  $Ca^{2+}$  influx and ATP release in primary urothelial cell cultures. *J Biol Chem* 284, 21257-21264.
- Montalbetti, N., Rued, A.C., Clayton, D.R., Ruiz, W.G., Bastacky, S.I., Prakasam, H.S., Eaton, A.F., Kullmann, F.A., Apodaca, G., and Carattino, M.D. (2015). Increased urothelial paracellular transport promotes cystitis. *Am J Physiol Renal Physiol* 309, F1070-1081.

- Montalbetti, N., Rued, A.C., Taiclet, S.N., Birder, L.A., Kullmann, F.A., and Carattino, M.D. (2017). Urothelial Tight Junction Barrier Dysfunction Sensitizes Bladder Afferents. *eNeuro* 4.
- Morimoto, S., Nishimura, N., Terai, T., Manabe, S., Yamamoto, Y., Shinahara, W., Miyake, H., Tashiro, S., Shimada, M., and Sasaki, T. (2005). Rab13 mediates the continuous endocytic recycling of occludin to the cell surface. *J Biol Chem* 280, 2220-2228.
- Morris, C.E., and Homann, U. (2001). Cell surface area regulation and membrane tension. *J Membr Biol* 179, 79-102.
- Moulton, D.E., Sulzer, V., Apodaca, G., Byrne, H.M., and Waters, S.L. (2016). Mathematical modelling of stretch-induced membrane traffic in bladder umbrella cells. *J Theor Biol* 409, 115-132.
- Mruk, D.D., Lau, A.S., Sarkar, O., and Xia, W. (2007). Rab4A GTPase catenin interactions are involved in cell junction dynamics in the testis. *J Androl* 28, 742-754.
- Muhamed, I., Wu, J., Sehgal, P., Kong, X., Tajik, A., Wang, N., and Leckband, D.E. (2016). E-cadherin-mediated force transduction signals regulate global cell mechanics. *J Cell Sci* 129, 1843-1854.
- Mulvey, M.A., Schilling, J.D., Martinez, J.J., and Hultgren, S.J. (2000). Bad bugs and beleaguered bladders: interplay between uropathogenic *Escherichia coli* and innate host defenses. *Proc Natl Acad Sci U S A* 97, 8829-8835.
- Nakanishi, K., Ogata, S., Hiroi, S., Tominaga, S., Aida, S., and Kawai, T. (2008). Expression of occludin and claudins 1, 3, 4, and 7 in urothelial carcinoma of the upper urinary tract. *Am J Clin Pathol* 130, 43-49.
- Nebenfuhr, A., Ritzenthaler, C., and Robinson, D.G. (2002). Brefeldin A: deciphering an enigmatic inhibitor of secretion. *Plant Physiol* 130, 1102-1108.
- Nieset, J.E., Redfield, A.R., Jin, F., Knudsen, K.A., Johnson, K.R., and Wheelock, M.J. (1997). Characterization of the interactions of alpha-catenin with alpha-actinin and beta-catenin/plakoglobin. *J Cell Sci* 110 ( Pt 8), 1013-1022.
- Niessen, C.M., and Gottardi, C.J. (2008). Molecular components of the adherens junction. *Biochim Biophys Acta* 1778, 562-571.
- Nolen, B.J., Tomasevic, N., Russell, A., Pierce, D.W., Jia, Z., McCormick, C.D., Hartman, J., Sakowicz, R., and Pollard, T.D. (2009). Characterization of two classes of small molecule inhibitors of Arp2/3 complex. *Nature* 460, 1031-1034.
- Noren, N.K., Niessen, C.M., Gumbiner, B.M., and Burridge, K. (2001). Cadherin engagement regulates Rho family GTPases. *J Biol Chem* 276, 33305-33308.
- Noria, S., Cowan, D.B., Gotlieb, A.I., and Langille, B.L. (1999). Transient and steady-state effects of shear stress on endothelial cell adherens junctions. *Circ Res* 85, 504-514.

- Nusrat, A., Giry, M., Turner, J.R., Colgan, S.P., Parkos, C.A., Carnes, D., Lemichez, E., Boquet, P., and Madara, J.L. (1995). Rho protein regulates tight junctions and perijunctional actin organization in polarized epithelia. *Proc Natl Acad Sci U S A* 92, 10629-10633.
- Nusrat, A., Turner, J.R., and Madara, J.L. (2000). Molecular physiology and pathophysiology of tight junctions. IV. Regulation of tight junctions by extracellular stimuli: nutrients, cytokines, and immune cells. *Am J Physiol Gastrointest Liver Physiol* 279, G851-857.
- Nusrat, A., von Eichel-Streiber, C., Turner, J.R., Verkade, P., Madara, J.L., and Parkos, C.A. (2001). Clostridium difficile toxins disrupt epithelial barrier function by altering membrane microdomain localization of tight junction proteins. *Infect Immun* 69, 1329-1336.
- O'Leary, C.J., Nourse, C.C., Lee, N.K., White, A., Langford, M., Sempert, K., Cole, S.J., and Cooper, H.M. (2017). Neogenin Recruitment of the WAVE Regulatory Complex to Ependymal and Radial Progenitor Adherens Junctions Prevents Hydrocephalus. *Cell Rep* 20, 370-383.
- Obert, G., Peiffer, I., and Servin, A.L. (2000). Rotavirus-induced structural and functional alterations in tight junctions of polarized intestinal Caco-2 cell monolayers. *J Virol* 74, 4645-4651.
- Onder, T.T., Gupta, P.B., Mani, S.A., Yang, J., Lander, E.S., and Weinberg, R.A. (2008). Loss of E-cadherin promotes metastasis via multiple downstream transcriptional pathways. *Cancer Res* 68, 3645-3654.
- Ooshio, T., Irie, K., Morimoto, K., Fukuhara, A., Imai, T., and Takai, Y. (2004). Involvement of LMO7 in the association of two cell-cell adhesion molecules, nectin and E-cadherin, through afadin and alpha-actinin in epithelial cells. *J Biol Chem* 279, 31365-31373.
- Ortega, E., Manso, J.A., Buey, R.M., Carballido, A.M., Carabias, A., Sonnenberg, A., and de Pereda, J.M. (2016). The Structure of the Plakin Domain of Plectin Reveals an Extended Rod-like Shape. *J Biol Chem* 291, 18643-18662.
- Otey, C.A., and Carpen, O. (2004). Alpha-actinin revisited: a fresh look at an old player. *Cell Motil Cytoskeleton* 58, 104-111.
- Pan, Y., Heemskerk, I., Ibar, C., Shraiman, B.I., and Irvine, K.D. (2016). Differential growth triggers mechanical feedback that elevates Hippo signaling. *Proc Natl Acad Sci U S A* 113, E6974-E6983.
- Papafotiou, G., Paraskevopoulou, V., Vasilaki, E., Kanaki, Z., Paschalidis, N., and Klinakis, A. (2016). KRT14 marks a subpopulation of bladder basal cells with pivotal role in regeneration and tumorigenesis. *Nat Commun* 7, 11914.
- Park, M., Kim, H.J., Lim, B., Wylegala, A., and Toborek, M. (2013). Methamphetamine-induced occludin endocytosis is mediated by the Arp2/3 complex-regulated actin rearrangement. *J Biol Chem* 288, 33324-33334.
- Parsons, C.L. (2007). The role of the urinary epithelium in the pathogenesis of interstitial cystitis/prostatitis/urethritis. *Urology* 69, 9-16.

- Parton, R.G., Prydz, K., Bomsel, M., Simons, K., and Griffiths, G. (1989). Meeting of the apical and basolateral endocytic pathways of the Madin-Darby canine kidney cell in late endosomes. *J Cell Biol* 109, 3259-3272.
- Paterson, A.D., Parton, R.G., Ferguson, C., Stow, J.L., and Yap, A.S. (2003). Characterization of E-cadherin endocytosis in isolated MCF-7 and chinese hamster ovary cells: the initial fate of unbound E-cadherin. *J Biol Chem* 278, 21050-21057.
- Pinheiro, D., and Bellaiche, Y. (2018). Mechanical Force-Driven Adherens Junction Remodeling and Epithelial Dynamics. *Dev Cell* 47, 3-19.
- Pitelka, D.R., Hamamoto, S.T., Duafala, J.G., and Nemanic, M.K. (1973). Cell contacts in the mouse mammary gland. I. Normal gland in postnatal development and the secretory cycle. *J Cell Biol* 56, 797-818.
- Pitelka, D.R., and Taggart, B.N. (1983). Mechanical tension induces lateral movement of intramembrane components of the tight junction: studies on mouse mammary cells in culture. *J Cell Biol* 96, 606-612.
- Plageman, T.F., Jr., Chauhan, B.K., Yang, C., Jaudon, F., Shang, X., Zheng, Y., Lou, M., Debant, A., Hildebrand, J.D., and Lang, R.A. (2011). A Trio-RhoA-Shroom3 pathway is required for apical constriction and epithelial invagination. *Development* 138, 5177-5188.
- Price, A.J., Cost, A.L., Ungewiss, H., Waschke, J., Dunn, A.R., and Grashoff, C. (2018). Mechanical loading of desmosomes depends on the magnitude and orientation of external stress. *Nat Commun* 9, 5284.
- Quinlan, R.A., Schwarz, N., Windoffer, R., Richardson, C., Hawkins, T., Broussard, J.A., Green, K.J., and Leube, R.E. (2017). A rim-and-spoke hypothesis to explain the biomechanical roles for cytoplasmic intermediate filament networks. *J Cell Sci* 130, 3437-3445.
- Rakshit, S., Zhang, Y., Manibog, K., Shafraz, O., and Sivasankar, S. (2012). Ideal, catch, and slip bonds in cadherin adhesion. *Proc Natl Acad Sci U S A* 109, 18815-18820.
- Raleigh, D.R., Marchiando, A.M., Zhang, Y., Shen, L., Sasaki, H., Wang, Y., Long, M., and Turner, J.R. (2010). Tight junction-associated MARVEL proteins marveld3, tricellulin, and occludin have distinct but overlapping functions. *Mol Biol Cell* 21, 1200-1213.
- Ramesh, N., Memarzadeh, B., Ge, Y., Frey, D., VanRoey, M., Rojas, V., and Yu, D.C. (2004). Identification of pretreatment agents to enhance adenovirus infection of bladder epithelium. *Mol Ther* 10, 697-705.
- Raucher, D., and Sheetz, M.P. (1999). Membrane expansion increases endocytosis rate during mitosis. *J Cell Biol* 144, 497-506.
- Rickard, A., Dorokhov, N., Ryerse, J., Klumpp, D.J., and McHowat, J. (2008). Characterization of tight junction proteins in cultured human urothelial cells. *In Vitro Cell Dev Biol Anim* 44, 261-267.
- Rief, M., Pascual, J., Saraste, M., and Gaub, H.E. (1999). Single molecule force spectroscopy of spectrin repeats: low unfolding forces in helix bundles. *J Mol Biol* 286, 553-561.

- Rizvi, S.A., Neidt, E.M., Cui, J., Feiger, Z., Skau, C.T., Gardel, M.L., Kozmin, S.A., and Kovar, D.R. (2009). Identification and characterization of a small molecule inhibitor of formin-mediated actin assembly. *Chem Biol* 16, 1158-1168.
- Roh-Johnson, M., Shemer, G., Higgins, C.D., McClellan, J.H., Werts, A.D., Tulu, U.S., Gao, L., Betzig, E., Kiehart, D.P., and Goldstein, B. (2012). Triggering a cell shape change by exploiting preexisting actomyosin contractions. *Science* 335, 1232-1235.
- Rojas, R., Ruiz, W.G., Leung, S.M., Jou, T.S., and Apodaca, G. (2001). Cdc42-dependent modulation of tight junctions and membrane protein traffic in polarized Madin-Darby canine kidney cells. *Mol Biol Cell* 12, 2257-2274.
- Rubsam, M., Broussard, J.A., Wickstrom, S.A., Nekrasova, O., Green, K.J., and Niessen, C.M. (2018). Adherens Junctions and Desmosomes Coordinate Mechanics and Signaling to Orchestrate Tissue Morphogenesis and Function: An Evolutionary Perspective. *Cold Spring Harb Perspect Biol* 10.
- Runkle, E.A., and Mu, D. (2013). Tight junction proteins: from barrier to tumorigenesis. *Cancer Lett* 337, 41-48.
- Russell, D., Andrews, P.D., James, J., and Lane, E.B. (2004). Mechanical stress induces profound remodelling of keratin filaments and cell junctions in epidermolysis bullosa simplex keratinocytes. *J Cell Sci* 117, 5233-5243.
- Sahai, E., and Marshall, C.J. (2002). ROCK and Dia have opposing effects on adherens junctions downstream of Rho. *Nat Cell Biol* 4, 408-415.
- Sai, X., Yonemura, S., and Ladher, R.K. (2014). Junctionally restricted RhoA activity is necessary for apical constriction during phase 2 inner ear placode invagination. *Dev Biol* 394, 206-216.
- Saias, L., Swoger, J., D'Angelo, A., Hayes, P., Colombelli, J., Sharpe, J., Salbreux, G., and Solon, J. (2015). Decrease in Cell Volume Generates Contractile Forces Driving Dorsal Closure. *Dev Cell* 33, 611-621.
- Sakane, A., Abdallah, A.A., Nakano, K., Honda, K., Ikeda, W., Nishikawa, Y., Matsumoto, M., Matsushita, N., Kitamura, T., and Sasaki, T. (2012). Rab13 small G protein and junctional Rab13-binding protein (JRAB) orchestrate actin cytoskeletal organization during epithelial junctional development. *J Biol Chem* 287, 42455-42468.
- Sakane, A., Yoshizawa, S., Nishimura, M., Tsuchiya, Y., Matsushita, N., Miyake, K., Horikawa, K., Imoto, I., Mizuguchi, C., Saito, H., Ueno, T., Matsushita, S., Haga, H., Deguchi, S., Mizuguchi, K., Yokota, H., and Sasaki, T. (2016). Conformational plasticity of JRAB/MICAL-L2 provides "law and order" in collective cell migration. *Mol Biol Cell* 27, 3095-3108.
- Samak, G., Gangwar, R., Crosby, L.M., Desai, L.P., Wilhelm, K., Waters, C.M., and Rao, R. (2014). Cyclic stretch disrupts apical junctional complexes in Caco-2 cell monolayers by a JNK-2-, c-Src-, and MLCK-dependent mechanism. *Am J Physiol Gastrointest Liver Physiol* 306, G947-958.

- Samak, G., Suzuki, T., Bhargava, A., and Rao, R.K. (2010). c-Jun NH2-terminal kinase-2 mediates osmotic stress-induced tight junction disruption in the intestinal epithelium. *Am J Physiol Gastrointest Liver Physiol* 299, G572-584.
- Samanta, P., Wang, Y., Fuladi, S., Zou, J., Li, Y., Shen, L., Weber, C., and Khalili-Araghi, F. (2018). Molecular determination of claudin-15 organization and channel selectivity. *J Gen Physiol* 150, 949-968.
- Sanchez-Pulido, L., Martin-Belmonte, F., Valencia, A., and Alonso, M.A. (2002). MARVEL: a conserved domain involved in membrane apposition events. *Trends Biochem Sci* 27, 599-601.
- Sarikas, S.N., and Chlapowski, F.J. (1989). The effect of thioglycolate on intermediate filaments and membrane translocation in rat urothelium during the expansion-contraction cycle. *Cell Tissue Res* 258, 393-401.
- Sato, T., Fujita, N., Yamada, A., Ooshio, T., Okamoto, R., Irie, K., and Takai, Y. (2006). Regulation of the assembly and adhesion activity of E-cadherin by nectin and afadin for the formation of adherens junctions in Madin-Darby canine kidney cells. *J Biol Chem* 281, 5288-5299.
- Sawyer, J.K., Harris, N.J., Slep, K.C., Gaul, U., and Peifer, M. (2009). The *Drosophila* afadin homologue Canoe regulates linkage of the actin cytoskeleton to adherens junctions during apical constriction. *J Cell Biol* 186, 57-73.
- Schiffhauer, E.S., Luo, T., Mohan, K., Srivastava, V., Qian, X., Griffis, E.R., Iglesias, P.A., and Robinson, D.N. (2016). Mechanoaccumulative Elements of the Mammalian Actin Cytoskeleton. *Curr Biol* 26, 1473-1479.
- Schneider-Poetsch, T., Ju, J., Eyler, D.E., Dang, Y., Bhat, S., Merrick, W.C., Green, R., Shen, B., and Liu, J.O. (2010). Inhibition of eukaryotic translation elongation by cycloheximide and lactimidomycin. *Nat Chem Biol* 6, 209-217.
- Schock, F., and Perrimon, N. (2002). Molecular mechanisms of epithelial morphogenesis. *Annu Rev Cell Dev Biol* 18, 463-493.
- Schwayer, C., Sikora, M., Slovakova, J., Kardos, R., and Heisenberg, C.P. (2016). Actin Rings of Power. *Dev Cell* 37, 493-506.
- Serrels, A., Canel, M., Brunton, V.G., and Frame, M.C. (2011). Src/FAK-mediated regulation of E-cadherin as a mechanism for controlling collective cell movement: insights from in vivo imaging. *Cell Adh Migr* 5, 360-365.
- Shams, H., Golji, J., and Mofrad, M.R. (2012). A molecular trajectory of alpha-actinin activation. *Biophys J* 103, 2050-2059.
- Shaye, D.D., Casanova, J., and Llimargas, M. (2008). Modulation of intracellular trafficking regulates cell intercalation in the *Drosophila* trachea. *Nat Cell Biol* 10, 964-970.
- Shen, L., and Turner, J.R. (2005). Actin depolymerization disrupts tight junctions via caveolae-mediated endocytosis. *Mol Biol Cell* 16, 3919-3936.

- Shen, L., Weber, C.R., and Turner, J.R. (2008). The tight junction protein complex undergoes rapid and continuous molecular remodeling at steady state. *J Cell Biol* 181, 683-695.
- Shewan, A.M., Maddugoda, M., Kraemer, A., Stehbens, S.J., Verma, S., Kovacs, E.M., and Yap, A.S. (2005). Myosin 2 is a key Rho kinase target necessary for the local concentration of E-cadherin at cell-cell contacts. *Mol Biol Cell* 16, 4531-4542.
- Siddharthan, V., Kim, Y.V., Liu, S., and Kim, K.S. (2007). Human astrocytes/astrocyte-conditioned medium and shear stress enhance the barrier properties of human brain microvascular endothelial cells. *Brain Res* 1147, 39-50.
- Singh, U., Mitic, L.L., Wieckowski, E.U., Anderson, J.M., and McClane, B.A. (2001). Comparative biochemical and immunocytochemical studies reveal differences in the effects of *Clostridium perfringens* enterotoxin on polarized CaCo-2 cells versus Vero cells. *J Biol Chem* 276, 33402-33412.
- Sivaramakrishnan, S., Schneider, J.L., Sitikov, A., Goldman, R.D., and Ridge, K.M. (2009). Shear stress induced reorganization of the keratin intermediate filament network requires phosphorylation by protein kinase C zeta. *Mol Biol Cell* 20, 2755-2765.
- Sluysmans, S., Vasileva, E., Spadaro, D., Shah, J., Rouaud, F., and Citi, S. (2017). The role of apical cell-cell junctions and associated cytoskeleton in mechanotransduction. *Biol Cell* 109, 139-161.
- Smith, N.J., Hinley, J., Varley, C.L., Eardley, I., Trejdosiewicz, L.K., and Southgate, J. (2015). The human urothelial tight junction: claudin 3 and the ZO-1alpha(+) switch. *Bladder (San Franc)* 2, e9.
- Smith, P.R., Mackler, S.A., Weiser, P.C., Brooker, D.R., Ahn, Y.J., Harte, B.J., McNulty, K.A., and Kleyman, T.R. (1998). Expression and localization of epithelial sodium channel in mammalian urinary bladder. *Am J Physiol* 274, F91-96.
- Sohet, F., Lin, C., Munji, R.N., Lee, S.Y., Ruderisch, N., Soung, A., Arnold, T.D., Derugin, N., Vexler, Z.S., Yen, F.T., and Daneman, R. (2015). LSR/angulin-1 is a tricellular tight junction protein involved in blood-brain barrier formation. *J Cell Biol* 208, 703-711.
- Solsona, C., Innocenti, B., and Fernandez, J.M. (1998). Regulation of exocytotic fusion by cell inflation. *Biophys J* 74, 1061-1073.
- Song, M.J., Davidovich, N., Lawrence, G.G., and Margulies, S.S. (2016). Superoxide mediates tight junction complex dissociation in cyclically stretched lung slices. *J Biomech* 49, 1330-1335.
- Song, S., Eckerle, S., Onichtchouk, D., Marrs, J.A., Nitschke, R., and Driever, W. (2013). Pou5f1-dependent EGF expression controls E-cadherin endocytosis, cell adhesion, and zebrafish epiboly movements. *Dev Cell* 24, 486-501.
- Soulet, F., Schmid, S.L., and Damke, H. (2006). Domain requirements for an endocytosis-independent, isoform-specific function of dynamin-2. *Exp Cell Res* 312, 3539-3545.

- Southgate, J., Varley, C.L., Garthwaite, M.A., Hinley, J., Marsh, F., Stahlschmidt, J., Trejdosiewicz, L.K., and Eardley, I. (2007). Differentiation potential of urothelium from patients with benign bladder dysfunction. *BJU Int* 99, 1506-1516.
- Spadaro, D., Le, S., Laroche, T., Mean, I., Jond, L., Yan, J., and Citi, S. (2017). Tension-Dependent Stretching Activates ZO-1 to Control the Junctional Localization of Its Interactors. *Curr Biol* 27, 3783-3795 e3788.
- Stenmark, H. (2009). Rab GTPases as coordinators of vesicle traffic. *Nat Rev Mol Cell Biol* 10, 513-525.
- Stevenson, B.R., Anderson, J.M., Goodenough, D.A., and Mooseker, M.S. (1988). Tight junction structure and ZO-1 content are identical in two strains of Madin-Darby canine kidney cells which differ in transepithelial resistance. *J Cell Biol* 107, 2401-2408.
- Subtil, A., Gaidarov, I., Kobylarz, K., Lampson, M.A., Keen, J.H., and McGraw, T.E. (1999). Acute cholesterol depletion inhibits clathrin-coated pit budding. *Proc Natl Acad Sci U S A* 96, 6775-6780.
- Sun, Y., Jaldin-Fincati, J., Liu, Z., Bilan, P.J., and Klip, A. (2016). A complex of Rab13 with MICAL-L2 and alpha-actinin-4 is essential for insulin-dependent GLUT4 exocytosis. *Mol Biol Cell* 27, 75-89.
- Surviladze, Z., Waller, A., Strouse, J.J., Bologa, C., Ursu, O., Salas, V., Parkinson, J.F., Phillips, G.K., Romero, E., Wandinger-Ness, A., Sklar, L.A., Schroeder, C., Simpson, D., Noth, J., Wang, J., Golden, J., and Aube, J. (2010). A Potent and Selective Inhibitor of Cdc42 GTPase. In: *Probe Reports from the NIH Molecular Libraries Program*, Bethesda (MD).
- Suzuki, H., Nishizawa, T., Tani, K., Yamazaki, Y., Tamura, A., Ishitani, R., Dohmae, N., Tsukita, S., Nureki, O., and Fujiyoshi, Y. (2014). Crystal structure of a claudin provides insight into the architecture of tight junctions. *Science* 344, 304-307.
- Suzuki, H., Tani, K., Tamura, A., Tsukita, S., and Fujiyoshi, Y. (2015). Model for the architecture of claudin-based paracellular ion channels through tight junctions. *J Mol Biol* 427, 291-297.
- Svitkina, T. (2018). *The Actin Cytoskeleton and Actin-Based Motility*. Cold Spring Harb Perspect Biol 10.
- Tabaries, S., and Siegel, P.M. (2017). The role of claudins in cancer metastasis. *Oncogene* 36, 1176-1190.
- Takai, Y., and Nakanishi, H. (2003). Nectin and afadin: novel organizers of intercellular junctions. *J Cell Sci* 116, 17-27.
- Takaishi, K., Sasaki, T., Kato, M., Yamochi, W., Kuroda, S., Nakamura, T., Takeichi, M., and Takai, Y. (1994). Involvement of Rho p21 small GTP-binding protein and its regulator in the HGF-induced cell motility. *Oncogene* 9, 273-279.
- Takeichi, M. (2014). Dynamic contacts: rearranging adherens junctions to drive epithelial remodelling. *Nat Rev Mol Cell Biol* 15, 397-410.

- Takeichi, M. (2018). Multiple functions of alpha-catenin beyond cell adhesion regulation. *Curr Opin Cell Biol* 54, 24-29.
- Talavera, D., Castillo, A.M., Dominguez, M.C., Gutierrez, A.E., and Meza, I. (2004). IL8 release, tight junction and cytoskeleton dynamic reorganization conducive to permeability increase are induced by dengue virus infection of microvascular endothelial monolayers. *J Gen Virol* 85, 1801-1813.
- Tanentzapf, G., and Tepass, U. (2003). Interactions between the crumbs, lethal giant larvae and bazooka pathways in epithelial polarization. *Nat Cell Biol* 5, 46-52.
- Tateishi, K., Nishida, T., Inoue, K., and Tsukita, S. (2017). Three-dimensional Organization of Layered Apical Cytoskeletal Networks Associated with Mouse Airway Tissue Development. *Sci Rep* 7, 43783.
- Terada, N., Ohno, N., Saitoh, S., Saitoh, Y., Fujii, Y., Kondo, T., Katoh, R., Chan, C., Abraham, S.N., and Ohno, S. (2009). Involvement of dynamin-2 in formation of discoid vesicles in urinary bladder umbrella cells. *Cell Tissue Res* 337, 91-102.
- Terai, T., Nishimura, N., Kanda, I., Yasui, N., and Sasaki, T. (2006). JRAB/MICAL-L2 is a junctional Rab13-binding protein mediating the endocytic recycling of occludin. *Mol Biol Cell* 17, 2465-2475.
- Thi, M.M., Tarbell, J.M., Weinbaum, S., and Spray, D.C. (2004). The role of the glycocalyx in reorganization of the actin cytoskeleton under fluid shear stress: a "bumper-car" model. *Proc Natl Acad Sci U S A* 101, 16483-16488.
- Toivola, D.M., Ku, N.O., Ghorri, N., Lowe, A.W., Michie, S.A., and Omary, M.B. (2000). Effects of keratin filament disruption on exocrine pancreas-stimulated secretion and susceptibility to injury. *Exp Cell Res* 255, 156-170.
- Tornavaca, O., Chia, M., Dufton, N., Almagro, L.O., Conway, D.E., Randi, A.M., Schwartz, M.A., Matter, K., and Balda, M.S. (2015). ZO-1 controls endothelial adherens junctions, cell-cell tension, angiogenesis, and barrier formation. *J Cell Biol* 208, 821-838.
- Truschel, S.T., Wang, E., Ruiz, W.G., Leung, S.M., Rojas, R., Lavelle, J., Zeidel, M., Stoffer, D., and Apodaca, G. (2002). Stretch-regulated exocytosis/endocytosis in bladder umbrella cells. *Mol Biol Cell* 13, 830-846.
- Tsang, S.M., Brown, L., Gadmor, H., Gammon, L., Fortune, F., Wheeler, A., and Wan, H. (2012a). Desmoglein 3 acting as an upstream regulator of Rho GTPases, Rac-1/Cdc42 in the regulation of actin organisation and dynamics. *Exp Cell Res* 318, 2269-2283.
- Tsang, S.M., Brown, L., Lin, K., Liu, L., Piper, K., O'Toole, E.A., Grose, R., Hart, I.R., Garrod, D.R., Fortune, F., and Wan, H. (2012b). Non-junctional human desmoglein 3 acts as an upstream regulator of Src in E-cadherin adhesion, a pathway possibly involved in the pathogenesis of pemphigus vulgaris. *J Pathol* 227, 81-93.
- Tzima, E., Irani-Tehrani, M., Kiosses, W.B., Dejana, E., Schultz, D.A., Engelhardt, B., Cao, G., DeLisser, H., and Schwartz, M.A. (2005). A mechanosensory complex that mediates the endothelial cell response to fluid shear stress. *Nature* 437, 426-431.

- Ulrich, F., Krieg, M., Schotz, E.M., Link, V., Castanon, I., Schnabel, V., Taubenberger, A., Mueller, D., Puech, P.H., and Heisenberg, C.P. (2005). Wnt11 functions in gastrulation by controlling cell cohesion through Rab5c and E-cadherin. *Dev Cell* 9, 555-564.
- Umeda, K., Ikenouchi, J., Katahira-Tayama, S., Furuse, K., Sasaki, H., Nakayama, M., Matsui, T., Tsukita, S., Furuse, M., and Tsukita, S. (2006). ZO-1 and ZO-2 independently determine where claudins are polymerized in tight-junction strand formation. *Cell* 126, 741-754.
- Umeda, K., Matsui, T., Nakayama, M., Furuse, K., Sasaki, H., Furuse, M., and Tsukita, S. (2004). Establishment and characterization of cultured epithelial cells lacking expression of ZO-1. *J Biol Chem* 279, 44785-44794.
- Valentijn, K., Valentijn, J.A., and Jamieson, J.D. (1999). Role of actin in regulated exocytosis and compensatory membrane retrieval: insights from an old acquaintance. *Biochem Biophys Res Commun* 266, 652-661.
- Van Itallie, C.M., Holmes, J., Bridges, A., Gookin, J.L., Coccaro, M.R., Proctor, W., Colegio, O.R., and Anderson, J.M. (2008). The density of small tight junction pores varies among cell types and is increased by expression of claudin-2. *J Cell Sci* 121, 298-305.
- Varley, C.L., Garthwaite, M.A., Cross, W., Hinley, J., Trejdosiewicz, L.K., and Southgate, J. (2006). PPARgamma-regulated tight junction development during human urothelial cytodifferentiation. *J Cell Physiol* 208, 407-417.
- Veranic, P., and Jezernik, K. (2002). Trajectorial organisation of cytokeratins within the subapical region of umbrella cells. *Cell Motil Cytoskeleton* 53, 317-325.
- Vielmuth, F., Hartlieb, E., Kugelmann, D., Waschke, J., and Spindler, V. (2015). Atomic force microscopy identifies regions of distinct desmoglein 3 adhesive properties on living keratinocytes. *Nanomedicine* 11, 511-520.
- Vlaskovska, M., Kasakov, L., Rong, W., Bodin, P., Bardini, M., Cockayne, D.A., Ford, A.P., and Burnstock, G. (2001). P2X3 knock-out mice reveal a major sensory role for urothelially released ATP. *J Neurosci* 21, 5670-5677.
- Vogler, G., Liu, J., Iafe, T.W., Migh, E., Mihaly, J., and Bodmer, R. (2014). Cdc42 and formin activity control non-muscle myosin dynamics during Drosophila heart morphogenesis. *J Cell Biol* 206, 909-922.
- von Kleist, L., Stahlschmidt, W., Bulut, H., Gromova, K., Puchkov, D., Robertson, M.J., MacGregor, K.A., Tomilin, N., Pechstein, A., Chau, N., Chircop, M., Sakoff, J., von Kries, J.P., Saenger, W., Krausslich, H.G., Shupliakov, O., Robinson, P.J., McCluskey, A., and Haucke, V. (2011). Role of the clathrin terminal domain in regulating coated pit dynamics revealed by small molecule inhibition. *Cell* 146, 471-484.
- Wang, E., Brown, P.S., Aroeti, B., Chapin, S.J., Mostov, K.E., and Dunn, K.W. (2000). Apical and basolateral endocytic pathways of MDCK cells meet in acidic common endosomes distinct from a nearly-neutral apical recycling endosome. *Traffic* 1, 480-493.

- Wang, E., Pennington, J.G., Goldenring, J.R., Hunziker, W., and Dunn, K.W. (2001). Brefeldin A rapidly disrupts plasma membrane polarity by blocking polar sorting in common endosomes of MDCK cells. *J Cell Sci* *114*, 3309-3321.
- Wang, E.C., Lee, J.M., Johnson, J.P., Kleyman, T.R., Bridges, R., and Apodaca, G. (2003). Hydrostatic pressure-regulated ion transport in bladder uroepithelium. *Am J Physiol Renal Physiol* *285*, F651-663.
- Wang, Y., Minshall, R.D., Schwartz, D.E., and Hu, G. (2011). Cyclic stretch induces alveolar epithelial barrier dysfunction via calpain-mediated degradation of p120-catenin. *Am J Physiol Lung Cell Mol Physiol* *301*, L197-206.
- Wankel, B., Ouyang, J., Guo, X., Hadjiolova, K., Miller, J., Liao, Y., Tham, D.K., Romih, R., Andrade, L.R., Gumper, I., Simon, J.P., Sachdeva, R., Tolmachova, T., Seabra, M.C., Fukuda, M., Schaeren-Wiemers, N., Hong, W.J., Sabatini, D.D., Wu, X.R., Kong, X., Kreibich, G., Rindler, M.J., and Sun, T.T. (2016). Sequential and compartmentalized action of Rabs, SNAREs, and MAL in the apical delivery of fusiform vesicles in urothelial umbrella cells. *Mol Biol Cell* *27*, 1621-1634.
- Warrington, S.J., Strutt, H., and Strutt, D. (2013). The Frizzled-dependent planar polarity pathway locally promotes E-cadherin turnover via recruitment of RhoGEF2. *Development* *140*, 1045-1054.
- Watson, C.J., Rowland, M., and Warhurst, G. (2001). Functional modeling of tight junctions in intestinal cell monolayers using polyethylene glycol oligomers. *Am J Physiol Cell Physiol* *281*, C388-397.
- Weber, C.R. (2012). Dynamic properties of the tight junction barrier. *Ann N Y Acad Sci* *1257*, 77-84.
- Weber, E., Berta, G., Tousson, A., St John, P., Green, M.W., Gopalokrishnan, U., Jilling, T., Sorscher, E.J., Elton, T.S., Abrahamson, D.R., and et al. (1994). Expression and polarized targeting of a rab3 isoform in epithelial cells. *J Cell Biol* *125*, 583-594.
- Welz, T., Wellbourne-Wood, J., and Kerkhoff, E. (2014). Orchestration of cell surface proteins by Rab11. *Trends Cell Biol* *24*, 407-415.
- Whitehead, J., Vignjevic, D., Futterer, C., Beaurepaire, E., Robine, S., and Farge, E. (2008). Mechanical factors activate beta-catenin-dependent oncogene expression in APC mouse colon. *HFSP J* *2*, 286-294.
- Wirtz, H.R., and Dobbs, L.G. (1990). Calcium mobilization and exocytosis after one mechanical stretch of lung epithelial cells. *Science* *250*, 1266-1269.
- Woichansky, I., Beretta, C.A., Berns, N., and Riechmann, V. (2016). Three mechanisms control E-cadherin localization to the zonula adherens. *Nat Commun* *7*, 10834.
- Wojciak-Stothard, B., Potempa, S., Eichholtz, T., and Ridley, A.J. (2001). Rho and Rac but not Cdc42 regulate endothelial cell permeability. *J Cell Sci* *114*, 1343-1355.

- Wood, M.W., Breitschwerdt, E.B., Nordone, S.K., Linder, K.E., and Gookin, J.L. (2012). Uropathogenic *E. coli* promote a paracellular urothelial barrier defect characterized by altered tight junction integrity, epithelial cell sloughing and cytokine release. *J Comp Pathol* **147**, 11-19.
- Xiao, K., Allison, D.F., Buckley, K.M., Kottke, M.D., Vincent, P.A., Faundez, V., and Kowalczyk, A.P. (2003). Cellular levels of p120 catenin function as a set point for cadherin expression levels in microvascular endothelial cells. *J Cell Biol* **163**, 535-545.
- Xu, J., Kausalya, P.J., Phua, D.C., Ali, S.M., Hossain, Z., and Hunziker, W. (2008). Early embryonic lethality of mice lacking ZO-2, but Not ZO-3, reveals critical and nonredundant roles for individual zonula occludens proteins in mammalian development. *Mol Cell Biol* **28**, 1669-1678.
- Yamamura, R., Nishimura, N., Nakatsuji, H., Arase, S., and Sasaki, T. (2008). The interaction of JRAB/MICAL-L2 with Rab8 and Rab13 coordinates the assembly of tight junctions and adherens junctions. *Mol Biol Cell* **19**, 971-983.
- Yano, S., Komine, M., Fujimoto, M., Okochi, H., and Tamaki, K. (2004). Mechanical stretching in vitro regulates signal transduction pathways and cellular proliferation in human epidermal keratinocytes. *J Invest Dermatol* **122**, 783-790.
- Yao, M., Qiu, W., Liu, R., Efremov, A.K., Cong, P., Seddiki, R., Payre, M., Lim, C.T., Ladoux, B., Mege, R.M., and Yan, J. (2014). Force-dependent conformational switch of alpha-catenin controls vinculin binding. *Nat Commun* **5**, 4525.
- Yap, A.S., Crampton, M.S., and Hardin, J. (2007). Making and breaking contacts: the cellular biology of cadherin regulation. *Curr Opin Cell Biol* **19**, 508-514.
- Yonemura, S. (2011). Cadherin-actin interactions at adherens junctions. *Curr Opin Cell Biol* **23**, 515-522.
- Yu, A.S., Cheng, M.H., Angelow, S., Gunzel, D., Kanzawa, S.A., Schneeberger, E.E., Fromm, M., and Coalson, R.D. (2009a). Molecular basis for cation selectivity in claudin-2-based paracellular pores: identification of an electrostatic interaction site. *J Gen Physiol* **133**, 111-127.
- Yu, C.H., Rafiq, N.B., Cao, F., Zhou, Y., Krishnasamy, A., Biswas, K.H., Ravasio, A., Chen, Z., Wang, Y.H., Kawauchi, K., Jones, G.E., and Sheetz, M.P. (2015). Integrin-beta3 clusters recruit clathrin-mediated endocytic machinery in the absence of traction force. *Nat Commun* **6**, 8672.
- Yu, D., Marchiando, A.M., Weber, C.R., Raleigh, D.R., Wang, Y., Shen, L., and Turner, J.R. (2010). MLCK-dependent exchange and actin binding region-dependent anchoring of ZO-1 regulate tight junction barrier function. *Proc Natl Acad Sci U S A* **107**, 8237-8241.
- Yu, D., and Turner, J.R. (2008). Stimulus-induced reorganization of tight junction structure: the role of membrane traffic. *Biochim Biophys Acta* **1778**, 709-716.
- Yu, J.C., and Fernandez-Gonzalez, R. (2016). Local mechanical forces promote polarized junctional assembly and axis elongation in *Drosophila*. *Elife* **5**.

- Yu, W., Hill, W.G., Apodaca, G., and Zeidel, M.L. (2011). Expression and distribution of transient receptor potential (TRP) channels in bladder epithelium. *Am J Physiol Renal Physiol* 300, F49-59.
- Yu, W., Khandelwal, P., and Apodaca, G. (2009b). Distinct apical and basolateral membrane requirements for stretch-induced membrane traffic at the apical surface of bladder umbrella cells. *Mol Biol Cell* 20, 282-295.
- Zahraoui, A., Joberty, G., Arpin, M., Fontaine, J.J., Hellio, R., Tavitian, A., and Louvard, D. (1994). A small rab GTPase is distributed in cytoplasmic vesicles in non polarized cells but colocalizes with the tight junction marker ZO-1 in polarized epithelial cells. *J Cell Biol* 124, 101-115.
- Zhang, H.M., Ji, H.H., Ni, T., Ma, R.N., Wang, A., and Li, X.D. (2017). Characterization of Blebbistatin Inhibition of Smooth Muscle Myosin and Nonmuscle Myosin-2. *Biochemistry* 56, 4235-4243.
- Zhou, K., Muroyama, A., Underwood, J., Leylek, R., Ray, S., Soderling, S.H., and Lechler, T. (2013). Actin-related protein2/3 complex regulates tight junctions and terminal differentiation to promote epidermal barrier formation. *Proc Natl Acad Sci U S A* 110, E3820-3829.